



Durham E-Theses

Elucidation of cytolinker function: periplakin-associated proteins in epithelial cells.

Boczonadi, Veronika

How to cite:

Boczonadi, Veronika (2009) *Elucidation of cytolinker function: periplakin-associated proteins in epithelial cells.*, Durham theses, Durham University. Available at Durham E-Theses Online:
<http://etheses.dur.ac.uk/2466/>

Use policy

The full-text may be used and/or reproduced, and given to third parties in any format or medium, without prior permission or charge, for personal research or study, educational, or not-for-profit purposes provided that:

- a full bibliographic reference is made to the original source
- a [link](#) is made to the metadata record in Durham E-Theses
- the full-text is not changed in any way

The full-text must not be sold in any format or medium without the formal permission of the copyright holders.

Please consult the [full Durham E-Theses policy](#) for further details.

Academic Support Office, Durham University, University Office, Old Elvet, Durham DH1 3HP
e-mail: e-theses.admin@dur.ac.uk Tel: +44 0191 334 6107
<http://etheses.dur.ac.uk>

**Elucidation of cytolinker function:
periplakin-associated proteins in
epithelial cells.**

By

Veronika Boczonadi

A thesis submitted at Durham University for the degree of
Doctor of Philosophy

School of Biological and Biomedical Sciences

Durham University

The copyright of this thesis rests with the author or the university to which it was submitted. No quotation from it, or information derived from it may be published without the prior written consent of the author or university, and any information derived from it should be acknowledged.

23 JUN 2009



DECLARATIONS

I declare that the experiments described in this thesis were carried out by myself in the School of Biological and Biomedical Sciences, University of Durham, under the supervision of Dr Arto Maatta. This thesis has been composed by myself and is a record of work that has not been submitted previously for a higher degree.

Veronika Boczonadi

I certify that the work reported in this thesis has been performed by Veronika Boczonadi, who, during the period of study, has fulfilled the conditions of the Ordinance and Regulations governing the Degree of Doctor of Philosophy.

Dr Arto Maatta

The copyright of this thesis rests with the author. No quotation from it should be published in any format, including electronics and the internet, without the author's prior consent. All information derived from this thesis must be acknowledged appropriately.

PRESENTATIONS AND PUBLICATIONS:

1. Heather A. Long¹, Veronika Boczonadi¹, Lorna Marshall, Martin Goldberg and Arto Määttä*. (2006) Role of intermediate filaments in epithelial migration: Periplakin-dependent re-organisation of keratin cytoskeleton and loss of collective migration in keratin 8 down-regulated epithelial sheets. *Journal of Cell Science.* (2006) 119 (Pt 24):5147-59.

2. Veronika Boczonadi, Lorna McInroy, Arto Maatta. (2007) Cytolinker cross-talk: Periplakin N-terminus interacts with plectin to regulate keratin organization and epithelial migration. *Experimental Cell Research* 313(2007)3579-3591.

- Poster at the British Society for Investigative Dermatology Annual conference (BSID) in Robinson College University of Cambridge 11-13 2 April 2005.
- Poster at the British Society for Investigative Dermatology (BSID) Annual conference in Hulme Hall University of Manchester 10-12 April 2006.
- Oral presentation at the 5th Intermediate Filament meeting, Durham University September 2007.
- Poster presentation at the British Society for Investigative Dermatology (BSID) conference, New Collage, Oxford, 7-9 April 2008.

ABSTRACT

Periplakin is a cytolinker protein which participates in the barrier formation of the skin by playing part in the cornified envelope assembly of epidermal cells. Previous studies had identified periplakin, envoplakin and involucrin as constituents of the cornified envelope, but gene-targeting studies had demonstrated that lack of the proteins individually or in any “double knock-out” combination did not disturb the epidermal differentiation or skin barrier function. In order to gain more information about periplakin, which is also expressed in simple epithelial cells, a stably transfected MCF-7 subclone overexpressing the HA-tagged periplakin N-terminus was generated. Co-immunoprecipitation was used for screening of protein complexes associated with the HA-tagged periplakin N-terminus to identify previously uncharacterised periplakin partners. Co-IP with anti-HA antibody and mass-spectrometry revealed a 500 kDa periplakin interacting protein, plectin and another protein around the size of 34 kDa identified as annexin A9. Endogenous periplakin co-localised with annexin A9 in the plasma membrane of MCF-7 cells and showed a similar staining pattern in newborn and adult mouse skin. Transient transfection of periplakin deletion constructs indicated that the first 133 amino acid residues are essential for the co-localisation with plectin at cell borders. Immunofluorescence analysis demonstrated that periplakin N-terminus and different plectin isoforms, such as plectin-1, -1f and 1k, are co-localise at cell borders of MCF-7 epithelia and also co-localise with endogenous periplakin at suprabasal layers of the skin. Ablation of the plectin by siRNA transfection in HaCaT keratinocytes resulted in aggregation of periplakin into small clusters in the cytoplasm. Scratch wounded MCF-7 epithelia expressing the N-terminal half of periplakin showed accelerated keratin re-organisation which was hampered by plectin downregulation. The role of periplakin and keratin IFs in the migration of simple epithelial cells was also investigated. Stable expression of periplakin C-terminus increased keratin bundling and Ser-431 phosphorylation of keratin 8 at the free wound edge, delaying wound closure. Depletion of periplakin or plectin by siRNA transfection impaired wound closure, while simultaneous ablation of both proteins reduced the speed of wound healing even further. Knockdown of keratin 8 IFs with siRNA resulted in the loss of desmoplakin at cell borders and the failure of different simple epithelial sheets migrating as a collective unit.

AKNOWLEDGEMENTS

Hereby I would like to take the opportunity to thank a number of people whose help is invaluable to me.:

First and foremost I would like to thank my supervisor Dr. Arto Maatta for giving me the opportunity to join his lab and for providing me solid guidance, support and inspiration throughout. I would like to thank people who helped me along the way so big thanks have to go to Heather and Lorna for helping me learn all the techniques, to Dr. Bill Simon and Joanne Robson for their great help with the 2-D gels and the proteomics work, and Mrs. Christine Richardson for her time with me at the confocal microscope. Also thanks to everyone in the ICBL lab who are not just colleagues but great friend also, and who made my time in Durham so enjoyable Vicky, Kem, Vanja, Georgia, and Fred.

This project was supported by the British Skin Foundation.

Special thanks have to go to my parents who not only throughout my PhD but during the undergraduate years have been so supportive, believing in my abilities even when I was doubting myself and let me go and leave them and my brother (Pocok) behind.

And last but not least huge big thanks have to go to my fiancée, Robek (Dr. Robert Pal) who encouraged me to start a new life in England. He has been always there for me when I needed to take my mind off work and helped me to smile and believing in myself.

KÖSZÖNET NYILVÁNÍTÁS

Ezennel szeretném megragadni az alkalmat hogy köszönetet nyilvánítsak mindazoknak akik segítsége felbecsülhetetlen volt a doktorandusz éveim alatt:

Mindenek előtt hatalmas köszönet témavezetőmnek Dr Arto Maatta-nak, aki lehetőséget nyújtott számomra hogy csatlakozzak a kutató csoportjához, folyamatos támogatásáért és ösztönzéséért. Köszönettel tartozom mindazoknak akik segítettek az elmúlt három évben különösképpen Heather-nek es Lorna-nak akik megtanítottak a laboratóriumi eszközök használatára és segítettek az nehézkes kezdeti időszakban. Köszönet Dr. Bill Simon-nak es Joanne Robson-nak akik hatalmas segítséget nyújtottak a 2-dimenziós fehérje elválsztásban, tömeg spektroszkópiás mérésekben, valamint Mrs. Christine Richardson-nak aki a konfokális mikroszkóp rejtelseibe vezetett be. Továbbá köszönettel tartozom mindenkinek az ICBL laborban akik nem csak munkatársak de barátok is: Vicky, Kem, Vanja, Georgia, és Fred.

Hálás köszönet szüleimnek akik nem csak a doktorandusz de az egyetemei éveim alatt is kitartóan támogattak, hittek a képességeimben még akkor is amikor én kételkedtem bennük és amiért képesek voltak elengedni, hogy új életet kezdjek Angliában.

Végül de nem utolsó sorban óriási köszönet a vőlegényemnek, Robeknak (Dr. Pál Róbertnek) kinek ösztönzése nélkül nem hagytam volna el Magyarországot és aki mindig mellettem állt mikor szükségem volt támogatásra valamint képes volt mosolyt varázsolni arcomra egy másodperc alatt

TABLE OF CONTENTS

DECLARATION.....	2
PRESENTATIONS AND PUBLICATIONS.....	3
ABSTRACT.....	4
ACKNOWLEDGEMENTS.....	5
KÖSZÖNET NYÍLVÁNÍTÁS.....	6
TABLE OF CONTENT.....	7
INDEX OF FIGURES.....	13
INDEX OF TABLES.....	16
ABBREVIATIONS.....	17

CHAPTER I – GENERAL INTRODUCTION

1.1 Prologue.....	21
1.2 Cytoskeleton.....	21
1.2.1 Introduction to cytoskeletal networks.....	21
1.2.2 Actin.....	24
1.2.3 Microtubules.....	25
1.2.4 Intermediate Filaments.	27
1.2.4.1 Intermediate filament structure.....	31
1.2.4.2 IF assembly properties <i>in vitro</i>	32
1.2.4.3 Remodelling of intermediate filaments.....	32
1.2.4.4 Major functions of intermediate filaments.....	34
1.3 Cytoskeletal Linker Proteins: Plakin Family.....	37
1.3.1 Structure of the cytolinkers.....	38
1.3.2 Periplakin.....	44
1.3.2.1 Overall structure of the periplakin.....	44
1.3.2.2 Role of periplakin in cornified envelope formation.....	46
1.3.2.3 Consequence of periplakin ablation.....	50
1.3.2.4 Periplakin in cancer progression.....	51
1.3.3 Envoplakin.....	51
1.3.4 Desmoplakin.....	52
1.3.4.1 Structure of desmoplakin.....	53
1.3.4.2 Function of desmoplakin in skin, cardiac muscle and during embryogenesis.....	53
1.3.5 Plectin.....	54
1.3.5.1 Role of plectin in cytoskeletal dynamics.....	55

1.3.5.2 Plectin and signal transduction.....	56
1.3.5.3 Mutations in the plectin gene.....	56
1.3.5.4 Plectin isoforms.....	57
1.3.6 Bullous pemphigoid antigen 1 (BPAG-1).....	60
1.3.6.1 Mutation in the BPAG-1 gene.....	60
1.3.7 Microtubule-Actin Cross-linking Factor 1 (MACF-1).....	61
1.3.8 Epiplakin.....	62
1.4 Epithelial cell junctions.....	66
1.4.1 Cell-Cell junctions.....	68
1.4.1.1 Tight junctions.....	68
1.4.1.2 Adherens junctions.....	69
1.4.1.3 Desmosomes.....	70
1.4.1.3.1 Desmosomes and signalling.....	72
1.4.1.3.2 Autoantibodies against periplakin and desmosomal components are detected in autoimmune skin diseases.....	73
1.4.1.4 Gap junctions.....	78
1.4.2 Cell-matrix junctions.....	83
1.4.2.1 Hemidesmosomes.....	83
1.4.2.2 Focal adhesions.....	84
AIM OF THIS THESIS.....	88

CHAPTER II – MATERIAL AND METHODS

Chemicals and reagents.....	90
2.1 Periplakin constructs	90
2.2 Mammalian cell culture.....	90
2.2.1 Cell cultures.....	91
2.2.2 Cryopreservation of the cells.....	92
2.2.3 Establishment of stably transfected cell lines.....	92
2.2.4 Generation of periplakin specific rabbit polyclonal antibody.....	93
2.3 Immunohistochemistry and confocal microscopy.....	93
2.3.1 Fixation.....	93
2.3.2 Primary antibodies.....	93
2.3.3 Secondary antibodies.....	94
2.3.4 Immunofluorescence staining of frozen tissue sections.....	94
2.3.5 Microscopy.....	95
2.4 Scratch wound assay.....	95
2.5 Protein analysis techniques.....	97

2.5.1 Whole cell protein extraction.....	97
2.5.2 Protein Quantification Using BCA-Assay.....	97
2.5.3 Subcellular Detergent Fractionation of Proteins.....	97
2.6 SDS-PolyAcrylamide Gel Electrophoresis (PAGE) for proteins	
with a molecular weight of 20-200 kDa.....	100
2.7 1-dimensional gel electrophoresis.....	102
2.8 Immunoblotting.....	102
2.9 Ponceau S staining of the nitrocellulose membrane.....	102
2.10 Immunodetection.....	103
2.11 Membrane stripping for reprobing.....	103
2.12 Immunoprecipitation.....	103
2.12.1 Cell lysis, Pre-clearing, Immunoprecipitation.....	103
2.12.2 Immunoprecipitation with the IP/CoIP kit.....	104
2.13 Gel staining.....	105
2.14 2-Dimensional gel electrophoresis.....	105
2.14.1 Re-Swelling of IPG strip.....	106
2.14.2 1 st Dimension run.....	106
2.14.3 2 nd dimension run.....	107
2.15 Matrix-assisted laser desorption/ionization time-of-flight (MALDI-TOF).....	108
2.15.1 Mass-Spectrometry.....	108
2.16 RNA interference (RNAi).....	109
2.16.1 Selection of siRNA sequence.....	113
2.16.2 Cell culture and transfection of siRNA.....	113
2.17 Student's T-test.....	114

CHAPTER III – CO-IMMUNOPRECIPITATION OF PLECTIN AND ANNEXIN A9 WITH PERIPLAKIN IN MCF-7 EPITHELIAL CELLS

3.1. Introduction.....	118
3.2 Results.....	120
3.2.1 Demonstration of periplakin BOCZ-1 antibody specificity by siRNA transfection experiments.....	120
3.2.2 Generation of ½ N-PPL overexpressing cell line.....	120
3.2.3 Characterization of stably transfected cell line.....	124
3.2.4 Cellular localization of HA-tagged protein and endogenous periplakin in MCF-7 cells by immunofluorescence microscopy.....	124
3.2.5 Periplakin N-terminus does not co-localised with keratin intermediate filaments in MCF-7 cells.....	127

3.2.6 Solubility properties of the HA-tagged protein by biochemical fractionation.....	127
3.2.7 Identification of plectin and annexin A9 as co-immunoprecipitating partners of periplakin.....	130
3.2.7.1 Strategy of co-immunoprecipitation experiments.....	130
3.2.8 Successful precipitation of periplakin ½ N-terminus with HA-antibody.....	130
3.2.9 Use of the Mammalian HA Tag IP/Co-IP Kit, to identify periplakin interacting partners.....	134
3.2.10 Results of the 2D gel electrophoresis.....	136
3.2.11 Verification of co-immunoprecipitation of periplakin and plectin by Western blot analysis.....	143
3.2.12 Co-localization of periplakin and plectin in MCF-7 and HaCaT cell line.....	145
3.2.13 The first 133 amino acids of the periplakin N-terminus are required for co-localization with plectin in simple epithelial cells.....	147
3.2.14. Co-localisation of plectin isoforms with periplakin.....	150
3.2.15 Investigation of Annexin A9 as a potential periplakin interacting partner.....	156
3.2.16 Confirmation of co-immunoprecipitation of periplakin and annexin A9 by Western blot analysis.....	156
3.2.17 Expression level of annexin A9 protein in untransfected, empty transfected and MCF-7 C6-PPL cell lines.....	157
3.2.18 Annexin A9 found in mostly in the Triton-X100 insoluble cytoskeletal fraction in MCF-7 cells.....	157
3.2.19 Cellular co-localization of periplakin and annexin A9 in simple epithelia by immunofluorescence microscopy.....	160
3.2.20 Annexin A9 and annexin A1 are not co-localised in MCF-7 cells.....	162
3.2.21 Expression of annexin A9 in newborn and adult mouse skin sections by immunofluorescence staining.....	164
3.3 Discussion.....	167
3.3.1 Why Co-immunoprecipitation?.....	167
3.3.2 MCF-7 ½ N-PPL cell line proved a suitable model for studying protein interactions.....	168
3.3.3 Plectin and Annexin A9 identified as co-immunoprecipitating partners of periplakin N-terminus.....	168
3.3.4 Periplakin-plectin co-localisation.....	169
3.3.5 Annexin A9 co-localise with periplakin in MCF-7 cells and in mouse skin.....	172

CHAPTER IV – KERATIN INTERMEDIATE FILAMENT ORGANISATION IS DEPENDENT ON PERIPLAKIN AND PLECTIN IN SIMPLE EPITHELIAL CELLS

4.1 Introduction	177
4.2 Results	179
4.2.1 Transfection of short interfering RNA (siRNA) to down-regulate periplakin, plectin and keratin 8 expression.....	179
4.2.2 Plectin knock-down impairs periplakin subcellular targeting in HaCaT keratinocytes.....	183
4.2.3 Periplakin ablation inhibits intermediate filament re-organisation at the wound site.....	189
4.2.4 Investigation of intracellular localization of periplakin C-terminus by confocal microscopy in simple epithelial cell.....	192
4.2.5 Investigation of expression levels of HA-tagged periplakin linker domain by Western blot analysis.....	195
4.2.6 Stable expression of the periplakin linker domain interferes with keratin reorganization at wound edge.....	197
4.2.7 Overexpression of periplakin C-terminus is associated with up-regulated Ser-431 phosphorylation in keratin 8 intermediate filament.....	197
4.2.8 Periplakin amino-terminus accelerates keratin intermediate filament bundling at the wound edge.....	201
4.2.9 Plectin downregulation in the 1/2N-PPL cell inhibits rapid keratin bundle formation.....	204
4.2.10 Simultaneous periplakin and plectin downregulation results in keratin intermediate filament disorganization in MCF-7 cells.....	206
4.3 Discussion	208
4.3.1 Effect of periplakin and plectin ablation in intact epithelial sheets.....	208
4.3.2 Keratin intermediate filament organization.....	208
4.3.3 Influence of periplakin linker domain on keratin intermediate filaments.....	209
4.3.4 Periplakin NH ₂ -terminus is required in normal wound healing processes.....	210

CHAPTER V – ROLE OF PLAKIN PROTEINS AND KERATIN 8 IN EPITHELIAL MIGRATION

5.1 Introduction	212
5.2 Results	215
5.2.1 Cell viability is not affected by either periplakin or keratin 8 siRNA transfections.....	215

5.2.2 Periplakin linker domain delays wound closure in MCF-7 cells.	215
5.2.3 <i>In vitro</i> wound closure is impaired by periplakin siRNA transfection in simple epithelial MCF-7 and HeLa cells	219
5.2.4 Depletion of either periplakin or plectin impairs MCF-7 wound closure in a similar manner.....	224
5.2.5 Ablation of keratin 8 shows disrupted desmosomes in HeLa and Panc-1 simple epithelial cell lines.....	227
5.3 Discussion.....	236
5.3.1 Effect on cell migration.....	236
5.3.2 Collective epithelial sheet migration.....	237
 CHAPTER VI – GENERAL DISCUSSION	
6.1 Implications of current work.....	243
6.2 Periplakin functions.....	243
6.3 General outlook on epithelial cell migration.....	244
6.4 Possible future directions.....	247
 REFERENCES.....	 249

INDEX OF FIGURES

Figure 1.1: Major cytoskeletal filament networks.....	23
Figure 1.2.: Schematic diagram highlighting members of the plakin family	40
Figure 1.3: Crystal structure displaying the first tandem pair of spectrin repeats found of plectin and an overlap comparison with BPAG-1.....	43
Figure 1.4: Detailed full structure of periplakin and plectin, also displaying the organization of their plakin domains.....	45
Figure 1.5: Schematic diagram of the skin structure and its terminal differentiation.....	48
Figure 1.6: Schematic diagram detailing the formation of cornified envelope.....	49
Figure 1.7: Genomic organisation of the mouse plectin gene.....	59
Figure 1.8: Schematic diagram detailing the interaction of plakins in epithelial cells.....	63
Figure 1.9: Schematic diagram detailing the organisation of simple and stratified epithelia.....	67
Figure 1.10: Composition and structure of the cell-cell junctions.....	80
Figure 1.11: Schematic diagram of cell-matrix junctions.....	86
Figure 2.1: Scratch wound assay.....	96
Figure 2.2: Experimental summary of subcellular detergent fractionation of proteins.....	99
Figure 2.3: Mechanism of gene silencing by siRNA transfection.....	111
Figure 3.1: Demonstration of periplakin BOCZ-1 antibody specificity by siRNA transfection experiments.....	122
Figure 3.2: Schematic diagram of the 1/2N-periplakin construct used for stable cell line establishment.....	123
Figure 3.3: Co-localization of the endogenous periplakin and the HA-tagged protein in MCF-7 1/2 N-PPL cell line.....	126
Figure 3.4: MCF-7 1/2 N-PPL cell line expressing the HA-tagged N-terminus of periplakin.....	129
Figure 3.5: Immunoprecipitation experiment of the anti-HA antibody using IgG beads.....	132
Figure 3.6: Co-immunoprecipitation of periplakin 1/2N-terminus with anti-HA-antibody and analysis by silver staining on a 1D 4-12% gradient pre-cast gel.....	135
Figure 3.7: Co-immunoprecipitation of periplakin amino-terminus with anti-HA antibody analysed on silver stained 2-D gels.....	137
Figure 3.8: MALDI-TOF spectrum for peptide identified as plectin by peptide mass fingerprinting.....	141
Figure 3.9: MALDI-TOF spectrum for peptide identified as annexin A9 by peptide mass fingerprinting.....	142
Figure 3.10: Co-immunoprecipitation of periplakin and plectin MCF-7 C6-PPL cells	144

Figure 3.11: Co-staining of MCF-7 and HaCaT cell with periplakin and plectin.....	146
Figure 3.12: Schematic diagram of N-terminal subdomains of the HA-tagged deletion constructs.....	148
Figure 3.13: Localization of periplakin deletion constructs in MCF-7 cells.....	149
Figure 3.14: Schematic diagram illustrating human N-terminal plectin isoforms.....	152
Figure 3.15: Co-localisation of periplakin and N-terminal plectin isoforms.....	153
Figure 3.16: Immunofluorescence staining of human skin.....	154
Figure 3.17: Immunoprecipitation of HA-tag periplakin N-terminus and characterization of annexin A9 expression level in untransfected, empty transfected (MCF-7 EV.) and MCF-7 1/2 N-PPL cell line.....	158
Figure 3.18: Characterization of Annexin A9 solubility in untransfected, MCF-7 EV and MCF-7 C6-PPL cells.....	159
Figure 3.19: Double staining of periplakin and annexin A9 in MCF-7 C6-PPL and untransfected MCF-7 cells.....	161
Figure 3.20: Expression of annexin A9 and annexin A1 on MCF-7 cells.....	163
Figure 3.21: Expression of annexin A9 and periplakin in newborn and adult mouse skin.....	165
Figure 4.1: Verification of the effect of siRNA oligonucleotides using Western blot analysis in MCF-7 cells.....	181
Figure 4.2: Periplakin and plectin downregulation in MCF-7 and HaCaT cells.....	185
Figure 4.3: Images showing clusters of periplakin in plectin siRNA transfected HaCaT keratinocytes.	187
Figure 4.4: Altered periplakin distribution after plectin siRNA transfection on subconfluent HaCaT keratinocytes.....	188
Figure 4.5: Keratin organization in periplakin downregulated wound edge cells.....	190
Figure 4.6: Schematic diagram of the periplakin construct used for stable cell line transfection.....	193
Figure 4.7: Localisation of periplakin linker domain in MCF-7 cells.....	194
Figure 4.8: Detection of periplakin C-terminal linker domain in MCF-7 C-PPL cells by immunoprecipitation and western blott analysis.....	196
Figure 4.9: Immunofluorescence staining of keratin 8 at wound edges.....	199
Figure 4.10: Expression of Ser-431-phosphorylated keratin expression at wound edges.....	200
Figure 4.11: Accelerated keratin bundling in MCF-7 1/2N-PPL cells.....	202
Figure 4.12: Fluorescence images observing that plectin is required for rapid keratin bundling at the wound edge.....	205

Figure 4.13: The lack of periplakin and plectin alter the appearance of keratin intermediate filament network in MCF-7 cells.....	207
Figure 5.1: Cell survival after siRNA transfections.....	217
Figure 5.2: Wound closure in control and PPL-C cell lines.....	218
Figure 5.3: Wound migration properties of periplakin depleted MCF- 7 cells.....	221
Figure 5.4: Effect of periplakin downregulation on wound healing in HeLa cells.....	223
Figure 5.5: Verification of effective periplakin and plectin downregulation in wound healing experiments.....	226
Figure 5.6: Phase contrast microscopy images showing that epithelial migration is impaired by ablation of periplakin or plectin.....	227
Figure 5.7: Protein expression of MCF-7 in comparison with two other cell lines (HeLa and Panc-1).....	229
Figure 5.8: The effect of keratin 8 knock-down in HeLa and Panc-1 cells.....	232
Figure 5.9: Phase contrast microscopy images of scratch wound closure in keratin 8 downregulated HeLa and Panc-1 monolayer.....	235

INDEX OF TABLES

Table 1.1: Classification of intermediate filament protein superfamily.....	28
Table 1.2: Summary of mammalian cytolinkers and their related diseases, studied mouse knockout phenotypes.....	64
Table 1.3: Summary of intraepidermal bullous diseases triggered by autoimmune response against components of desmosomes.....	77
Table 2.1: Summary of cell lines used in this study.....	91
Table 2.2: Preparation of different SDS-PAGE gel.....	101
Table 2.3: siRNA sequences from what highlighted (bald) were used in this study.....	113
Table 2.4: List of primary antibodies used in this study.....	115
Table 2.5: List of secondary antibodies used in this study.....	116
Table 3.1: Summary of mass spectroscopic identification of proteins co-immunoprecipitating with periplakin amino-terminus on 1D and 2D gels.....	139
Table 3.2: Members of the annexin family indicating interacting partners and knock-out studies.....	175

ABBREVIATIONS

1-D	1-dimension
2-D	2-dimension
aa	amino acid
ABD	actin binding domain
ADP	adenosine diphosphate
APS	ammonium persulphate
ATP	adenosine triphosphate
BM	basement membrane
bp	base pairs
BPAG-1	bullous pemphigoid antigen-1
BPAG-2	bullous pemphigoid antigen-2
BSA	bovine serum albumin
°C	centigrade
cDNA	complementary DNA
CE	cornified envelope
CH	calponin homology
cm	centimetre
CO ₂	carbon dioxide
Co-IP	co-immunoprecipitation
Cx	connexin
DICER	RNAase III enzyme
DMEM	Dulbecco's modified Eagle's medium
DMSO	dimethyl sulphoxid
DNA	deoxyribonucleic acid
DP	desmoplakin
Dsc	desmocollin
Dsg	desmoglein
EBS-MD	epidemolysis bullosa simplex with muscular dystrophy
EDC	epidermal differentiation complex
EDTA	ethyle diamine tetra-acetic acid
EGF	epidermal growth factor
EGFP	enhanced green fluorescent protein
EGTA	ethylene glycol tetra-acetic acid
F-actin	filamentous-actin
FAK	focal adhesion kinase
FCS	foetal calf serum
g	gram
G-actin	globular actin
GFAP	glial fibrillary acidic protein
GPS	L-glutamin/penicillin/streptomycin
GSR	glycine-serine-arginine domain
GTP	guanosine-triphosphate

h	hour
HA	hemagglutinin
HaCaT	immortalised human keratinocyte cell line
HRP	horse radish peroxidase
HT29	human colon adenocarcinoma cell line
IBD	inflammatory bowel disease
IF	intermediate filaments
Ig	immunoglobulin
IPTG	isopropylthio- β -D-galactosidase
JAM	junctional adhesion molecule
K	keratin
KCl	potassium chloride
kDa	kilo Dalton
KO	knock-out
L	litre
LB	lammellar bodies
LCE	late cornified envelope genes
LEP	late envelope protein genes
LSB	Laemmli sample buffer
μ g	microgram
μ l	microlitre
μ M	micromolar
μ m	micron (micrometre)
M	molar
MACF-1	microtubule-Actin Cross-linking Factor 1
MAGUK	membrane associated guanylate kinase
MALDI-TOF	matrix-assisted laser desorption/ionisation-time of flight mass spectrometry
MAP	microtubule associated proteins
MCF-7	human breast adenocarcinoma cell line
MDCK	Madin-Darby canine kidney epithelial cells
min	minutes
ml	millilitre
mm	millimetre
mM	millimolar
MOWSE	molecular weight search
mRNA	messenger RNA
MT	microtubule
MTOC	microtubule organising centre
NaN ₃	sodium azide
NaCl	sodium chloride
NF-H	neurofilament heavy chain
NF-L	neurofilament light chain
NF-M	neurofilament medium chain
ng	nanogram
NH ₂	amino-terminus
nm	nanometre

NP40	nonident P40
PAGE	polyacrylamide gel electrophoresis
PBS	phosphate buffered saline
PCR	polymerase chain reaction
PF	pemphigus foiaceus
PG	pakoglobin
PMF	peptide mass fingerprinting
PMSF	phenylmethylsulfonyl fluoride
PNP	paraneoplastic pemphigus
PRD	plectin repeat domain
PV	pemphigus vulgaris
RISC	RNA induced silencing complex
rpm	revolutions per minute
SDS	sodyum dodecyl sulphate
sec	second
siRNA	small double-stranded RNA
SPR	spectrin repeat domain
SPRs	small-prolin rich proteins
SR	spectrin repeats
TBS	tris buffered saline
TEM	transmission electron microscopy
TEMED	N,N,N',N'-tetramethylethylenediamine
TEN	toxic epidermal necrolysis
TG	transglutaminase
Tris	tris-(hydroxy-methyl)methylamine
Triton X-100	t-octylphenoxypolyethoxyethanol
TTBS	tris-bufferd saline containing Tween 20
ULF	unit length filament
UV	ultraviolet
v/v	volume for volume
w/v	weight for volume
ZO	zonula occludens

CHAPTER I

GENERAL INTRODUCTION

1.1 Prologue

Periplakin is widely studied as a protein of the cornified layers of the epidermis, which are essential for the barrier function of the skin. Furthermore, periplakin is one of the cytolinker proteins that binds to intermediate filaments and localises to desmosomes. This thesis proposes that periplakin forms protein complexes with other proteins and has a role in cell migration and in organisation of the keratin intermediate filaments in simple epithelial cells. This chapter will give an overview of the cytoskeleton, cytolinker proteins and adhesion junctions, relating this to relevant autoimmune skin diseases.

Each of the results chapters to follow will then give a focused insight on the specific subject that it addresses.

1.2 Cytoskeleton

1.2.1 Introduction to cytoskeletal networks

The cytoskeleton of a cell is a complex mixture of structural proteins which are essential for the integrity of cell shape, motility and internal movement or transport of particles, vesicles and organelles within the cytoplasm. All the cytoskeletal networks are polymers built from small subunits and held together by non-covalent bonds. Instead of being a disorganised array, the cytoskeleton is organized into discrete structures. The mammalian cytoskeleton is composed of three main networks, microtubules (MTs), actin filaments and intermediate filaments (IFs), each of which has a specific role within the cell. IFs provide mechanical strength and resistance to stress (Fuchs & Cleveland, 1998; Omary *et al.*, 2004), microtubules serve as tracks for intracellular transport (Vale, 1987) and form the mitotic spindle (Cooper, 2000), while actin filaments are necessary for whole cell locomotion (Bray, 1992).

These three types of filaments often have distinct localisations. In the lumen of the intestine, this distribution is easily distinguishable. Actin microfilaments are abundant in the apical and lateral regions of the cell (Drenckhahn & Dermietzel, 1988), whereas IFs form a meshwork that is tethered to junctions between cells (Franke *et al.*, 1979). In contrast,

microtubules align with the axis of the cell in close proximity to major organelles such as the Golgi complex (Rogalski & Singer, 1984) or endoplasmic reticulum (Buckley & Porter, K, 1975) (**Figure 1.1 A', B', C'**). The three networks will be discussed in turn below.

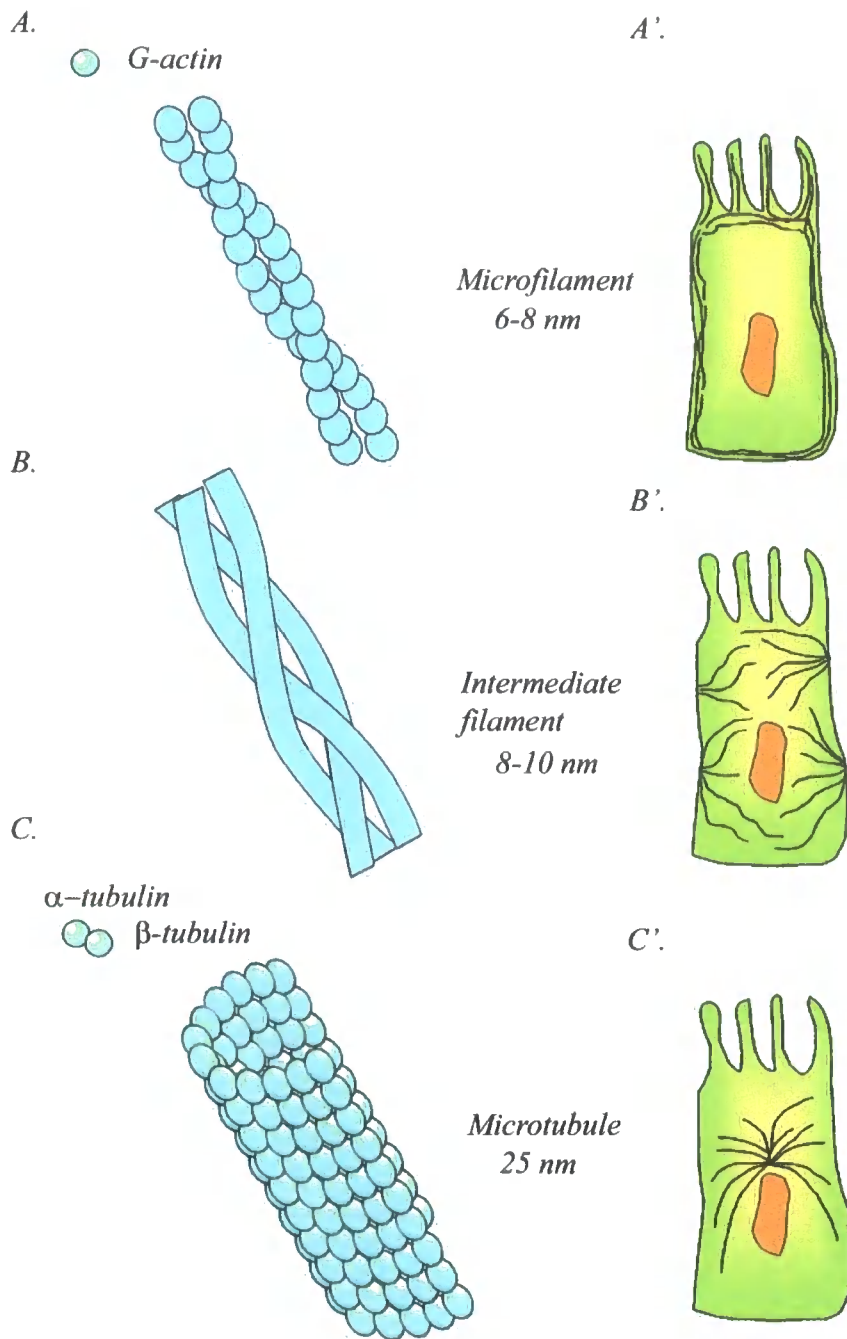


Figure 1.1: Major cytoskeletal filament networks.

A. Actin filaments (6-8 nm), also known as microfilaments, are two stranded helical polymers of the actin protein. **A'.** Although microfilaments are dispersed throughout the cell, they are mostly concentrated beneath the plasma membrane. **B.** Intermediate filaments (8-10 nm) are rope like fibers consist of intermediate filament proteins. **B'.** In epithelial tissues intermediate filaments extend across the cytoplasm from one cell-cell junction to another giving cells mechanical strength. **C.** Microtubules are long, hollow cylinders composed of α and β tubulin heterodimers that arrange to form protofilaments (25 nm). **C'.** Microtubules are long, straight and typically possess one end attached to the microtubule-organising center (MTOC).

1.2.2 Actin

Actin is encoded by a highly conserved gene family and is the most abundant intracellular protein in most eukaryotic cells, with a molecular weight of 42 kDa. Actin, along with myosin, was discovered in 1861 by Kuhne, but was first isolated in 1939-1942 by Straub, Bonga and Szent-Gyorgyi (Szent-Gyorgyi, 1951). Actin filaments are about 6-8 nm in diameter and are the contractile elements of the cell. Actin plays an important role in cell movement, cell contractility, cell remodelling, cell polarity, intracellular transport and phagocytosis. The organization of actin is regulated by many signalling proteins, including Rho, Rac and Cdc42, that are activated by extracellular signals (Schmidt & Hall, 1998). Actin exists in two forms, globular or G-actin, which polymerizes into the other form, called filamentous or F-actin. Filamentous actin can be found as bundles called stress fibers, or as a fine network called microfilaments. There is also a third filamentous structure known as the contractile ring, which is critical for the separation of the cell during cytokinesis.

Each actin microfilament has two distinct ends, at which polymerization takes place at different rates. There is a fast growing (or plus) end and a slow-growing (or minus) end. Within the cell, the plus end of the filaments is oriented towards the cell membrane, whereas the minus end is oriented towards the cytoplasm (Begg *et al.*, 1978; Stossel, 1984). Actin assembly is coupled with continuous ATP hydrolysis as actin is an ATPase. Under physiological conditions, Mg^{2+} -ATP bound G-actin is incorporated into growing filaments at the plus end. ATP-actin is then converted to ADP-actin by slow hydrolysis as actin monomers are shifted along the filament toward the minus ends (Carrier, 1991a; Carrier, 1991b). At a significant concentration of G-actin, the plus end of the microfilament will constantly grow while the minus end simultaneously dissolves, so the length of the microfilament remains constant - a process known as treadmilling (Bonder *et al.*, 1983; Bonder & Mooseker, 1983).

The actin cytoskeleton consists of polymers of actin along with a large number of actin binding proteins and associated proteins (Stossel, 1993; Winsor & Schiebe, 1997). Their binding to G- or F-actin has various functions: they serve to control the length of filaments (e.g. villin, cofilin, gelsolin, fragmin, and severin), to produce bundles of actin filaments (e.g. villin, filamin, and fimbrin), to cross-link actin filaments to form a meshwork such as that found in association with the cell membrane (e.g. fibrin, vinculin, α -actinin, and talin) or to

control the G-actin pool by preventing the polymerization of actin (e.g. profilin). Additionally, the family of myosins is an important class of actin-associated proteins which convert chemical energy to produce movement of actin filaments. When actin is associated with myosin it forms actinomyosin (Szent-Györgyi, 1949). The best characterised myosin, myosin II, slides actin filaments past each other either to power contraction of the contractile ring during cytokinesis or to produce cell migration (Maciver, 1996).

During cell migration, actin filaments exist in two alternative forms at the leading edge of the motile cells, known as lamellipodia and filopodia (also known as microspikes) (Mitchison & Cramer, 1996; Mejillano *et al.*, 2004). These protrusions seem to rely on forces generated by actin polymerization to push the plasma membrane outward. Cells use these structures to explore their territory and pull themselves around. Lamellipodia are two-dimensional sheet-like structures containing a cross-linked mesh of actin filaments with unbranched filaments at the base (Small, 1995; Svitkina & Borisy, 1999). Filopodia contain long bundled actin filaments and have been implicated in epithelial sheet closure in development, wound healing and metastasis in cancer (Jacinto & Wolpert, 2001).

1.2.3 Microtubules

Microtubules (MT), which were discovered by electron microscopy by Marton and Clarke (1952) and Fawcett and Porter (1954), are large polar filaments composed of heterodimers of the globular proteins α and β tubulin, which create a cylindrical ring of 13 linear protofilaments (linear polymers), 25 nm in diameter. α and β tubulins are homologous but not identical, with each containing a nucleotide binding site and having a molecular weight of approximately 55 kDa. Most microtubules occur as single tubes and form cellular structures such as the mitotic spindle, which positions, aligns and separates chromosomes.

Microtubules grow from the microtubule organising centre (Tucker, 1992) and undergo rapid remodelling with frequent shortening and growth transitions (Waterman-Storer & Salmon, 1998). Microtubules are able to undergo treadmilling, in a similar manner to actin, with addition of tubulin heterodimers at the plus end and dissociation of tubulin heterodimers at the minus end. Microtubules are highly dynamic between growing and shrinking phases both

in vivo and *in vitro* (Desai & Mitchison, 1997). Microtubule elongation proceeds when the concentration of free subunits exceeds the critical concentration, while below this concentration, microtubules depolymerize (Alberts *et al.*, 2002). This non-equilibrium behaviour, known as dynamic instability (Mitchison & Kirschner, 1984), is also based on the binding and hydrolysis of GTP at the nucleotide binding site. Each α and β monomer possesses a binding site for one molecule of GTP. The GTP that is bound to the α -tubulin is physically trapped and is never hydrolysed (Spiegelman *et al.*, 1977). The nucleotide on the β -tubulin, in contrast, is exchangeable, and may be either GTP or GDP. Shortly after incorporation of a tubulin subunit into a filament, GTP hydrolysis occurs, but the nucleotide diphosphate remains trapped in the filament structure. Microtubule structure is stabilized by a layer of GTP tubulin subunits (Mitchison & Kirschner, 1984). When this cap is lost, the protofilaments peel outward and the microtubule rapidly depolymerizes. This dynamic instability is important in cell motility as well as in the positioning of organelles and movement of vesicles in the cell. Microtubules associate with a variety of proteins known as microtubule associated proteins (MAPs).

There are two main classes of microtubule motor proteins that carry out ATP-dependent movement along microtubules (Mitchison & Kirschner, 1984; Gross *et al.*, 2007). Kinesins are a large family of motor proteins, most of which walk along microtubules toward the plus end (Hollenbeck & Swanson, 1990; Coy *et al.*, 1999), whereas dyneins walk along microtubules towards the minus end (Hirokawa, 1998; Vale, 2003). Motility arises from conformational changes in the motor domain, as ATP is bound and hydrolyzed, and products are released.

Microtubules are key organizers of the cell interior as they serve as a track for organelle movements driven by molecular motors. Plus end directed motors such as kinesins distribute the endoplasmic reticulum, Golgi complex (Lippincott-Schwartz *et al.*, 1995) and mitochondria along microtubules (Fujita *et al.*, 2007). Also, different kinesins are involved in chromosome movement during mitosis and meiosis as well as in microtubule spindle formation (Chang *et al.*, 2004). In human keratinocytes, the retrograde microtubule motor dynein mediates the perinuclear aggregation of melanosomes, which protects the nucleus from UV-induced DNA damage (Byers *et al.*, 2003).

1.2.4 Intermediate Filaments

Evolutionarily, IFs appeared more recently than the other two cytoskeleton networks (Rash *et al.*, 1970; Fuchs & Cleveland, 1998), and were first described by Holtzer and colleagues, from studies of muscle, in the late 1960s (Ishikawa *et al.*, 1968). They have been described as ubiquitous cytoskeletal scaffolds in both the nucleus and cytoplasm of higher metazoans (with the exception of arthropods) (Erber *et al.*, 1998). The name “Intermediate Filament” comes from the fact that their size (10 nm) is intermediate in thickness between the thin actin (6-8 nm) and thick microtubule (25 nm) filaments. IFs are rope-like fibres, forming an internal framework that stretches from the nuclear envelope to the plasma membrane. IFs are encoded by one of the largest families of genes in the human genome (Hesse *et al.*, 2001). More than 65 different IF protein have been identified and classified into six groups based on similarities between their amino acid sequences (**Table 1.1**).

Table 1.1: Classification of intermediate filament protein superfamily and their associated diseases.

Intermediate filament type			Specificity of expression	Disease
I.	Acidic keratins	K9-K24	Soft epithelia	K14-Epidermis bullosa simplex
		K31-K40	Hard epithelia	K10, K16, K14-Keratoderma disorder K12-Meesmann corneal dystrophy
		K25-K28	Inner root Sheet (hair)	K13-White sponge nevus of Cannon K16-Pachyonychia congenital type I K17- Pachyonychia congenital type II
II.	Neutral, basic keratins	K1-K8	Soft epithelia	K1, K9, K2-Keratoderma disorders
		K81-K86	Hard epithelia	K3-Meesmann corneal dystrophy K4- White sponge nevus of cannon
		K71-K80	Inner root Sheet (hair)	K6a- Pachyonychia congenital type I K6b- Pachyonychia congenital type II K81 (Hb1), K83 (Hb3), K86 (Hb6)- Monilethrix K85 (Hb5)-Pure hair-nail type ectodermal dysplasia
III.	Desmin	Muscles	Dilated cardiomyopathy 11, Familial restrictive cardiomyopathy 2	
	GFAP(glial fibrillary acidic protein)	Astrocytes, glia	Alexander disease	

	Vimentin	Fibroblast, endothelium, leukocytes	
	Peripherin	PSN Neurons	Amyotrophic lateral sclerosis
IV.	Neurofilaments (L,M,H)	Neurons	NF-L, M, and H- Amyotrophic lateral sclerosis
	α -Internexin		NF-L-Charcot-Marie-Tooth disease NF-M-Parkinson's disease NF-H-Neuronal IF inclusion disease
	Nestin	Neuroepithelial stem cells	
	Synemin	Muscle	
	Desmuslin	Muscle	
V.	Lamin A/C	Ubiquitous , Nuclear lamina	Lamin A/C-muscular dystrophies (Emery-Dreifuss muscular dystrophy, EDMD), progeria, (Hutchinson-Gilford progeria syndrome), neuropathy (Charcot-Marie-Tooth disease).
	Lamin B1	Ubiquitous (nucleus)	
	Lamin B2	Ubiquitous (nucleus)	Lamin B-lipodystrophies (Barraquer- Simons syndrome), leukodystrophy (Pelizaeus-Merzbacher disease).
Others	Filensin Phakinin	Eye lens	Filensin- Autosomal recessive cataract disease Phakinin- Autosomal dominant cataract disease

Table 1.1: Classification of intermediate filament protein superfamily and their associated diseases.

This classification was based on the new keratin nomenclature which was published recently (Porter, 2006; Schweizer et al., 2006). With the exception of eye lens specific proteins, IFs are divided into five groups based on their sequence homology. Group I-IV are localised to the cell cytoplasm whereas the type V nuclear lamins build up the nuclear envelope and karyoplasms. The keratins are by far the most diverse group of the IFs, containing over 54 genes (Hesse et al., 2001; Hesse et al., 2004; Rogers et al., 2004; Rogers et al., 2005). Keratins are subdivided into type I and type II comprising 17 and 20 different proteins respectively, which are expressed in epithelial cells. Some of the type I and II keratins, called hard keratins, are used for production of structures such as hair and nails. In contrast, soft keratins are abundant in the cytoplasm of epithelial cells. Type III proteins of the IF family include vimentin, GFAP, peripherin and desmin. The type IV IF consists of the three-neurofilament proteins. These form the major IF of many types of mature neurons and were identified by axonal transport studies (Hoffman & Lasek, 1975). Other proteins in this group are α -internexin, expressed at the early stage of neuron development (Pachter & Liem, 1985), nestin, which plays a role in developmental processes and two other proteins expressed in muscle, synemin and desmuslin. Type V IFs consist of nuclear lamins, which are important organisers of the nuclear envelope. Mutations in IFs comprise a large group of human diseases. These are represented in all IF groups (Godsel et al., 2008).

Similarly to microtubules and microfilaments, IFs are dynamically regulated, fully integrated within the cellular framework, and interact with a range of cellular proteins. However there are several basic characteristics that are unique to IFs compared to microfilaments and microtubules. They lack the structural polarity that is observed for actin and microtubules, they are linear rather than globular proteins and are unable to bind or hydrolyze nucleotides as a means of regulating filament dynamics. The small size of the soluble pool of IF subunits *in vivo*, and their mode and location of assembly and turnover in cells, suggest unique organisation properties (Coulombe *et al.*, 2001; Windoffer *et al.*, 2004). Furthermore, IFs display unique mechanical and biochemical properties. Unlike microfilaments and microtubules, IFs are flexible and able to cope with stretching to more than three times their resting length without breaking. (Fudge *et al.*, 2003; Kreplak *et al.*, 2005). Under strain, IFs become thinner and more resistant to further deformation (“strain stiffening”) Moreover, as most of the changes are reversible, they regain their previous conformation once the strain is dissipated. This cytoskeletal filament network, with all the accessory proteins that link the filament to cell components and other cytoskeletal network systems, contribute to the tensile strength necessary for maintaining cell integrity (Kreplak *et al.*, 2005; Herrmann *et al.*, 2007).

1.2.4.1 Intermediate filament structure

Intermediate filaments show a conserved tripartite domain structure. Most IFs contain a conserved central α helical rod domain that is usually 310-350 amino acids long. This is flanked by non-helical carboxyl and amino terminal domains that differ in length, sequence, substructure and properties, leading to the heterogeneity in IF protein size (~40–240 kDa) and other characteristics (Kim & Coulombe, 2007). The rod domain contains heptad repeats (subdomains 1A, 1B, 2A, 2B) that facilitate dimerisation between the rod domains (Coulombe *et al.*, 2001). These dimers constitute the fundamental building blocks of IFs which, depending on the IF type, can be either heterodimeric (keratin) or homodimeric (vimentin). The head and tail domains mediate interactions with other filaments and cellular proteins, as well as serving as a substrate for post-translational modifications that regulate function, structure and

organisation of the filament (Green *et al.*, 2005; Omary *et al.*, 2006a; Izawa & Inagaki, 2006; Coulombe & Wong, 2004).

1.2.4.2 IF assembly properties *in vitro*

The central "rod" domain of IFs mediates coiled-coil dimer formation and represents the major driving force for self-assembly (Chan *et al.*, 1994; Herrmann & Aebi, 2004; Lin *et al.*, 2005). The assembly of the IFs includes several steps, starting with the formation of parallel dimers. Due to the long repeats in the rod domain, cytoplasmic IF proteins form highly stable coiled-coil dimers (42–44 nm in length) in which the two participating monomers show polar, parallel alignment (Kim & Coulombe, 2007). Subsequently, dimers spontaneously assemble into anti-parallel, non-polar tetramers in the absence of ATP or GTP (Strelkov *et al.*, 2003), with a diameter of 8-9 nm (Sokolova *et al.*, 2006; Mücke *et al.*, 2004). Tetramers laterally interact and form octamers, with four of these building up a unit length filament (ULF) (Sokolova *et al.*, 2006), which undergo reorganisation and elongation by longitudinal annealing to form immature IFs. The final step is radial compaction of the filament via lateral rearrangements of protein subunits that reduce the diameter from 16 nm to 10-12 nm (Sokolova *et al.*, 2006; Herrmann *et al.*, 2007; Parry *et al.*, 2007) without increasing the length of the filament.

1.2.4.3 Remodeling of intermediate filaments

IFs are highly dynamic cell components which undergo disassembly and reassembly during many processes such as cell spreading, wound healing processes, cell division and in response to environmental stresses. Phosphorylation is a major post-translational event that is involved in the regulation and reorganisation of the intermediate filament network in cells. IFs have specific kinases associated with them that control solubility, assembly, interactions and disassembly events. Initial experiments highlighted phosphorylation as a major regulatory event, with IF proteins observed to be hyperphosphorylated in mitosis (Evans & Fink, 1982). Other work showed that vimentin-type IFs were rapidly hyperphosphorylated and disassembled in cells

exposed to phosphatase inhibitors, which suggested that the assembly of IFs in interphase cells is controlled by equilibrium between phosphatases and kinases (Lee & Cleveland, 1996). All kinases phosphorylate their target proteins at specific residues (Inagaki *et al.*, 1996; Kosako *et al.*, 1997; Matsuzawa *et al.*, 1998; Goto *et al.*, 2006). In most cases, this targeted phosphorylation leads to an inhibition of IF assembly or facilitates disassembly of the filaments. Those sites of phosphorylation closest to the central rod domain appear to affect filament assembly, whilst those further from the rod domain are important for regulating the interaction of IFs with other cellular components (Inagaki *et al.*, 1996). *In vivo* phosphorylation of IFs may also influence the protein conformation as demonstrated by interference with the binding of antibodies to a distinct site (Tao *et al.*, 2006). It has been suggested that IF turnover might occur via exchanging particles within the filament network (Vikstrom *et al.*, 1992) based on vimentin fluorescence recovery after photobleaching (FRAP) analysis. More recently, phosphorylation of the vimentin end domains have been suggested to regulate IF assembly *in vivo* (Eriksson *et al.*, 2004; Omary *et al.*, 2006b). Studies using fluorescent tagged proteins have identified non-filamentous “particles” and small filamentous portions of IFs called “squiggles” which are able to incorporate into the polymerizing network of the cell (Windoffer & Leube, 1999; Prahlad *et al.*, 1998; Yoon *et al.*, 1998). Keratin particles merge to form squiggles containing IF aggregates such as ULFs and polymerized ULFs building up small filaments (Mücke *et al.*, 2004; Liovic *et al.*, 2003; Kirmse *et al.*, 2007) The cell periphery has been proposed as a “hot spot” for initiation of IF assembly (Windoffer *et al.*, 2006). It is been shown that fluorescent keratin probes initially become incorporated into small particles at the cell periphery, close to actin rich regions such as focal contacts. They then move towards the cell center, becoming rodlets, and eventually integrate into the existing IF network (Windoffer *et al.*, 2004). This connection between keratin filaments and focal adhesions became evident after experiments where the focal adhesion component talin was downregulated and resulted in the inhibition of keratin filament precursor formation (Windoffer *et al.*, 2006). Plectin has also been proposed as a possible candidate for regulating IF polymerization and dynamics. In addition to having an IF binding site on the C-terminus, recently another site (the first CH domain) has been shown to bind IFs. Interestingly, this site is not able to bind filamentous vimentin, suggesting that it might regulate the dynamics of IF polymerization (Sevcik *et al.*, 2004).

Live cell imaging studies of peripherin revealed that 30% of the non-filamentous particles are assembled into a cytoplasmic mRNA complex by a process called dynamic co-translation, in which IF protein particles are initially formed (Chang *et al.*, 2006). Intermediate filaments, such as keratin and vimentin precursors, are motile elements due to their association with MTs (Helfand *et al.*, 2004) and actin filament based motor proteins (Windoffer *et al.*, 2006). This characteristic of IFs is required for proper assembly into extensive cytoskeletal networks (Yoon *et al.*, 1998; Yoon *et al.*, 2001). The direction and rate of movement of IF particles varies depending on IF type, cell type and size of the precursor. However, neurofilaments, vimentin and peripherin have several dynamic behaviors in common. They move 60% of the time in the anterograde and 40% of the time in the retrograde direction (Wang *et al.*, 2000; Helfand *et al.*, 2003). For anterograde movement of vimentin and neurofilaments, kinesin has been implicated (Yoon *et al.*, 1998; Prahlad *et al.*, 1998; Motil *et al.*, 2006) while dynein has been associated with retrograde translocation. Keratin precursors have been demonstrated to move more frequently in the retrograde direction compared to type III and IV IFs. In addition, the kinetics of keratin precursors can be divided into two classes, one of which represents slower kinetics requiring actin filaments and one, with a more rapid kinetics involving microtubules (Wöll *et al.*, 2005).

1.2.4.4 Major functions of intermediate filaments

In contrast to microfilaments and microtubules, intermediate filaments are not fundamentally essential for life at the single cell level. Unicellular eukaryotes (such as *Saccharomyces cerevisiae*) do not have genes encoding IFs (Erber *et al.*, 1998) and some mammalian cells can grow in the absence of a cytoplasmic IF network (Venetianer *et al.*, 1983). Until recently, the main role of IFs was considered to be to hold the cell together because of their remarkable mechanical properties. Today, it is known that they are dynamic, mobile, and in the case of simple epithelia, that they have a role in apico-basal polarization (Oriolo *et al.*, 2007). The major role of IFs in higher vertebrates is to protect epithelial cells, muscle cells and astrocytes from either mechanical or non-mechanical stresses that cause cell death. Besides structural scaffolding, IFs also fulfil specific functions in different cell types. For example, neurofilaments contribute to the radial growth of axons (Lee & Cleveland, 1996),

vimentin IFs play roles in sphingolipid synthesis (Gillard *et al.*, 1998) and keratin 8/18 filaments protect hepatocytes in the liver against drug-induced apoptotic stress (Ku *et al.*, 1998b).

IFs are connected to desmosomes and hemidesmosomes, via a variety of linker proteins. This IF network gives shape and rigidity to the cells, allowing them to resist mechanical stress. Disruption of these fibres can occur in certain genetic disorders, resulting in skin fragility, laminopathies, myopathies, neuropathies, cataracts and premature aging (Omary *et al.*, 2004; Magin *et al.*, 2004; Godsel *et al.*, 2008) (Human Intermediate Filament Mutation Database, <http://www.interfil.org>) (**Table 1.1**). The importance and function of keratin intermediate filaments in skin integrity is well-studied in multiple skin blistering diseases caused by mutations in the keratin genes (Magin *et al.*, 2007; Omary *et al.*, 2004; Gu & Coulombe, 2007). It is clear that mechanical resilience is compromised in epidermal diseases with keratin mutations, notably in epidermolysis bullosa simplex (EBS), which is a group of heritable blistering disorders of keratin 5 and keratin 14. The mechanical function of keratins is highlighted in murine knockout experiments where the worst phenotypes occur in cells where compensation by other keratins is not possible. An excellent example of this is shown by the targeted deletion of keratin 5, the only type II keratin in basal cells, that results in neonatal death (Peters *et al.*, 2001). In contrast, keratin 14 knockout mice have a mild phenotype, most likely due to the compensatory expression of K15 (Lloyd *et al.*, 1995). Similarly, patients lacking keratin 5 have not been identified, as it is associated with early lethality, whereas humans lacking keratin 14 display less pronounced phenotypes (Chan *et al.*, 1994; Batta *et al.*, 2000; Rugg *et al.*, 1994). This mechanical function of keratin is also suggested by heterozygous desmoplakin gene mutations in mice which lead to truncated proteins lacking keratin binding domains. These result in neonatal death, accompanied by excessive blister formation, nail loss and neonatal teeth (Jonkman *et al.*, 2005).

There is emerging evidence suggesting regulatory functions for the keratin intermediate filaments, besides the well known structural properties. Recently, it has been suggested that the control of cell size, cell proliferation and the response to stress, are dependent on the expression of certain keratins (Pallari & Eriksson, 2006; Gu & Coulombe, 2007). IFs, similar to other proteins, are regulated by associated proteins and post-translational modifications.

With regard to keratin associated proteins, several members of the 14-3-3 protein family associate reversibly with keratin 8/18 in cultured cells, in a phosphorylation dependent manner (Liao & Omary, 1996). The 14-3-3 protein family, the first member of which was identified in rabbit brain and named because of its migration in starch gels (Moore & Perez, 1967), consists of seven highly conserved proteins that regulate the subcellular distribution and activity of many proteins, mostly in a serine/threonine phosphorylation-dependent manner (Izawa & Inagaki, 2006). In response to intra- or extracellular signals, reorganisation of the keratin intermediate filaments occurs, leading to generation of IF granules and increases in the soluble pool of IF subunits. At the same time, serine phosphorylation creates binding sites for the 14-3-3 σ adapter protein, as is observed for keratin 18 (Ku *et al.*, 1998a). This binding is a requirement for cell cycle progression (Margolis *et al.*, 2006; Kim *et al.*, 2006). Recruitment of the 14-3-3 proteins to keratin 17 has been shown to regulate protein biosynthesis and cell growth via the Akt/mTOR (the mammalian target of rapamycin) signalling pathway, which plays an important role in rapid cell growth in response to injury (Kim *et al.*, 2006). Lately, another aspect of keratin function has emerged, suggesting a role in melanosome transport. Mutations residing in the head domain of keratin 5 and keratin 14 appear to be a common genetic mechanism in Dowling–Degos disease (DDD), a pigmentation defect resulting in hyperpigmented macules and papules affecting major areas of the skin (Betz *et al.*, 2006; Liao *et al.*, 2007). These mutations are also observed in EBS with mottled pigmentation (Harel *et al.*, 2006) and in Naegeli-Franceschetti-Jadassohn syndrome, a hyperpigmentation of the skin that tends to slowly disappear with age (Lugassy *et al.*, 2006). Emerging data have also shown involvement of keratin IFs in multiple kinds of stresses and apoptosis. As an example, transgenic mice overexpressing the keratin 8 G61C mutation showed induced vulnerability to stress-induced liver injury and apoptosis (Ku & Omary, 2006).

Taken together, there is evidence supporting the involvement of intermediate filaments in six broadly defined functions: structural support, cytoarchitecture, stress response, regulation of signalling pathways towards apoptosis, protein synthesis and organelle/vesicle distribution.

1.3 Cytoskeletal Linker Proteins: Plakin Family

Recently, it has become increasingly obvious that the cytoskeletal network systems are not fulfilling their roles in isolation, but are connected to each other to play dynamic roles in cell architecture and cell integrity. The proteins that interlink the cytoskeletal network systems are known as plakins (Uitto *et al.*, 1996) or cytolinkers (Wiche, 1998). Further studies have opened up this family's role and cytolinkers have been found to link to actin and microtubules in the nervous system (Yang *et al.*, 1999) and to play a role in scaffolding of signalling events (Sonnenberg & Liem, 2007).

Plakins were first identified in epithelial cells, where they tethered IFs to membrane-associated adhesive junctions, such as desmosomes and hemidesmosomes, and cell-matrix junctions (Ruhrberg & Watt, 1997). The members of this family are periplakin, envoplakin, plectin, desmoplakin, epiplakin, bullous pemphigoid antigen 1 (BPAG-1) and the microtubule-actin crosslinking factor (MACF). These proteins have been proposed to preserve the mechanical integrity of the cell in tissues that are exposed to continuous stress, such as the skin, heart and muscle, by networking intermediate filaments and linking them to their membrane attachment sites. They have also been found in the nervous system, where they appear more complex (Leung *et al.*, 2001). Each plakin protein shows a characteristic tissue-specific expression pattern and subcellular distribution, suggesting a distinct functional role for each individual protein. Plakins may have additional roles in signal transduction as they can interact with a variety of signalling molecules. Mutations in plakin family genes lead to defects in tissue integrity and function of the skin, muscle and the nervous system both in human and mouse (**Table 1.2**).

Plakins are highly conserved through evolution, with plectin-like proteins also present in cells of algae, *Chlamydomonas eugametos* (Hendrychová *et al.*, 2002). The invertebrate plakins in *Drosophila melanogaster* and *Caenorhabditis elegans* were discovered from genetic screens (Jefferson *et al.*, 2004). The *Drosophila* gene *Shortstop* (*Shot*) was identified in a screen for genes that control neuromuscular specificity (Vactor *et al.*, 1993). Subsequently, it was found to be allelic to another mutation called *Kakapo* (Lee *et al.*, 2000) which was identified in a screen to isolate genes required for integrin-mediated adhesion (Prout *et al.*, 1997; Gregory & Brown, 1998). There are three known *Shot* isoforms. *Shot I* mediates cell-

matrix adhesion, Shot II mediates lateral cell adhesion (Röper & Brown, 2003) and the third variant, Shot III, has been described in one report, but no function has yet been described (Lee *et al.*, 2000; Röper & Brown, 2003). The *C. elegans* plakin, *vab-10*, was identified in a genetic screen for embryonic morphological defects (Bosher *et al.*, 2003). *vab-10* generates protein isoforms with distinct distribution and function in the epidermis (Bosher *et al.*, 2003). These isoforms are termed VAB-10A and VAB-10B.

1.3.1 Structure of the cytolinkers

All plakin family members are built from a combination of different modules illustrated in **Figure 1.2**, which builds up a head-rod-tail structure, with a specific function for each domain (Green *et al.*, 1992). In some family members, an N-terminal calponin-type actin binding domain (ABD) (Bañuelos *et al.*, 1998) is present. This calponin-homology (CH) domain contains four α -helices connected by loops and short helices. Each domain contains approximately 10 residues and is present in signalling and cytoskeletal proteins (Stradal *et al.*, 1998; Gimona *et al.*, 2002). CH domains are subgrouped into CH1 and CH2 due to functional diversity, and are able to homodimerise and heterodimerise (Fontao *et al.*, 2001; Young *et al.*, 2003). CH1 and CH2 are responsible for actin binding in some cytolinkers. The affinity to bind actin is lower in the case of CH2 and CH1-CH2, than in CH1 alone (Winder *et al.*, 1995). The ABD is followed by a plakin domain which is proposed to contain six α -helical bundles and play a role in protein-protein interactions (Leung *et al.*, 2002; Rezniczek *et al.*, 2004; Jefferson *et al.*, 2007). These regions were named as NN, Z, Y, X, W and V (Green *et al.*, 1992). Plakins are evolutionarily related to the spectraplakins, cytoskeletal giants with characteristics of both plakins and spectrin (Röper *et al.*, 2002; Määttä *et al.*, 2004). The spectraplakins were named by Röper and colleagues in 2002, to encompass all proteins that have similarities to plakins and spectrin family proteins. This includes the *Shot* gene in *Drosophila* and the *dystonin/BPAG1* and *MACF1* genes in mammals. This relationship was confirmed after crystallography studies of both plectin and BPAG-1 (Jefferson *et al.*, 2007; Sonnenberg *et al.*, 2007). The crystal structure of the plectin N-terminus revealed the structure of the first two tandem repeats of the plakin domain. This domain is formed by two spectrin repeats (SR1, SR2) connected with a α -helix that spans between these two regions (Sonnenberg *et al.*, 2007). Although these two

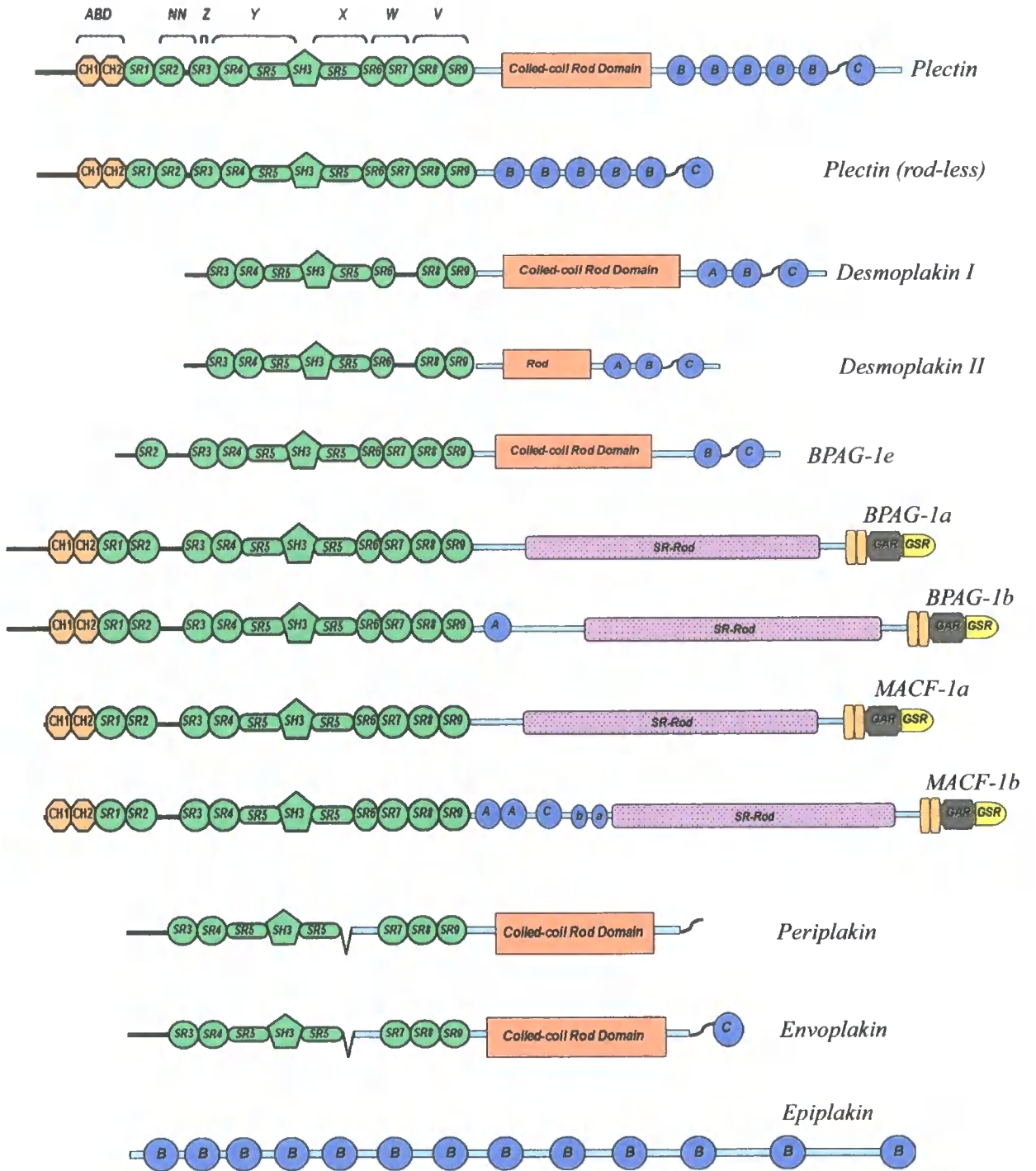
spectrin repeats are very similar, they differ in the hydrophobic core of the second repeat, which slightly alters the structure. This domain is adjacent to the ABD, suggesting that it may act as a functional unit. Sequence analysis of the plakin domain revealed further repeats, with up to eight or nine consecutive spectrin repeats. This region is organized into an array of tandem modules, with a Src-homology 3 domain (SH3) inserted in the middle of the fifth repeat (SR5) (Sonnenberg *et al.*, 2007). The centre of the protein forms a coiled coil rod-domain (CC-rod) which can adopt many different conformations, suggesting that it may give flexibility to the protein, facilitating the response to mechanical stress in muscles and skin. The coiled-coil rod domain contains heptad repeats that mediate homodimerisation or heterodimerisation. The C-terminal region harbours plakin repeat domains (PRD) with intermediate filament-binding properties that in some cases require an associated linker (L) subdomain. The plakin repeat domain comprises varying numbers of repeating unit subdomains which are termed A, B or C, depending on their degree of similarity to each other. All plakin repeat domains consist of 4.5 copies of a 38 amino acid repeat that adopts a globular structure with a unique fold (Choi *et al.*, 2002) which is important for binding to IFs (Fontao *et al.*, 2003). The flexible linker region that is present between the B and C subdomains in some cytolinkers might be required to allow these motifs to simultaneously bind to IFs (Sonnenberg *et al.*, 2007). However, in the case of periplakin, only the linker domain is able to bind the protein to IFs.

In some proteins such as BPAG-1a, BAPG-1b, MACF-1a and MACF-1b, the spectrin repeat (SR)-containing rod domain is followed by two calcium binding motifs (putative calmodulin-like EF hands), a Gas2-homology region called the GAR domain and finally a domain containing GSR (Gly-Ser-Arg) repeats. The GAR domain is thought to be required for MT binding. Other cytolinkers without a GAR domain, bind to MT through their GSR repeats (Sun *et al.*, 2001; Yang *et al.*, 1999).

N-terminus

C-terminus

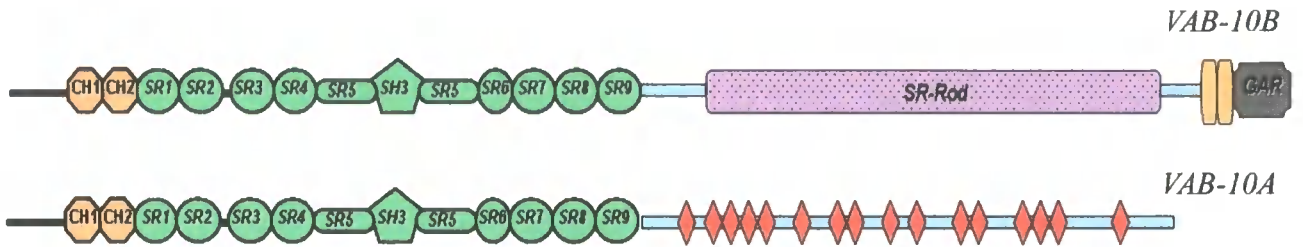
Mammalian plakins



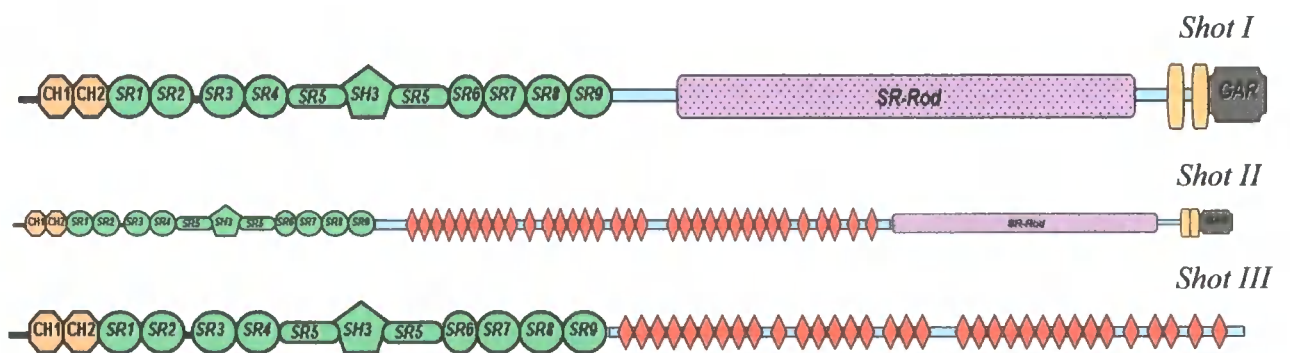
N-terminus

C-terminus

Caenorhabditis elegans plakins



Drosophila melanogaster plakins



Actin binding domain



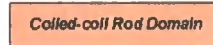
Spectrin repeats (SR1-SR9)



SH3 domain



Coiled coil domain



Plakin repeat domain (A, B, C, a,b)



Linker region



Spectrin repeat domain



EF-hands



GAR domain



GSR domain



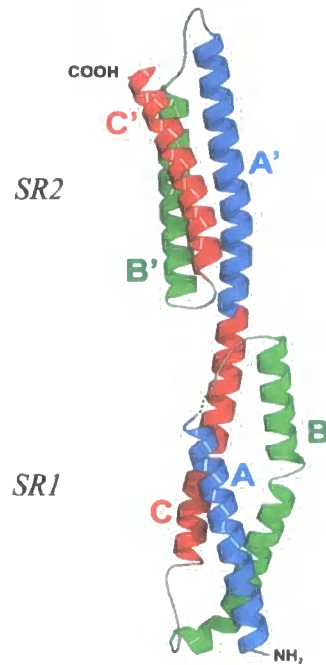
Plakin repeat



Figure 1.2: Schematic diagram of the plakin family members.

The CH actin binding domain is present in plectin, BPAG-1a/b, MACF-1a/b and in the invertebrate VAB-10A/B and Shot I/II/III proteins. Plakins (with the exception of epiplakin) also contain an N-terminal region consisting of 4-9 spectrin repeats with a central SH3 domain and a central coiled-coil rod domain. The spectrin rod domain is present in BPAG-1 and MACF-1 and the invertebrate plakins VAB-10B and Shot I/II. This is followed by a microtubule binding domain, consisting of EF hands and a Gas2 related (GAR) domain with a glycine-serine-arginine (GSR) domain. In the other plakins lacking in the microtubule binding site, there are three plakin repeat domains (PRD). These are marked as A, B and C or in case of incomplete A 'a' and B 'b' (PRD) domains. In the invertebrate plakins, there are a series of plakin repeats that are not organized into PRD. The C-terminal linker region found in the epithelial plakins plays a role in the interaction with intermediate filaments.

A.



B.

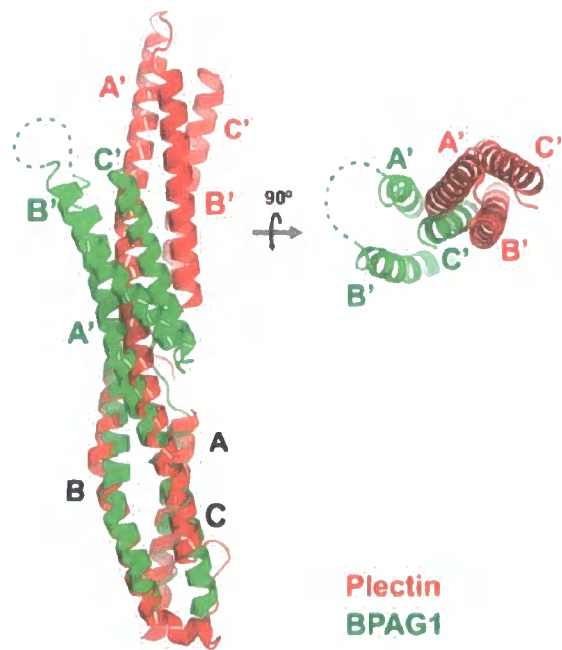


Figure 1.3: Crystal structure displaying the first tandem pair of spectrin repeats found in plectin and an overlap comparison with BPAG-1.

*A. Cartoon representation of the first two spectrin repeats in plectin. Each of them built up from three α -helices arranged in a left handed supercoil. The first bundle contains helices A, B and C, while the second bundle contains helices A', B' and C'. The first bundle referred as SR1 (Spectrin Repeats 1) and the second as SR2. Similar α -helices in each domain are presented in the same colour. **B.** Comparison, highlighting the orientation of the spectrin repeats in plectin and another cytolinker BPAG-1. Crystal structures adopted from Sonnenberg et al., 2007.*

1.3.2 Periplakin

Originally, periplakin (195kD) was identified as a precursor of the cornified cell envelope (CE) in terminally differentiated epidermal keratinocytes (Simon & Green, 1984; Ma & Sun, 1986; Ruhrberg *et al.*, 1997). Periplakin has also been found in two-layered and transitional epithelia such as the mammary gland and bladder (Ruhrberg *et al.*, 1996; Ruhrberg *et al.*, 1997; Aho *et al.*, 1998) and it is highly expressed in some non-epithelial tissues, such as in the brain (Aho *et al.*, 1998). Periplakin was also found in lens fibre cells, forming a cortical complex with ezrin, periaxin, and desmoyokin (Straub *et al.*, 2003). In both the brain and lens, the primary function of periplakin remains unclear.

1.3.2.1 Overall structure of periplakin

Figure 1.4 shows a detailed structure of periplakin in comparison with another cytolinker, plectin. Periplakin is predicted to contain a globular NH₂-terminal domain, but is distinguished from the other cytolinkers, such as plectin, as it lacks the actin-binding domain (ABD) and the first, second and sixth (SR1, SR2, SR6) spectrin repeats at the amino terminus. The domain connecting the first spectrin pair to the next pair of periplakin, approximately corresponds to the NN region of the plakin domain, the SR3 to the Z region, the first half of SR4-SR5 to the Y region, X to the SR5 region, W to the SR7 and finally V to the SR8-SR9 region (Sonnenberg *et al.*, 2007). The central rod domain mediates assembly of periplakin into parallel homodimers, or heterodimers with envoplakin (Ruhrberg & Watt, 1997; DiColandrea *et al.*, 2000). The C-terminus of periplakin also differs from other plakin proteins as it lacks any of the sequence-related subdomains. However, it does contain the α -helical linker region that connects the C-subdomain to intermediate filaments (Karashima & Watt, 2002).

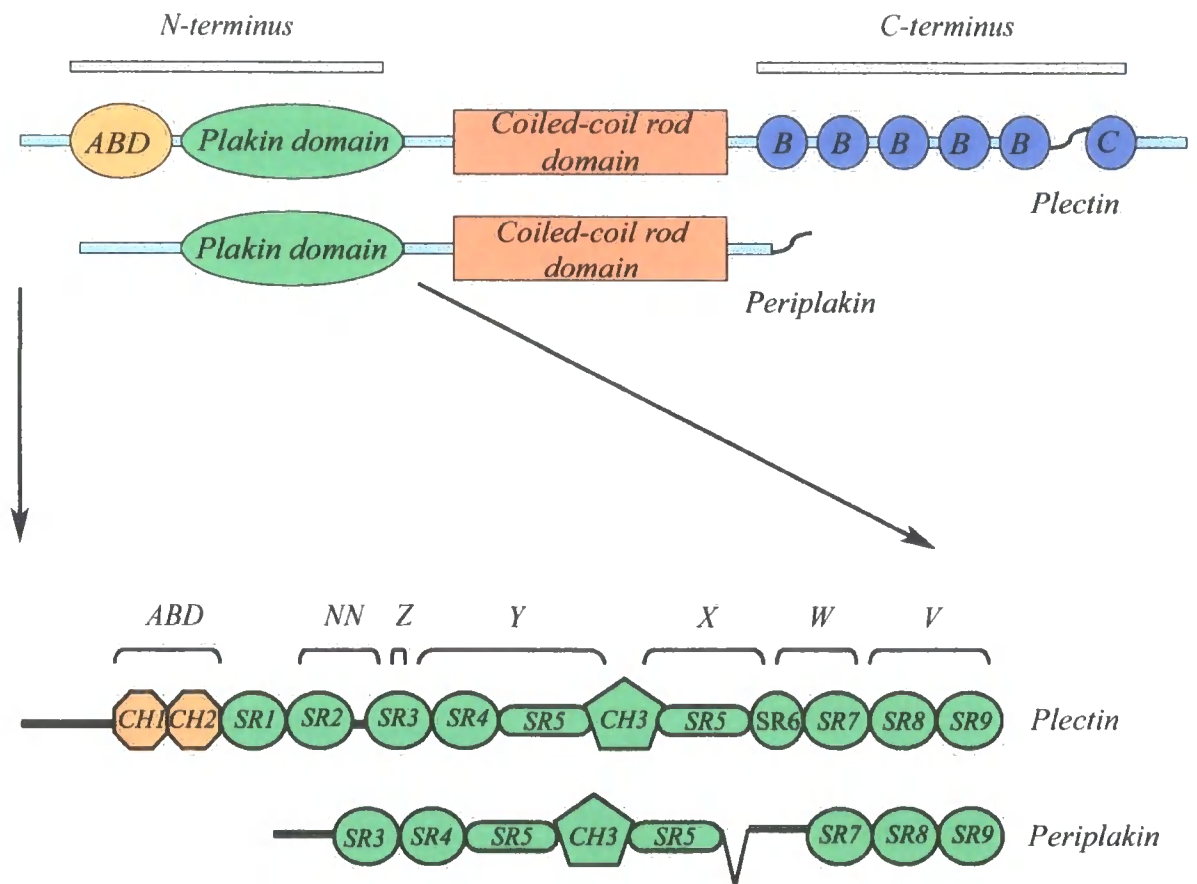


Figure 1.4: Detailed full structure of periplakin and plectin, also displaying the organization of their plakin domains.

Schematic representation of plectin and periplakin, highlighting that periplakin lacks actin binding domain along with spectrin repeats SR1, SR2 and SR6 on the amino terminus. It also lacks in all PRD (plectin repeat domain) on the C-terminus, but importantly still contains the linker domain.

1.3.2.2 Role of periplakin in cornified envelope formation

The outermost, cornified, layers of the epidermis are composed of terminally differentiated keratinocytes known as corneocytes. This specialised structure develops as a result of a complex terminal differentiation of stratified squamous epithelia (**Figure 1.5**). Corneocytes provide an insoluble protein structure that is assembled to replace the plasma membrane, functioning as a scaffold for lipid attachment. This protein and lipid structure is called the cornified cell envelope (CE) and is assembled from a great variety of precursor proteins (Jarnik *et al.*, 1998). The CE is extremely insoluble, and is composed of two major parts. The 10nm (approximately) thick protein envelope is formed by covalent cross-linking of specific structural proteins by sulphhydryl oxidases and transglutaminases (TGases) (Hohl, 1990; Polakowska *et al.*, 1991; Eckert *et al.*, 1997). TG1/3 and 5 are involved in CE formation, and these enzymes are essential for normal barrier assembly (Matsuki *et al.*, 1998). This protein layer is coated by the lipid envelope which is approximately 5nm thick, with layers of lipids that are covalently attached to the exterior of protein envelope (Wertz & Downing, 1990).

The first step in the formation of the CE takes place in the spinous layers (**Figure 1.6**) and involves the synthesis of the cornified envelope structural proteins. It is believed that the assembly of the CE is regulated and triggered by a rise in intracellular calcium concentration, coincidental with signals to initiate terminal differentiation in epithelia. As the intracellular calcium concentration rises in suprabasal cells, the level of envoplakin and periplakin is increased (Ruhrberg *et al.*, 1996; Ruhrberg *et al.*, 1997). A short time later, involucrin is expressed, which was the first described CE precursor (Rice & Green, 1977). TG1 and TG5 enzymes are expressed and crosslink envoplakin and periplakin to form stable heterodimers thereby anchoring them to the desmosomes as the calcium level rises. Then, TGs join together the plakins and involucrin by forming lysine isopeptide crosslinks (Steinert & Marekov, 1997; Nemes & Steinert, 1999) in a calcium-dependent manner. TG1 also crosslinks other membrane-associated and desmosomal proteins, which leads to changes in cell-cell connections and communication (Kee & Steinert, 2001). Gradually, the involucrin-envoplakin-periplakin protein complexes form a monomolecular layer along the whole inner surface of the cell membrane, including desmosomes, forming a “scaffold” (Kalinin *et al.*, 2001).

Loricrin and small proline-rich proteins (SPRs) together constitute the main component of the epidermal CE, and seem to function as main strengthening proteins for the CE on its cytoplasmic face (Steinert & Marekov, 1995). Although loricrin is an insoluble protein and is localized in the cytoplasm of the granular layer cells, the SPRs are very soluble. Therefore when these proteins are cross-linked, loricrin is solubilised assisting translocalisation to the cell periphery (Kalinin *et al.*, 2001). Minor amounts of other proteins, including repetin, trichohyalin, cystatin α and elafin also become crosslinked to the CE (Steinert & Marekov, 1995).

The epidermal differentiation complex (EDC) on human chromosome 1 (1q21) is enriched in genes associated with epidermal terminal differentiation (Backendorf & Hohl, 1992; Engelkamp *et al.*, 1993; Mischke *et al.*, 1996). As well as encoding single-terminal differentiation genes, the EDC also contains “clusters” of related genes, such as S100 genes, small proline-rich region (SPRR) genes, and a recently identified gene cluster, the late cornified envelope (LCE) genes (previously XP5, EIG, small proline-rich-like, late envelope protein (LEP) genes) (Zhao & Elder, 1997; Marshall *et al.*, 2001; Wang *et al.*, 2001). Analysis of LCE genes revealed that the cluster is organised into three groups, with these genes responding as a group to environmental stimuli such as calcium levels and ultraviolet (UV) light, highlighting the functional significance of these groups (Jackson *et al.*, 2005).

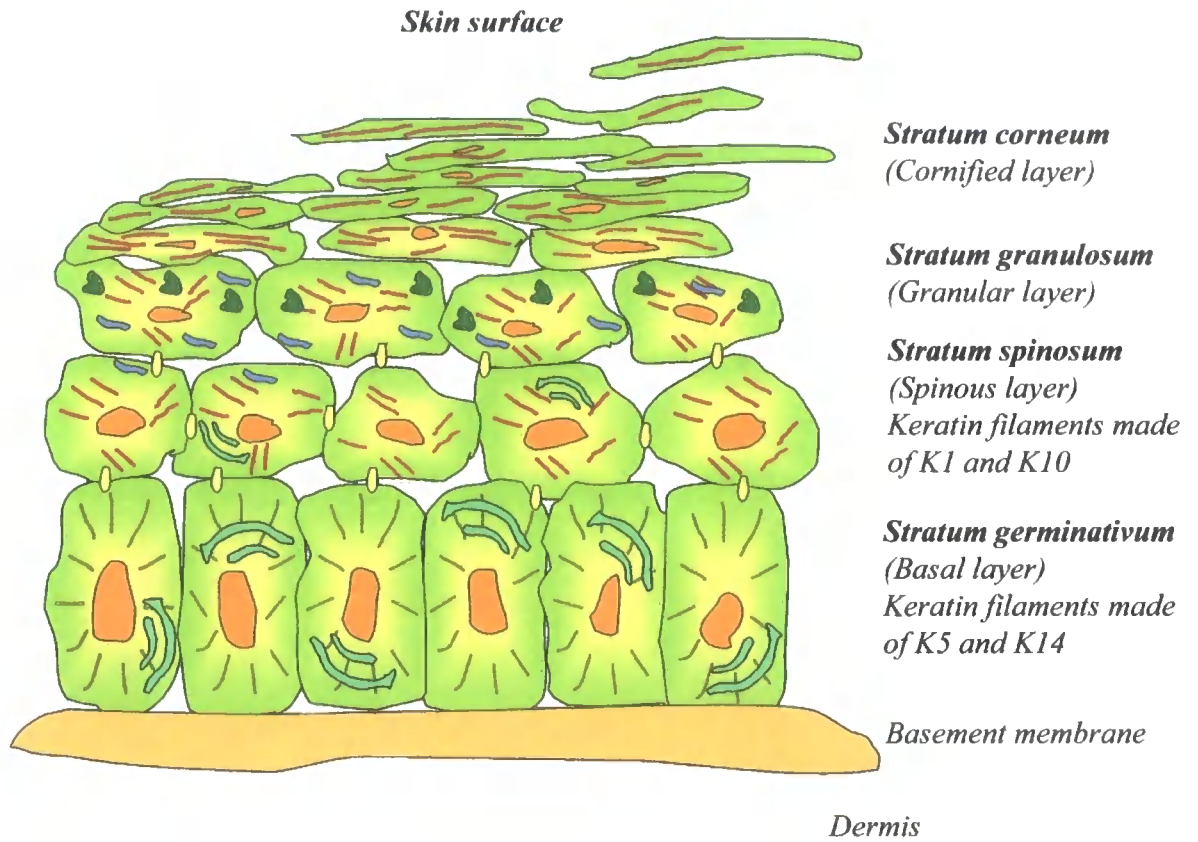
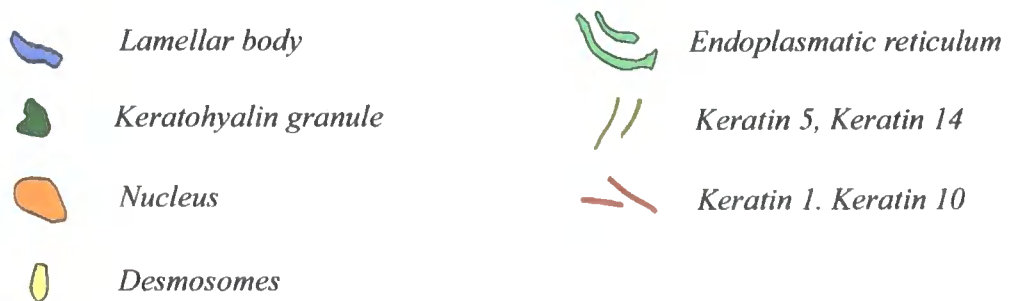


Figure 1.5: Schematic diagram of the skin structure and its terminal differentiation.

The basal layer of the epidermis consists of undifferentiated mitotically active keratinocytes that are attached to the basement membrane. In the granular layer keratinocytes detach from the basal lamina and start to undergo terminal differentiation. The cells flatten and differentiation specific proteins are expressed such as keratin 1 and keratin 10. The granular layer of the epidermis is characterized by the presence of keratohyalin granules. In the same layer organelles are disintegrated and the plasma membrane is replaced by the cornified envelope. The cornified layer consists of dead cells that shed into the environment during desquamation.



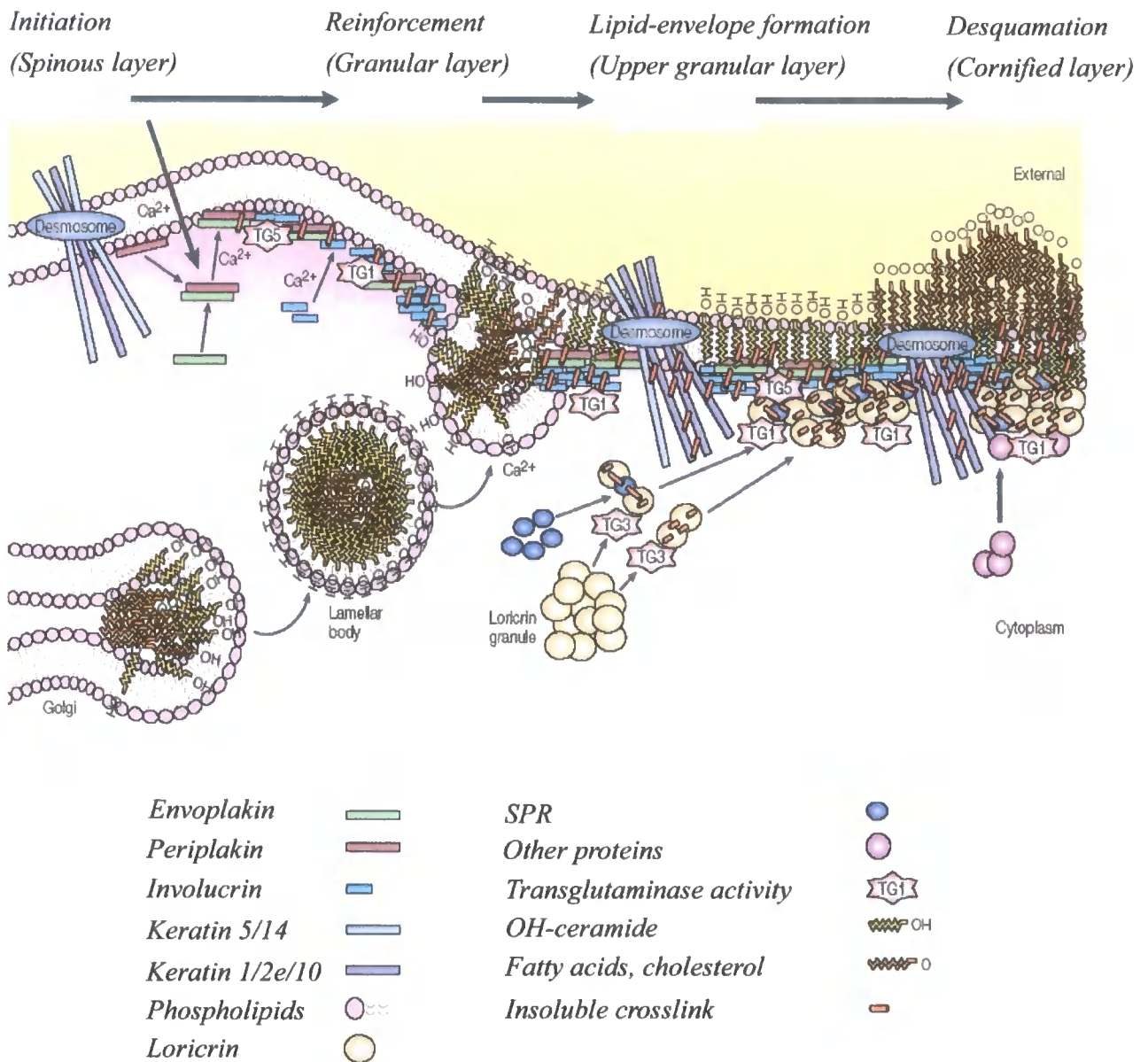


Figure 1.6: Schematic diagram detailing the formation of the cornified envelope.

As an initiation step structural proteins of the cornified envelope are synthesised in the spinous layer. Transglutaminases 1 and 5 (TG1 and TG5) crosslink periplakin and envoplakin under the cell membrane anchoring them to desmosomes. In the second step, which takes place in the granular layer, lipids are covalently attached to the cornified envelope proteins whilst loricrin and small proline rich proteins become crosslinked. In the granular layer during the formation of the lipid envelope, lipids form lamellar bodies, which are linked to the cornified proteins by TG1 and TG5. The desquamation phase in the cornified layer involves further crosslinking of loricrin and other proteins to the protein scaffold by TG1. The location of these progressive steps are presented in the figure above (Figure adapted from Candi et al., 2005).

1.3.2.3 Consequence of periplakin ablation

It has been reported that when periplakin is deleted by gene targeting in mice, there is normal epidermal barrier formation (Aho *et al.*, 2004). In line with this result, mutations in the gene encoding periplakin are not associated with genetic disease in humans. Furthermore, the loss of expression of other scaffold proteins that build up the CE, such as envoplakin and involucrin, also results in normal CE assembly and produces viable, fertile mice, suggesting that this might be achieved through compensatory mechanisms (Dijan *et al.*, 2000; Määttä *et al.*, 2001). This has been demonstrated in loricrin-deficient mice, where an increased expression of members of the SRP family and repetin are thought to compensate for the loricrin deficiency (Jarnik *et al.*, 2002). Thus, no single molecule has been found to be critical for CE integrity. Surprisingly, the lack of periplakin did not alter the expression level of other epidermal proteins such as envoplakin or involucrin (Aho *et al.*, 2004). Some studies speculate that cross-linking between periplakin and the CE is a result of a default mechanism for disposing of these proteins during terminal differentiation (Aho *et al.*, 2004). This is known as the “dust-bin” hypothesis and predicts that the composition of the CE might be determined by the availability of substrate proteins at the moment when TGs mediate cross-linking (Michel *et al.*, 1988; Regnier *et al.*, 1993). This hypothesis is supported by the observation that the breakdown of organelles during terminal differentiation correlates with the appearance of a morphologically defined CE. On the other hand, not all proteins that had been targeted for destruction (such as filaggrin and keratin1 and 10) were necessarily cross-linked to the CE (Steven & Steinert, 1994). Recently, triple knock-out mice for envoplakin, involucrin and periplakin were generated, which demonstrated delayed epidermal barrier formation during embryonic development, defects in the cornified layer and signs of hyperkeratosis postnatally (Sevilla *et al.*, 2007). Simultaneous loss of periplakin, envoplakin and involucrin also triggered an accumulation of CD3⁺, CD4⁺ T cells in the skin, and down-regulation of proteases, resulting in defective filaggrin processing (Sevilla *et al.*, 2007). Thus, envoplakin, periplakin and involucrin have been proposed to contribute to pathological human skin conditions such as ichthyosis vulgaris and atopic dermatitis (Sevilla *et al.*, 2007).

1.3.2.4 Periplakin in cancer progression

In excised tissues from patients with primary oesophageal cancer, immunoblotting revealed that periplakin was significantly downregulated in oesophageal cancer. Immunohistochemistry subsequently showed that periplakin was mainly localized at cell-cell boundaries in normal epithelium, whereas it disappeared from cell boundaries, shifting to the cytoplasm, in early cancers, and was scarcely expressed in advanced cancers. Therefore, it has been suggested that periplakin could be a useful marker for detection of early oesophageal cancer and evaluation of tumor progression (Nishimori *et al.*, 2006). Other plakins have also been implicated in cancer progression, with downregulation of desmoplakin found in poorly differentiated breast tumours (Davies *et al.*, 1999) and mutations of MACF-1 also found in breast tumours (Sjöblom *et al.*, 2006).

1.3.3 Envoplakin

Envoplakin (210kD), similarly to periplakin (195kD), was identified in a proteomic search for CE proteins in keratinocytes (Simon & Green, 1984). It was also found in terminally differentiated keratinocytes where it partially colocalised with desmoplakin at desmosomes (Ruhrberg *et al.*, 1996). Envoplakin is expressed in the suprabasal layers of stratified squamous epithelia, but not in simple epithelia or non-epithelial tissues. The structure of envoplakin is very similar to periplakin, as described above, although a PRD, called the C subdomain, exists in the envoplakin C-terminus. Envoplakin and periplakin have smaller C-terminal domains than the other plakins and they also have the potential to form heterodimers with each other (Ruhrberg *et al.*, 1997). A detailed analysis of periplakin and envoplakin revealed that the rod domains of each protein are more closely related to each other than to those of other plakins. It was suggested that the two proteins could form two-stranded, parallel homodimers or heterodimers which could be stabilized by extensive inter-chain ion pairing (Ruhrberg *et al.*, 1997). Envoplakin knockout mice do not have any obvious pathological phenotype in the skin or other epithelia and also show no evidence of epidermal fragility or blistering (Määttä *et al.*, 2001). There was only a slight delay observed in epidermal barrier

formation, which had no effect later in life. This mild effect of envoplakin loss could explain why no inherited human disease caused by envoplakin mutation has been reported to date.

1.3.4 Desmoplakin

Desmoplakin (DP) was first discovered as a protein linked to the desmosomes in isolated epidermis (Skerrow & Matoltsy, 1974). The cytoplasmic proteins of the desmosome interact with the IF-binding protein desmoplakin, which anchors stress-bearing IFs to the desmosomal plaque (Godsel *et al.*, 2004). Alternative splicing in the region of the central rod domain results in two isoforms of desmoplakin. Desmoplakin I (DPI) is a 322-kDa protein and is expressed in all tissues with desmosomes. The other isoform, desmoplakin II (DPII) weighing 259-kDa, is expressed in non-stratified tissues at low level and is absent from the heart (Green *et al.*, 1990). DPII also lacks most of the rod domain and therefore can be found as a monomer (O'Keefe *et al.*, 1989). Desmoplakin is targeted at the desmosomal inner plaque through interaction of its N-terminal plakin domain with plakoglobin and plakophilins, which then link to desmosomal cadherins (Kowalczyk *et al.*, 1997; Bornslaeger *et al.*, 2001). However, there is also evidence that desmoplakin is able to bind desmosomal cadherins directly (Smith & Fuchs, 1998; Bornslaeger *et al.*, 2001). Recently, desmoplakin was found in non-classical desmosome-related junctions in different tissues, where the junctional structure is considerably different from epithelial desmosomes. Desmoplakin (with cadherins and plakoglobin) is also a constituent of a specialized vascular and lymphatic endothelial cell junction called the “complexus adhaerens” (Borrmann *et al.*, 2006; Hämmerling *et al.*, 2006). Moreover, the composition of the intercalated disk in heart muscle revealed a specialized region of the cardiomyocyte membrane where desmoplakin is combined with cadherin components. As a result, these junctions have been reclassified as “area composita” of adhering junctions (Franke *et al.*, 2006).

1.3.4.1 Structure of desmoplakin

The study of the protein structure of desmoplakin reveals several spectrin repeats that are interrupted by a SH3 region (Röper *et al.*, 2002; Green *et al.*, 1992; Koster *et al.*, 2004). The central coiled-coil rod domain is followed by the C-terminal region with three homologous plakin repeat domains (PRDs), A, B, and C. The B and C subdomains of desmoplakin adopt a globular structure that can directly bind to the IF protein vimentin (Fontao *et al.*, 2003). Furthermore, DP-IFs interactions are regulated by phosphorylation of Ser2849 within the DP C-terminus (Fontao *et al.*, 2003; Godsel *et al.*, 2005).

1.3.4.2 Function of desmoplakin in skin, cardiac muscle and during embryogenesis

Epidermis-specific knock-out of desmoplakin in the developing mouse embryo had little effect on desmosome structure and only the interaction with IFs was affected, resulting in skin fragility (Vasioukhin *et al.*, 2001). Interestingly, in humans haplo-insufficient for desmoplakin, the recruitment of desmoplakin into desmosomes decreases (Armstrong *et al.*, 1999; Whittock *et al.*, 1999) causing blistered areas on the palms of the hands and soles of the feet (palmoplantar keratoderma). No such phenotype was observed in heterozygous desmoplakin knockout mice (Gallicano *et al.*, 1998). However, in some patients, the heterozygous phenotype did not result in skin fragility but a missense mutation on the other allele triggered the abnormalities to occur (Whittock *et al.*, 1999). This underlies the fact that a certain amount of functional desmoplakin has to be produced to maintain normal skin integrity. Desmoplakin has recently been implicated in the rearrangement of the microtubule cytoskeleton during epithelial differentiation. In the suprabasal layers of the skin of wild type mice, microtubules were concentrated at the cell junctions, whereas in desmoplakin knock-out mice, the microtubules were found to be aggregated in the cytoplasm (Lechler & Fuchs, 2007). Mutations in the desmoplakin gene are responsible for other diseases as well. A recessive homozygous mutation (7901delG) in the human desmoplakin gene produces a premature stop codon leading to a truncated desmoplakin protein missing the C domain of the tail region. This truncated desmoplakin causes a generalized striate keratoderma particularly affecting the palmoplantar epidermis, woolly hair and a dilated left ventricular cardiomyopathy (Norgett *et*

al., 2000). A lethal condition called acantholytic epidermolysis bullosa was shown to result from compound heterozygous mutations that truncate the desmoplakin C-terminus (Jonkman *et al.*, 2005). A dominant missense mutation (S299R) in desmoplakin, located in the plakoin domain, results in a form of arrhythmogenic right ventricular cardiomyopathy (AVCR) (Rampazzo *et al.*, 2002). Other missense mutations in the plakoin domain that affect both the heart and skin have also been reported (Whitlock *et al.*, 2002). These are likely to be caused by a failure of desmoplakin to bind plakoglobin, since plakoglobin mutations cause similar disorders in both humans and mice (Ruiz *et al.*, 1996; McKoy *et al.*, 2000).

Desmoplakin null mouse embryos do not survive beyond E6.5 of gestation due to the failure of the surface endoderm to resist mechanical stress (Gallicano *et al.*, 1998). Desmoplakin *-/-* embryos showed morphological abnormalities, with the endoderm of these mutant embryos mechanically fragile and the embryos significantly smaller than normal. These defects are directly related to the reduction in the number of desmosomes in developing embryos, and the few desmosomes still present were not attached to keratin IFs. Interestingly, the reduction in the numbers of desmosomes resulting from desmoplakin deletion in epidermis, was not observed in mice (Vasioukhin *et al.*, 2001). In order to overcome the early embryonic death when desmoplakin is completely absent from the embryo, tetraploid (wild-type) and diploid (mutant) morulae were aggregated. In this case, embryos develop beyond E6.5, but die after gastrulation due to major defects in heart muscle, the neuroepithelium, skin and the microvasculature (Gallicano *et al.*, 2001). Recently it was shown that desmoplakin also plays a role in formation of microvascular tubes in culture, in addition to its function to stabilizing these vessels (Zhou *et al.*, 2004).

1.3.5 Plectin

Plectin, a protein of high molecular mass (approximately 500 kDa), was first isolated from cultured cells as a major IF-associated protein (Pytela & Wiche, 1980). Additionally, a novel hemidesmosome protein named as HD1 was isolated from bovine corneal epithelial cells, and was later identified as plectin (Owaribe *et al.*, 1991; Hieda *et al.*, 1992). Plectin is widely expressed in a variety of cell types, including skin and striated muscle. Plectin play roles in cell

and tissue integrity by cross-linking between the three cytoskeletal networks and stabilising cell-matrix and cell-cell contacts (Wiche, 1998; Leung *et al.*, 2002). Plectin has an ABD consisting of calponin-homology subdomains at the N-terminus, and a plakin domain which is followed by a central rod domain. At the C-terminus, plectin harbours six plectin repeat domains (PRD), with the last two PRD joined by a linker domain which is critical for IF binding (Nikolic *et al.*, 1996).

Plectin serves as an anchorage site for IFs to the cytoplasmic domain of integrin $\alpha6\beta4$ ($\beta4$ subunit) and BPAG-2 in hemidesmosomes (Niessen *et al.*, 1997; Litjens *et al.*, 2006), mediating firm adhesion of the basal cells to the basement membrane (Jones *et al.*, 1998; Borradori & Sonnenberg, 1999). Interestingly, the integrin $\beta4$ binding site and the actin binding sites are overlapping, which might prevent plectin from binding these two proteins simultaneously, possibly explaining the absence of actin from hemidesmosomes (Geerts *et al.*, 1999; Koster *et al.*, 2003). Furthermore, plectin is present in focal adhesion contacts and stress fibres (Seifert *et al.*, 1992; Sánchez-Aparicio *et al.*, 1997), as well as being a component of desmosomes (Eger *et al.*, 1997). In other studies, plectin has also been localised to Z-discs and dense plaques of striated muscle (Wiche *et al.*, 1983; Zernig & Wiche, 1985).

1.3.5.1 Role of plectin in cytoskeletal dynamics

Another important function of plectin is to cross-link intermediate filaments to microtubules and to the actin cytoskeleton. Plectin has been shown to interact with actin, and also bundle actin filaments via dimerisation of the ABD (Fontao *et al.*, 2001). Plectin is also understood to regulate actin filament dynamics via phosphatidylinositol, 4,5-bisphosphate (PIP2) (Andrä *et al.*, 1998). Plectin is an early substrate for capsase 8, suggesting that it may play roles in reorganisation of the actin cytoskeleton during death receptor-mediated apoptosis (Stegh *et al.*, 2000). In addition, plectin is an important organiser of the IF system. Plectin-deficient keratinocytes lose proper orthogonal IF cross-linking, making them more vulnerable to stress induced IF disruption; this additionally leads to changes in cell signalling and cell migration (Osmanagic-Myers *et al.*, 2006). Similar results were observed when the interaction of plectin and integrin $\beta4$ was disturbed (Geuijen & Sonnenberg, 2002).

1.3.5.2 Plectin and signal transduction

The role of plectin in signalling pathways is beginning to be explored. It has been shown that in plectin deficient keratinocytes, Erk1/2, c-Src and PKC δ are upregulated (Osmanagic-Myers *et al.*, 2006). Mapping of the protein-protein interactions of plectin has identified binding sites for several signalling molecules, including RACK1 (receptor for activated C kinase- 1) (Osmanagic-Myers & Wiche, 2004), the non-receptor tyrosine kinase Fer (Lunter & Wiche, 2002) and the regulatory γ 1 subunit of AMP-activated protein kinase (Gregor *et al.*, 2006).

1.3.5.3 Mutations in the plectin gene

Mutations in the plectin gene result in fragility of the skin, demonstrating blister formation. These blistering disorders belong to the spectrum of epidermolysis bullosa (EB) phenotypes, and three distinct variants have been identified. Plectin-deficient mice exhibit severe skin blistering and abnormalities in skeletal heart and muscle, in association with a reduction in hemidesmosomes (Andrä *et al.*, 1997). Mutations in human *PLEC1* result in defects in, or loss of, plectin protein and cause autosomal recessive epidermolysis bullosa with muscular dystrophy (EBS-MD) (McLean *et al.*, 1996). The majority of patients carry nonsense mutations in the rod-domain-encoding exon, leading to premature termination of translation and loss of expression of the full-length plectin. In these cases, hemidesmosomes are still formed, but their anchorage to IFs is impaired. As a consequence, blister formation occurs (Sonnenberg & Liem, 2007). A rod-less variant of plectin has been described which, in a similar manner to full length plectin, is widely expressed in cells and tissues including keratinocytes and muscle (Elliott *et al.*, 1997; Koster *et al.*, 2004). This particular variant of the plectin is believed to play an important function, and to compensate for the loss of the full-length plectin in EBS-MD patients. The lack of both plectin variants results in a more severe phenotype and patients die shortly after birth (Charlesworth *et al.*, 2003). Plectin mutations at the end of the coiled-coiled rod domain have also been found in patients with EB simplex of the Oagna type, which is a rare autosomal disorder leading to skin changes in the absence of muscular symptoms (Koss-Harnes *et al.*, 2002). Recent studies have reported plectin mutations

in patients with EB with pyloric atresia, an autosomal recessive syndrome which is frequently lethal (Pfundner & Uitto, 2005).

1.3.5.4 Plectin isoforms

Alternative splicing provides a mechanism for generating transcript diversity. Mouse plectin resides on chromosome 15 and extensive analysis has shown that it contains over 40 exons and exhibits an unusual complexity of 5' isoforms (Fuchs *et al.*, 1999; Rezniczek *et al.*, 2003). The mouse plectin gene is organized into variable and constant regions (**Figure 1.7**). Each variable exon is separately spliced to the first constant exon to generate diverse plectin mRNAs. However, not all variable exons are coding and the variable exons of the plectin gene do not display sequence similarity to each other (Zhang *et al.*, 2004). 16 mouse plectin isoforms have been identified, of which 11 (1-1j) are spliced onto a common exon two. In addition, two short alternative exons were found for both the 2nd and 3rd exons (2 α and 3 α), increasing the diversity in the region of the gene that encodes the calponin homology ABD (exons 2-8). Finally, three non coding exons (named exons -1, 0a, and 0), that are located 5' to the first coding exons, 1c, were identified (Fuchs *et al.*, 1999). In humans, the plectin gene spans over 32 exons located at the telomeric region of chromosome 8 (McLean *et al.*, 1996). Bioinformatics searches identified eight putative first exons in the human plectin gene, corresponding to the previously identified mouse exons (Zhang *et al.*, 2004). In the last year, an additional human plectin N-terminal isoform, that was named plectin 1-k, was discovered in our research group by Dr. Lorna McInroy (unpublished data). Notably, all plectin isoforms discovered so far have been found to contain alternative exons at the 5' end of the gene, with only the rod-less form being an exception (Elliott *et al.*, 1997).

This large versatility in plectin splicing allows for distinct isoforms to be expressed in different cell types and tissues. Plectin-1 is the major isoform expressed in tissues of mesenchymal origin (Fuchs *et al.*, 1999). It has been shown that plectin-1 and plectin 1-f can associate with the sarcolemma, whereas plectin-1d localises exclusively to Z-disc (Rezniczek *et al.*, 2007). In epidermal keratinocytes, isoforms 1-a and 1-c were shown to interact with integrin β 4 (Litjens *et al.*, 2003). In contrast to plectin-null mice (lacking all plectin isoforms),

which die shortly after birth because of severe skin blistering, plectin isoform-1 deficient mice were viable at birth, had a normal lifespan, and did not display the skin blistering phenotype (Abrahamsberg *et al.*, 2005). However, dermal fibroblasts isolated from plectin 1-deficient mice exhibited abnormalities in their actin cytoskeleton and impaired migration potential (Abrahamsberg *et al.*, 2005). Similarly, plectin-1 deficient T cells isolated from lymph nodes showed diminished chemotactic migration *in vitro*. Most strikingly, leukocyte infiltration during wound healing was reduced in the plectin-1 mutant mice (Abrahamsberg *et al.*, 2005). These data show a specific role for a specific plectin isoform in immune cell motility. It has been suggested that N-terminal sequences can determine the interaction of plectin with other structures of the cell. For example, the plectin-1b isoform is found mostly associated to the mitochondria, providing a connection of these organelles to IFs (Rezniczek *et al.*, 2003). The N-terminal domain also contains sequences important for regulating the binding activity of plectin-ABD. Indeed, deletion of the N-terminal sequences increased the affinity of ADB for integrin $\beta 4$ in hemidesmosomes, whilst decreasing the actin contacts in focal adhesions (Litjens *et al.*, 2003). Plectin-1a is the major epithelial isoform and most likely responsible for the skin blistering observed in EBS-MD, as in transient transfection experiments, expression of full length plectin-1a rescued the hemidesmosomal defects in plectin $-/-$ keratinocytes (Andrä *et al.*, 2003).

Mouse plectin gene

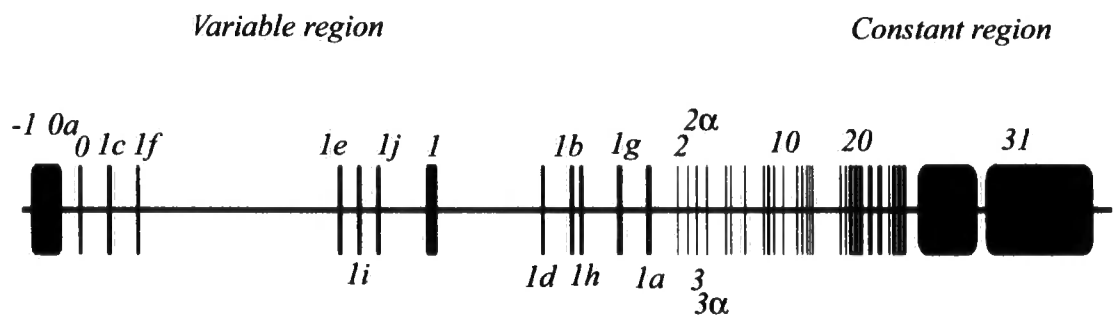


Figure 1.7: Genomic organisation of the mouse plectin gene.

The gene contains an array of multiple first exons in the variable region, each of these is separately spliced into a common set of downstream constant exons. The -1, 0a and 0 regions are non coding exons. The first coding exon in the murin plectin gene is exon 1c. 11 plectin isoforms (1-1j) are spliced into a common exon 2, which with exon 3 also contain alternative coding exons (2 α , 3 α) increasing the variety of plectin isoforms. (This figure was plotted according to a similar diagram from Fuchs et al., 1999 and Zhang et al., 2004).

1.3.6 Bullous pemphigoid antigen 1 (BPAG-1)

There are three different isoform-specific variants of the BPAG-1 gene. Interestingly these isoforms have specific expression patterns in various tissues, which may indicate distinct functions. The epithelial form of BPAG-1 (BPAG-1e) was identified, with BPAG-2, in hemidesmosomes of patients with the skin blistering disease Bullous Pemphigoid (Stanley *et al.*, 1988). BPAG-1e is expressed in basal epithelial cells, localizing close to hemidesmosomes (Leung *et al.*, 2002). Along with plectin, BPAG-1e is positioned in the inner cytoplasmic plaque and links keratin intermediate filaments to hemidesmosomes by the interactions of $\beta 4$ integrin and BPAG-2. The structure of the epithelial isoform is similar to that of desmoplakin, consisting of a plakin domain followed by a coiled-coil rod domain and two sets of PRDs at the C-terminus. This C-terminus interacts with cytoplasmic IFs, whilst the plakin domain is responsible for mediating the localization of this protein to the hemidesmosomal plaque (Koster *et al.*, 2004). BPAG-1a is a huge protein of approximately 600 kDa in molecular weight, and is expressed in the nervous system (Leung *et al.*, 2001). It has all the properties of the spectrin family, and it is likely that they are evolutionary related (Röper *et al.*, 2002). BPAG-1a has also been reported to directly interact with dynactin, a member of the dynein complex, and retrolinkin, via its structurally and functionally unique ezrin/radixin/moesin (ERM) domain. Disruption of their associations results in defects in retrograde axonal transport (Liu *et al.*, 2003; Liu *et al.*, 2007). BPAG-1b is the predominant isoform (800 kDa) in muscle cells (Lin *et al.*, 2005), but it is also expressed in the heart, bone and cartilage of developing mouse embryos (Leung *et al.*, 2001).

1.3.6.1 Mutations in the BPAG-1 gene

Over 40 years ago, a spontaneous mouse mutant, *dystonia muscolorum* (*dt*) was characterized as a heritable neuropathy that primarily affects sensory neurons and results in death at 3-5 weeks of age (Duchen *et al.*, 1964). In 1995, two reports (Guo *et al.*, 1995; Brown *et al.*, 1995) described the gene affected in *dt* mice as being an orthologue of BPAG-1. BPAG1^{-/-} mice show obvious degeneration of sensory neurons and also have muscular weakness with instability of the cytoarchitecture of mature muscles (Bernier *et al.*, 1995; Dalpé *et al.*, 1998; Dalpé *et al.*, 1999). One case study reports the disruption of BPAG-1a and BPAG-

1b in a girl with a chromosome 6;15 translocation, resulting in encephalopathy with motor and mental retardation and delayed visual maturation (Giorda *et al.*, 2004). BPAG-1 has also been identified as a component in the “disrupted in schizophrenia 1” (Disc1) interactome (Camargo L *et al.*, 2007). Accordingly, it is possible that BPAG-1 has other, as yet unidentified, functions.

1.3.7 Microtubule-Actin Cross-linking Factor 1 (MACF-1)

MACF-1 was first isolated in a screen for members of the actin cross-linking family. The full length murine ACF1 cDNA, called MACF-1, encodes a protein with a molecular weight of 600 kDa (Sun *et al.*, 1999). The human cDNA was cloned by two different groups and called trabeculin and macrophin (Okuda *et al.*, 1999; Sun *et al.*, 1999). MACF-1 is expressed in mouse embryos, with the highest levels in the nervous system, followed by skeletal muscles and the myocardium (Leung *et al.*, 1999). In keratinocytes, MACF-1 colocalises with microtubules and actin at the cell periphery and relocates to sites of cell–cell contact upon stimulation (Karakesisoglou *et al.*, 2000). MACF-1a is similar to BPAG-1a, whereas MACF-1b is similar to BPAG-1b (Lin *et al.*, 2005). MACF-1a has the same domain structure as BPAG-1a and they are expressed in the same tissues, except that the latter is more abundant in dorsal root ganglia. MACF-1b has a more complicated PRD region than BPAG-1b, comprising three full and two partial PRDs. Interestingly, this isoform has been shown to interact with the Golgi apparatus (Lin *et al.*, 2005).

MACF-1 null mice die shortly after gastrulation, with embryos with defects in the formation of the primitive streak, node and mesoderm similar to Wnt3a null embryos (Chen *et al.*, 2006). These results suggest a role for MACF-1 downstream of Wnt signalling. No human disease has yet been reported to be linked to mutations in MACF-1. Both BPAG-1 and MACF-1 have been identified as part of the Disc1 interactome, interacting with Disc1 and Dysbindin, another gene product that has been implicated in schizophrenia (Camargo L *et al.*, 2007). In a recent screen of breast and colorectal cancers, MACF-1 appeared to be mutated in 12% of the breast cancer tumors, although its function still needs to be identified (Sjöblom *et al.*, 2006).

1.3.8 Epiplakin

Epiplakin was initially identified as an autoantigen in a patient suffering from a skin blistering disease. It is believed to play a role in bundling keratin intermediate filaments (Fujiwara *et al.*, 2001; Spazierer *et al.*, 2003). This particular protein contains only plakin repeat domains and the last six domains are almost identical. It is encoded by a single large exon and expressed widely in a variety of tissues, with higher levels in the epidermis, liver, salivary gland and the digestive tract. Epiplakin RNAi knockdown in simple epithelial cells resulted in IF disruption, although this was not seen in epidermal cells (Jang *et al.*, 2005). However, epiplakin knockout mice had no obvious defects, except that their keratinocytes showed accelerated migration in culture (Goto *et al.*, 2006; Spazierer *et al.*, 2006). Recently, it has been revealed that epiplakin plays a role in keratin filament reorganization in response to stress, probably by protecting keratin filaments against disruption in a chaperone-like fashion (Spazierer *et al.*, 2008).

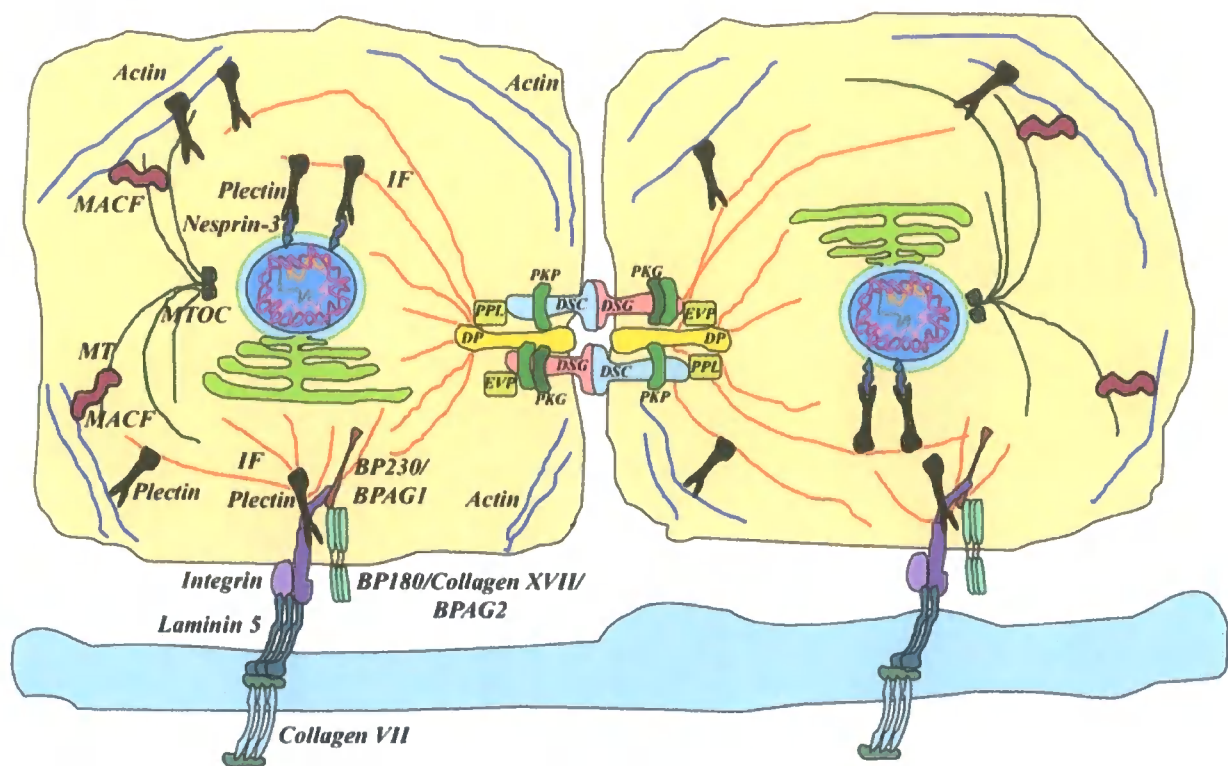


Figure 1.8: Schematic diagram detailing the interaction of plakins in epithelial cells.

Plectin and BPAG-1e are present in hemidesmosomes, where they attach to the $\alpha 6 \beta 4$ integrin and BPAG-2 mediating anchorage of intermediate filaments to the plasma membrane. Plectin is also involved in linking intermediate filaments to the nuclear envelope via nesprin-3, also interconnecting actin filaments with intermediate filaments and microtubules. MACF-1 interacts with both actin filaments and microtubules, binding them together in the cytoplasm. Desmoplakin is involved in the anchorage of intermediate filaments to the desmosomes, where it binds to plakoglobin and plakophilins, which in turn interact with the desmosomal cadherins. Periplakin and envoplakin colocalise with desmosomes rising the possibility that they are involved in anchoring keratin filaments to desmosomes.

Table 1.2: Summary of mammalian cytolinkers and their related diseases in humans and in mice.






Plakin	Human disease	Phenotype of knock-out mice
<p>Desmoplakin</p>	<p><u>Autoimmune diseases:</u></p> <p>Paraneoplastic pemphigus</p> <p>Erythema multiforme</p> <p><u>Genetic diseases:</u></p> <p>Striate palmoplantar keratoderma</p> <p>Arrhythmogenic right ventricular cardiomyopathy</p>	<p>Embryonic lethal at egg cylinder stage (Gallicano <i>et al.</i>, 1998)</p>
<p>Plectin</p>	<p><u>Autoimmune diseases:</u></p> <p>Paraneoplastic pemphigus</p> <p>Bullous pemphigoid</p> <p><u>Genetic diseases:</u></p> <p>Epidermolysis bullosa simplex with muscular dystrophy</p> <p>Epidermolysis bullosa with pyloric atresia</p> <p>Epidermolysis simplex Ogna variant</p>	<p>Lethal at postnatal day 2-3, skin blistering, skeletal and cardiac abnormalities (Andrä <i>et al.</i>, 1997)</p>

<p>BPAG1</p>	<p><u>Autoimmune diseases:</u></p> <p>Bullous pemphigoid Paraneoplastic pemphigus</p> <p><u>Genetic diseases:</u></p> <p>Single case of patient with 6;15 chromosome translocation resulting in encephalopathy, severe motor and mental retardation and delayed visual maturation</p>	<p>Lethal at 4-5 weeks after birth, sensory neuron degeneration, skin blistering upon mechanical trauma (Brown <i>et al.</i>, 1995; Guo <i>et al.</i>, 1995)</p>
<p>MACF-1</p>	<p>None reported</p>	<p>Lethal at gastrulation (Chen <i>et al.</i>, 2006)</p>
<p>Envoplakin</p>	<p><u>Autoimmune diseases:</u></p> <p>Paraneoplastic pemphigus pemphigus foliaceus</p>	<p>Subtle phenotypes, slight delay in epidermal barrier formation (Määttä <i>et al.</i>, 2001)</p>
<p>Periplakin</p>	<p><u>Autoimmune diseases:</u></p> <p>Paraneoplastic pemphigus Pemphigus foliaceus Pemphigus vegetans Neumann type</p>	<p>No discernible phenotype (Aho <i>et al.</i>, 2004)</p>
<p>Epiplakin</p>	<p><u>Autoimmune diseases:</u></p> <p>Subepidermal blistering disease</p>	<p>No discernible phenotype (Goto <i>et al.</i>, 2006; Spazierer <i>et al.</i>, 2006)</p>

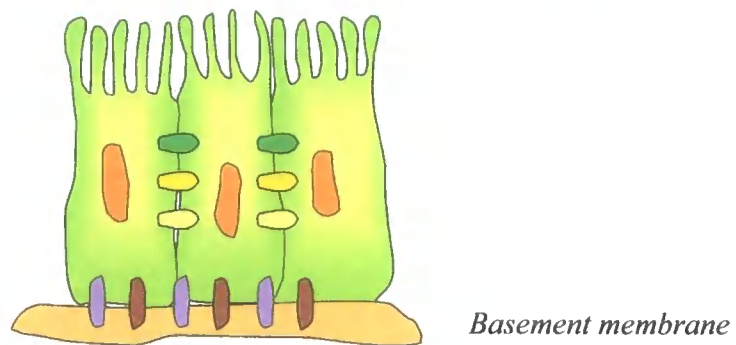
Table 1.2: Summary of mammalian cytollinkers and their related diseases in humans and in mice. Adapted from (Leung *et al.*, 2002; Sonnenberg & Liem, 2007) and (Uitto *et al.*, 2007).

1.4 Epithelial cell junctions.

Epithelia, found in multi-cellular organisms, are cohesive sheets of ordered epithelial cells (Perez-Moreno *et al.*, 2003). The main types are the stratified epithelia of the skin, simple epithelia, transitional epithelia and pseudostratified epithelia. Cell adhesion is very important for the assembly of individual cells into a three-dimensional tissue. In order to function as a tissue, epithelial cells must have the correct shape and structure to pack together with their neighbours. In simple epithelia, such as the lining of the intestine or the kidney tubule, the cells have two surfaces with different adhesive structures. The lateral surface is specialized for adhesion to adjacent cells, whilst the basal surface strengthens the connection with the underlying matrix (**Figure 1.9 A**). In stratified epithelia like the epidermis, the basal cells adhere to the basement membrane below, to each other laterally, and to the suprabasal cells apically. The suprabasal cells, however, lose their connection to the matrix and instead adhere to similar cells on all sides, until they reach the cornified layer of the skin and eventually slough off (**Figure 1.9 B**). These junctions, and the cytoskeletal network systems, contribute to the distinct shape, polarity and cellular movements of developing tissue.

-  Tight junction
-  Adherens junction
-  Desmosome
-  Hemidesmosome
-  Focal adhesion

A. Simple epithelia



B. Stratified epithelia

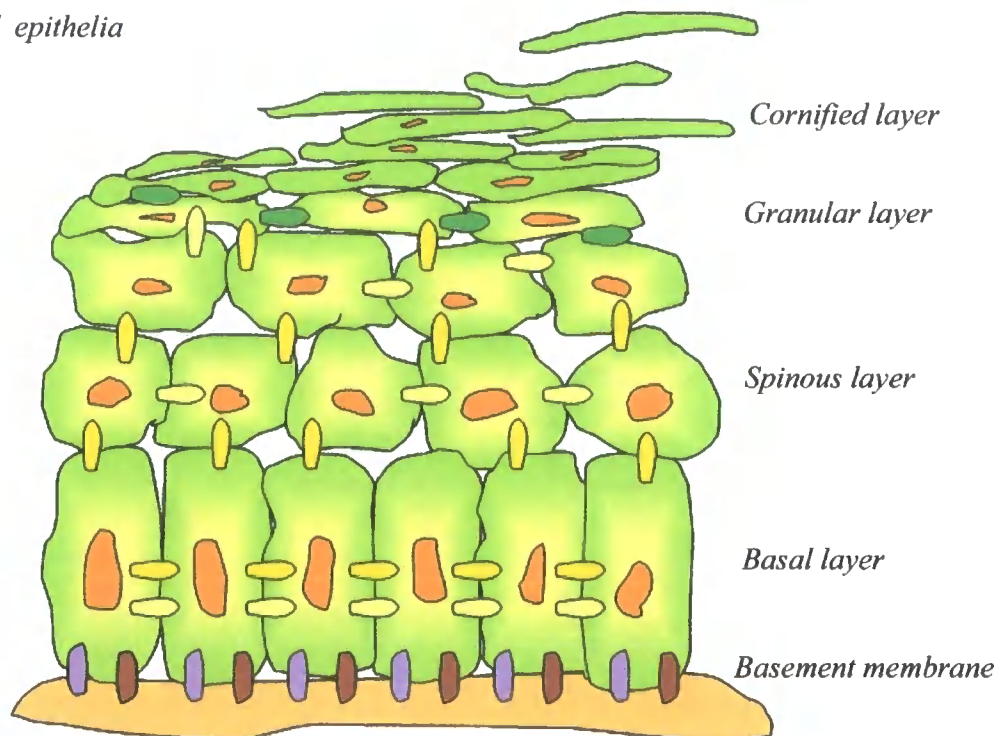


Figure 1.9: Schematic diagram detailing the organization of simple and stratified epithelia.

A. Simple epithelia containing only one cell layer anchored to the basal lamina by hemidesmosomes and focal adhesions. Adjacent cells are linked together via adherens junctions and desmosomes. Cell polarity is maintained by tight junctions. *B. Stratified epithelia* is made up from four distinct layers. Neighbouring cells are attached together via desmosomes and adherens junctions in the basal and spinous layer. In the upper part of the stratum spinosum and stratum granulosum, tight junctions appear and hold cells together. Hemidesmosomes and focal adhesions anchor keratinocytes to the stratum basale. (The diagram above is based on a similar figure published by Perez-Moreno et al., 2003)

1.4.1 Cell-Cell junctions

There are four types of cell-cell junction found in epithelial layers: tight junctions, adherens junctions, gap junctions and desmosomes, which together constitute the Intracellular Junctional Complex (IJC) (**Figure 1.10 A**). This linkage of cell–cell junctions to the cytoskeleton allows adjacent cells to function as coupled tissue. Adhesion complexes can be connected through intermediate filaments at desmosomes, or through microfilaments at adherens junctions and tight junctions (Braga, 2002).

1.4.1.1 Tight junctions

In epithelial and endothelial cells, tight junctions are the most apical intercellular junctions that function as a selective (semi-permeable) size- and ion-specific diffusion barrier between individual cells (Anderson *et al.*, 2004). They also maintain different concentrations of ions, solutes, proteins and lipids between the apical and basolateral plasma membrane domains. Furthermore, tight junctions regulate the growth and differentiation of epithelial and endothelial cells. (Balda & Matter, 1998; Tsukita *et al.*, 1999). The tight junction is identified as a belt-like structure in which two lipid-apposing membranes lie close together (tight junction strands), with the tight junction strands of adjacent cells forming tightly connected pairs. The proteins involved in the formation of tight junctions are divided into two categories: 1) integral membrane proteins, such as occludin, claudin and junctional adhesion molecule (JAM); and 2) peripheral membrane proteins (cytoplasmic plaque proteins) and MAGUK (membrane-associated guanylate kinase) homologue proteins, such as ZO-1, 2, 3, cingulin and symplekin (**Figure 1.10 B**). Moreover, various signalling proteins, including protein kinases, heterotrimeric G-proteins and small GTP-binding proteins, are either localized at the cytoplasmic plaque domain of the tight junction, or they have a central role in the assembly or function of the junction (Tsukita *et al.*, 2001). Tight junctions are crucial for proper barrier function in mammalian skin, with deficiency of claudin-1 resulting in water loss and ultimately neonatal death in mice (Furuse *et al.*, 2002). It is also recognized that the variety in strength, size and ion specificity of tight junctions in different epithelia is largely due to the different

type of claudins present in specific tight junctions (Anderson *et al.*, 2004; Furuse & Tsukita, 2006).

1.4.1.2 Adherens junctions

In epithelial cells, cadherin-based cell-cell contacts are specialised regions of the plasma membrane, where cadherin molecules of the adjacent cells interact in a homophilic calcium-dependent manner. In tissues, the establishment of strong adhesion or contractility is dependent on the assembly of adherens junction. In epithelial cells, the apico-lateral belt of adherens junctions strengthens adhesion by linking the actin cytoskeleton to sites of strong adhesion. Actin filaments are associated with adherens junctions through catenins located at the adherens junction (Geiger & Ginsberg, 1991; Rimm *et al.*, 1995; Takeichi, 1995). Classical cadherins have an extracellular part consisting of five distinct domains and a conserved cytoplasmic domain. This extracellular region interacts, homotypically, with cadherins of neighbouring cells. E-cadherin is the best described member of the family that is expressed in epithelia. It mediates the assembly of adherens junctions and affects the formation of desmosomes and tight junctions (Gumbiner, 1988; Wheelock & Jensen, 1992). It has been demonstrated that E-cadherin, through its transmembrane domain, is able to bind directly to a special catenin, called p120 catenin (Reynolds *et al.*, 1994; Yap *et al.*, 1998; Thoreson *et al.*, 2000), which was originally characterised as a substrate of v-Src kinase (Reynolds *et al.*, 1992). The cytoplasmic tail of E-cadherin is linked to the actin cytoskeleton through many peripheral membrane proteins, including α -catenin, β -catenin, vinculin, and α -actinin, which strengthen the cell-cell adhesion activity of E-cadherin (Nagafuchi, 2001) (**Figure 1.10 C**). The absence of E-cadherin weakens intercellular adhesion by affecting other junctional proteins, and loss of its expression or function is associated with tumor cell invasion in epithelial cancers (Birchmeier & Behrens, 1994). However, the function of cadherins is not limited to formation of protein complexes inside cells, or to linkage of the cells, but also includes regulation of signalling events during differentiation, proliferation and migration (Knudsen *et al.*, 1998). Besides the typical cadherin-catenin complex, there is also another intracellular adhesion unit in adherens junctions consisting of a complex of nectin and afadin. Nectin, is a Ca^{2+} -independent immunoglobulin (Ig)-like adhesion receptor, whereas afadin is a

nectin- and actin filament binding protein that connects nectin to the actin cytoskeleton (Takai & Nakanishi, 2003). Evidence has accumulated that the trans-interactions of nectins recruit cadherins to the nectin-based adhesion unit, resulting in formation of adherens junctions in epithelial cells and fibroblasts, and in formation of synapses in neurons (Takai & Nakanishi, 2003).

D. melanogaster lacks the genes that encode cytoplasmic IFs, which indicates that the invertebrate spectraplakins protein Shot, also mediates functions that are unrelated to IF binding (Röper & Brown, 2003). The largest isoform of Shot (Shot II), containing plakin repeats at internal sites, is localised to adherens junctions in the embryonic epithelia of *Drosophila*, and in the epithelial cells that surround the developing oocyte. Loss of this Shot isoform leads to tears in the epidermis which indicates that this isoform is required in actin filament-associated lateral cell junctions to maintain cell adhesion (Röper & Brown, 2003). It has also been suggested that if the plakin repeats are localised at internal sites of the plakin proteins, the protein has alternative binding partners (Röper & Brown, 2003).

1.4.1.3 Desmosomes

Desmosomes are specialized junctional structures that are important in tissue architecture as they connect intermediate filaments to adjacent cells providing a continuous network throughout tissues (Green *et al.*, 1990). They function as cell-cell attachment sites in epithelia, cardiac muscle, and dendritic cells of the lymphoid system. The particular type of intermediate filaments attached to the desmosomes depends on the cell type, with keratin filaments in most epithelial cells and desmin filaments in heart muscle cells. The complex desmosomal structure consists of several transmembrane adhesive glycoproteins and cytoplasmic plaque proteins (Garrod, 1993). The glycoproteins, such as desmogleins (Dsg) and desmocollins (Dsc), belong to the cadherin superfamily and form an adhesive interface (Garrod *et al.*, 2002), although the precise manner in which they mediate adhesion remains elusive. In simple epithelia, only the Dsg2 and Dsc2 pair are expressed, whereas in stratified epithelia such as the epidermis, Dsg1/3 and Dsc1/3 are expressed in the upper granular layer, with low levels of Dsg2 and Dsc2 in the basal layers (North *et al.*, 1996; Shimizu *et al.*, 1995; Nuber *et al.*, 1996). It has been proposed

that the ratios of desmosomal cadherins and their specific differentiation patterns may regulate epidermal development and differentiation (Garrod, 1996; Ishii & Green, 2001).

The cytoplasmic tails of desmosomal cadherins interact with plakoglobins and plakophilins (Schmidt & Jäger, 2005). These cytoplasmic plaque proteins interact with plakin proteins such as desmoplakin I and II (Godsel *et al.*, 2005) and cell envelope proteins including envoplakin, periplakin and plectin, which links the IF at the desmosomal plaque (Leung *et al.*, 2002) (**Figure 1.10 D**). Although desmoplakin is the main candidate for mediating the IF linkage in stratified cells, it is suggested that plectin might participate in this linkage in simple epithelial cells (Eger *et al.*, 1997), as *in vitro* binding studies revealed interaction between plectin and desmoplakin in MDCK cells.

In the suprabasal cornified layers of the skin, desmosomes are modified and referred to as corneodesmosomes. These structures include a secreted glycoprotein corneodesmosin (Jonca *et al.*, 2002). These modified desmosomal junctions are proteolytically degraded as the desmosomes lose their cytoplasmic plaque in the top layer of the epidermis to allow desquamation (Serre *et al.*, 1991). Plakin family members, armadillo family members and desmosomal plaque proteins might have a role in modifying desmosomes during differentiation in different tissues or histological layers (Hatzfeld, 1999; DiColandrea *et al.*, 2000; Getsios *et al.*, 2004). Normally, corneodesmosomes are degraded in the lower stratum corneum, however in epidermis lacking periplakin, envoplakin and involucrin, these structures are present in the outer cornified layers which is a sign of defective desquamation (Sevilla *et al.*, 2007).

The crucial importance of desmosomes during embryogenesis, and in the adult, is highlighted by defects in the skin, hair and heart in animal models and human patients with mutations in desmosomal proteins (McGrath, 2005). Mutations in genes encoding transmembrane proteins and desmosomal plaque proteins that anchor the IF cytoskeleton, lead to many different phenotypes. Ablation of desmoplakin in the heart, or the lack of plakoglobin and plakophilin leads to animals with cardiac abnormalities and early embryonic lethality (Bierkamp *et al.*, 1996; Ruiz *et al.*, 1996; Grossmann *et al.*, 2004). Plakoglobin (γ -catenin) null embryos survived until birth but skin fragility was observed (Bierkamp *et al.*, 1996). Desmosomal cadherin mutations, for example in desmoglein 1 gene which displays limited expression in stratified epithelia, have restricted phenotypes that include skin fragility and skin

barrier defects (Hunt *et al.*, 2001). Changing the Dsg3 to Dsg1 ratio in transgenic epidermis, so that it is similar to what is observed in mucous membranes, results in an epidermal stratum corneum that histologically and ultrastructurally resembles the stratum corneum of mucosal epithelia (Elias & Feingold, 2001). This observation supports an idea that was originally proposed by Garrod (1996), that the tightly regulated expression profile of desmosomal cadherins might be essential for proper patterning of the stratified tissues (Garrod *et al.*, 1996). Dsg4 is mainly localised in the granular layer of the epidermis and in hair follicles (Kljuic *et al.*, 2003), with a possible role in morphogenesis of the hair follicle. Ablation of Dsg2 (which is expressed early in embryogenesis and throughout epithelial tissues) suggests a desmosome-independent function during early development and embryonic stem cell proliferation. Thus, it is needed for early embryonic survival (Eshkind *et al.*, 2002). Surprisingly, Dsc3, which is prominently present in the lower layers of stratified epithelia, has been proposed to operate independently from desmosomes, as Dsc3 null embryos die in the first two days of pre-implantation development, before desmosomes appear (Den *et al.*, 2006).

1.4.1.3.1 Desmosomes and signalling

Plakoglobin and plakophilin have multiple functions inside and outside the desmosome. Plakoglobin (PG) is a potential candidate in adhesion-independent signalling as it is highly homologous to β -catenin, and a well established mediator of canonical Wnt/wingless pathways (Zhurinsky *et al.*, 2000; Yin & Green, 2004). Canonical Wnt signalling initiates a cascade of events that allows β -catenin to escape the proteasome degradation machinery which normally ensures its low cytoplasmic levels. β -catenin can then translocate to the nucleus where it complexes with transcription factors and activates transcription of target genes involved in developmental patterning, cell fate decisions, cell growth and survival (Zhurinsky *et al.*, 2000). Recent reports have demonstrated that PG is able to compensate for deficient β -catenin, including its regulatory role in keratinocyte differentiation and proliferation (Maeda *et al.*, 2004; Teulière *et al.*, 2004). PG can be phosphorylated by multiple protein tyrosine kinases, with the specific effect dependent on the phosphorylation site. These phosphorylation events modulate PGs associations with intracellular junctions and regulate signalling (Miravet *et al.*, 2003). EGF receptor-dependent tyrosine phosphorylation of PG can impair desmoplakin

recruitment to junctions, weakening desmosomal adhesion (Yin *et al.*, 2005). Loss of desmoplakin from cell junctions in cardiomyocytes can also be a result of translocation of PG into the nucleus (Garcia-Gras *et al.*, 2006). Furthermore, another desmosomal protein, plakophilin 2, may play a role in the transcriptional machinery as part of the RNA polymerase III holoenzyme complex (Mertens *et al.*, 2001). Plakophilins 1 and 3 were found to associate with RNA-binding proteins and may participate in RNA metabolism (Hofmann *et al.*, 2006).

In tissues or cells that have been cultured for extended periods, desmosomes are found in a hyper-adhesive state known as “Ca²⁺ independence”, in which they are insensitive to the absence of extracellular calcium (Watt *et al.*, 1984; Garrod *et al.*, 2005; Kimura *et al.*, 2007). Normally, low Ca²⁺ would disrupt desmosomes and cause their rapid internalisation (Mattey & Garrod, 1986; Windoffer *et al.*, 2002). Subconfluent cells never acquire Ca²⁺-independent desmosomes, but once they reach a confluent state, almost 100% of cells become Ca²⁺ independent (Wallis *et al.*, 2000). If this confluent epithelial sheet is scratch wounded, the cells at the wound edge rapidly revert to calcium dependence (Wallis *et al.*, 2000; Garrod *et al.*, 2005). Interestingly, the activation of PKC α , which has been shown to occur at wound edges, alters the calcium-dependent state (Wallis *et al.*, 2000). It has been speculated (Garrod *et al.*, 2005) that the PKC activity may change the phosphorylation state of desmosomal proteins such as desmoplakin, affecting their interactions and associations with intermediate filaments which could modulate adhesive strength and stability.

1.4.1.3.2 Autoantibodies against periplakin and desmosomal components are detected in autoimmune skin diseases

Desmosome membrane glycoproteins are not only subject to gene mutations but also to inactivation by autoimmune antibodies. Emerging data suggests that cadherin stability and internalization are key components of a group of autoimmune diseases, known as pemphigus. Pemphigus vulgaris (PV) is the most frequently diagnosed form of pemphigus, where the sores and blisters usually start in the mouth. PV is an autoimmune, intraepithelial blistering disease, affecting the skin and the mucous membranes, mediated by circulating auto-antibodies to cell surface proteins of keratinocytes (Beutner & Jordon, 1964). These intercellular or PV antibodies bind to keratinocyte desmosome proteins and result in a loss of cell-cell adhesion, a

process termed acantholysis (Stanley *et al.*, 1982; Stanley, 1998). In the mucosal type of PV, auto-antibodies are found only against desmoglein 3, but in the muco-cutaneous type, auto-antibodies against both desmoglein 3 and desmoglein 1 are present (Amagai *et al.*, 1999). Recently, periplakin auto-antibodies were detected in the sera from patients with a rare variant of PV, called pemphigus vegetans Neumann type (Cozzani *et al.*, 2007). However, the pathophysiological significance of anti-periplakin reactivity in this pemphigus variant remains to be determined.

Pemphigus foliaceus (PF) is an autoimmune skin disorder characterized by the loss of intracellular adhesion of keratinocytes in the top, dry layer of skin. In PF, crusted, scaly sores or fragile blisters usually appear first on the scalp, later involve the face, chest and back, but not the mouth. The auto-antibodies bind to desmoglein 1, resulting in a formation of superficial blisters that are induced by immunoglobulin G (Hashimoto *et al.*, 2001). Auto-antibodies against periplakin and envoplakin have also been found in sera from patients with PF (Kazerounian *et al.*, 2000).

The most serious form of pemphigus is paraneoplastic pemphigus (PNP). PNP, as an entity, has evolved from initial observations that pemphigus occurred more frequently in patients with known malignancy (Younus & Ahmed, 1990; Anhalt *et al.*, 1990). It is now understood that PNP is a malignancy-driven autoimmune phenomenon which involves the detection of circulating antibodies to a variety of polypeptides that constitute the desmosomes and hemidesmosomes of epithelial structures (Stanley, 1993). Painful sores of the mouth, lips and oesophagus are almost always present, and skin lesions of different types occur. This disease is not usually responsive to treatment. In some cases, the tumor will be benign and the disease will improve if the tumor is surgically removed. More recently, it has been suggested that the condition should be renamed paraneoplastic autoimmune multiorgan syndrome, because the antigens that are the target of autoantibodies in the presence of a malignancy are not limited to the skin, but are found in many organs of the body (Nguyen *et al.*, 2001). Combining the antibody profile of all the cases in the literature, antibodies to desmoglein 3 occur in most cases and antibodies to desmoglein 1 are found in approximately two-thirds of cases. The general consensus is that desmoglein 1 and 3 are most likely to be the principal antigenic precipitants. Envoplakin and periplakin are the next two most commonly targeted

antigens (Nagata *et al.*, 2001; Joly *et al.*, 2000), followed by desmoplakin. BPAG-1 is also an important antigen and could be considered the hemidesmosomal equivalent of desmoplakin, attaching to anchoring fibrils. In fact, BPAG-1 shares 60% homology with desmoplakin I (Anhalt, 1999). Taken together, PNP sera contains autoantibodies against both shared and unique epitopes within the linker regions of the plakin family of proteins (Mahoney *et al.*, 1998). “Epitope spreading” is the phenomenon of auto-antibody induction to proteins that are structurally similar or physically close to the original autoantigens, which widens the range of clinical morphology seen in PNP (Anhalt, 1999).

Periplakin has consistently been detected in PNP using immunoblotting techniques, but recently another severe skin disease with life-threatening mucocutaneous reactions (toxic epidermal necrolysis; TEN), was associated with auto-antibodies against periplakin (Park *et al.*, 2006). TEN is induced by drugs (sulphonamides and nonsteroidal anti-inflammatory drugs) which lead to the separation of large areas of the skin at the epidermal-dermal junction, producing the appearance of burnt skin (Wolkenstein *et al.*, 1996). The clinical features of TEN are strikingly similar to those observed for PNP (Anhalt *et al.*, 1990). It is thus speculated that periplakin might be involved in the epidermal pathology of TEN. However, it cannot currently be ruled out that the periplakin autoantibodies are a secondary phenomenon due to the exposure of desmosomal epitopes, as part of the damage to the epidermis (Park *et al.*, 2006).

Until recently, it was generally accepted that autoantibodies against desmoglein molecules prevented the formation of desmoglein-mediated adhesion, resulting in cellular dissociation and pemphigus (Amagai, 2003). Based on a recent study of PF, IgGs do not inhibit homophilic transinteraction of Dsg1 molecules between adjacent cells (Waschke *et al.*, 2005), suggesting that disruption of adhesion may not be a primary disease mechanism. However other mechanisms, including antibody-induced activation of extracellular proteolysis, phosphorylation of Dsgs, and activation of protein kinase C followed by plakoglobin dislocation and subsequent depletion of Dsgs from desmosomes, appear to be important for pemphigus pathogenesis (Kitajima *et al.*, 1999; Aoyama *et al.*, 1999). It has also been shown that high levels of Fas ligand in pemphigus sera induced apoptosis in cultured human keratinocytes through the activation of the caspase-8 (Puviani *et al.*, 2003) and mitogen

activated protein (MAP)-kinase pathways (Berkowitz *et al.*, 2005). Emerging data suggest that binding of autoantibodies to desmogleins, or to other molecules at the cell surface, triggers a series of events that results in desmosome disassembly (Calkins *et al.*, 2006).

Disease	Antigen	Antibody	Reference
Pemphigus vulgaris	Desmoglein 3 Desmoglein 1	IgG	(Stanley, 1993; Amagai <i>et al.</i> , 1998) (Ding <i>et al.</i> , 1999)
Pemphigus vegetans Neumann type	Desmoglein 3 Desmoglein 1 Periplakin	IgG	(Cozzani <i>et al.</i> , 2007)
Pemphigus foliaceus	Desmoglein 1 Periplakin Envoplakin	IgG	(Ding <i>et al.</i> , 1999; Kazerounian <i>et al.</i> , 2000)
Paraneoplastic pemphigus	Envoplakin, Periplakin Desmoglein Desmoplakin 3 BP230	IgG	(Amagai <i>et al.</i> , 1998) (Kiyokawa <i>et al.</i> , 1998) (Kazerounian <i>et al.</i> , 2000) (Stanley, 1993)

Table 1.3: Intraepidermal bullous diseases due to autoimmune response to components of the desmosome.

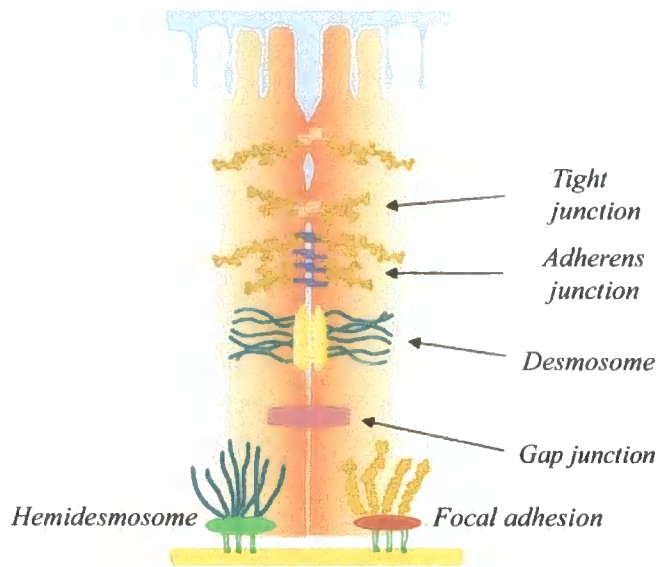
1.4.1.4 Gap junctions

Gap junctions provide communication between neighbouring cells via intercellular channels that cluster in specialized regions of the plasma membrane (Robertson, 1963; Revel & Karnovsky, 1967; Wei *et al.*, 2004). This intercellular space is connected by transmembrane proteins (connexins) that, six by six, form two hemichannels (connexons) which join in mirror symmetry to permit direct communication between the cytosol of the connected cells (Stauffer & Unwin, 1992) (**Figure 1.10 E**). There are at least 21 connexin isoforms in the human genome and nearly all cells in the body express at least one of these genes at some point during development. Moreover, in adult life, connexins show overlapping expression patterns, where an individual cell can use more than one type of isoform (Wiszniewski *et al.*, 2000; Kretz *et al.*, 2003). At least nine connexin genes, including Cx26, Cx30, Cx30.3, Cx31 and Cx43 have been shown to be expressed during keratinocyte differentiation (Kelsell *et al.*, 2000; Di *et al.*, 2001). Various processes are driven by gap junctions, such as rapid transmission of action potentials in heart and in neuronal tissue (Simon *et al.*, 1998; Kirchhoff *et al.*, 1998). Diffusion of metabolites and nutrients, such as nucleotides and glucose, also occurs through gap junctions (Goldberg *et al.*, 1999). This is dependent on the channel type: Cx32 channels are more permeable to adenosine than Cx43 channels. ATP, however, passes more readily through Cx43 channels (Goldberg *et al.*, 2002). Diffusion of second messengers, such as Ca^{2+} , inositol-trisphosphate (IP3) and cyclic nucleotides (Saez *et al.*, 1989; Alexander & Goldberg, 2003) might be involved in induction of apoptosis, gene transcription and growth control. Gap junctional communication is also essential for many other physiological events, including cell synchronization, differentiation and metabolic coordination of avascular organs including epidermis and lens (White & Paul, 1999; Vinken *et al.*, 2006). Furthermore, it has been shown that transfer of small interfering RNAs through gap junctions, thus between adjacent cells, was possible, although it remains unclear if they are normally exchanged via this route *in vivo* (Valiunas *et al.*, 2005). Biosynthesis and assembly of the gap junctions is strictly regulated and intercellular junctions have a short half-life of only a few hours (Musil *et al.*, 2000). Mutations in the connexin genes Cx31, Cx30.3 and Cx43 are associated with skin diseases such as erythrokeratoderma variabilis and hyperkeratosis, highlighting the role of gap junctions in the epidermis (Richard *et al.*, 1998a; Richard *et al.*, 1988; Macari *et al.*, 2000; Paznekas *et al.*, 2003; Gong *et al.*, 2006). In addition, mutation in the Cx26 gene cause non-syndromic

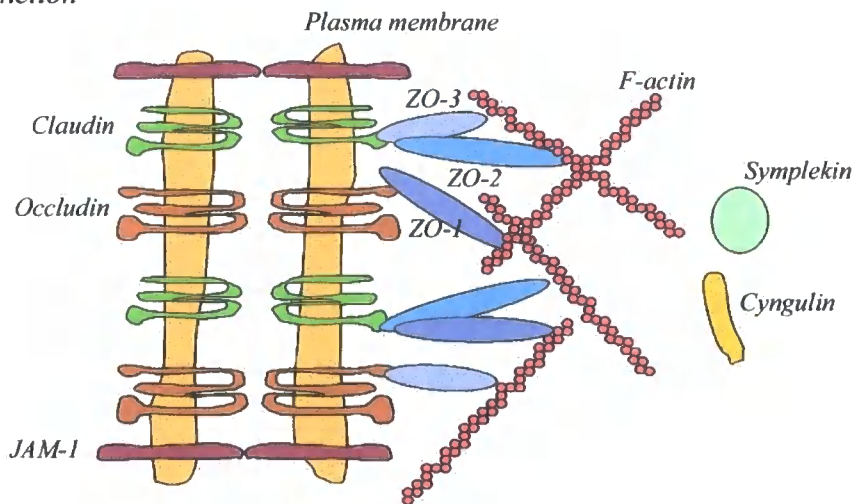
deafness with palmoplantar keratoderma (Richard *et al.*, 1998b). Reduced gap junction activity has also been implicated in tumorigenesis. Decreased connexin expression may be an important marker of skin tumours, as normal melanocytes are coupled with keratinocytes by gap junctions, whereas melanoma cells are not (Budunova *et al.*, 1995). Melanoma cells, instead, communicate amongst themselves and with fibroblasts.

The spectrins are an increasingly diverse group of cytoskeletal proteins containing spectrin-repeat domains and a calponin-type actin-binding domain with homology to similar domains found in plakin proteins (Röper *et al.*, 2002). Spectrins are found in virtually every mammalian cell and play important roles in membrane stability, membrane domain organization and cytoskeletal structure. Spectrin has as many as five isoforms found in heart cells (Vybiral *et al.*, 2001). Recently an alternatively spliced isoform of α II-spectrin has been found that directs its localization to gap junctions in cardiomyocytes (Ursitti *et al.*, 2007). α II-spectrin binds to Cx43 via the first 20 amino-acids adjacent to the SH3 domain to regulate stress activated protein kinase and modulate intracellular communication (Ursitti *et al.*, 2007). However, no interactions between plakin or spectraplakin proteins and gap junction components have, so far, been described.

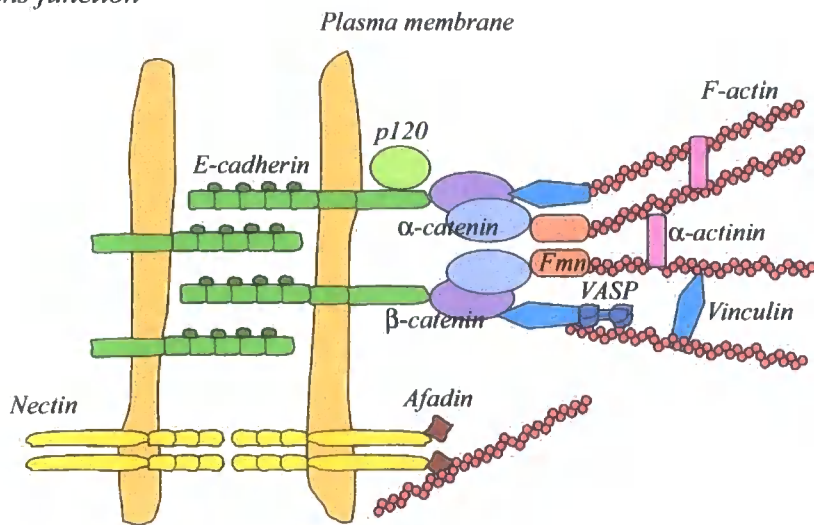
A.



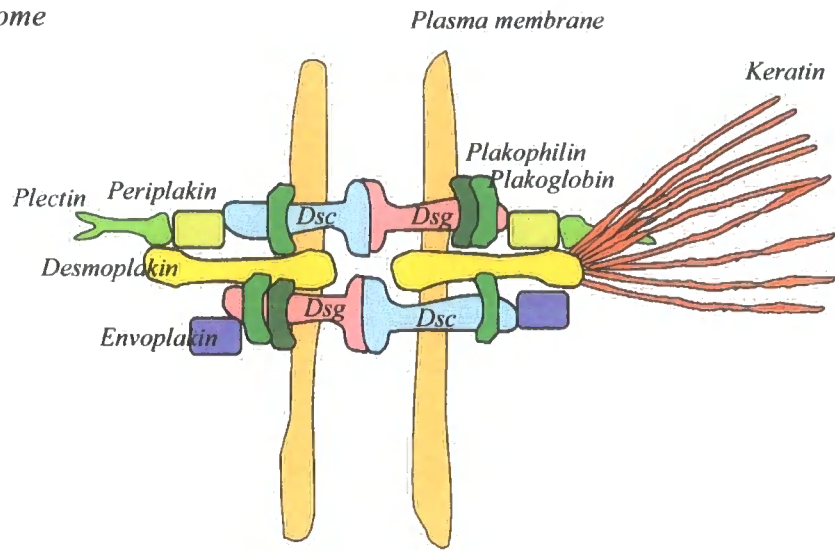
B. Tight junction



C. Adherens junction



D. Desmosome



E. Gap junction

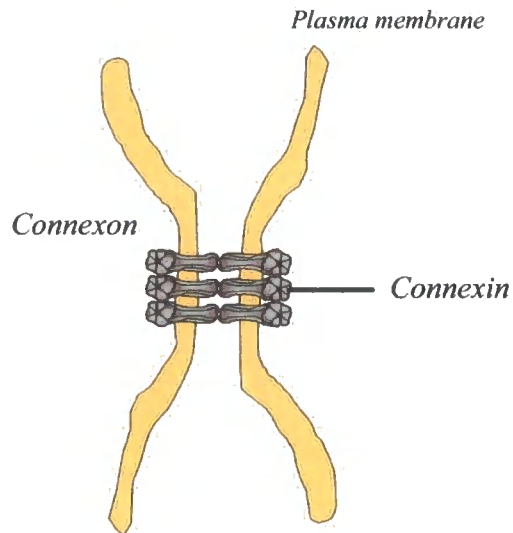


Figure 1.10: Composition and structure of the cell-cell junctions.

A. Schematic diagram detailing the intracellular junctions (B-E) in epithelial cells. Tight junctions provide a physical barrier between the apical and basolateral regions of the cell. Adherens junctions hold together adjacent cells by their actin filaments through transmembrane cadherins. Desmosomes link keratin intermediate filaments via desmosomal cadherins. Gap junctions permit rapid diffusion of water soluble molecules between the cytoplasm of adjacent cells. Tight junctions are the most apical cell-cell junctions, in which occludins and claudins mediate extracellular binding, whilst ZO-1, 2 and 3 bind to actin filaments. C. Adherens junctions are E-cadherin-based junctions where E-cadherin is a direct binding partner of β -catenin which interacts with several proteins. It binds to α -catenin and links cadherin/catenin complexes to the actin cytoskeleton. D. Desmosomes contain two cadherin subgroups (the desmogleins (Dsg) and desmocollins (Dsc)) and also other specialized proteins such as plakophilin, plakoglobin (Armadillo proteins), desmoplakin, plectin, envoplakin and periplakin (plakin proteins), anchoring bundled intermediate filaments between cells. E. Six connexins oligomerise to form hemichannels called connexons, which align in the extracellular space to complete the formation of gap junction channels.

1.4.2 Cell-matrix junctions

The basal layer of epithelial sheets is anchored to the basement membrane via cell-matrix attachments such as hemidesmosomes and focal adhesions (**Figure 1.10 A**). These junctions include plakin proteins such as BPAG-1 and plectin, which connect the actin cytoskeleton to these adhesion sites. The transmembrane adhesion proteins in these junctions are integrins which are a large family of proteins, distinct from cadherins.

1.4.2.1 Hemidesmosomes

Hemidesmosomes are complex protein junctions present in stratified epithelia that attach epithelial cells to their underlying extracellular matrix (Jones *et al.*, 1998; Borradori & Sonnenberg, 1999). They also serve as cell surface anchorage sites for the keratin cytoskeleton and as a channel for signals from the extracellular matrix to the cytoplasm of the cell (Giancotti, 1996; Jones *et al.*, 1998; Borradori & Sonnenberg, 1999). In spite of the morphological similarities (cytoplasmic plaques and connection to cytokeratin filaments) with desmosomes, the protein composition is distinct and contains at least six proteins. The plakin proteins BPAG-1 (also named BP230) and plectin form the hemidesmosomal plaque proteins that bind intermediate filaments to the hemidesmosomes (Stanley *et al.*, 1981; Gache *et al.*, 1996; Borradori & Sonnenberg, 1996; Green *et al.*, 1999; Burgeson & Christiano, 1997). Along with the hemidesmosomal plaque proteins, the transmembrane integrins $\alpha 6\beta 4$, the tetraspanin CD151 (Sterk *et al.*, 2000) and BPAG-2 (also named BP180) mediate anchorage of the basal epithelial cells to the basement membrane (Sonnenberg *et al.*, 1991; Jones *et al.*, 1991; Lee *et al.*, 1992). The integrin $\alpha 6\beta 4$ binds particularly to laminin-5 (a non-collagenous glycoprotein) which is prominently expressed in the basement membrane of epithelial layers (Niessen *et al.*, 1994) (**Figure 1.11 A**). Type II hemidesmosomes form an adhesion complex lacking BPAG-1 (BP230) and BPAG-2 (BP180) but containing plectin and $\alpha 6\beta 4$ integrin; this structure has been described in various cell types and tissues including intestinal epithelium (Jones *et al.*, 1991; Uematsu *et al.*, 1994; Orian-Rousseau *et al.*, 1996; Fontao *et al.*, 1997). Fontao and colleagues characterised type II hemidesmosomes in HT29 cells with electron microscopy, observing electron dense regions connected to cytokeratin filaments that could be modulated by the

extracellular matrix. They found that assembly requires actin filaments but not microtubules (Fontao *et al.*, 1999).

The binding of plectin to $\alpha 6\beta 4$ integrin is essential for the integrity of the adhesive complex in both hemidesmosome types, as indicated by patients with mutations in the $\alpha 4$ integrin subunit or mutations in the plectin gene that prevented this interaction (Pulkkinen & Uitto, 1999; McLean *et al.*, 1996). Mutations in either genes resulted in skin blistering. Furthermore, it has previously been reported that the recruitment of plectin by $\alpha 6\beta 4$ integrin is one of the first steps in type I hemidesmosome assembly, as neither BPAG-1 nor BPAG-2 are recruited efficiently when integrin $\beta 4$ can not bind plectin (Koster *et al.*, 2004). Tetraspanin (CD151) binds to another integrin ($\alpha 3\beta 1$), forming “pre-hemidesmosomal” clusters in keratinocytes (Sterk *et al.*, 2000). However, it is not required for the formation of true hemidesmosomes (Geuijen & Sonnenberg, 2002). Interestingly, tetraspanin deficient mice showed defective wound healing without any effect on epidermal integrity (Cowin, 2006), whereas mutations in the human tetraspanin gene lead to skin blistering (Karamatic *et al.*, 2004). The $\beta 4$ subunit of integrin is unique as its cytoplasmic domain contains two pairs of fibronectin type III repeats (Borradori & Sonnenberg, 1999). The first and second fibronectin repeats form a complex with plectin (Spinardi *et al.*, 1993), with two proline residues of the $\beta 4$ integrin having been found to be critical for this interaction (Koster *et al.*, 2004). The third fibronectin repeat is essential for BPAG-2 binding (Borradori *et al.*, 1997). In contrast, the third and fourth fibronectin repeats are important for binding of BPAG-1 (Hopkinson & Jones, 2000; Koster *et al.*, 2003). It has been suggested that the formation of hemidesmosomes is regulated both within the cells via the plectin - integrin $\beta 4$ interaction, and from outside the cell via binding of integrin $\alpha 6\beta 4$ to laminin-5 (Litjens *et al.*, 2006).

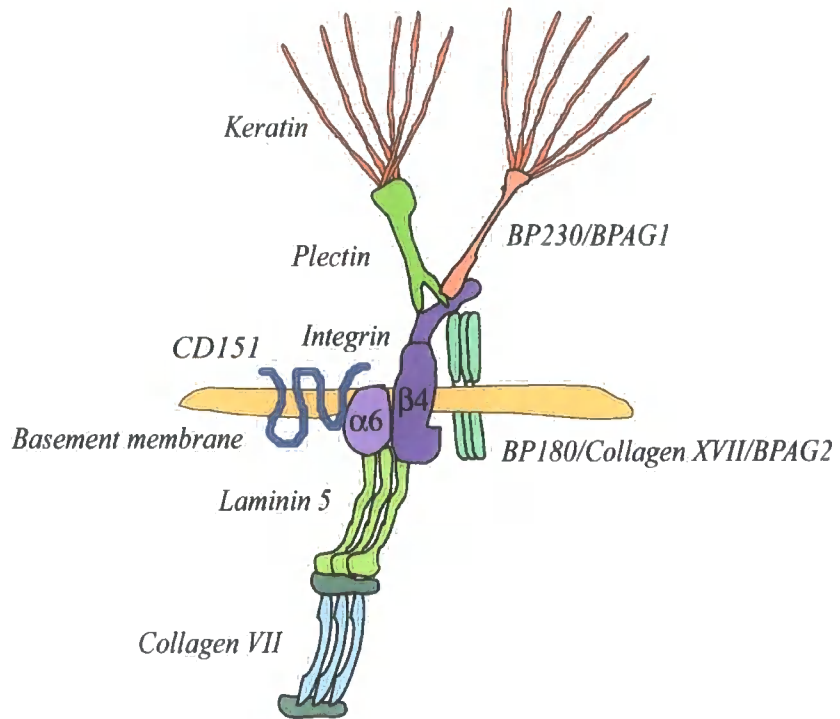
1.4.2.2 Focal adhesions

Most cultured and stationary cells adhere tightly to the underlying substrate through distinct regions of their plasma membrane called cell-matrix junctions, otherwise known as focal adhesion plaques, focal contacts, or focal adhesions (FAs) (Burrige *et al.*, 1988). At these sites, integrins span the cell membrane to link the extracellular matrix (ECM) proteins,

such as fibronectin, collagens, laminins and vitronectin, to various intracellular molecules including the cytoskeleton (Luo & Springer, 2006). On the cytoplasmic side of focal adhesions, integrins and cytoskeletal proteins link the large bundles of microfilaments and stress fibres to these structures (**Figure 1.11 B**). The short cytoplasmic domain of the integrin exposes a relatively large accessible binding surface for protein ligands, as in the absence of these proteins the integrin tail domain appears unstructured (Ulmer *et al.*, 2003). Cytoskeletal anchoring molecules recruited to FAs include talin, vinculin, α -actinin, paxillin, zyxin, and focal adhesion kinase (FAK) (Zamir & Geiger, 2001). FAs are dynamically assembled and disassembled by cells. Continuous remodelling of FAs is critical for cell movement (Lauffenburger & Horwitz, 1996) and dynamic responses to mechanical forces (Choquet *et al.*, 1997). Several regulators of adhesion turnover, including paxillin (Webb *et al.*, 2004), G protein-coupled receptor kinase-interacting protein 1 (GIT1) (Zhao *et al.*, 2000), FAK (Ren *et al.*, 2000), Src (Webb *et al.*, 2004) and p21-activated kinase (PAK) (Manser *et al.*, 1997) are known. Paxillin is a key regulator of adhesion turnover, as it interacts with several adhesion proteins such as FAK, GIT1 (Brown & Turner, 2004) and a serine/threonine phosphatase PP2A which might regulate it via its S273 phosphorylation site (Nayal *et al.*, 2006). Talin is a large intracellular molecule that binds integrin tails and actin (Critchley, 2005) and that has also been shown to be a key regulator of integrin activation (Tadokoro *et al.*, 2003).

Although plectin has been well characterized for its role in hemidesmosomes as a plaque protein, a link has also been shown to vimentin-positive focal adhesions (Gonzales *et al.*, 2001). Distinct localization of the plectin-1f isoform was shown to concentrate at vinculin-positive focal adhesion contacts in mouse fibroblasts (Rezniczek *et al.*, 2003). Recently, plectin downregulation in breast carcinoma and colon carcinoma cells indicated that plectin plays a key role in modulating cell migration and invasion of tumour cells (unpublished data).

A. Hemidesmosome



B. Focal adhesion

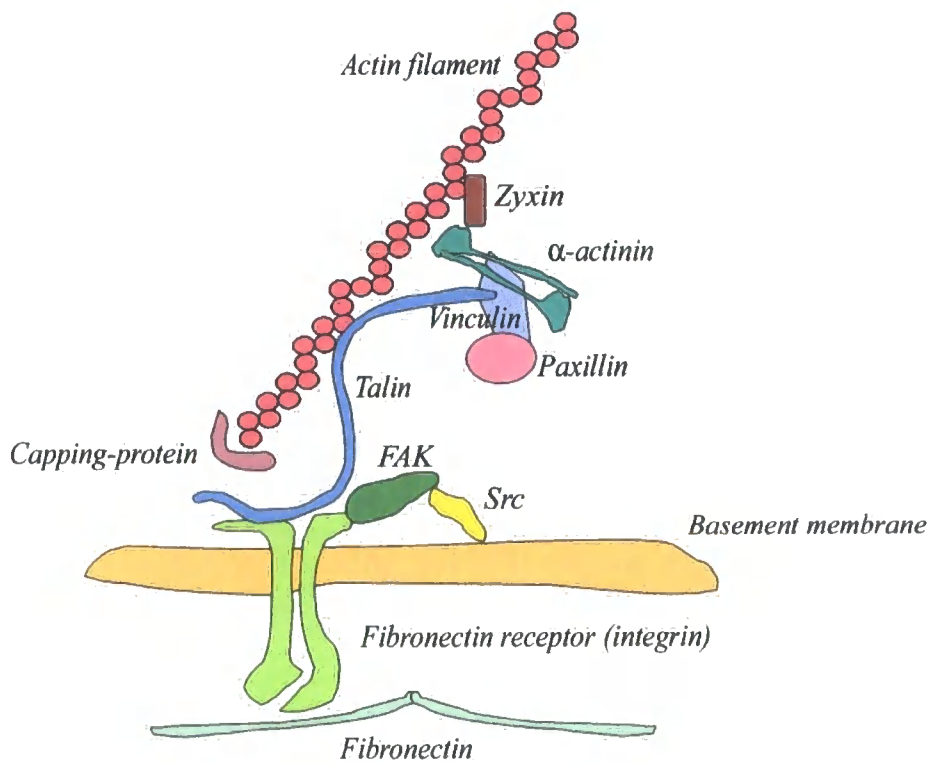


Figure 1.11: Cell-matrix junctions.

A. Hemidesmosomes are complex junctions anchoring cells to the basement membrane providing stable adhesion of the cell. The major component of the inner cytoplasmic plaque consists of two plakin proteins BPAG-1 and plectin. The transmembrane proteins tetraspanin (CD151), BPAG-2 and integrin $\alpha 6 \beta 4$ are also part of the hemidesmosome. The integrin is linked to laminin 5 and collagen VII in the extracellular matrix. **B.** Focal adhesions are specific type of large macromolecular assemblies. Connection between focal adhesions and proteins of the extracellular matrix generally involves integrins. Integrins bind to extracellular proteins such as fibronectin or laminin via their C-terminal domain, while the intracellular domain of integrin binds to the cytoskeleton via adapter proteins such as talin, α -actinin, paxillin and vinculin.

AIM OF THIS THESIS

In this chapter, cytolinkers have been discussed, particularly in relation to the cytoskeleton and to different junctional complexes. The importance of the cytolinkers as cytoskeletal organiser and/or constituents of junctional complexes is clearly unquestionable. Analysis of gene targeted mouse models and human inherited diseases underlines the role plakins in the maintenance of tissue integrity. Periplakin is a component of the CE and also associated with desmosomes in cultured keratinocytes. Remarkably, periplakin has been found to be dispensable in CE formation and in maintaining tissue integrity. This raises the question of what is the primary role of this cytolinker.

With the ultimate goal to contribute to the understanding of the function of periplakin, this work was conducted with the following aims:

1. To study the specific subcellular localisation of the C-terminal and N-terminal constructs of periplakin in simple epithelial MCF-7 cells.
2. To identify any molecular interactions of periplakin N-terminus by co-immunoprecipitation experiments using stably transfected MCF-7 cells.
3. As a next step, to investigate the functional correlation between co-immunoprecipitated proteins through siRNA transfection and immunofluorescence staining.
4. To investigate the role of keratin 8 intermediate filaments in collective epithelial migration during wound healing in human cervical cancer (HeLa) and human pancreatic carcinoma cell lines (Panc-1).

CHAPTER II

MATERIALS AND METHODS

Chemicals and reagents

All chemicals and reagents used in this study were of analytical grade and were purchased from VWR International Ltd., Sigma Aldrich UK or BDH Laboratory Supplies, unless otherwise stated.

2.1 Periplakin constructs

pCI-neo plasmids containing the first half of the N-terminus and C-terminus of periplakin were used to create stable cell lines. These vectors were a kind gift from Dr. Theresa DiColandrea (Keratinocyte Laboratory, Imperial Cancer Research Fund, London, England). The following mutant constructs were created by deletion from the original N-terminal region of periplakin. These were as follows: Ppl-133, Ppl-80, Ppl-63 and Ppl16-133. All the deletion constructs were a kind gift from Dr. Lisa M. Sevilla, Keratinocyte Laboratory, Imperial Cancer Research Fund, London WC2A 3PX, England)

2.2 Mammalian cell culture

Cell line	Type	Media conditions	Reference
MCF-7	Human Caucasian breast adenocarcinoma	DMEM (Sigma)	(Soule <i>et al.</i> , 1973)
HeLa	Human cervical cancer	DMEM (Sigma)	(Puck <i>et al.</i> , 1956)
Panc-1	Human pancreatic carcinoma	DMEM (Sigma)	(Lieber <i>et al.</i> , 1975)
HaCaT	Immortalized human keratinocyte	DMEM (Sigma)	(Fusenig <i>et al.</i> , 1982)

Table 2.1: Cell lines used in this study.

2.2.1 Cell cultures

Cells were maintained in Dulbecco's minimum essential medium (DMEM Sigma, UK) supplemented with 10% foetal calf serum and 5% GPS (L-glutamine, glucose, penicillin, streptomycin), and incubated at 37 C° in humidified air with 5% CO₂. Standard sterile tissue culture techniques were used and cells were propagated in T-25 or T-75 flasks (Greiner Bio-one UK), where appropriate. Cells were passaged using 0.05% Trypsin EDTA (Sigma Aldrich UK) and all washes performed with 1x PBS (Sigma Aldrich UK tissue culture grade).

2.2.2 Cryopreservation of the cells

Cells were stored at -80°C and -130°C , thawed quickly in a 37°C circulating water bath, diluted into complete media, pelleted for 5 minutes at 1000 rpm at 4°C , resuspended in complete media, and plated into the appropriate sized culture vessel. Passages of cells were carried out as follows. The media was removed from the flask by aspiration, the cells were washed with $1\times$ PBS and then 2 ml prewarmed $1\times$ trypsin EDTA (Sigma) was added to the T-75 flask. After 5 minutes incubation at 37°C , the flasks were firmly tapped so that the cells were dislodged from the inner surface. Cells were diluted at a 1:10 ratio using DMEM containing 10% serum, to inhibit the trypsin solution. Cells were divided into flasks according to requirements. For long term storage, cells were centrifuged at 1000 rpm for 5 minutes to remove old media, and were resuspended on ice in antibiotic-free media containing 10% dimethyl sulphoxide (DMSO), before final transferral to a -130°C freezer.

2.2.3 Establishment of stably transfected cell lines

MCF-7 cells were grown in 6-well plate (Greiner Bio-one UK) at a density of 50-60 % confluence before being stably transfected, using GeneJuice transfection reagent (Merck Biosciences, UK), with pCI-neo mammalian expression vector, containing the half-N terminal of the periplakin, whole C-terminal of the periplakin or the empty vector. In each case, cells were transfected with $1\ \mu\text{g}$ of plasmid and $3\ \mu\text{l}$ of GeneJuice. The transfection reagent uses a non-toxic cellular protein and a polyamine to introduce plasmids into the cell. Once inside the cell, the plasmid can express the gene of interest from the internal plasmid promoter using the cell's transcriptional machinery. Cells were allowed to recover for 48 hours after transfection, before starting the selection with $500\ \mu\text{g/ml}$ neomycin. The medium was changed every two days for 3-4 weeks until only isolated colonies remained. After the selection stage, individual colonies were picked and grown initially in 96-well-plates, then later in 24-well-plates before finally being transferred to T-25 flasks. At the 24 well stage, cells were grown on coverslips to screen for expression of the transfected genes. This was confirmed by immunoblotting.

2.2.4 Generation of periplakin specific rabbit polyclonal antibody

A polyclonal antibody was raised against the C-terminal region of periplakin. The peptide sequence PDTGRELSPEEAHRA was chosen as it is conserved between human and mouse and as it is the most hydrophilic (antigenic) region. A cysteine residue was added to the start of the peptide sequence to allow conjugation to the carrier protein, keyhole limpet hemocyanin (KLH). Carrier proteins, once coupled to the peptides, provide additional motifs required for association with Class II molecules and T-cell receptors and in turn generate a stronger antibody response. Peptide synthesis, raising of antibodies and collection of serum was conducted by Cambridge Research Biochemicals, Billingham, UK.

2.3 Immunohistochemistry and confocal microscopy

2.3.1 Fixation

Cells were seeded on sterile glass coverslips in 24-well plates in the presence of DMEM (10% FCS and 5% GPS) medium and grown for three days to obtain the required degree of confluence. All cultures were washed 3 times in PBS and either fixed with 4% formaldehyde in phosphate-buffered saline (PBS) for 10 minutes at room temperature and permeabilised in 0.5% Triton X-100 for 15 minutes, or fixed with ice-cold methanol:acetone (1:1) for 15 minutes. Following fixation, cultures were washed 3 times with PBS containing 0.5% bovine serum albumin (BSA) and 0.02% sodium azide (NaN₃). Subsequently, cultures were blocked with 0.5% Fish Skin Collagen Solution diluted in 1x PBS for 40 minutes at room temperature.

2.3.2 Primary antibodies

After blocking, the coverslips were placed on Parafilm and primary antibodies were applied for 1 hour at room temperature, after which cells were washed 3 times in PBS/BSA/NaN₃. Primary antibodies used and their dilutions are described in **Table 2.4**. All primary antibodies were diluted in PBS/BSA/NaN₃ buffer.

2.3.3 Secondary antibodies

Secondary antibodies were applied for 1 hour in the dark at room temperature, after which the cells were washed 3 times in washing buffer. All the Alexa 488 and Alexa 594-labelled secondary antibodies were diluted in the same buffer as their respective primary antibodies. The cell nucleus was visualised using 100 ng/ml DAPI (Invitrogen UK) which binds to double stranded DNA. Secondary antibodies used in this study and their dilutions are summarized in **Table 2.5**. After several washes in PBS, the coverslips were mounted face-down in one drop of Immunomount (Thermo UK) and used for microscopy immediately or stored at 4°C.

2.3.4 Immunofluorescence staining of frozen tissue sections

Frozen tissue blocks were cut with a LEICA CM 3050S cryostat and placed on slides before air drying and storing at -80 °C. Prior to tissue staining, the slides were removed from the -80 °C freezer and allowed to equilibrate to room temperature for 30 minutes-1 hour before transferring into 1 X PBS/BSA/NaN₃ for 5 minutes. A wax pen was used to circle the sections, ensuring the solutions covered the sections at all times. 0.5 % fish skin gelatin was applied to the sections for 40 minutes as a blocking step. Sections were washed 3 times in PBS/BSA/NaN₃ for 5 minutes. Primary antibodies were diluted in PBS/BSA/NaN₃ and tissue sections were incubated in the dark for 90 minutes at room temperature, or alternatively overnight at 4°C. Sections were washed 3 times in PBS/BSA/NaN₃ and secondary antibody was applied for 1 hour at room temperature, again in the dark. Slides were washed in PBS/BSA/NaN₃ before the coverslips were positioned cell-side down onto glass slides using Immunomount (Thermo UK) Slides were dried overnight in the dark and stored at 4°C.

2.3.5 Microscopy

For viewing and imaging cells, a Zeiss LSM 510 META confocal microscope imaging system, equipped with 40X N/A1.3 and 63X/1.10 oil immersion objectives, was used. A dynamic range adjustment was set up to optimise the signal for the fluorophores and the same optimised conditions were used for comparisons of the intensity of signals between different cultures. The images were collected at a scan speed of 12.8 μ s per pixel and a resolution of 1024 x 1044. Composite images were generated using Adobe Photoshop CS (Adobe System) and LSM510 image browser software (Carl Zeiss). Only linear adjustments to brightness and contrast were made. On some occasions, a BioRad Radiance 2000 confocal microscope imaging system with LaserSharp software (Bio-Rad) was used equipped with 40X and 63X/1.40 oil immersion lens. Images were collected in Sequential Mode (Bio-Rad) or Multi-Track Mode (Zeiss).

2.4 Scratch wound assay

Cells were grown to 100% confluence under standard conditions and wounded using the scratch wound assay technique (Lampugnani, 1999). Briefly, once the cells had formed a monolayer in culture, they were wounded using a 200 μ l pipette tip (Star Lab UK). For immunoblotting analysis, cells were harvested at different time points (30 minutes or 2 hours) post wounding, or the cells were washed 3 times with PBS and used for immunofluorescence imaging. For real time wound healing experiments, the wounded area was captured using a phase contrast microscope (Axiovert 10 Zeiss, Colorview System) using the x10 objective. Progression of the cells during healing of the wounded area was observed under the microscope for a period of time ranging from hours to several days (Figure 2.1).

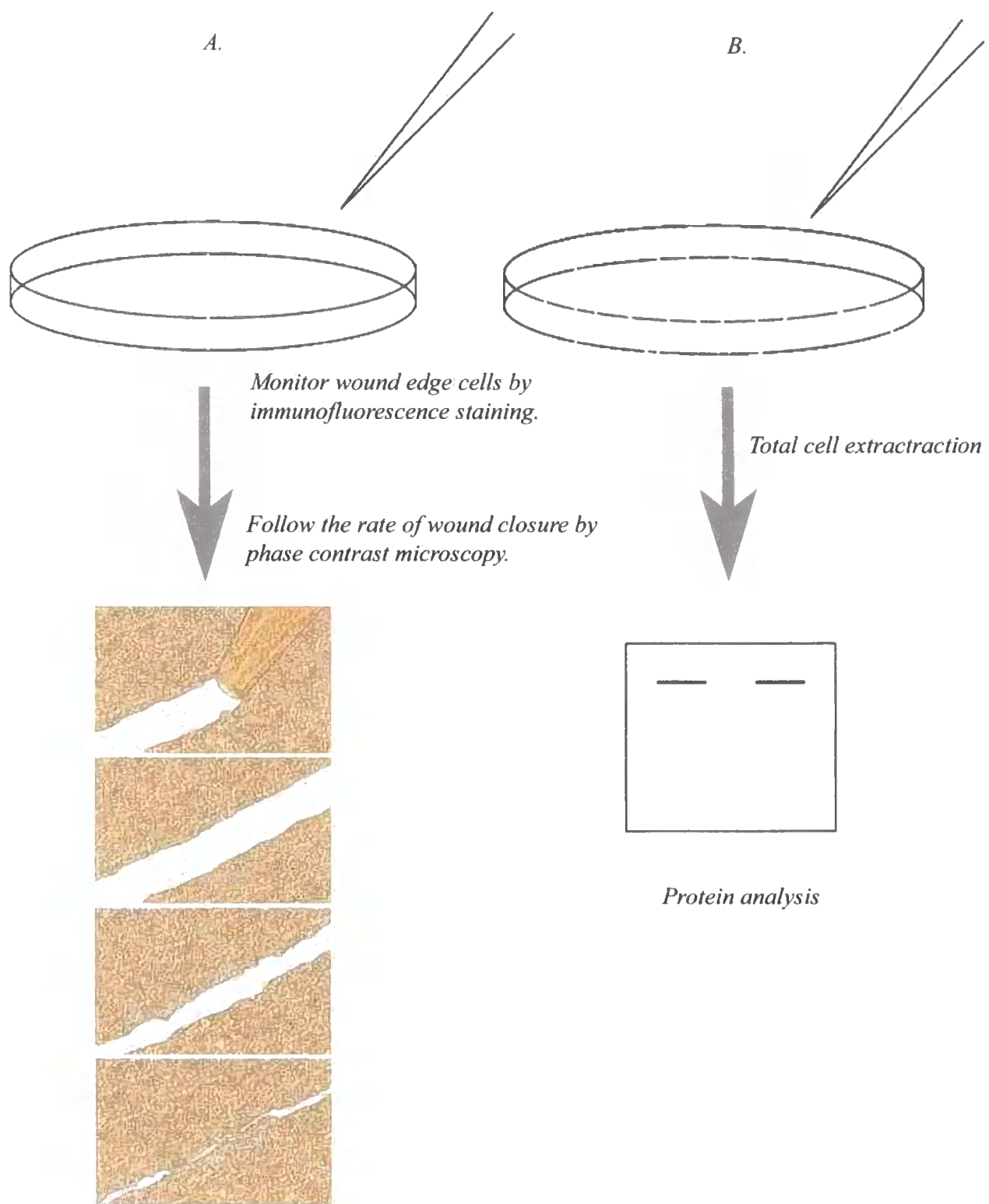


Figure 2.1: Scratch wound assay.

A. In order to perform a wound healing assay, a wound is introduced into a monolayer of cells using a sterile pipette tip by scratching a line through the layer. The open gap is then monitored by phase contrast microscopy focusing on the wound edge cells and/or following the rate of wound healing. The monolayers recover and heal the wound in a process that can be observed over a distinct timecourse depending on the specific cell type, conditions, and the extent of the “wounded” region. **B.** Scratch wound assay is also a useful tool for monitoring protein expression alterations after wounding the monolayer (images displayed were adopted from public site: www.biophysics.com/.../woundhealing.html).

2.5 Protein analysis techniques

2.5.1 Whole cell protein extraction

All protein analysis procedures were performed on ice. Whole cell protein was extracted after washing 3 times with ice-cold PBS. Cells were lysed on ice in 2x Laemmli sample buffer (LSB) (0.5M Tris-HCl pH 6.8, 20% v/v Glycerol, 1% SDS; 1mM EDTA), supplemented with Complete Protease Inhibitor Cocktail (Roche UK), containing a mixture of protease inhibitors including serine-, cysteine- and metalloproteases. 1 tablet was added to 5 ml of sample buffer. Keeping the samples on ice during protein extraction, and the use of protease inhibitors, are important steps to stop degradation of the proteins. Cells were scraped off the dishes with a cell scraper and transferred into microcentrifuge tubes. The samples were boiled for at least 5 minutes and homogenised with a 25G needle to shear the genomic DNA. Samples were used fresh or aliquoted and stored at -80°C until needed.

2.5.2 Protein Quantification Using BCA-Assay

Extracted proteins were quantified using a BCA (bicinchoninic acid) protein assay reagent kit (Pierce UK), which is a colorimetric assay where the samples are read at 562 nm. Standards were made using BSA (Sigma Aldrich UK) diluted in the same sample buffer that the protein samples were stored in. Standard concentrations were: 0, 0.1, 0.25, 0.5, 1.0, 1.5, and 2.5 mg/ml, and the protein samples were used at dilutions of 1:5 in the assay. Samples were read on a Beckman DU-600 spectrophotometer, which produces a standard curve which can be used to determine the concentration of unknown samples, based on their absorbance.

2.5.3 Subcellular Detergent Fractionation of Proteins

MCF-7 cells were grown to confluence in 10 cm² dishes and extracted using saponin, with some modifications of the protocol described by Palka and Green (Palka & Green, 1997). Briefly, cells were washed in PBS to remove any medium and extracted with saponin buffer (0.01% w/v saponin, 10mM Tris pH 7.5, 140mM NaCl, 5mM EDTA, 2mM

EGTA, 1mM PMSF and Complete Protease Inhibitor Cocktail (Roche UK)) on ice, for 10 minutes. After this, the cells were removed from the dishes using cell scrapers and centrifuged at 14,000 x g for 30 minutes at 4 °C. The saponin soluble fraction was transferred to a separate Eppendorf tube and the pellet was further extracted using ice-cold Triton buffer (1% v/v, TritonX-100, 10mM Tris pH 7.5, 140mM NaCl, 5 mM EDTA, 2mM EGTA, 1 mM PMSF and proteinase inhibitor cocktail). After vortexing the pellet for 30 sec, the sample was centrifuged for 30 minutes at 14,000 x g, at 4°C. The supernatant (Triton soluble fraction) was transferred to a separate tube, leaving the Triton insoluble fraction as the pellet (**Figure 2.2**). All samples were adjusted to the same volume with 4 x LSB and equal volumes were loaded on a 4-12% Bis-Tris gel (Invitrogen) for analysis by immunoblotting. Quantification of individual proteins in each fraction was determined using Image Gauge version 4.0 (Fuji photo film co. Ltd).

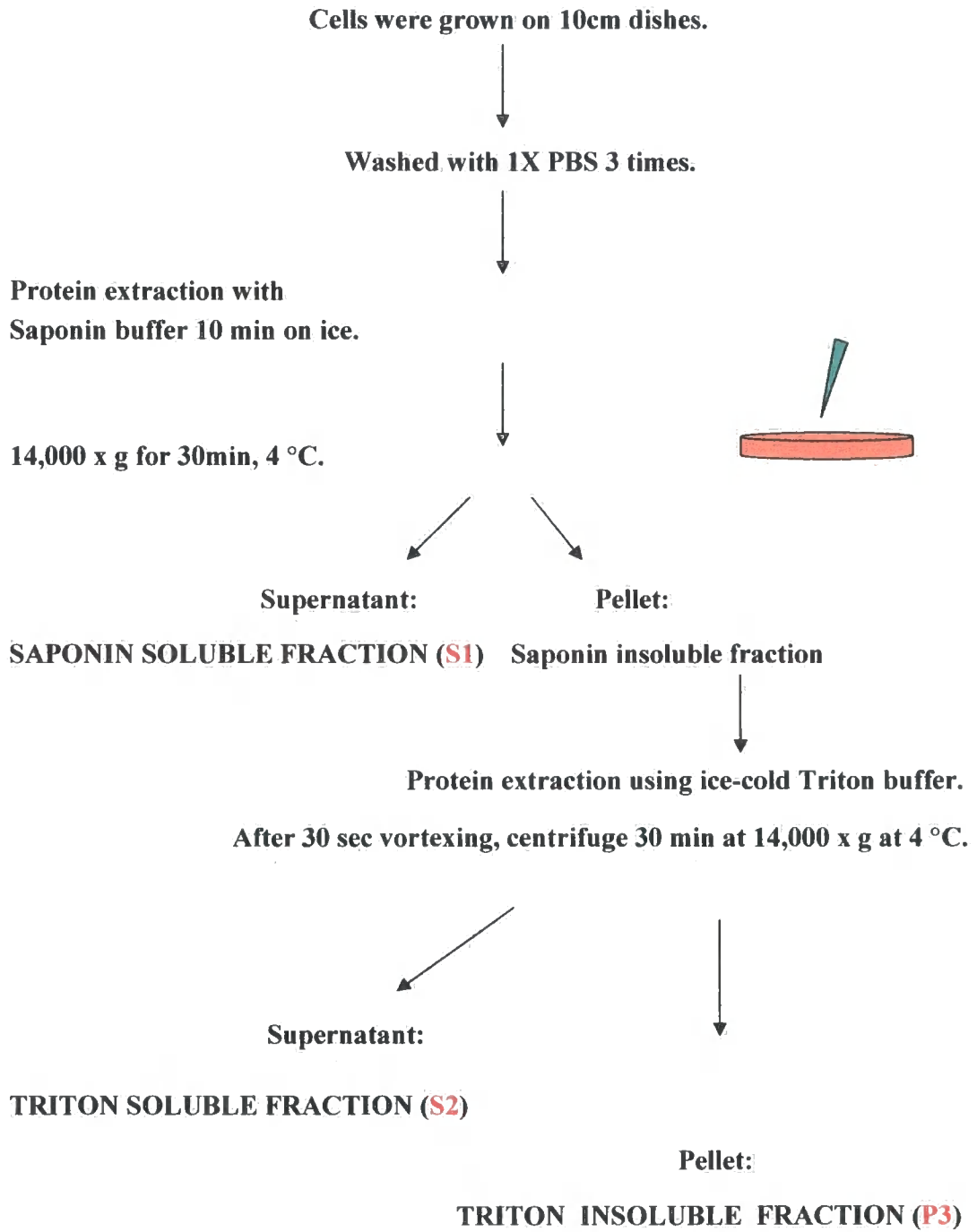


Figure 2.2: Experimental summary of subcellular detergent fractionation of proteins.

2.6 SDS-PolyAcrylamide Gel Electrophoresis (PAGE) for proteins with a molecular weight of 20-200 kDa

Proteins were separated by SDS polyacrylamide gel electrophoresis (PAGE) using the Thermo Electron mini gel system. Sodium dodecyl sulphate (SDS) is an anionic detergent which denatures proteins by "wrapping around" the polypeptide backbone. Polymerisation of the acrylamide was initiated by the addition of ammonium persulphate (Sigma, U.K.) to a final concentration of 0.1% and 1 in 2,500 dilution of N,N,N',N'-tetramethylethylenediamin (TEMED; Sigma, UK.). The mixture was immediately poured between glass plates on the casting rig, leaving approximately 1 cm at the top for the stacking gel mix. Saturated butanol was overlaid on top of the gel for a smooth inter-phase. Following polymerisation of the separating gel, the saturated butanol was removed and washed away with distilled water several times. The stacking gel (final concentration 4% acrylamide, 0.5 mM Tris-HCL pH 6.8; 20% SDS (w/v), 10% (w/v) ammonium persulphate and 1 in 2500 dilution of TEMED) was mixed and poured on top of the separating gel and the comb inserted between the plates. The comb was removed after the stacking gel had polymerised. The required amount of each protein sample was denatured by adding an equal volume of loading buffer dye (sample buffer supplemented with 0.2% bromophenol blue and 1% β -mercaptoethanol) and resolved on SDS-PAGE gels, at 100 V through the stacking and 200 V in the resolving gel in 1 X SDS-PAGE buffer (25mM Tris, 250mM glycine, 0.1% SDS). Depending on the size of the proteins of interest, resolving gels of 7% to 15% were used for higher resolution in the upper and lower part of the gel, respectively (**Table 2.2**).

Stacking Gel Solution (4% Acrylamide)	
H ₂ O	3.075 ml
0.5 M Tris-HCl, pH 6.8	1.25 ml
20% (w/v) SDS	0.025 ml
Acrylamide/Bis-acrylamide (30%/0.8% w/v)	0.67 ml
10% (w/v) ammonium persulphate (APS)	0.025 ml
TEMED	0.005 ml

Separating gel Solutions:	7%	10%	12%	15%
H ₂ O	15.3 ml	12.3 ml	10.2 ml	7.2 ml
1.5 M Tris-HCl, pH 8.8	7.5 ml	7.5 ml	7.5 ml	7.5 ml
20% (w/v) SDS	0.15 ml	0.15 ml	0.15 ml	0.15 ml
Acrylamide/Bis-acrylamide (30%/0.8% w/v)	6.9 ml	9.9 ml	12.0 ml	15.0 ml
10% (w/v) ammonium persulphate (APS)	0.15 ml	0.15 ml	0.15 ml	0.15 ml
TEMED	0.02 ml	0.02 ml	0.02 ml	0.02 ml

Table 2.2: Preparation of SDS-PAGE gels.



2.7 1-dimensional gradient gel electrophoresis

For improved separation, protein samples were separated on NuPAGE 4-12% Bis-Tris (Invitrogen), or in the case of high molecular weight proteins such as plectin, NuPAGE 3-8% Tris-acetate gradient gels using the NuPAGE Mini-Cell system. Proteins were resolved on NuPAGE 4-12% Bis-Tris gradient gels using 1X MOPS running buffer. In contrast, proteins were resolved on NuPAGE 3-8% Tris-acetate gradient gels using 1X NuPAGE Tris-acetate running buffer.

2.8 Immunoblotting

Immunoblotting was performed using the semi-dry blotting technique (Trans-Blot SD Semi-Dry Transfer Cell Bio-Rad). Proteins were separated on SDS-PAGE gels (Invitrogen) and transferred to Hybond nitrocellulose membranes (Amersham Pharmacia Biotech) using anode buffer I (0.3 M Tris, 10% methanol, pH 10.4), anode buffer II (25 mM Tris, 10% methanol, pH 10.4) and cathode buffer (25 mM Tris, 40 mM glycine, 10% methanol, pH 9.4) for 0.8 mA/cm².

2.9 Ponceau S staining of the nitrocellulose membrane

The nitrocellulose membranes, containing the transferred proteins were stained with Ponceau S (Sigma Chemical U.K.) for 3-5 minutes and the excess dye was washed off with distilled water until protein bands were visible. Ponceau S was used to check that protein transfer had occurred and that this transfer was uniform and also to verify equal loading of proteins. Membranes were destained in Tris-buffered saline (1×TBS; 20 mM Tris-HCl, pH 7.4, 150 mM NaCl) for 5 minutes.

2.10 Immunodetection

For the detection of protein using antibodies, non-specific binding sites on the membranes were blocked by incubation with blocking solution consisting of 5% (wt/vol) dried non-fat milk powder in TBS containing 0.2% (vol/vol) Tween-20 for 2 hours at room temperature or at 4°C overnight. The membranes were probed with an antibody diluted in blocking solution for 1 hour. After several washes with TBS containing 0.2% (vol/vol) Tween 20, the membrane was incubated with horseradish peroxidase-conjugated secondary antibody (diluted 1:800) in blocking solution for 1 hour, followed by washing with 1X TTBS for 30 minutes. Antibody labelling was detected by enhanced chemiluminescence using an ECL Plus Western Blotting Detection System (Amersham), visualized with a luminescent image analyser (LAS-1000plus; Fuji Photo Film (UK), London, United Kingdom).

2.11 Membrane stripping for reprobing

Hybond PTM nitrocellulose membranes were incubated at 55°C for 1 hour in stripping buffer (100 mM β -mercaptoethanol, 2% SDS, 62.5 mM Tris-HCL, pH 6.7). The membranes were washed twice, for 3 minutes, in TBS-T and then blocked in 10% (w/v) non-fat milk in TBS-T for 1 hour at 37°C. Removal of the protein signal was verified by treatment of the membranes with ECL Plus. Following a further three 5-min TBS-T washes, the membranes were ready for reuse and probing with other antibodies.

2.12 Immunoprecipitation

2.12.1 Cell lysis, Pre-clearing, Immunoprecipitation

Cells were washed 3 times in ice-cold PBS (1mM KH_2PO_4 , 10mM Na_2HPO_4 , 137mM NaCl , 2.7 mM KCl, pH 7.4) and lysed in Lysis buffer (50mM Tris-HCl pH 7.5, 150mM NaCl, 1% Nonident P40, 0.5% sodium deoxycholate, Complete Protease Inhibitor Cocktail (1 tablet/15ml). The cells were scraped into an Eppendorf tube and homogenised

on ice, then centrifuged for 10 min at 12,000×g at 4°C to remove debris. 50µl homogenous protein G agarose suspension (Roche) were added to the sample (containing 25 µl bed volume of the resin) to 1-3 ml sample and pre-cleared for 3 hours at 4°C on a rocking platform. After centrifugation to pellet the beads, 10 µl of antibody (diluted 1:100) was added to the supernatant and incubated for 1 hour at 4°C on a rotating mixer. After incubation with 50 µl Protein G beads, proteins were immunoprecipitated overnight at 4°C on a rotating mixer. Immunoprecipitated samples were then washed three times, first with 1ml lysis buffer, then with 1ml wash buffer 2 (50mM Tris-HCl pH 7.5, 500 mM NaCl, 0.1 % Nonident P40, 0.05 % sodium deoxycholate) and finally with 1 ml wash buffer 3 (50mM Tris-HCl pH 7.5, 0.1 % Nonident P40, 0.05 % sodium deoxycholate) for 20 minutes at 4°C. This step is crucial to remove non-specifically bound proteins. For a less stringent washing procedure, immunoprecipitated complexes were washed 3 times in lysis buffer for 20 minutes at 4°C. In order to denature proteins and release them from the beads, samples were heated to 100°C for 3 minutes in the presence of 25-75 µl electrophoresis sample buffer. After pelleting the beads, proteins from the solubilized supernatant were separated by electrophoresis using SDS-PAGE gels, or 4-12% Bis-Tris gradient gels (Invitrogen) for better resolution.

2.12.2 Immunoprecipitation with the IP/CoIP kit

Cells were grown under the usual conditions for each line. Having reached 100% confluency, culture media was decanted off and the cells were rinsed once with ice-cold TBS. Total protein was extracted with mammalian lysis buffer (M-PER Reagent; Pro-Found Mammalian HA-tag IP/CoIP kit and Application Set; Pierce) for 5 minutes with gentle shaking. The lysate was collected and transferred to a microcentrifuge tube. Samples were centrifuged at 16,000 x g at 4°C for 20 minutes to pellet the cell debris. Supernatants were transferred to a clean microcentrifuge tube and were used immediately or stored at -80°C until further analysis. The immunoprecipitation procedure was carried out with immobilized anti-HA antibody, overnight at 4°C, with end-over-end mixing. Samples were washed 3 times with TTBS (0.05% Tween-20 in TBS). 25µl of 2X non-reducing sample

buffer was added to the samples before placing on a heated block (95-100°C) for 5 minutes. For reducing gel analysis, 3 µl of 1M DTT was added to each sample.

2.13 Gel staining

After electrophoresis, gels were stained with normal Coomassie Brilliant Blue. Gels were placed directly in the dye (consisting of 40% methanol, 10% acetic acid, 0.1% Coomassie Blue G-250; Sigma Aldrich UK) and stained overnight at room temperature with constant agitation. Gels were destained with 40% methanol, 10% acetic acid for up to 24 hours with several changes of the solution.

Protein gels were also visualized by Silver staining (Silver Snap Stain Kit II; Pierce). Gels were washed in ultrapure water and fixed in fixing solution (30% ethanol: 10% acetic acid) for 30 minutes. The gels were then washed in 10% ethanol for 10 minutes and in ultrapure water for 5 minutes, sensitized for 1 minute in sensitizer working solution (SilverSNAP Sensitizer diluted in ultrapure water, 1:500), and stained for 30 minutes. After washing the gels with water, they were developed for 2-3 minutes and the reaction was stopped with 5% acetic acid for 10 minutes. Unknown proteins were identified by isolating the relevant band from the gel, before processing for peptide mass fingerprinting [matrix-assisted laser desorption ionisation mass spectrometry (MALDI-TOF)] and amino acid sequence analysis.

2.14 2-Dimensional gel electrophoresis

As the co-immunoprecipitation kit leaves the proteins contaminated with charged detergents which are incompatible with the isoelectric focusing, SDS had to be removed from the samples. The samples (25 µl) were diluted with 100 µl double distilled water and 400 µl of acetone was added. After 30 minutes incubation at room temperature, centrifugation at 13,000 rpm resulted in a pellet with only a minimal amount of SDS. With

the addition of 60µl lysis buffer containing urea, thiourea and CHAPS (see below), proteins were unfolded and their solubility was increased.

2.14.1 Re-Swelling of IPG strip

Preparing the protein samples for the first dimension run, lysis buffer (9M urea; 2M thiourea; 4% CHAPS; 1% DTT; 2% 3-10 ampholytes and a trace of bromophenol blue) was added to make the volume 120 µl. With the addition of 2.5 µl 50% DDT and 2.5 µl ampholyte buffer, this made a final volume of 125 µl, which was sufficient to re-hydrate a 7 cm IPG strip. The samples were pipetted into a well of the Immobiline Drystrip Re-swelling Tray, and the IPG strips were placed into the well over the sample, gel side down, avoiding trapping of air bubbles underneath. Paraffin oil was placed over the sample and the strip was rehydrated overnight.

2.14.2 1st Dimension run.

After washing and blotting dry, the IPG strips were placed into the grooves of the strip tray, gel side up. Electro focusing electrode strips were cut to size, soaked in water, dried and placed across the IPG strips. Paraffin oil was added to completely cover the IPG strips. The Multidrive XL power was linearly increased and programmed as shown below (running conditions: temperature 20°C; current 2 mA; power 5 W total).

	Voltage(V)	mA	W	Time (h)	kVh
1. step	200	2	5	0:01	
2.step	3500	2	5	1:30	2.8
3.step	3500	2	5	0:35-1:05	2.2-3.7

Following electrophoresis in the first dimension, IPG strips were removed from the tank, rinsed with MilliQ (MQ) water and placed into an equilibration tray, gel side up. Equilibration buffer (50mM Tris-HCl, 10mg/ml dithiothreitol, 10% (w/v) SDS, 6M urea, and 30% glycerol) was placed over the strips (4-5 ml per strip) and put on a shaker for 15 minutes.

The strips were removed and rinsed with MQ water and placed into equilibration buffer containing iodoacetimide (48mg/ml) (instead of DTT) and put back on the shaker for a further 15 minutes.

2.14.3. 2nd dimension run

The second dimension gels (70 x 80 mm) were 10% SDS-PAGE gels, prepared using a multi-gel casting system with 1mm spacers, and made in batches of three. The gel was filled to approximately 0.8 cm from the top of the lower glass plate and butan-2-ol was added. However, a stacking gel was not required. A standard SDS-PAGE electrophoresis buffer system was used. Once the gel had polymerized, the butanol-2-ol was washed out with MQ water and gel was covered with 1X running buffer to the top. IPG strips were transferred from the tray, allowing them to displace the water. Strips were pushed down with the spacer to prevent bubbles, and excess water was removed with blotting paper.

Warm 1% agarose was made with 1X running buffer and poured on top of the strips. The agarose was allowed to cool and solidify before moving on to the

electrophoresis step. The gels were run at 200 V for two hours, by which time the bromophenol blue dye had reached the end of the gel. Gels were removed from the plates and silver stained.

2.15 Matrix-assisted laser desorption/ionization time-of-flight (MALDI-TOF)

Proteomics is an important new field of study of protein properties (expression levels, interactions, post-translational modifications etc.) and thus can be described as functional genomics at the protein level. Matrix-assisted laser desorption/ionisation-time of flight mass spectrometry (MALDI-TOF MS) is a relatively novel technique in which a co-precipitate of an UV-light absorbing matrix and a biomolecule is ionised by a nanosecond laser pulse. Most of the laser energy is absorbed by the matrix, which protects against fragmentation of the biomolecule. The ionized biomolecules are accelerated by an electric field and enter the flight tube where the different molecules are separated according to their mass to charge ratio (m/z) and hence reach the detector at different times. In this way, each molecule yields a distinct signal. The method is used for detection and characterization of biomolecules, such as proteins, peptides, oligosaccharides and oligonucleotides, with molecular masses between 400 and 350,000 kDa. Protein identification by this technique has the advantages of a short measuring time (minutes) and negligible sample consumption (less than 1 pmol) and also yields additional information regarding microheterogeneity (e.g. glycosylation) and the presence of by-products. The mass accuracy of MALDI-TOF MS is sufficient to characterise proteins (after tryptic digestion) from completely sequenced genomes (e.g. methanogens, yeast). In addition, important progress has been made in the use of MALDI-TOF MS for typing of single nucleotide polymorphisms using single nucleotide primer extension.

2.15.1 Mass-Spectrometry

Tryptic digestion was performed on a ProGest Workstation from Genomic Solutions using the standard ProGest long trypsin protocol. Briefly, gel spots were washed

in 25mM bicarbonate buffer (pH 8), destained and dried out in concentrated acetonitrile. The gel pieces were rehydrated in 50mM bicarbonate buffer and the protein spots were reductively alkylated with DTT and iodoacetamide. After several washes in bicarbonate buffer, 200 ng/sample of buffered modified trypsin was added and the digestion was performed for 8 hours at 37C°. Following digestion, the peptide extracts were lyophilized in a vacuum concentrator, resuspended in 10 ml 0.1% formic acid and introduced into a Voyager DE-STR mass spectrometer (Applied Biosystems). All MALDI spectra acquired were internally calibrated using the trypsin autolysis peaks 842.5 and 2211.11 m/z present in the spectra. The generated peptide masses for each sample (fingerprints) were then matched to theoretical trypsin digests of proteins from a complete non-redundant human NCBLnn database. The database search was performed using the MASCOT (www.matrixscience.com) software at a mass accuracy of 50 parts per million (ppm). The MASCOT search algorithm takes into account the number of peptides that match, the number of fragment ions that match, the accuracy at which they match, and a weighing for large peptide matches (Pappin *et al.*, 1993). For each sample, the protein with the highest MOWSE (molecular weight search) score was reported as a positive result.

2.16 RNA interference (RNAi).

Until recently, the functional characterization of a particular mammalian gene or gene product involved either elimination by gene knock-out strategies in mouse models, inactivation using ribozymes, antisense strategies or overexpression of a dominant-negative form of the protein product in cell culture systems. The recent discovery of the natural process termed RNA interference (RNAi) offers an alternate tool to functionally characterize a gene product (Fire *et al.*, 1998). RNAi is an antiviral post-transcription gene silencing defense mechanism in animals and plants caused by the introduction of double-stranded RNA homologous to the silenced gene (Paddison & Hannon, 2002; Denli *et al.*, 2003). This mechanism of RNAi has been found to be conserved in most organisms, with the notable exception of the yeast *Saccharomyces cerevisiae* (Hutvagner & Zamore, 2002). RNAi involves the cleavage of the double stranded RNA by an RNAase III enzyme (DICER) into smaller fragments of 21-23 nucleotides (nt) in length with characteristic dinucleotide 3'

overhangs referred to a small interfering RNA (siRNA) (Zamore *et al.*, 2000). The siRNA is then recruited into a multienzyme complex called the RNA induced silencing complex (RISC) which binds specifically to a complementary mRNA transcript to target it for cleavage and degradation. In mammalian cells, *in vitro* synthesized 21-nucleotide siRNA duplexes provide a new tool for studying gene function (Elbashir *et al.*, 2001; Harborth *et al.*, 2001) as longer dsRNAs resulted in blockage of initiation of protein synthesis and mRNA degradation (Bass, 2001). There are several different methods of carrying out RNAi including *in vitro* transcription, siRNA vector or chemical synthesis. In this study, chemically-synthesized siRNAs have been used because of their purity and ease of use.

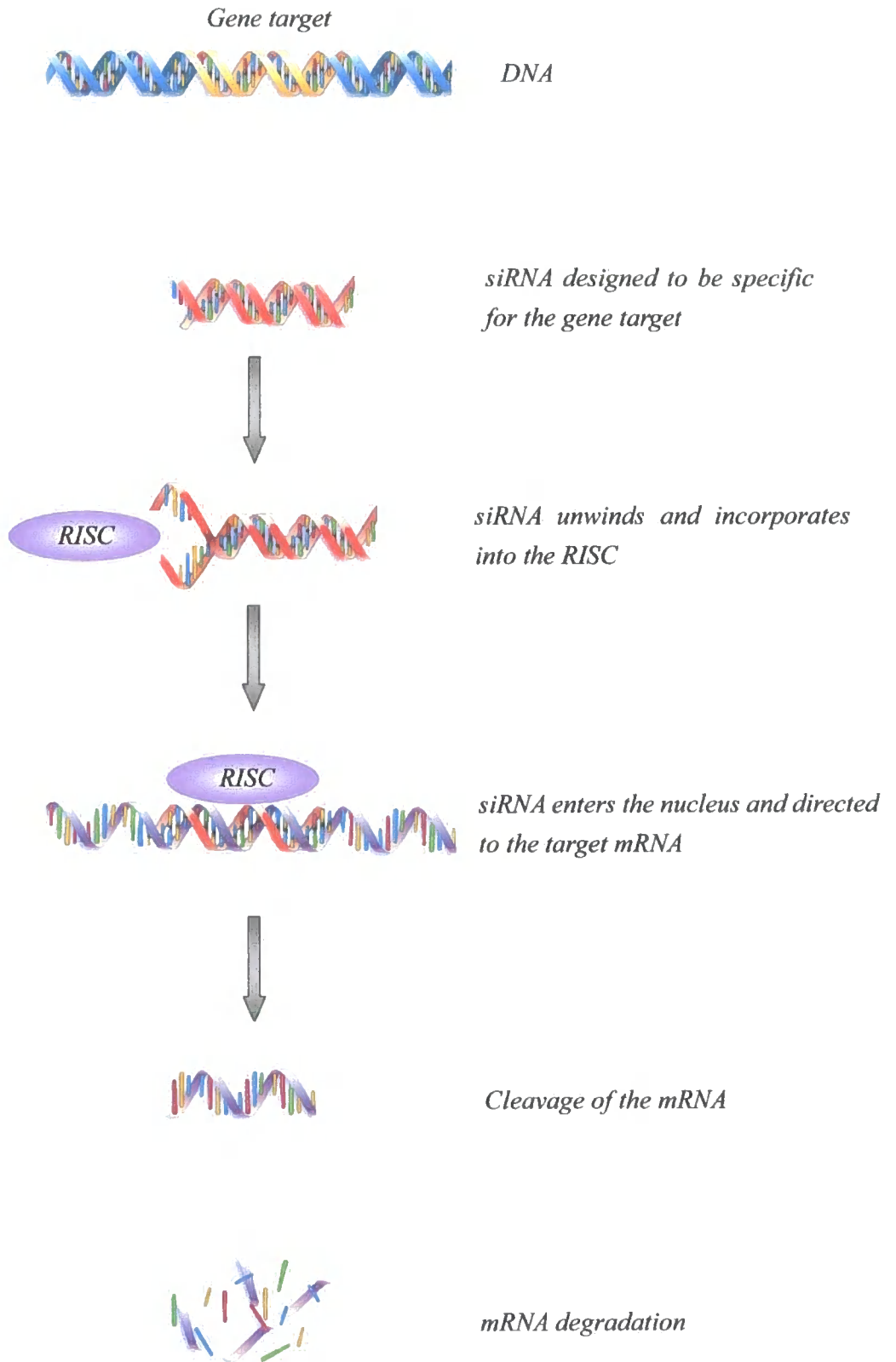


Figure 2.3: Mechanism of gene silencing by siRNA transfection.

Expression of individual genes can be inhibited by interfering with the transcribed mRNA. This is done via synthetic small double-stranded RNAs (siRNA). Within the cell, double stranded siRNA unwinds and is incorporated into the RISC (RNA induced silencing complex) forming a stable protein-RNA complex. The RISC then captures an endogenous mRNA molecule that complements the short siRNA sequence. If the pairing (native RNA and siRNA piece) is perfect, the native mRNA is severed and the mRNA undergoes degradation. If the pairing is less complete, however, the RISC complex binds to the mRNA and blocks ribosome movement along the native mRNA to stop translation, again resulting in no protein production.

2.16.1 Selection of siRNA sequence

Specific siRNA duplexes were designed to target the required DNA sequences which were selected from the open reading frame of periplakin, keratin 8 and plectin, in order to obtain sense and antisense strands with symmetric 3' overhangs of identical sequence. All sequences were submitted to a BLAST search against the human genome to ensure that only the desired mRNA was targeted.

siRNA oligo	Sequence	Target region	Knock down efficiency
PPL-1	AUGUAUAAAUGCUUGGCCtg	C-ter, exon22	>95%
PPL-2	UGCUCGUAUUUCCGGUUGGtg	N-ter, exon15	>95%
PPL-3	GAGGGUAUGUAUAAAUGCtt	C-ter, exon22	>95%
K8-1	CAUGUUGCUUCGAGCCGUCtt	N-ter head domain	50-80%
K8-2	AAUAUCCUCGUACUGUGCCtt	Rod, exon 6	>5%
Plectin-1	GGAAUGAUGACAUCGCUGAtt	C-ter Exon 5	>95%

Table 2.3: siRNA sequences used in this study.

2.16.2 Cell culture and transfection of siRNA

Wild type MCF-7, HaCaT, HeLa and Panc-1 cells were grown in normal DMEM medium for several days in T-75 flasks. One day before performing the transfection,

confluent (90%) cultures were trypsinised and diluted with fresh DMEM. Cells were seeded on sterile glass coverslips in 24-well plates in the presence of 10% FCS and 5% GPS. One day before transfection, cells were plated in 0.5 ml medium without antibiotics so that they would be 30-50% confluent at the time of transfection. siRNA transfections were carried out using oligofectamine reagent (Life Technology). Prior to transfection, 60 pmol siRNA was diluted in 50 μ l serum-free DMEM medium. At the same time, 3 μ l oligofectamine was diluted in 12 μ l serum-free DMEM medium and incubated for 5 minutes at room temperature. The diluted siRNA and the diluted oligofectamine were gently mixed and incubated for 20 minutes at room temperature to allow the siRNA-oligofectamine complex to form. The siRNA-oligofectamine mixture was then added to the culture dish well which was gently rocked back and forth. Complexes were removed from the cells and the media replaced after 24 hours, without affecting the transfection efficiency. Cells were processed for immunofluorescence, immunoblotting or scratch wound assay 48-96 hours after transfection.

2.17 Student's T-test

The Student's t-test was used to compare the quantitative data after siRNA transfections. Means of the scratch wound widths from 3 to 5 independent wounds were compared by using the Student's t-test at different time-points (10 minutes, 8 hours, 20 hours and 24 hours). The results were considered significant if the p value was less than 0.05 ($p < 0.05$).

Primary antibody	Species	Name	Source	IF	WB
α -tubulin	Mouse	Ab11304	Abcam	100	1000
Actin	Mouse	AC40	Sigma	NA	1000
Annexin A1	Rabbit	ANXA1	Abcam	200	N/A
Annexin A9	Chicken	ANXA9	Abcam	200	2000
Anti-HA	Rat	clone 3F10	Roche	200	200
Anti-HA	Rabbit	Ab9110	Abcam	200	200
Desmoplakin	Mouse	DP1/2	ICN	100	1000
Desmoplakin	Rabbit	AHP320	Serotec	100	1000
HA-probe	Rabbit	Y-11	Santa Cruz	200	500
Keratin 14	Rabbit	MK14	Covance	500	1000
Keratin 18	Mouse	Ab-2	Oncogene	100	1000
Keratin 8	Mouse	LE41	B.Lane	2	NA
Keratin 8	Mouse	ab9287 AE3	Abcam	100	1000
Keratin8 Pser431	Mouse	Ab-5 (5B3)	Strattech	100	1000
Periplakin	Rabbit	TD2	F. Watt	100	200
Periplakin	Rabbit	BOCZ-1	This study	500	500
Plectin	Goat	C-20	Santa Cruz	200	500
plectin isoform l	Rabbit	(LM2) plec1	L. McInroy	200	500
plectin isoform lf	Rabbit	(LM5) plec1f	L. McInroy	200	500
plectin isoform lk	Rabbit	(LM7) plec1k	L. McInroy	200	500
Vimentin	Rabbit	3052	R. Quinlan	NA	2000
Vinculin	Mouse	V-11-5	Sigma	500	100

Table 2.4: List of used primary antibodies used in this study. Immunofluorescence (IF), Western Blot (WB).

Secondary antibody	Species	Company	IF	WB
Rabbit	Anti-goat immunoglobulins-HRP	DakoCytomation		1:1000
Swine	Anti-rabbit immunoglobulins-HRP	DakoCytomation		1:1000
Goat	Anti-mouse immunoglobulins-HRP	DakoCytomation		1:1000
Donkey	Anti-chicken immunoglobulins-HRP	DakoCytomation		1:1000
Goat	Anti-chicken immunoglobulins-HRP	DakoCytomation		1:1000
Goat	Alexa-Fluor Anti-chicken IgG 594	Invitroge molecular probes	1:800	
Goat	Alexa-Fluor Anti-mouse IgG 594	Invitroge molecular probes	1:800	
Goat	Alexa-Fluor Anti-rabbit IgG 488	Invitroge molecular probes	1:800	
Goat	Alexa-Fluor Anti-mouse IgG 488	Invitroge molecular probes	1:800	
Donkey	Alexa-Fluor Anti-mouse IgG 488	Invitroge molecular probes	1:800	
Goat	Alexa-Fluor Anti-chicken IgG 488	Invitroge molecular probes	1:800	
Donkey	Alexa-Fluor Anti-mouse IgG 594	Invitroge molecular probes	1:800	
Donkey	Alexa-Fluor Anti-rabbit IgG 488	Invitroge molecular probes	1:800	
Donkey	Alexa-Fluor Anti-rabbit IgG 594	Invitrogen molecular probes	1:800	
Dapi		Invitrogen	1:1000	

Table 2.5: List of secondary antibodies used in this study. Immunofluorescence (IF), Western Blot (WB).

CHAPTER III

CO-IMMUNOPRECIPITATION OF PLECTIN AND ANNEXIN A9 WITH PERIPLAKIN IN MCF-7 EPITHELIAL CELLS

3.1. Introduction

Several studies have looked at the interactions of the periplakin C-terminal domain, but the molecular interactions of the N-terminus have been studied to a lesser extent.

The N-terminal domains of the cytolinker proteins display a high degree of structural homology and have been noted to be involved in a variety of interactions. The ABD of plectin can bind to actin and the same region is also able to bind to the first two cytoplasmic domains of integrin $\beta 4$ (fibronectin type III domains) contained within hemidesmosomes (Geerts *et al.*, 1999). Adjacent to the ABD is the plakin domain, which mediates further plectin interaction with $\beta 4$ integrin (Koster *et al.*, 2004). This plakin domain also contains the binding site for the hemidesmosomal transmembrane protein BPAG-2 (Koster *et al.*, 2003). The interaction of BPAG-1 with erbin is also known to occur at this site (Favre *et al.*, 2001). In desmoplakin, this plakin domain is known to interact with desmosomal proteins, such as plakophilin and plakoglobin, and also desmosomal cadherins (Bornslaeger *et al.*, 1996; Smith & Fuchs, 1998). In addition, the N-terminal head domain of desmoplakin has been suggested to play an important role in the development and maturation of the actin cytoskeleton (Huen *et al.*, 2002).

In contrast, the periplakin N-terminus has only two known protein binding partners. Recently, a yeast two hybrid analysis identified a protein called kazrin which interacts with the N-terminus of periplakin in keratinocytes (Groot *et al.*, 2004). Kazrin is not exclusively associated with desmosomes, as it also appears at the plasma membrane between desmosomes, as does periplakin. It has been proposed that kazrin might help to form heterodimers with envoplakin (Sonnenberg & Liem, 2007). Although the periplakin N-terminus is lacking in the ABD, periplakin has been shown to co-localise with cortical actin (DiColandrea *et al.*, 2000) in cultured keratinocytes. Based on F-actin co-sedimentation assays, it has been suggested that periplakin head domain may bind directly to actin filaments in MDCK cells (Kalinin *et al.*, 2005).

Thus, relatively little is known about the interacting partners of periplakin head domain and the mechanisms that regulate periplakin localization and function. This chapter reports the investigations of the molecular interactions of the periplakin $\frac{1}{2}$ N-

terminus by co-immunoprecipitation on a stably transfected cell line expressing HA-tagged periplakin N-terminus. Experiments in which tagged periplakin C-terminus was created and used to identify interacting partners have been performed in the past (van den Heuvel *et al.*, 2002; Beekman *et al.*, 2004). In this study, I focused on the N-terminus of periplakin and total cell extracts from MCF-7 cells were used to identify interacting partners. Following co-immunoprecipitation experiments, MALDI-TOF Mass Spectrometry was employed for the identification of periplakin binding proteins via peptide mass fingerprinting. Specifically, 1-D and 2-D gels were carefully examined and any bands or spots that might correspond to periplakin interacting proteins were selected from the gel and subjected to trypsin digestion. Two different sets of experiments identified plectin and annexin A9 as potential periplakin binding partners. These observations were also confirmed by Western blot analysis. Subsequent immunofluorescence labelling of the stable cell line and untransfected MCF-7 cells revealed co-localisation of the co-immunoprecipitated proteins.

The trypsin digestion, mass spectrometry and database search for identification of periplakin binding proteins were performed with the help of the Proteomics facility staff at the University of Durham.

3.2 Results

3.2.1 Demonstration of periplakin BOCZ-1 antibody specificity by siRNA transfection experiments

The antibody was characterised by siRNA transfection and immunoblotting to determine that it is specific for the endogenous protein to which it was raised. Depletion of periplakin by siRNA transfection in MCF-7 cells was carried out to downregulate the expression of the target protein. Total cell lysates of control and siRNA transfected cells were loaded onto gel and immunoblotted with BOCZ-1 periplakin antibody in a dilution of 1:500. While the 195kDa protein band was still present in untransfected and control transfected cells, the siRNA transfection reduced the signal when BOCZ-1 antibody was used for immunoblotting. These results confirm the specificity of the periplakin antibody (**Figure 3.1**).

3.2.2 Generation of ½ N-PPL overexpressing cell line

Previous immunofluorescence studies had demonstrated that periplakin N-terminus displays the same subcellular distribution as the whole protein in cultured human keratinocytes (DiColandrea *et al.*, 2000; Groot *et al.*, 2004). The first half of the N-terminus was used to identify unknown proteins that regulate periplakin localization to different membrane and cytoplasmic locations, as it is able to show all the properties previously demonstrated for the entire periplakin N-terminus. The periplakin ½ N construct used for stable transfection (DiColandrea *et al.*, 2000) contained subdomains NN, Z, Y and X (Ruhrberg & Watt, 1997) (**Figure 3.2**).

A stably transfected subclone of MCF-7 breast adenocarcinoma cell line referred to as MCF-7 ½ N-PPL was generated, overexpressing HA-tagged periplakin ½-N-terminus with a modified pCI-neo vector. Transfection was performed at 50% confluence. Selection medium, containing neomycin, was applied to cells two days after transfection and the cells were left to grow for three weeks with regular medium changes. The cells that remained alive carried the neomycin resistance gene, indicating successful transfection with the pCI-neo vector. Such colonies of cells were picked and grown in 96-well plates in the first instance and then in 24-well plates, 6 cm dishes, 10

cm dishes and T-75 flasks. A stably transfected control cell line carrying an empty pCI-Neo vector (MCF-7 EV) was also established.

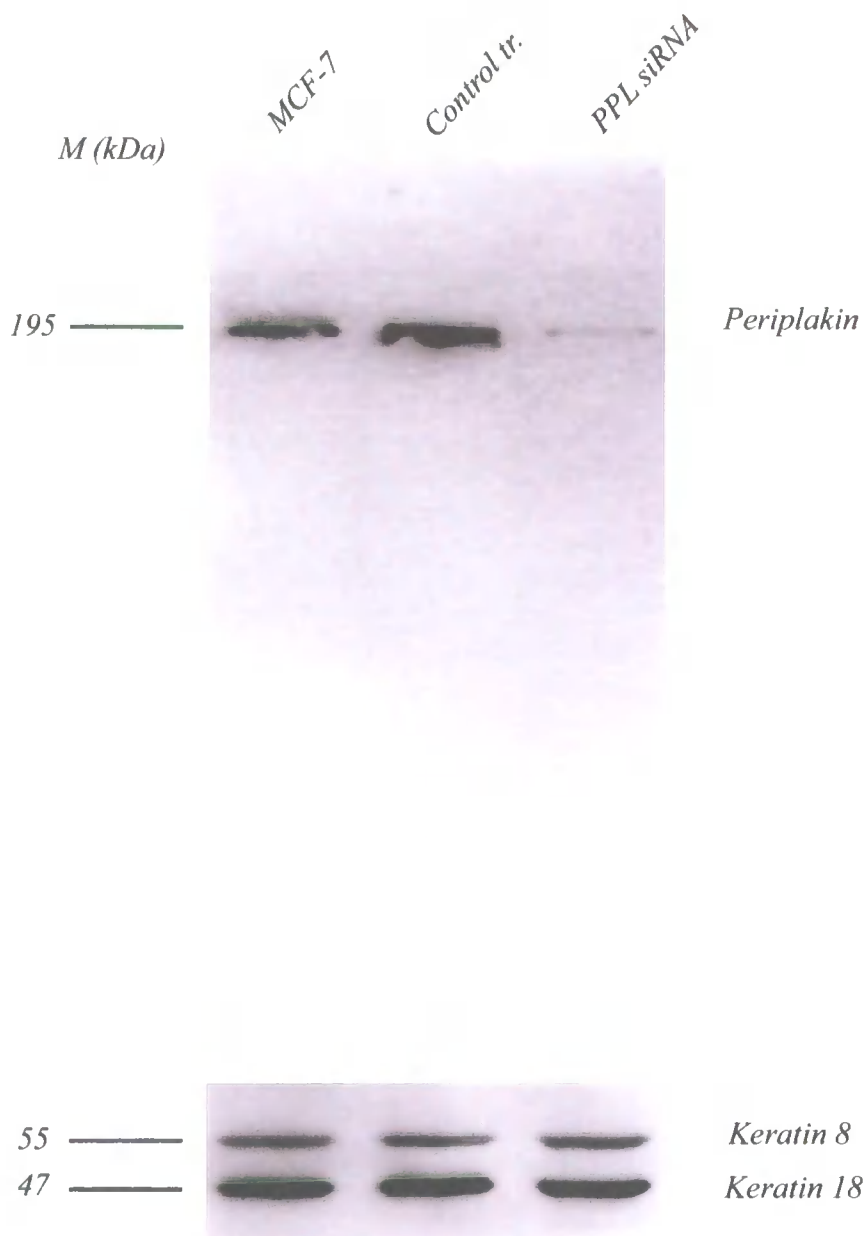
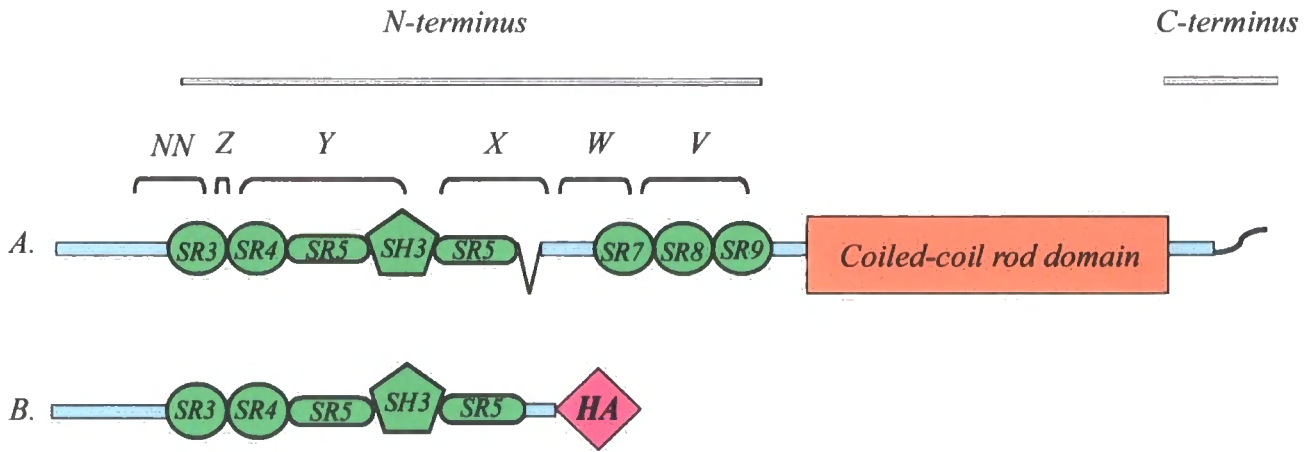


Figure 3.1: Confirmation of BOCZ-1 polyclonal antibody specificity by siRNA.

The polyclonal antibody, BOCZ-1 used here, was received from Cambridge Research Biochemicals. To test the specificity of the antibody, total cell extracts from untransfected, control transfected and periplakin siRNA transfected MCF-7 cells were immunoblotted with BOCZ-1 antibody (1:500 dilution). The antibody recognized a 195 kDa protein in control extracts while only a faint band is detected in the extracts from periplakin siRNA transfected cells.



Full length periplakin : 1-1756 aa

1/2N-terminus of periplakin : 1-496 aa

Figure 3.2: Schematic diagram of the 1/2N-periplakin construct used for stable cell line establishment.

A. Structure of periplakin. **B.** Structure of the periplakin construct containing HA-tagged periplakin half N-terminal domain used for the generation of MCF-7 1/2 N-PPL cell line.

3.2.3 Characterization of the stably transfected cell line

The periplakin ½ N-terminus construct was fused with hemagglutinin (HA) protein coding sequences within the plasmid to assist in intracellular localisation studies. The HA-tag is a common epitope tag, which consists of nine amino acids (YPYDVPDYA) derived from influenza virus and which is avidly recognized by anti-HA antibodies. Thus, the cellular localization of the tagged proteins can be determined and immunoprecipitation of the epitope-tagged proteins can be performed to identify interactions with other proteins, thus aiding further molecular characterization of the gene product. Furthermore, detection of HA-tagged proteins using anti-HA antibodies clearly distinguishes the expressed protein from the endogenous protein pool.

Immunoblot analysis and immunofluorescence staining on 8 different stably transfected cell colonies were performed in order to monitor the expression level and cellular distribution of the construct. All cell lines indicated constant expression level of the HA-tagged protein. Subcellular localisation of the ½ N-terminal periplakin domain in all 8 different cell lines showed reasonably similar decoration of the plasma membrane. A cell line which best mimicked the sub-cellular distribution of the endogenous periplakin protein was selected and utilized throughout this research (MCF-7 ½ N-PPL).

3.2.4 Cellular localization of HA-tagged protein and endogenous periplakin in MCF-7 cells by immunofluorescence microscopy

To investigate the expression level of the HA-tagged protein and the specificity of anti-HA antibody in the MCF-7 ½ N-PPL cell line, total cell lysates of confluent untransfected MCF-7, empty vector transfected (MCF-7 EV) and MCF-7 ½ N-PPL cells were loaded onto a gel. Immunoblotting with anti-HA antibody (monoclonal rat antibody, 1:200) resulted in a clear 53 kDa band in the MCF-7 ½ N-PPL cell line. In contrast, no bands were detected in the two control cell lines, suggesting that the antibody was specific for the HA-tag (**Figure 3.3 A**). As a control to demonstrate equal loading of lanes, the membrane was probed with a cytokeratin 8/18 mouse antibody (AB-2, Oncogene) at a dilution of 1:1000. The results obtained demonstrated the same amounts of keratin protein in all three lanes (**Figure 3.3 A**).

Whilst immunostaining of the N-terminus of periplakin was associated with the lateral plasma membranes, it also appeared in the cytoplasm to a lesser degree (**Figure 3.3 B**). This distribution was rather similar to that observed in keratinocytes where the endogenous periplakin demonstrated staining at the cell borders, but overexpression led to its redistribution towards IFs (Ma & Sun, 1986; Ruhrberg & Watt, 1997; DiColandrea *et al.*, 2000). The staining pattern which was obtained suggested that the periplakin might fulfil the same role in keratinocytes as in simple epithelia, as they share the same localization in both cases. Although it has been proposed that this domain of periplakin has the same distribution as the full-length protein in keratinocytes, it was important to confirm this in the simple epithelial cell line used throughout this study. When the subcellular localization of periplakin N-terminal construct and endogenous periplakin was investigated by double staining, it was found that both co-localised at cell borders. Double staining of HA-tagged protein (rat monoclonal, 1:200) and endogenous periplakin staining with BOCZ-1 antibody (rabbit polyclonal, 1:200) showed substantial co-localization in the stable cell line (**Figure 3.3 B**).

To further investigate the localization of these proteins at lateral plasma membranes, vertical confocal sections of the MCF-7 $\frac{1}{2}$ N-PPL cells (confocal axis: x-z) were produced. This profile was constructed by scanning a single line across the cells (in the x-axis) at different z-axis depths and displaying the series as a merged image. From the images obtained, it was evident that the periplakin $\frac{1}{2}$ N-HA constructs localised along the lateral cell border in the same way as the endogenous full-length protein (**Figure 3.3 C**).

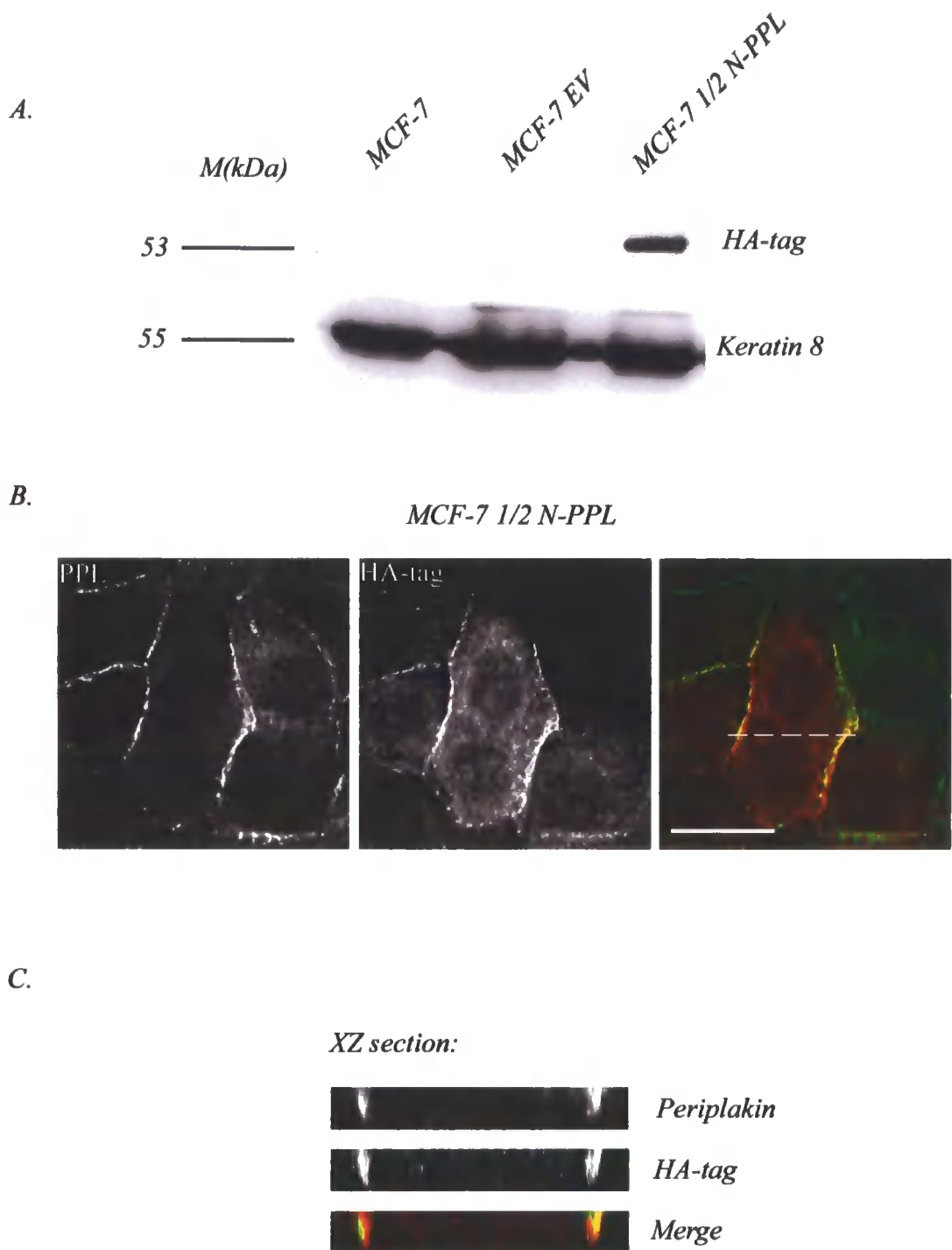


Figure 3.3: Co-localisation of the endogenous periplakin and the HA-tagged protein in MCF-7 1/2N-PPL cell line.

A. Western blot analysis showing the expression of the fusion protein. Cytokeratin 8 blot is shown as control for even loading. Anti-HA rabbit monoclonal antibody was used in 1:200 dilution and mouse monoclonal cytokeratin 8 antibody (Ab-2) in 1:1000 dilution. **B.** Co-localisation of the full length of periplakin (green) and the fusion protein (red channel) at cell borders (Scale bar equals 20 μm). **C.** Optical Z sectioning demonstrating colocalization of the endogenous periplakin and HA-tagged protein at the lateral cell borders in the MCF-7 1/2 N-PPL subclone. Dotted line in the merged image in panel A. indicates location of XZ slice.

3.2.5 Periplakin N-terminus does not co-localise with keratin intermediate filaments in MCF-7 cells

Immunofluorescence staining was also used to examine the localisation of the keratin 8 filaments and half-N terminal periplakin in MCF-7 $\frac{1}{2}$ N-PLL cell line, to ensure that overexpressed HA-tagged protein was not associated with intermediate filaments. This was important as keratin could potentially confound subsequent studies if it acted as a link between various immunoprecipitating proteins. Cells were grown to 50-60% confluence and fixed in methanol/acetone (1:1). The fixed cells were stained with anti-HA antibody (high affinity rat monoclonal antibody, clone 3F10, Roche) at a dilution of 1:200 and LE41 supernatant for keratin 8 detection at a dilution of 1:2. For the immunodetection of the HA-tagged protein and keratin 8, goat anti-rabbit Alexa-Fluor 488 (at a dilution of 1:800; Invitrogen Molecular Probes) and goat anti-mouse Alexa-Fluor 594 (at a dilution of 1:800, Invitrogen Molecular Probes) secondary antibodies were used, respectively. The results excluded significant co-localisation of the periplakin N-terminus with keratin filaments. (**Figure 3.4 A**) In addition, the stably transfected control cell line (MCF-7 EV) did not show any cell border staining with anti-HA antibody (**Figure 3.4 A**).

3.2.6 Solubility properties of the HA-tagged protein by biochemical fractionation

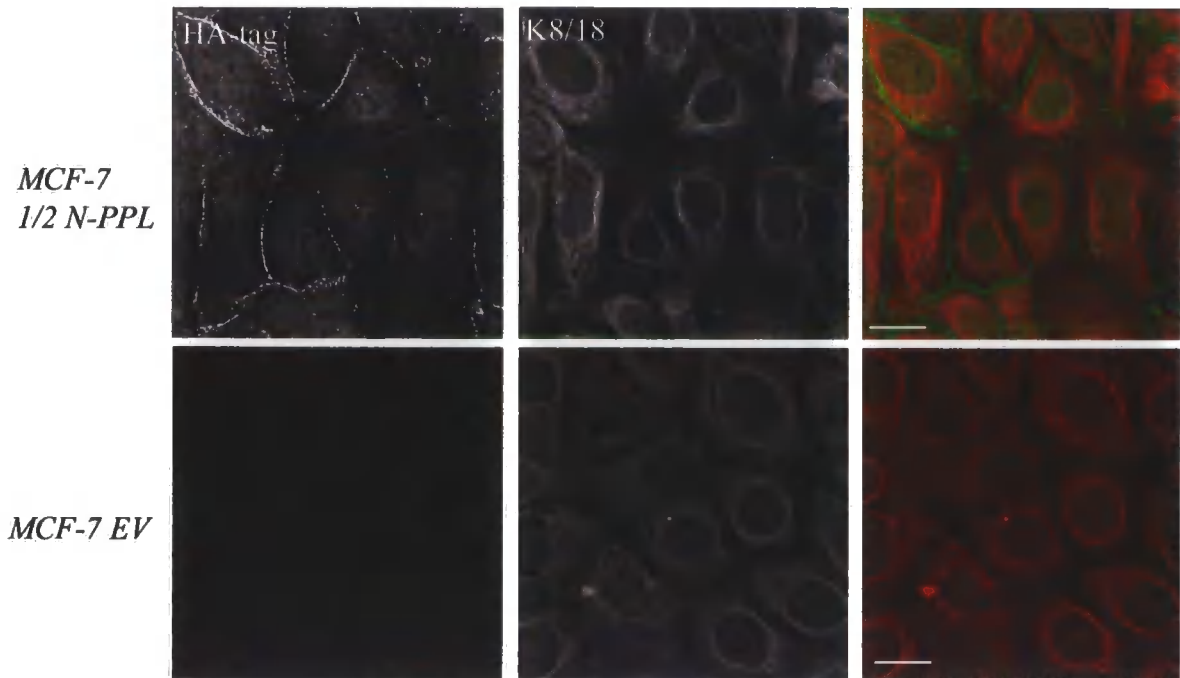
Although the immunofluorescence staining showed co-localization of the HA-tagged PPL NH₂-terminus with endogenous periplakin in the MCF-7 $\frac{1}{2}$ N-PPL cell line, this study further investigated the cellular compartments occupied by these proteins with regard to their solubility properties. The technique of subcellular biochemical fractionation isolates different proteins of the cell based on their biochemical solubility, enabling studies of their function and distribution. By sequential addition of different extraction buffers to a cell or cell pellet, proteins in different cell compartments can be selected. Cells were grown to 100% confluence and extracted with saponin buffer on ice. Saponin is a mild detergent, which allows extraction of cytosolic proteins (S1). Saponin insoluble proteins were pelleted and extracted in Triton-X100, a stronger detergent which solubilises plasma membrane associated proteins (S2) and finally the Triton-X100 insoluble pellet was extracted in urea, separating the insoluble cytoskeletal proteins in a third fraction (P3).

These cell fractionation experiments were performed on the MCF-7 ½ N-PPL cell line and an untransfected MCF-7 cell line, which served as a control. The half N-terminus of the plakin domain was detected at an expected molecular weight of 53 kDa in cytosolic (S1), Triton-soluble (S2) and Triton-insoluble (P3) fractions. Likewise, the 195-kDa endogenous periplakin was also present in all three fractions (**Figure 3.4 B**).

The representative Western blot shows that periplakin was distributed in approximately equal proportions in the saponin-soluble cytosolic pool, the Triton-X100 soluble pool and in the Triton-X insoluble cytoskeletal pool, whereas a lower proportion of the HA-tagged periplakin N-terminus was found in Triton insoluble cytoskeletal fraction (P3) compared to the distribution of the endogenous periplakin. This was probably due to the fact that the HA-tagged ½ N-PPL construct lacks in the IF-binding domain. This was also evident from the immunofluorescence study showing that the HA-tagged construct does not co-localise with keratin intermediate filaments in the cytoplasm (**Figure 3.4 A**).

From these data, it can be concluded that the MCF-7 ½ N-PPL cell line, expressing the half N-terminus of periplakin, is targeted to the plasma membrane where it co-localises with the endogenous periplakin at the lateral cell borders. Cellular fractionation studies also supported the finding that endogenous periplakin and ½ N-terminus of periplakin shows similar biochemical characteristics in MCF-7 cells being present in both soluble and insoluble fractions. Moreover, the fact that periplakin ½ N domain is not co-localised with the keratin intermediate filament network is likely to limit non-specific interactions in co-immunoprecipitation experiments. For these reasons, the chosen periplakin ½ N-terminal domain and the expressing cell line is a suitable model for identifying protein forming complexes with periplakin in all three subcellular fractions.

A.



B.

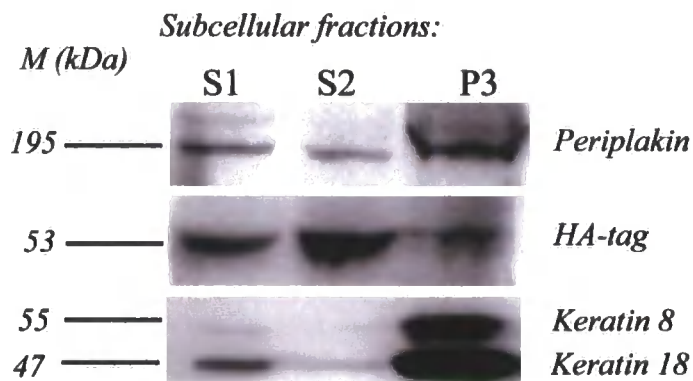


Figure 3.4: MCF-7 1/2 N-PPL cell line expressing the HA-tagged N-terminus of periplakin.
A. Immunofluorescence staining was carried out with anti-HA rabbit monoclonal antibody (Abcam) in 1:200 dilution and monoclonal anti-keratin 8/18 (LE41) in 1:2 dilution after methanol/acetone (1:1) fixation. HA-tagged protein (green) and epithelial cytokeratin 8/18 (red) are shown in MCF-7 1/2 N-PPL and control empty pCI-neo vector transfected (MCF-7 EV) cell lines. The images were taken as single optical slices and scale bar equals 20 μm . **B.** Subcellular distribution of endogenous periplakin, 1/2N-PPL-HA fusion protein and keratin 8/18 in the cytosolic fraction (S1), Triton soluble supernatant (S2) and in Triton insoluble pellet (P3) of MCF-7 1/2 N-PPL cells.

3.2.7 Identification of plectin and annexin A9 as co-immunoprecipitating partners of periplakin

Co-immunoprecipitation experiments to identify new binding partners for periplakin N-terminus were performed on confluent MCF-7 ½ N-PPL cells, empty vector transfected control cells (MCF-7 EV) and parental MCF-7 cells. Samples were immunoprecipitated with anti-HA antibody and were studied by electrophoresis after running them on SDS-PAGE and pre-cast gradient gels.

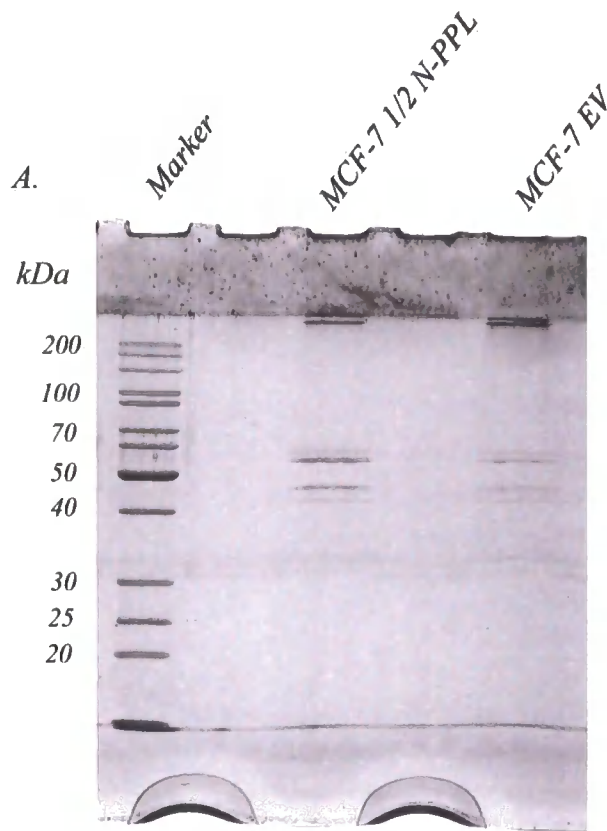
3.2.7.1 Strategy of co-immunoprecipitation experiments

1. As a first step, routine immunoprecipitation experiments were carried out following the protocol described in section 2.12.1 in order to demonstrate that HA-tag protein produced by the periplakin construct can be successfully precipitated with anti HA-antibodies.
2. Secondly, a high-affinity immobilized anti-HA antibody (anti-HA agarose) co-immunoprecipitation kit was optimised. This kit enabled the isolation and identification of tagged proteins, regardless of their expression levels, on regular 1-dimensional SDS-PAGE gels.
3. Finally, after co-immunoprecipitation experiments, the precipitated protein samples were examined on 2-dimensional gels.

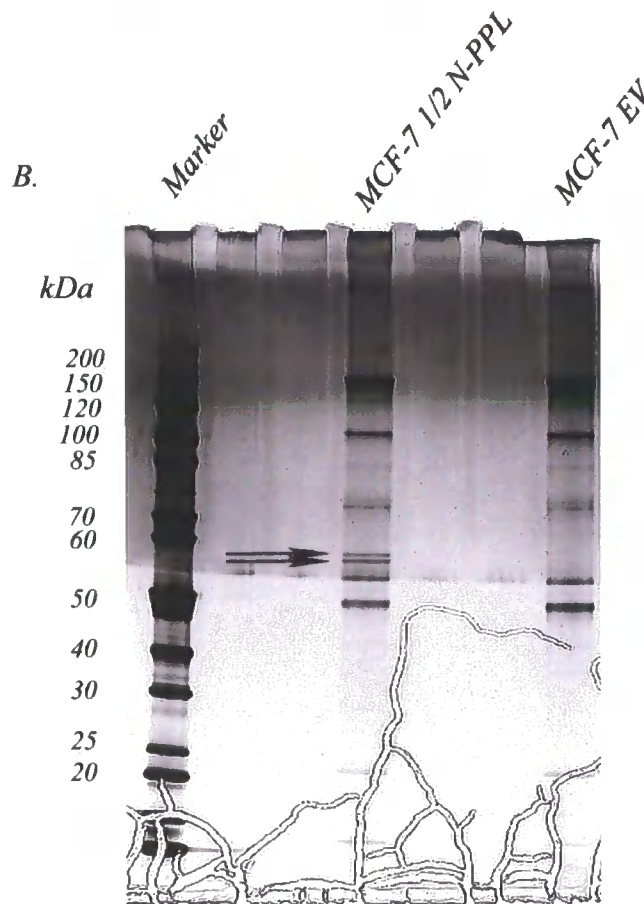
3.2.8 Successful precipitation of periplakin ½ N-terminus with HA-antibody

Following the immunoprecipitation steps with monoclonal rat anti-HA antibody (Roche) described in section 2.12.1 all samples were run on 1-dimensional 12% SDS-PAGE gels. The gels were stained with Coomassie-blue after electrophoresis. The immunoprecipitation experiment was repeated several times as described above but no specific proteins were detected in the elution fraction. To examine the possibility that proteins may have been washed away in the process, less stringent washing buffers were used. Afterwards all washing steps were carried out with the lysis buffer, which resulted in visible bands in the samples.

Initial Coomassie-blue staining failed to demonstrate unique bands in the MCF-7 ½ N-PPL samples when compared to empty vector transfected control cells (**Figure 3.5 A**). To increase the sensitivity of the staining and achieve better band separation, samples were run on pre-cast gradient gel 4-12% (Invitrogen) and were visualized by silver staining. Two bands that were unique to the MCF-7 ½ N-PPL sample when compared to controls were cut out from the gel and sent for identification. Both proteins were recognized as periplakin (**Figure 3.5 B**).



*12 % SDS-PAGE gel
Coomassie blue staining*



*4-12 % pre-cast gradient gel
Silver staining*

Figure 3.5: Immunoprecipitation experiment of the anti-HA antibody using IgG beads

A. MCF-7 $\frac{1}{2}$ N-PPL and control MCF-7 EV total cell lysates were pre-cleared and incubated with an anti-HA (3F10, 1:100 dilution, Roche) antibody and IgG beads overnight. Samples were separated on a 12% SDS-PAGE gel and stained with Coomassie blue. No bands were found exclusively in the MCF-7 $\frac{1}{2}$ N-PPL cell extract.

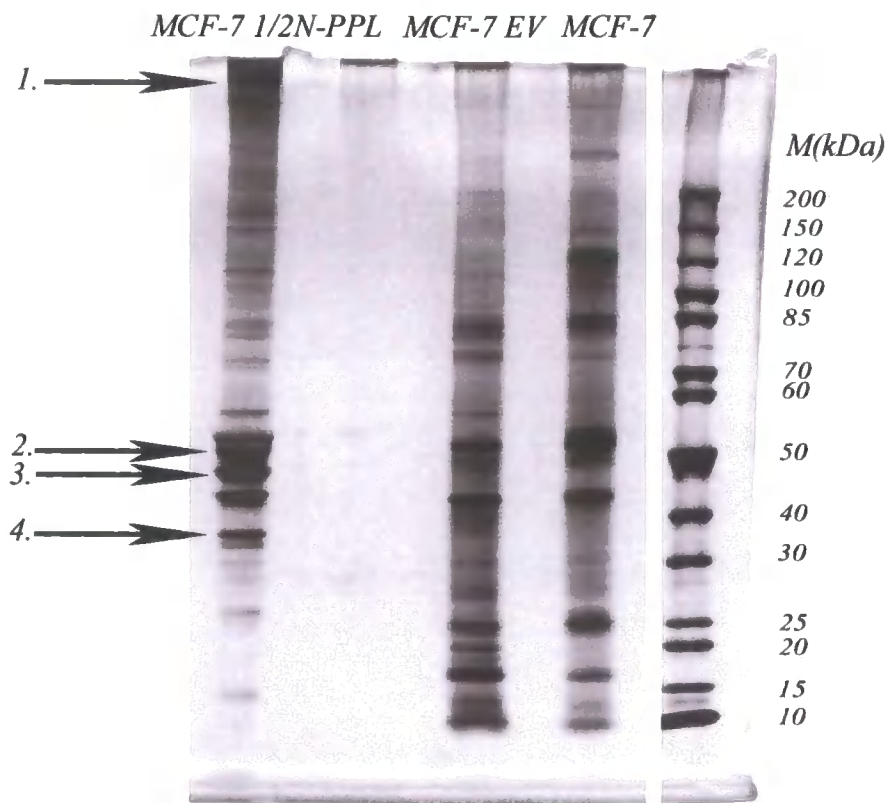
B. Following overnight immunoprecipitation procedures samples were separated on 4-12% pre-cast gel for better separation and silver staining was used for more sensitive visualisation. Arrowheads showing two bands in the MCF-7 $\frac{1}{2}$ N-PPL cell line approximately at a size of 53 kDa. Bands were cut out and both identified as periplakin by mass-spectrometry.

3.2.9 Use of the Mammalian HA Tag IP/Co-IP Kit, to identify periplakin interacting partners

To increase the chances to find new binding partners for the periplakin the ProFound™ Mammalian HA Tag IP/Co-IP Kit (Pierce) was used and the manufacturers protocol followed (section 2.12.2). As a result, four bands were identified as potential targets (**Figure 3.6**). Due to the low resolution, other faint bands were not excised from gel, as those would appear as no hits in Mascot search. Furthermore, some of the signals were very close to others, making it difficult to cut out a clear band. Bands that were present in both the control and sample lanes were ignored.

The results of the mass spectrometry from the 1D gel showed 4 bands, (**Figure 3.6 A**) one at high molecular weight, which had a very weak score resulting in no significant hits. Higher magnification shows this band in **Figure 3.6 B** when less sample was loaded. However, when a larger amount of sample was loaded on the gels, it became difficult to distinguish between different bands leading to protein mixtures. One of the clear hits obtained was the HA-tagged periplakin having the size of 53 kDa with the score of 123, Keratin 8 with the score of 71 and Annexin A9 with a yield of 176 peptide matches in a Mascot search (**Table 3.1**).

A.



B.

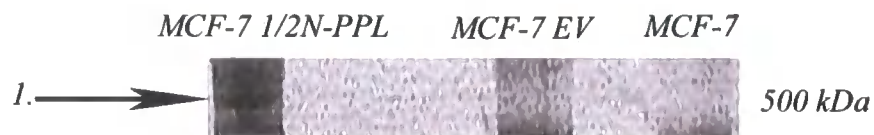


Figure 3.6: Co-immunoprecipitation of periplakin 1/2N-terminus with anti-HA-antibody and analysis using silver staining on 1D 4-12% gradient pre-cast gel.

A. MCF-7 1/2N-PPL: is the stable cell line overexpressing the HA-tagged N-terminal of periplakin. MCF-7 EV: is the control, empty transfected cell line. MCF-7 lane represent the untransfected cells. Bands marked with black arrow were cut out from the gel and sent for mass spectroscopy. **B.** Higher magnification of the 500 kDa co-immunoprecipitated protein in the MCF-7 1/2N-PPL cell line. (Numbers shown on the left were given to each sample that was sent for mass spectrometry.)

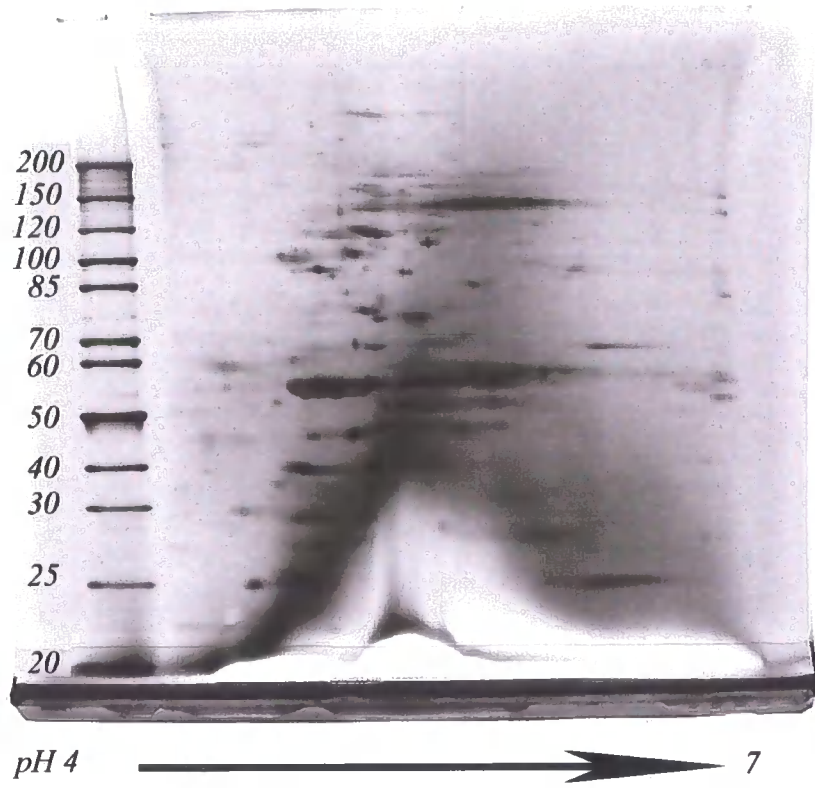
3.2.10 Results of the 2D gel electrophoresis

In order to obtain better results with the mass spectrometry, all samples were run on 2-D gels, allowing the similar-sized bands to be separated on the basis of their electric charge (isoelectric focusing, IEF).

Analysis of silver-stained 2D gels revealed 14 different unique spots. Each spot was cut out from the gel and sent for analysis by mass spectrometry (**Figure 3.7**). Interestingly, one of the unique spots (1), an approximately 500-kDa protein precipitated from MCF-7 ½ N-PPL extracts previously seen in 1D gels, was also present in the 2D gel. Mass spectrometry of tryptic peptides was used to identify this protein as plectin, another member of plakin cytolinkers family (Leung *et al.*, 2002; Jefferson *et al.*, 2004; Rezniczek *et al.*, 2003) as it yielded 67 exact peptide matches in a Mascot search (score 175, with protein scores greater than 77 considered significant, $p < 0.05$).

Many other selected spots resulted in no hits as shown in **table 3.1** below. Those giving significant scores included periplakin, as expected, because this protein is HA-tagged and therefore would obviously bind to the anti-HA antibody. Similarly, keratin 18, keratin 19, alpha-tubulin and beta-tubulin were pulled down as potential partners. However, these proteins were not considered direct interacting partners, as the periplakin N-terminus has no intermediate filament binding domain. Nevertheless, as plectin is able to bind intermediate filaments and microtubules, it is possible that these proteins were pulled down in a complex with plectin and not directly with the periplakin half N-terminus.

A.



B.

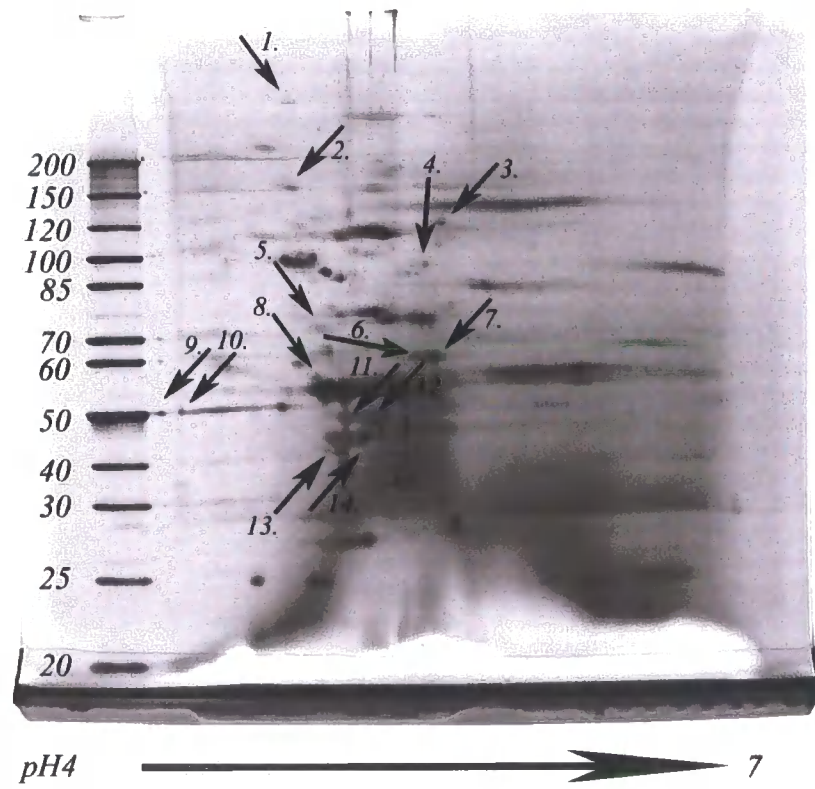


Figure 3.7: Co-immunoprecipitation of periplakin amino-terminus with anti-HA antibody analysed on silver stained 2-D gels

A. Immunoprecipitated proteins from control empty transfected MCF-7 cell line.

B. Immunoprecipitated proteins from MCF-7 $\frac{1}{2}$ N-PPL cell line. Arrows indicate protein spots that were sent for mass spectroscopic analysis. Black arrow below the gels indicates the separation as a function of pH.

Table 3.1: Summary of mass spectroscopic identification of proteins co-immunoprecipitating with periplakin N-terminus on 1D and 2D gels.

Sample	Highest match	Mass	Score
1-D gel bands			
1.			No hits
2.	Periplakin	205150	115
3.	Keratin 8	55874	71
4.	Annexin A9	37908	176
2-D gel spots			
1.	Plectin	520111	175
2.			No hits
3.			No hits
4.			No hits
5.			No hits
6.	Periplakin	205150	96
7.	Periplakin	205150	180
8.			No hits
9.	Keratin 18	47957	110
10.	Keratin 18	47957	89
11.	Keratin 19	44065	354
12.	Keratin 19	45870	190
13.	Beta-tubulin 2	50264	163
14.	Alpha-tubulin	58252	169

Table 3.1: Summary of mass spectroscopic identification of proteins co-immunoprecipitating with periplakin N-terminus on 1D and 2D gels.

Bands and spots that were selected from 1D and 2D gels (Figure 3.6, Figure 3.7) were identified by peptide mass fingerprinting. The table summarises the results showing the highest corresponding match, its molecular weight and its score.

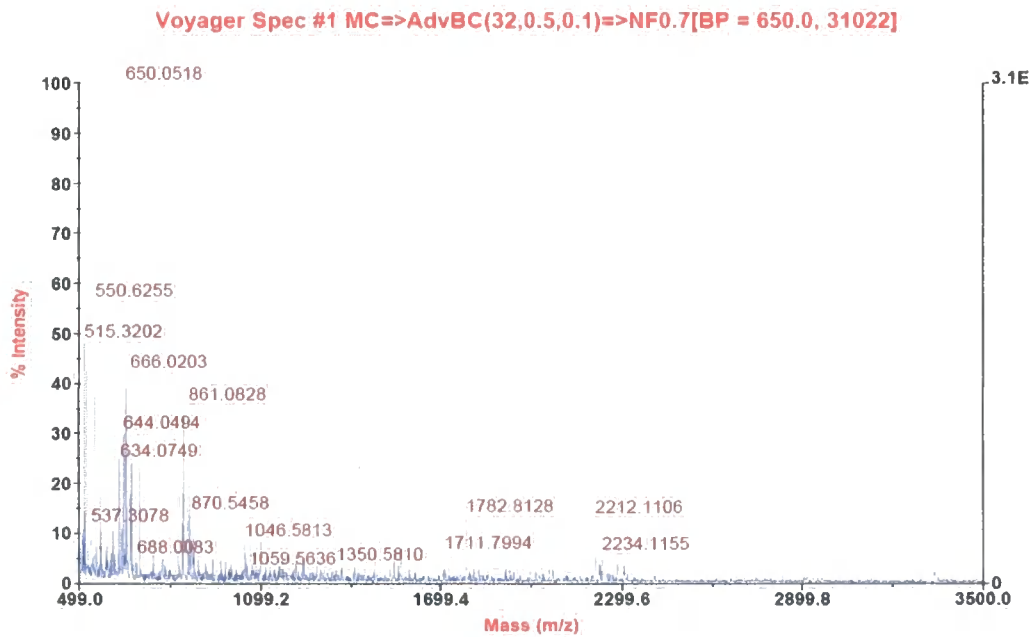


Figure 3.8: MS spectrum for the peptide identified as plectin by peptide mass fingerprinting.

From the spectrum the number of peptides generated after trypsin digestion and their corresponding mass/charge ratio (m/z) can be seen. Plectin was identified with a significant score of 175.

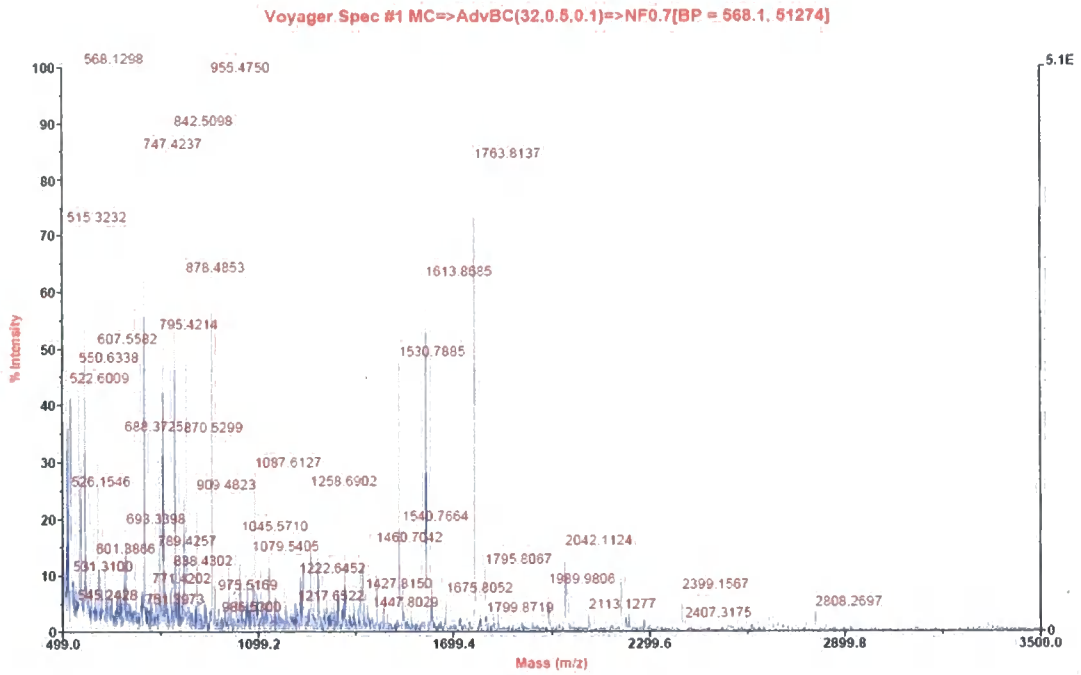


Figure 3.9: MS spectrum for the peptide identified as annexin A9 by peptide mass fingerprinting. From the spectrum the number of peptides generated after trypsin digestion and their corresponding mass/charge ratio (m/z) can be seen. Annexin A9 was identified with a significant score of 176.

On the basis of these results, two potential binding partners of the periplakin N-terminus in MCF-7 cells have been successfully identified.

3.2.11 Verification of co-immunoprecipitation of periplakin and plectin by Western blot analysis

The presence of HA-tagged periplakin N-terminus and plectin in the immunoprecipitated protein complexes was confirmed by immunoblotting. Samples were run on 3-8% pre-cast gradient gel (Invitrogen) and immunoblotted with anti-HA antibody (monoclonal rabbit antibody, Ab9110, 1:200, Abcam) and plectin (goat polyclonal, c-20, 1:200 Santa Cruz) antibody. **Figure 3.10 A** shows the HA-tagged periplakin domain in the MCF-7 ½ N-PPL cell line at a predicted size of 53 kDa next to the two control lanes, where no signal was detected. Immunoblotting with plectin (c-20) antibody revealed a plectin band only in the MCF-7 ½ N-PPL sample verifying the mass spectroscopic results (**Figure 3.10 B**). Plectin was not detected by immunoblotting in anti-HA immunoprecipitations of either of the empty vector transfected cell line or of untransfected MCF-7 cells, which confirms that plectin does not interact non-specifically with HA antibody conjugated beads used in the assays.

It was important to investigate whether the observed link between periplakin N-terminus and plectin is also applicable for the endogenous proteins. Therefore, co-immunoprecipitations were carried out on untransfected MCF-7 cells. The immunoprecipitation with plectin antibody (c-20) against endogenously expressed proteins was also successful producing a clear periplakin band after immunoblotting with BOCZ-1 antibody (**Figure 3.10 C**).

Standard immunoprecipitation of untransfected MCF-7 and HaCaT cell extracts with a different anti-plectin antibody, against the plectin-1f isoform, were also performed. The results demonstrated interaction between plectin and full-length periplakin. Consequently, the co-immunoprecipitation was not due to over-expression of the HA-tagged periplakin domain. (**Figure 3.10 D**) Moreover, no periplakin protein was immunoprecipitated with protein G beads alone as shown in the control lanes.

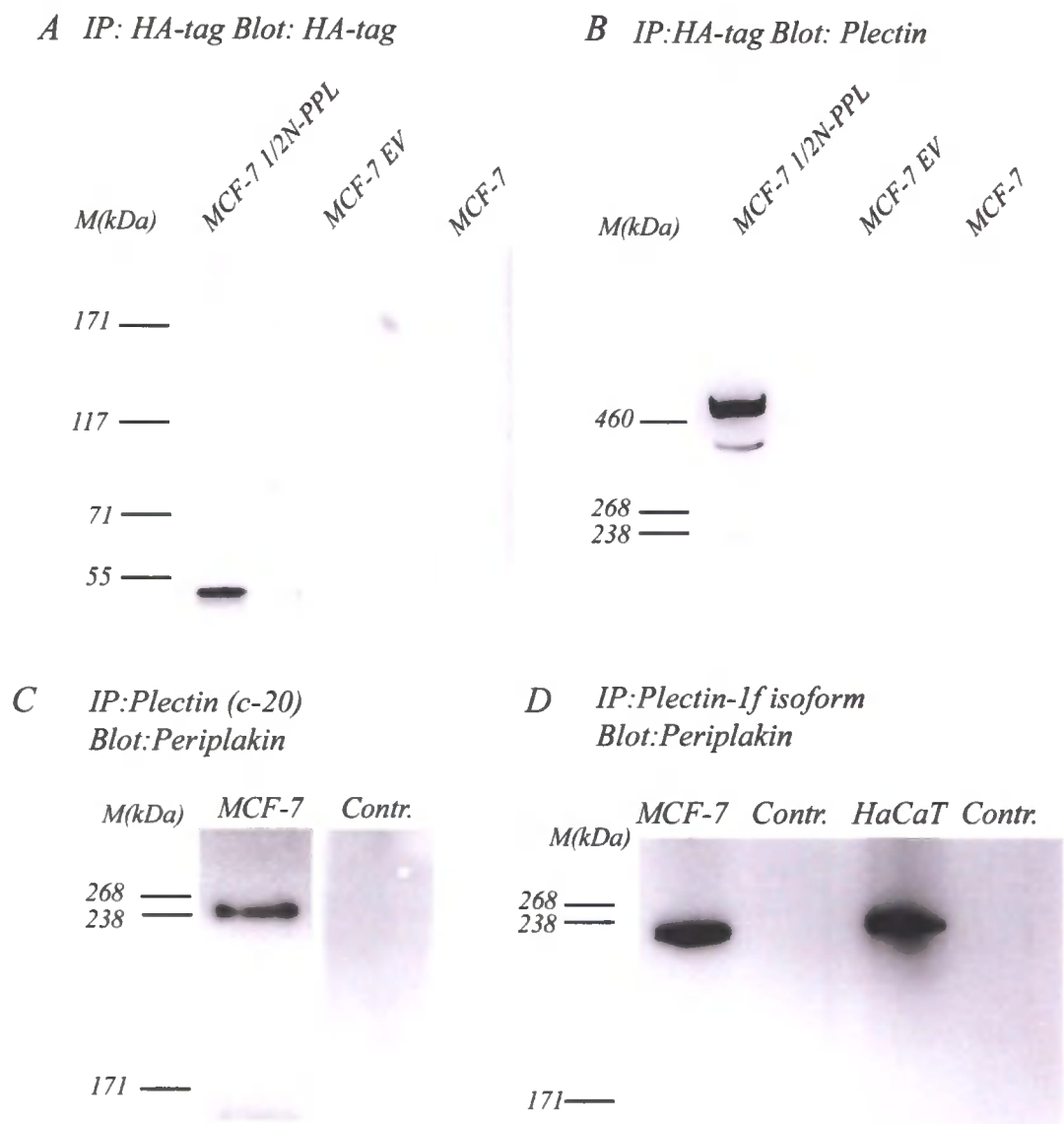


Figure 3.10: Co-immunoprecipitation of periplakin and plectin in MCF-7 1/2N-PPL cells.

A.,B. MCF-7 1/2 N-PPL cells, empty vector transfected control cells (MCF-7 EV) and untransfected cells were immunoprecipitated with an anti-HA antibody. Precipitated protein complexes were immunoblotted with anti-HA (Ab9110, 1:200 dilution, Abcam) and plectin (c-20) antibodies. Visible protein bands were found only in MCF-7 1/2N-PPL samples. **C.** Untransfected MCF-7 cell extracts were immunoprecipitated with plectin antibody (c-20, 1:100 dilution) against endogenous plectin and the samples were immunoblotted with BOCZ-1 periplakin antibody (1:500 dilution). **D.** Plectin-1f isoform specific rabbit polyclonal antibody (LM-5, 1:100 dilution) was used for immunoprecipitation in untransfected MCF-7 and HaCaT cells. IP samples were immunoblotted with BOCZ-1 periplakin antibody. Control lanes show that periplakin antibody does not interact non-specifically with protein G beads.

3.2.12 Co-localization of periplakin and plectin in MCF-7 and HaCaT cell line

Double staining was carried out to investigate the localisation of periplakin $\frac{1}{2}$ N-terminus and endogenous plectin. MCF-7 $\frac{1}{2}$ N-PPL cells were grown on coverslips to 80-90% confluence and immunolabelled for HA-tag (Ab9110, 1:200 dilution) and endogenous plectin (c-20, 1:200 dilution). The immunofluorescence study revealed that both proteins were mainly localized to cell borders, which, in the case of HA-tagged periplakin, was expected in light of previous investigations. This co-localisation at cell borders was more evident in MCF-7 $\frac{1}{2}$ N-PPL cells with greater confluence (**Figure 3.11 A**).

Having demonstrated co-localization between the HA-tagged periplakin head domain and endogenous plectin in the MCF-7 $\frac{1}{2}$ N-PPL cell line, it was necessary to explore whether the native proteins co-localized in un-transfected MCF-7 cells. Double immunofluorescence labelling was repeated using antibodies against endogenous periplakin (BOCZ-1) and plectin (c-20) in untransfected MCF-7 cells and in HaCaT keratinocytes.

These immunofluorescence studies demonstrated that the endogenous periplakin and plectin proteins mainly co-localised at cell membranes in MCF-7 cells although co-localisation was also detected in the cytoplasmic, cytoskeletal region in HaCaT cells (**Figure 3.11 B**). Immunofluorescence microscopy also revealed that the cell membrane localisation of periplakin and plectin was much more evident in MCF-7 cells than in HaCaT cells, where the amount of periplakin labelling seen at the cell borders increased after the formation of a confluent monolayer, as well as during differentiation.

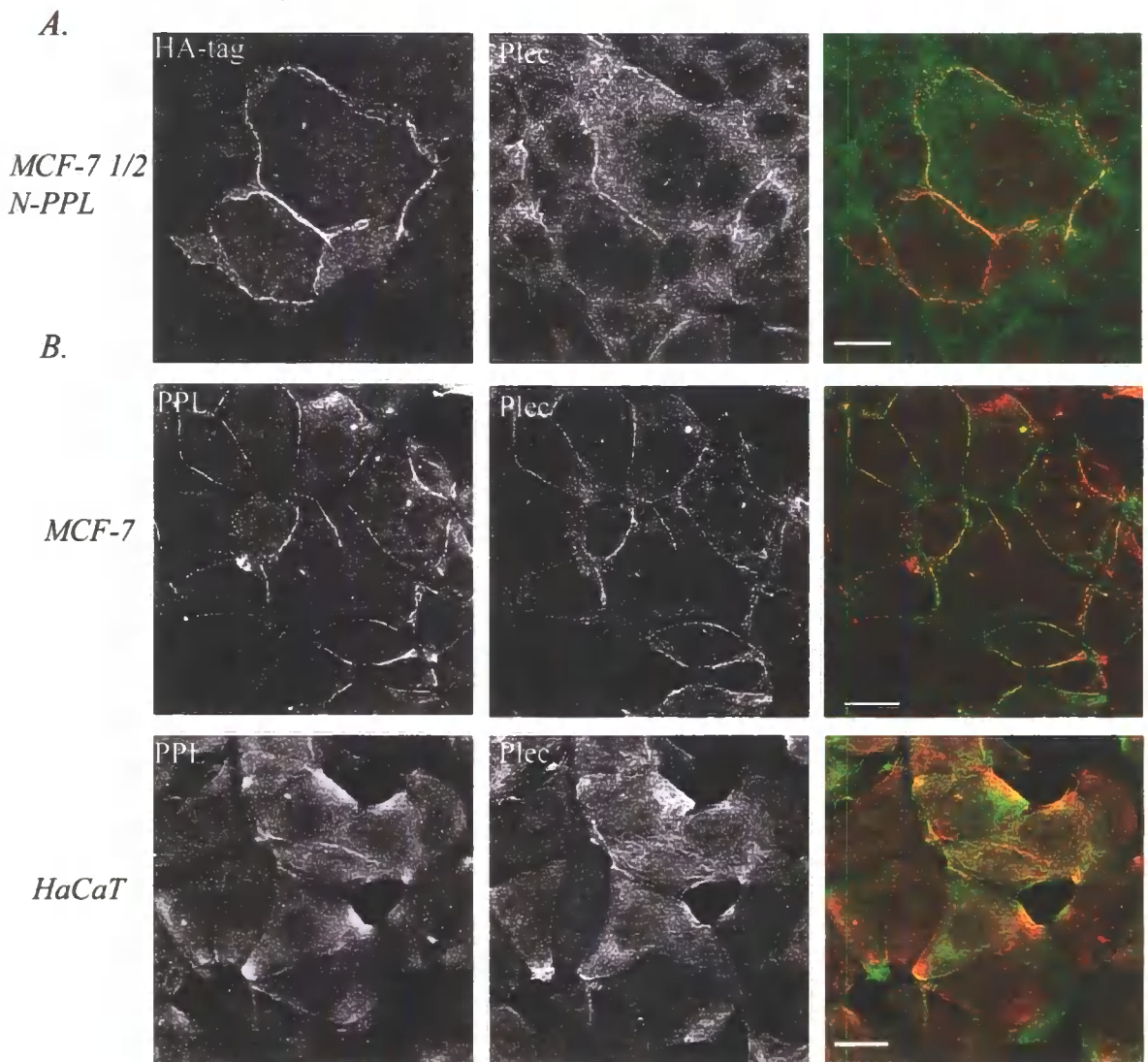


Figure 3.11: Co-staining of MCF-7 and HaCaT cell with periplakin and plectin.

A. Immunofluorescence staining of plectin (c-20 antibody, green) and HA-tagged periplakin N-terminus (red) in MCF-7 1/2N-PPL cell line. The images were captured as single optical section. **B.** Immunofluorescence staining of periplakin (BOCZ-1 antibody, green) and plectin (c-20 antibody, red) in untransfected MCF-7 epithelial and HaCaT keratinocyte cell line (Scale bar equals 20 μm).

3.2.13 The first 133 amino acids of the periplakin N-terminus are required for co-localization with plectin in simple epithelial cells

In order to further map the region in the periplakin N-terminus that is required for co-localisation with plectin, five different deletion constructs were used, which were kind gift from Dr. Lisa Sevilla (Keratinocyte Laboratory, Cancer Research UK, London). **Figure 3.12** shows schematic diagrams of all five N-terminal subdomain deletion constructs used in this experiment.

Transient transfections with the periplakin deletion constructs were carried out when cells reached 50% confluence. After the transfection, cells were grown for two days, fixed and stained with anti-HA antibody (Ab9110, 1:200 dilution) and plectin (c-20, 1:200 dilution) antibody.

The results obtained by immunofluorescence indicated that periplakin N terminal domains comprising the first 63 amino acid residues and the first 80 amino acid residues were not targeted to cells borders and did not co-localise with cytoplasmic plectin (**Figure 3.13**). However, the constructs containing the first 133 amino acid residues (encoding the entire NN subdomain) were localized at cell borders, where they partially co-localised with plectin. Surprisingly, a construct which lacked the first 16 amino acid but had the remainder of the first 133 amino acid residues could still be identified at cell borders. However, in keratinocytes, all of the first 133 residues (PPL-133 construct) were required for periplakin to localize efficiently to the plasma membrane and associate with the cortical actin (Groot et al., 2004).

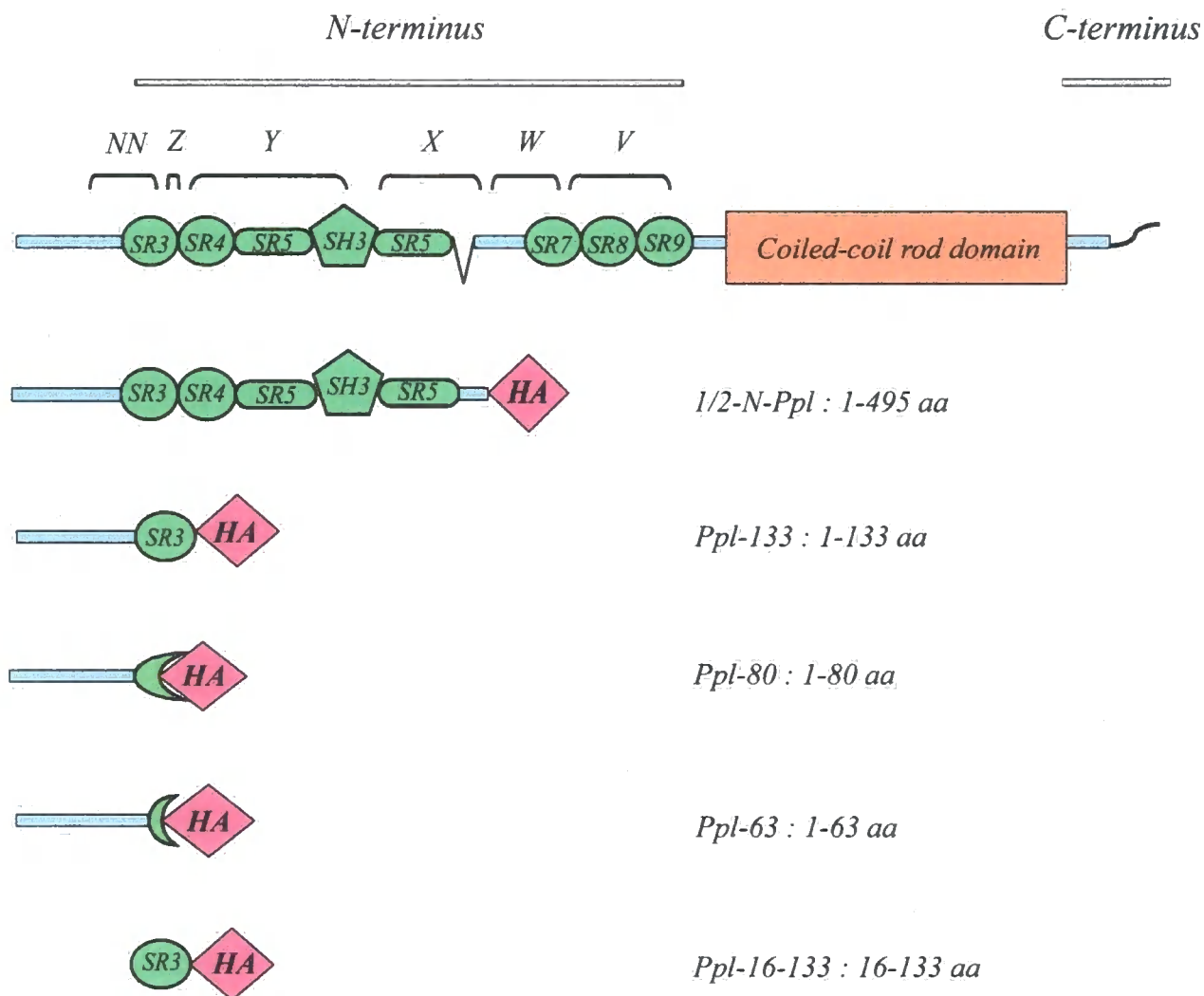


Figure 3.12: Schematic diagram of N-terminal subdomains of the HA-tagged deletion constructs (Groot et al., 2004).

Top part of the figure details the periplakin in full length. The subsequent five schematic drawings detail different constructs that were used for transient transfections (namely: *1/2N-Ppl*, *Ppl-133*, *Ppl-80*, *Ppl-63* and *Ppl-16-133*).

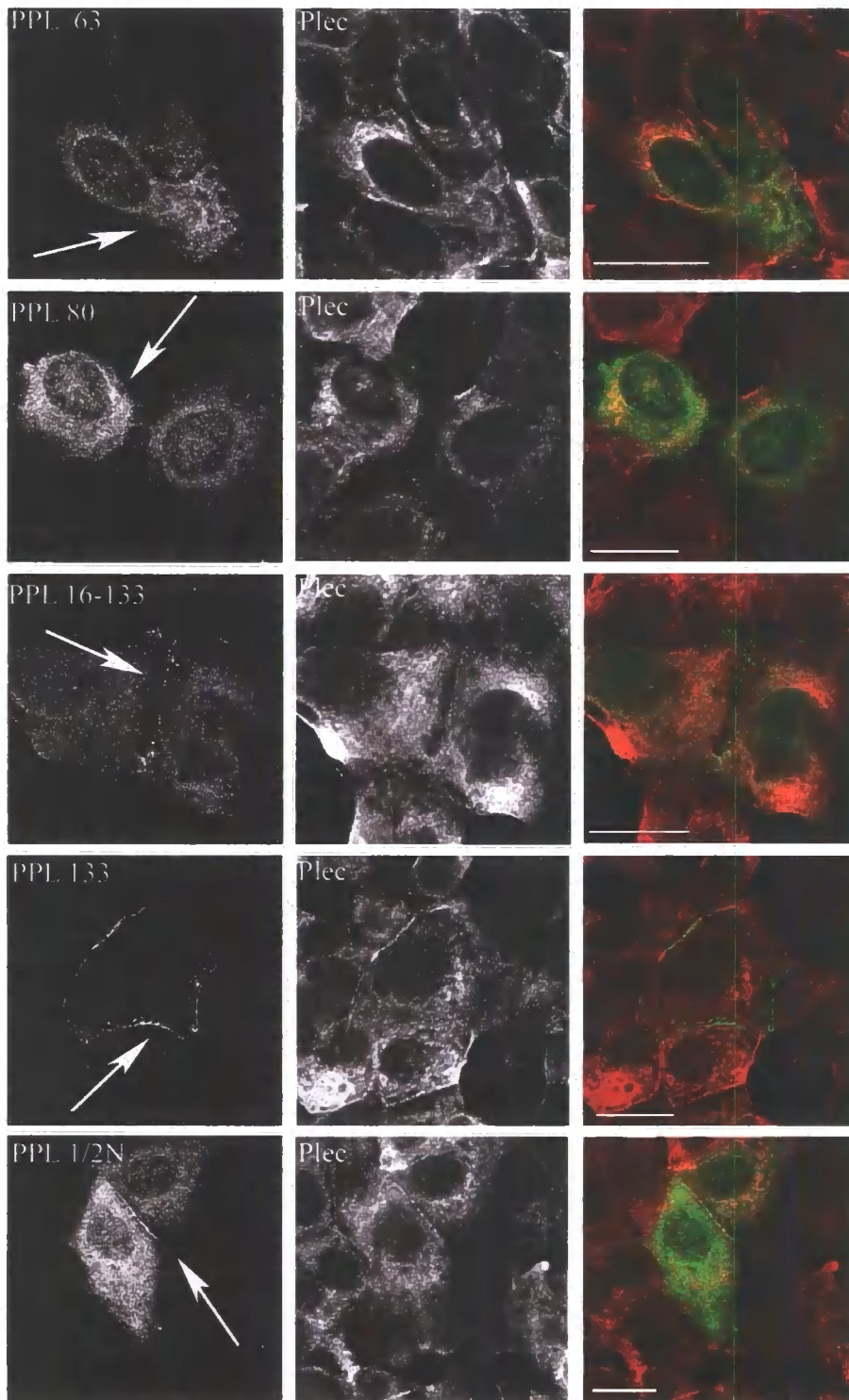


Figure 3.13: Localization of periplakin deletion constructs in MCF-7 cells.

Representative images of MCF-7 cells were transiently transfected with the indicated constructs (see Figure 3.12. for clarification) and stained with anti-HA (green) and plectin (red) antibodies after methanol/acetone fixation. It appears that PPL-133, PPL-16-133 and PPL 1/2N constructs are targeted to lateral plasma membranes and partially co-localise with plectin. Arrowheads indicate the main localisation of the constructs (scale bars equal 20 μm).

3.2.14. Co-localisation of plectin isoforms with periplakin

In the previous section, different constructs of the periplakin N-terminus demonstrated co-localization with the endogenous plectin protein in MCF-7 cells. However, alternative splicing is known to generate an extensive array of plectin isoforms. Specifically, nine alternative first exons are used to encode N-terminal plectin isoforms that are targeted to distinct subcellular locations (Rezniczek *et al.*, 2003). This work therefore sought to determine which of these alternative isoforms is able to co-localise with endogenous periplakin protein. Polyclonal isoform-specific antibodies against plectin-1 (this study), plectin-1f (this study) and plectin-1k (McInroy and Määttä, unpublished data) were generated (**Figure 3.14**).

To characterize these isoform specific antibodies, total protein extracts of control MCF-7 cells and plectin siRNA transfected MCF-7 cells were generated. Immunoblotting was performed to confirm that antibodies generated against plectin-1, plectin-1f and plectin-1k recognised plectin and that this could be prevented by siRNA knock-down of plectin protein. Actin was used as a reference to standardise loading, but Ponceau S staining and the BCA protein assay were also used to ensure accurate protein loadings for each lane (**Figure 3.15 A**). In some cases, such as for the c-20 and plectin-1 (LM-1) antibodies, two high-molecular weight proteins were detected. It is possible that the lower band observed in immunoblotting using C-terminal plectin antibodies could be a rodless plectin splice variant which lacks exon 31 (Elliott *et al.*, 1997).

All the isoform-specific plectin antibodies studied were able to co-localise with periplakin at cell borders (**Figure 3.15 B**) suggesting that co-localisation of plectin and periplakin is not restricted to only one particular plectin isoform. In addition to investigating the MCF-7 cells, human epidermis was also studied to see if these proteins co-localise within the same epidermal layers *in vivo*, as their potential functions may specially restrict their expression within the skin. For example, a major function of plectin in the epidermis is to connect keratin filaments to $\alpha 6\beta 4$ integrin in hemidesmosomes (Litjens *et al.*, 2006). Periplakin expression, however, is upregulated upon keratinocyte differentiation and the strong expression of periplakin at cell borders of suprabasal cells is consistent with its proposed role as a scaffold protein involved in cornified envelope assembly (Ruhrberg & Watt, 1997; DiColandrea *et al.*, 2000). The *in vivo* analysis revealed low levels of plectin-1 staining in the suprabasal layers - apart

from some individual cells in the spinous layer. In contrast, both plectin-1f and 1k antibodies localised to the cell borders of differentiated epidermal cell layers in a similar manner as periplakin. **(Figure 3.16)** Thus, it appears that a specific subset of plectin splice isoforms show similar distribution to periplakin in differentiated epidermal keratinocytes within the granular and cornified cell layers of the human epidermis.

Plectin

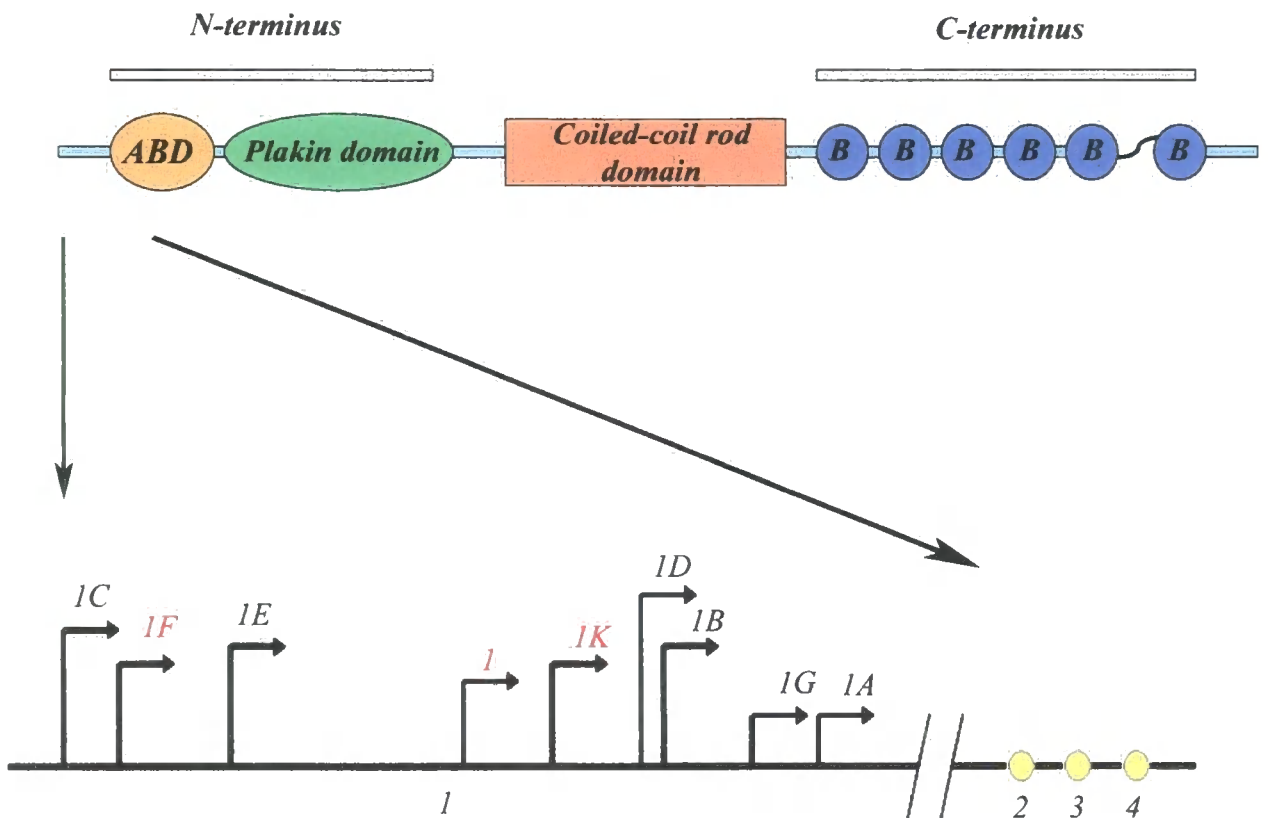
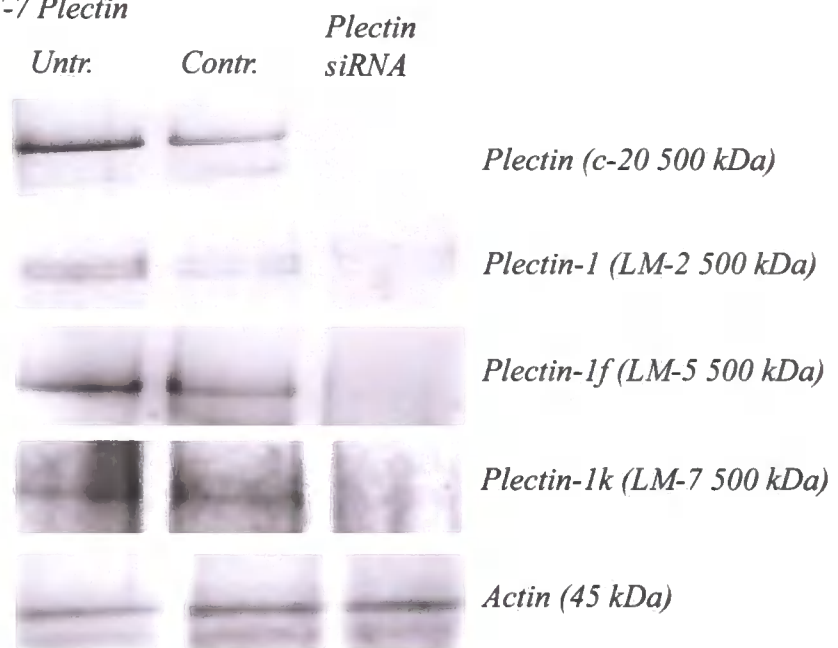


Figure 3.14: Schematic diagram illustrating human N-terminal plectin isoforms.

The 'map' of the human plectin gene presented here indicates the localisation of the 9 encoding first exons. All human N-terminal first exons spliced directly into exon 2. Plectin 1, 1F, and 1K isoforms shown in red were investigated in this study. Plectin 1K is a new isoform identified by Dr. Lorna McInroy.

A.

WB: MCF-7 Plectin



B.

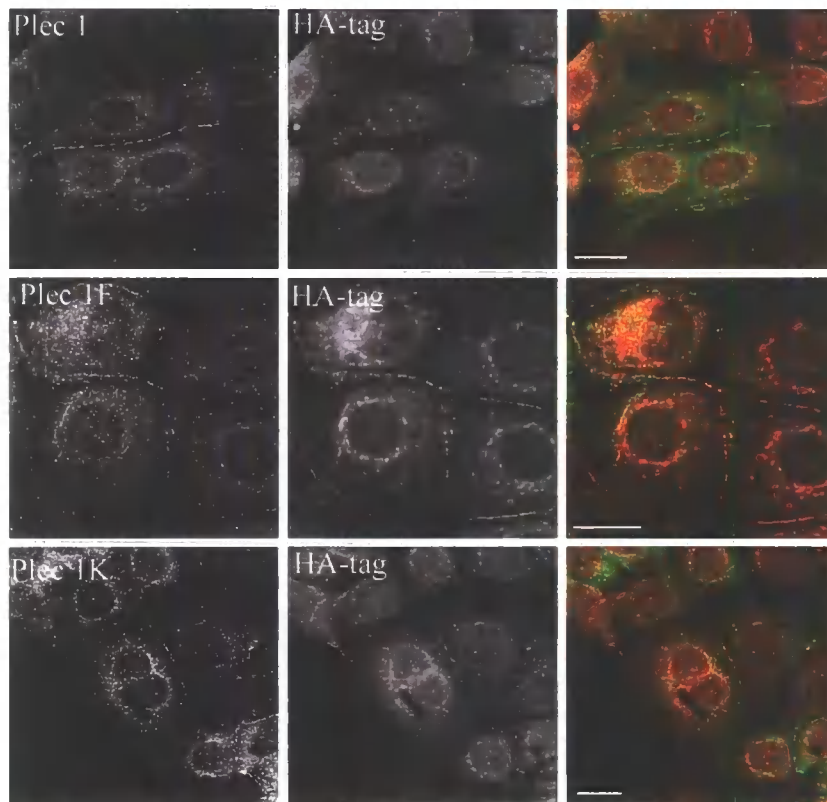


Figure 3.15: Co-localisation of periplakin and N-terminal plectin isoforms.

A. Western blot analysis of plectin isoform specific antibodies in plectin siRNA transfected cells. LM-2, LM-5 and LM-7 recognize plectin in untransfected MCF-7 cells (Untr.) and in control transfected cells with control siRNA (Contr.), while only very faint bands can be detected in plectin siRNA transfected cells. **B.** Immunofluorescence staining of plectin isoforms (green) and HA-tagged 1/2N-terminal periplakin (red) in MCF-7 1/2N-PPL cells. Plectin-1f (LM-5 antibody, top row) along with Plectin-1 (LM-1, middle row) and plectin-1k (LM-7, bottom row) were localised at the plasma membrane in MCF-7 1/2 N-PPL cells (scale bar equals 20 μ m).

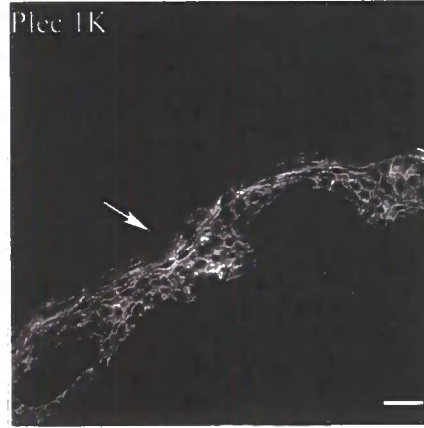
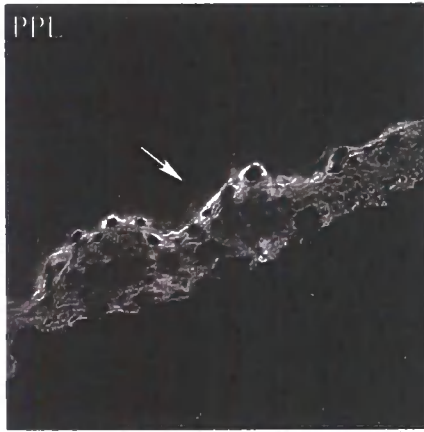


Figure 3.16: Immunofluorescence staining of human skin.

Skin sections stained with periplakin (TD-2,) and plectin isoform antibodies, plectin-1 (LM-1), plectin-1f (LM-5) and plectin-1k (LM-7). Arrows indicate prominent membrane staining in upper suprabasal cell layers with periplakin, plectin-1f and plectin-1k antibodies. Scale bar = 20 μ m.

3.2.15 Investigation of Annexin A9 as a potential periplakin interacting partner

Immunoprecipitation experiments on MCF-7 ½ N-PPL simple epithelial cell line indicated that the amino terminus of periplakin was capable of interacting with a protein approximately 34 kDa in size. Mass spectrometry of tryptic peptides identified this protein as Annexin A9, a Ca²⁺ and phospholipid binding protein (yielding 60 exact peptide matches and scoring 176 in a Mascot search. Protein scores greater than 77 were considered significant, $p < 0.05$).

3.2.16 Confirmation of co-immunoprecipitation of periplakin and annexin A9 by Western blot analysis

In order to validate the co-immunoprecipitation of periplakin and annexin A9 , the immunoprecipitation step was repeated. The immunoprecipitated proteins were loaded on 12% pre-cast gel (Invitrogen) and to provide controls, immunoprecipitation was carried out in a similar manner on untransfected and empty transfected MCF-7 cells. Following electrophoresis, proteins were blotted onto nitrocellulose membrane and probed with anti-HA (Ab9110, Abcam) and Annexin A9 (chicken polyclonal, ANXA9, Abcam) antibodies at dilutions of 1:200 and 1:2000, respectively. As expected, annexin A9 protein was present in the immunoprecipitated sample derived from MCF-7 ½ N-PPL cells, but missing in both empty vector and untransfected immunoprecipitation samples (**Figure 3.17 A**). Similarly, an HA-tagged periplakin N-terminus band was clearly seen in the sample from the MCF-7 ½ N-PPL cell line and was absent from both control samples.

3.2.17 Expression levels of annexin A9 protein in untransfected, empty transfected and MCF-7 C6-PPL cell lines

Annexin A9 has not been extensively studied. Thus, having immunoprecipitated the protein, (**Figure 3.17 A**) the relative levels of annexin A9 expression were investigated. Total cell extracts from untransfected, empty transfected and MCF-7 ½ N-PPL cell lines were subjected to gel electrophoresis and Western blotting. Immunoblotting for HA-tagged protein, which was only present in the cells overexpressing periplakin N-terminus, and annexin A9 demonstrated reasonably constant annexin A9 levels in all three cell lines (**Figure 3.17 B**).

3.2.18 Annexin A9 found in mostly in the Triton-X100 insoluble cytoskeletal fraction in MCF-7 cells

To further investigate the sub-cellular localisation of annexin A9 in MCF-7 cells, sub-cellular biochemical fractionation experiments were performed using 100% confluent monolayers. This confirmed the presence of annexin A9 in the cytoplasmic, Triton-soluble cytoskeletal and Triton-insoluble cytoskeletal fractions, but with a greater proportion in the (P3) cytoskeletal fraction than in the soluble fractions. Immunoblot analysis with BOCZ-1 periplakin antibody revealed similar subcellular distribution (**Figure 3.18 A**). This observation also suggests that the amount of periplakin in the cytoskeletal fraction increases once cells have formed a confluent monolayer, while in less confluent circumstances the quantity of periplakin is almost equally distributed throughout all three fractions (previously shown in **Figure 3.5 B**).

Further experiments were carried out to investigate whether the overexpression of periplakin N-terminus would alter the annexin A9 protein level and distribution. For this comparison, untransfected, empty transfected and periplakin ½ N-terminal overexpressing cell lines were studied. Following biochemical detergent extraction, protein fractions were run on 12% pre-cast gels. Immunoblotting with the annexin A9 antibody is shown in **figure 3.18 B**. This analysis demonstrated that overexpression of the periplakin amino terminus in MCF-7 cells did not alter annexin A9 expression level in any subcellular fraction.

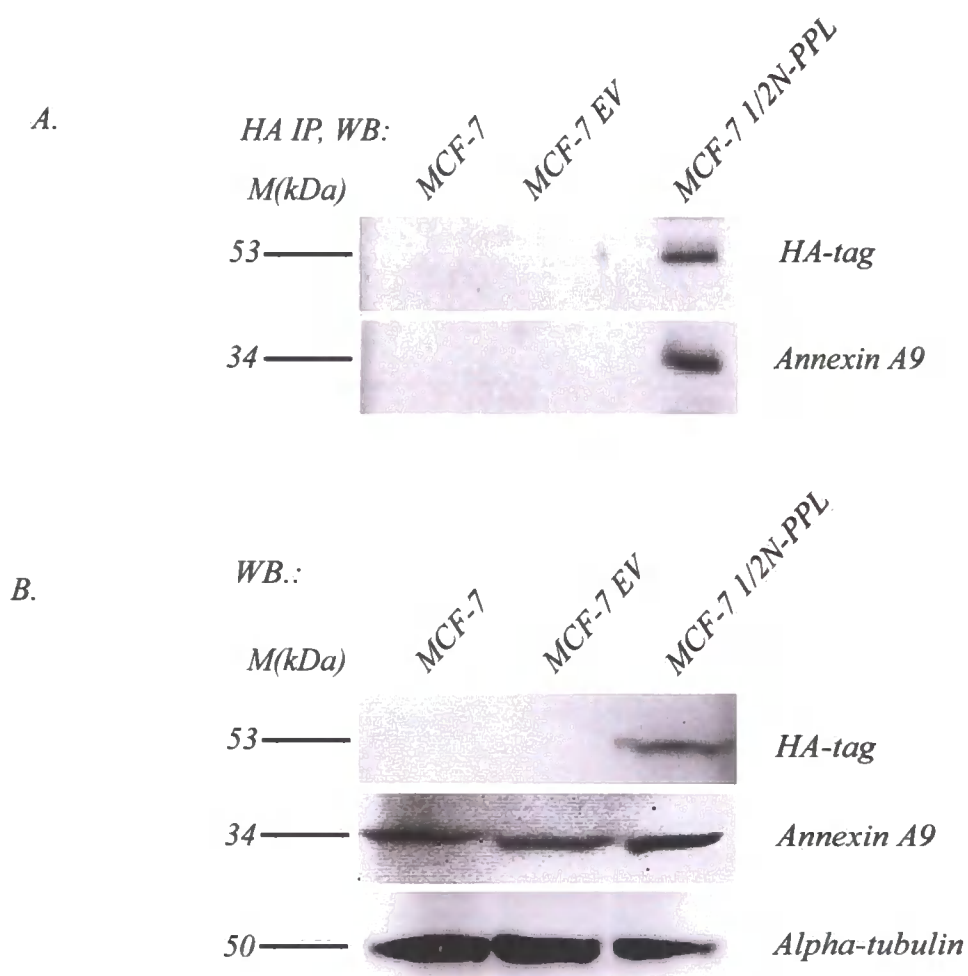
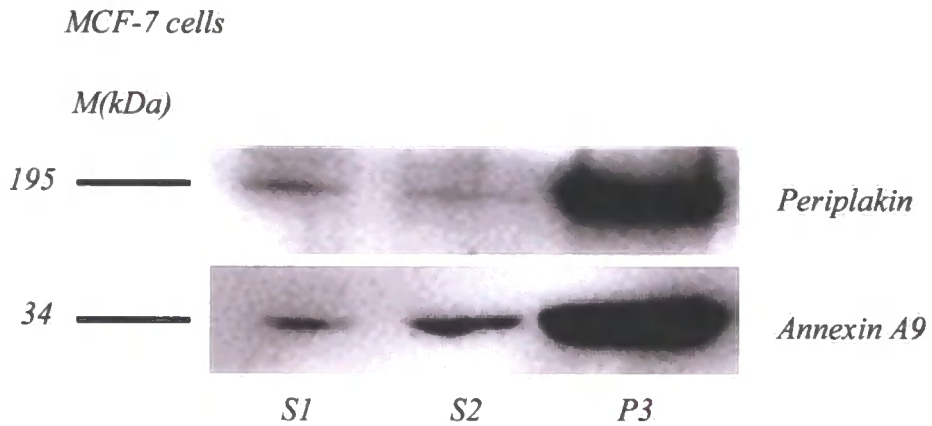


Figure 3.17: Immunoprecipitation of HA-tag periplakin N-terminus and characterisation of the annexin A9 expression level in untransfected, empty transfected (MCF-7 EV) and MCF-7 1/2 N-PPL cell lines.

A. Immunoblot analysis after immunoprecipitation with anti-HA antibody. Precipitated annexin A9 (34 kDa) appeared specifically in the MCF-7 1/2N-PPL cell line. **B.** Immunoblot analysis showing HA-tagged periplakin N-terminus, annexin A9 and alpha-tubulin (1:1000 dilution, Abcam) expression in untransfected MCF-7, MCF-7 EV control and in MCF-7 1/2N-PPL cell lines.

A.



B.

Annexin A9 blot

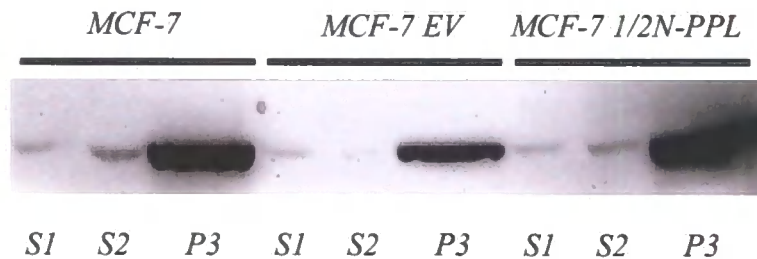


Figure 3.18: Characterization of annexin A9 solubility in untransfected, MCF-7 EV and MCF-7 1/2N-PPL cells.

A. Immunoblot analysis of periplakin and annexin A9 after subcellular detergent fractionation. Proteins were visualized with specific periplakin (BOCZ-1, 1:200 dilution) and annexin A9 (1:2000 dilution) antibodies. Both proteins share the similar subcellular distribution in confluent epithelial sheets. **B.** Subcellular distribution of annexin A9 in three different cell line (MCF-7, MCF-7 EV, MCF-7 1/2N-PPL) showing similar distribution in all cases.

3.2.19 Cellular co-localization of periplakin and annexin A9 in simple epithelia by immunofluorescence microscopy

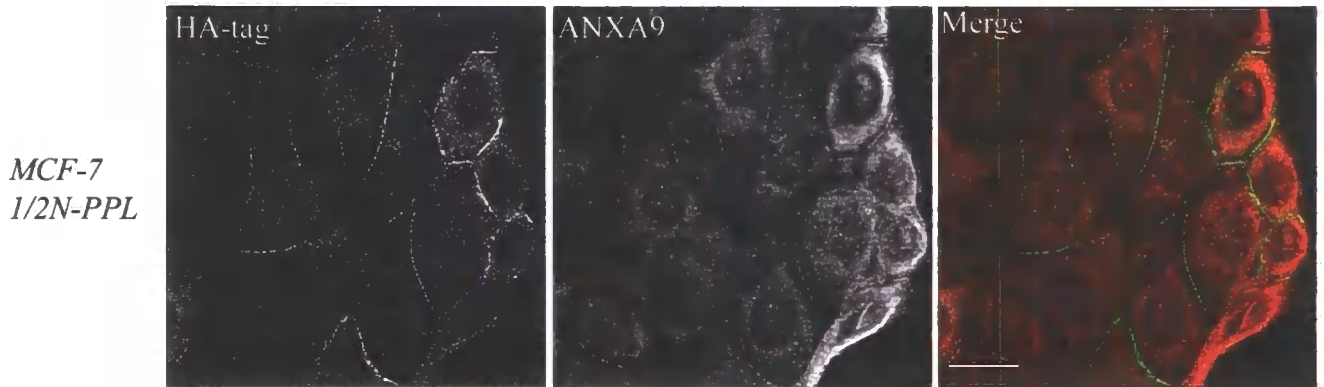
Subcellular distribution of these proteins indicated that periplakin and annexin A9 could potentially co-localise within the intact cell as they were found in the same detergent fractions. Having established that both proteins were found in the cytosolic, plasma membrane and cytoskeletal fractions, their localizations within intact cells were then observed.

In order to directly compare the localization of the periplakin amino-terminus and endogenous annexin A9, both proteins were simultaneously immunolabelled in the MCF-7 ½ N-PPL cell line. The anti-HA antibody (Ab9110, Abcam) and annexin A9 (ANXA9, Abcam) were used in dilutions of 1:200 and 1:2000, respectively. The results showed that whilst the periplakin head domain mainly decorated the plasma membrane, the annexin A9 antibody was localised throughout the cytosolic area as well as the plasma membrane (**Figure 3.19 A**).

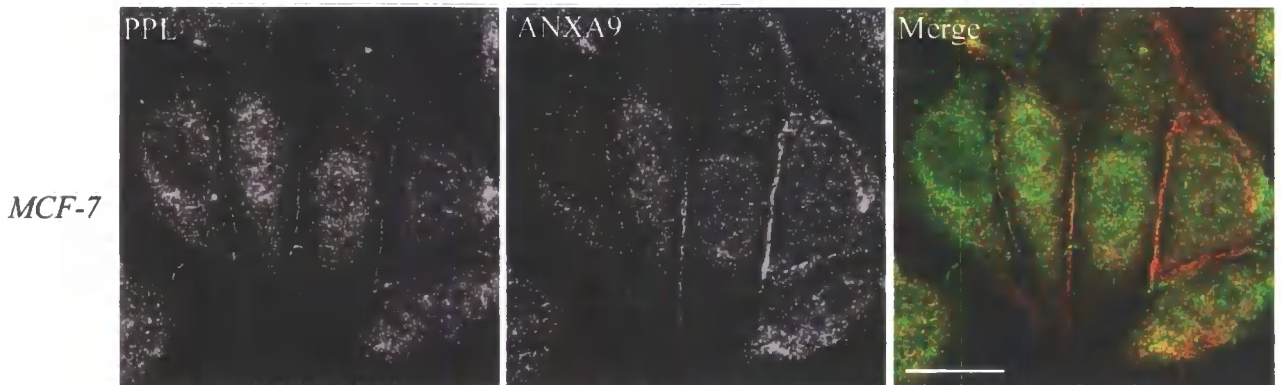
This localisation was further confirmed with antibodies directed against the endogenous proteins in untransfected MCF-7 cells. Likewise, the endogenous periplakin and annexin A9 showed rather similar distributions, having both cytosolic and cell border stainings (**Figure 3.19 B**).

A detailed analysis of co-localization at the cell border was performed using confocal microscopy. Images were constructed by scanning the cells at different depths (z-axis) and then finally merging these images into a single picture (**Figure 3.19 C**). These studies indicated that the localization of annexin A9 was very similar to that of periplakin, and both were distributed along the lateral cell border showing nearly overlapping labelling.

A.



B.



C.

XZ-section

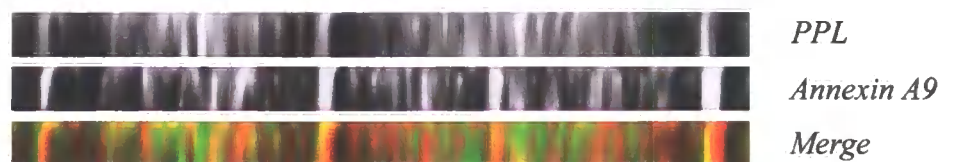


Figure 3.19: Double staining of periplakin and annexin A9 in MCF-7 1/2N-PPL and untransfected MCF-7 cells.

A. Immunofluorescence staining showing colocalization of periplakin N-terminus and annexin A9 at the cell borders in MCF-7 1/2N-PPL cells. **B.** Endogenous periplakin and annexin A9 localisation in untransfected MCF-7 cells indicate similar localisation in the cytoplasm and at the cell borders. **C.** Optical Z-sectioning demonstrate lateral cell border staining with periplakin (BOCZ-1) and annexin A9 (ANXA9) antibodies in MCF-7 cells (scale bar equals 20µm).

3.2.20 Annexin A9 and annexin A1 are not co-localised at MCF-7 cell borders

The polyclonal annexin A9 antibody (ANXA9, Abcam) was the only commercially-available antibody at the beginning of these studies. Although it showed very good results with immunoblotting, giving only one strong band at the expected size of 34 kDa, the potential for cross-reaction with other annexin family members remained. It was therefore interesting to investigate whether the expression pattern of annexin A1 might suggest cross-reaction with annexin A9 by immunofluorescence. Therefore double immunolabelling with annexin A9 and annexin A1 (another member of the annexin family) antibodies was carried out on untransfected MCF-7 cells.

The annexin A9 antibody decorated the plasma membrane of the cells as shown previously, but the annexin A1 antibody was associated mainly in the cytoplasmic region (**Figure 3.20**). Only the perinuclear area of the cell showed some partial co-localization. In addition, the results of this immunofluorescence staining demonstrated that not all annexin family members are able to co-localise with periplakin.

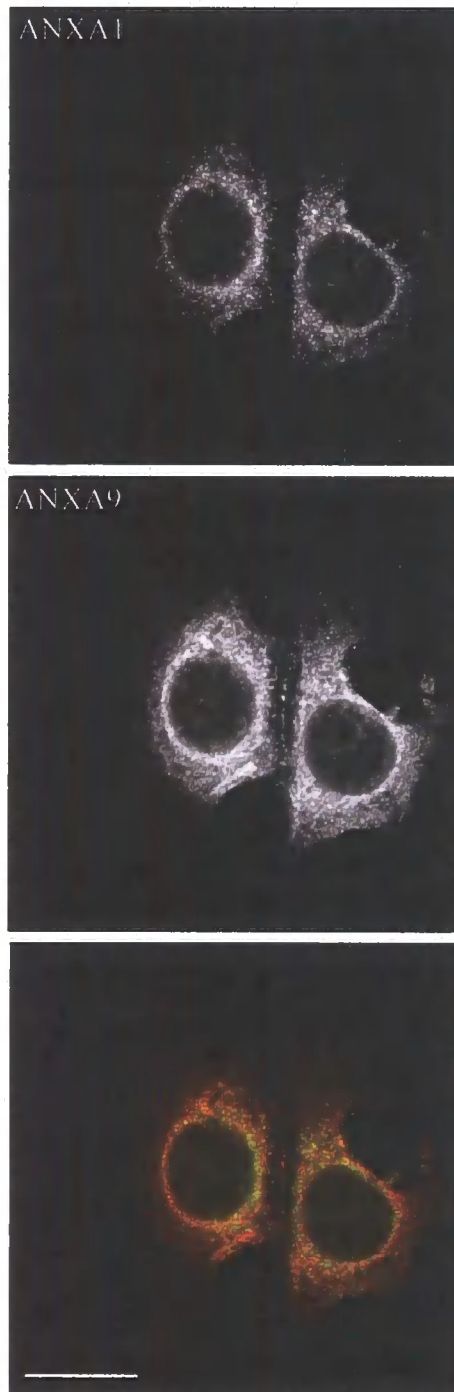


Figure 3.20: Expression of annexin A9 and annexin A1 in MCF-7 cells.

Double staining in untransfected MCF-7 cells with annexin A9 and annexin A1 antibodies (both in 1:200 dilution) was carried out. Immunofluorescence staining shows no cell border staining with annexin A1 which indicate that the annexin A9 is specifically localised at the lateral cell borders (scale bar equals 20 μm).

3.2.21 Expression of annexin A9 in newborn and adult mouse skin

Based on the immunofluorescence staining, both in adult and newborn mouse skin, the annexin A9 protein was expressed from the basal to the stratified layers. Annexin A9 showed reasonably even distribution in these skin layers and co-localised with the endogenous periplakin. Note that in this figure non-specific labelling of annexin A9 observed above the stratified layers owing to the secondary antibody (Alexa-Fluor anti-chicken IgG 488, 1:800). The observation above indicates that annexin A9, along with periplakin, is expressed in both undifferentiated and differentiated epidermis (**Figure 3.21**).

Whilst the function of the periplakin in the stratified layer of the skin as a member of the CE is known, the presence of annexin A9 as an epidermal protein is shown here for the first time. It remains for future studies to investigate the role of annexin A9 in skin.

Newborn mouse skin

Adult mouse skin

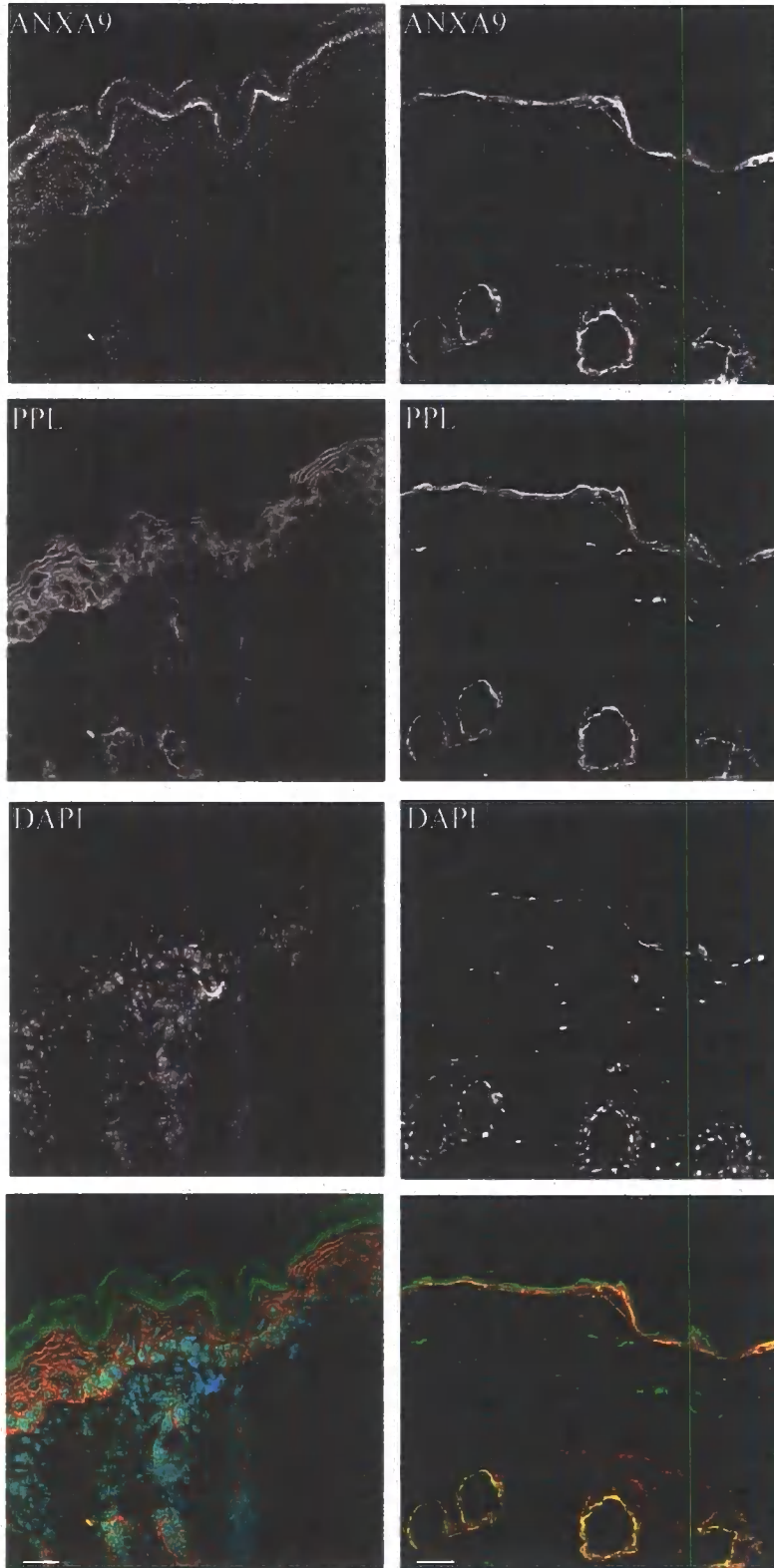


Figure 3.21: Immunofluorescence staining of annexin A9 and periplakin in newborn and adult mouse skin

Immunolabelling was performed without fixation using annexin A9 (ANXA9, 1:200 dilution, Abcam) and periplakin (BOCZ-1, 1:500) antibodies. Yellow colour indicates co-localisation of periplakin and annexin A9 in newborn and adult mouse skin. Scale bar equals 20 μm .

3.3 Discussion

This chapter has reported work which aimed to identify previously uncharacterised interacting partners for periplakin. A stable MCF-7 subclone was created using a pCI-neo vector carrying the first half N-terminus of periplakin tagged with HA. Two other cell lines, untransfected MCF-7 cells and empty pCI-neo transfected stable cell line were used as controls. Interacting partners were identified by a combination of co-immunoprecipitation, gel electrophoresis, mass spectrometry and peptide mass fingerprinting.

3.3.1 Why co-immunoprecipitation?

The analysis of protein-protein interactions (PPI) yields important insights into cell signalling and is essential for revealing protein function in the post-genomic era. The traditional yeast two-hybrid (Y2H) screen detects interactions of 'bait' and 'prey' proteins fused to transcriptional activators in the yeast nucleus. Although this method is sensitive and can be used to identify transient interactions, a major limitation is its high false positive and false negative rates (Bader et al., 2004). Moreover, the yeast 2 hybrid assay detects protein-protein interactions outside their normal cellular environment and does not take into account the specific subcellular localization, post-translational modifications and dynamic changes in the interaction between bait and prey proteins. Another successful method identifying PPIs depends on overexpression of a tagged protein in relevant cell lines (Zhu et al., 2003) where the interacting partners that precipitate with the tagged protein can be identified by mass spectrometry-based proteomics (Aebersold & Mann, 2003). This study used the technique of co-immunoprecipitation as it can identify interacting proteins or protein complexes from eukaryotic total cell extracts (regardless of direct or indirect binding). However, both tagging and overexpression can alter the properties of the protein of interest and yield false results. Therefore, PPIs were also confirmed by co-immunoprecipitating the untagged endogenously expressed proteins.

3.3.2 MCF-7 ½ N-PPL cell line proved a suitable model for studying protein interactions

Screening of the stable MCF-7 ½ N-PPL cell line proved that periplakin N-terminal domain is localised at the same cytoplasmic and plasma membrane locations as the endogenous periplakin in MCF-7 cells. Other workers have shown that full length of periplakin expressed in simple epithelial COS-7 cells showed characteristic IF staining (DiColandrea *et al.*, 2000; Karashima & Watt, 2002). However, in cultured kidney epithelial cells (MDCK) overexpression of periplakin showed filamentous cytoplasmic staining and in confluent cells periplakin became localized to cell borders (Kalinin *et al.*, 2005). Overall, the periplakin N-terminal construct which was used mimicked the distribution of the endogenous periplakin, indicating that the stable cell line can be used as a functional model in further experiments.

3.3.3 Plectin and Annexin A9 identified as co-immunoprecipitating partners of the periplakin N-terminus

Initial immunoprecipitation samples were analysed by 1D gel electrophoresis. To avoid false positive results, two controls were used. However, despite the use of 4-12% gradient gel that separates better than a normal SDS-PAGE gel, some of the bands obtained were identified to be a mixture of proteins. 1-D gel electrophoresis, although simple to perform and reproducible, has a limited resolving power as it separates proteins only based on their molecular mass. In contrast, 2-D gel electrophoresis resolves proteins according their net charge in the first dimension and according to their molecular mass in the second dimension. It is capable of resolving thousands of proteins and peptides from a single complex mixture in a single experiment and produces a resolution far exceeding that obtained for 1-D gels (Fey & Larsen, 2001). Application of this technique revealed clearer results. Careful examination of 1D and 2D gels revealed 4 bands and 13 spots that were uniquely present in the MCF-7 ½ N-PPL samples and these were selected and analysed by mass spectrometry. Unfortunately, some bands and spots were identified as contaminating proteins such as keratin 8/18, keratin 19 and tubulin, or having such a low score that they gave statistically insignificant matching score. Among these results, two candidate proteins were identified. Firstly, plectin, a

major cytolinker protein and member of the plakin family; and secondly, annexin A9, a Ca^{2+} and phospholipid-binding protein.

Peptide mass fingerprinting (PMF) has its limitations. Its ability to identify a protein depends on the presence of the protein in the database. PMF is a very effective method in the analysis of proteins from different organisms. A study on the origins of uninterpretable masses in PMF revealed a number of other reasons that lead to the non identification of a protein (Karty *et al.*, 2002). Among these were errors in the published genome such as incorrectly assigned protein start codons and protein modifications like deamidation and guanidination that give rise to masses cannot be correctly matched.

This study has identified proteins such as keratin 18 and keratin 19 and tubulin as possible contaminants characteristic for the MCF-7 ½ N-PPL cell line as these proteins appeared very well distinguished bands or spots on the gels. Although periplakin is an interacting partner of the keratin and vimentin intermediate filaments these interactions are mediated by the tail domain, this minimizes the chance that the periplakin NH_2 -domain responsible for the appearance of these cytoskeletal proteins. Based on the 2-D gel analysis that implies plectin as a possible binding partner for periplakin, it is possible that plectin pulled down keratin and tubulin.

Based on the evidence provided so far, plectin has been identified as a periplakin co-immunoprecipitating partner in the experiments analysed on 2-D gel electrophoresis. A band around the size of plectin (500 kDa) was also recognizable on 1-D gel but mass fingerprinting could not identify the trypsin digested protein as it appeared to be a mixture of proteins.

3.3.4 Periplakin-plectin co-localisation

Plectin was identified as an interaction partner for periplakin in a proteomic screen of protein complexes co-immunoprecipitated from MCF-7 cells expressing HA-tagged periplakin N-terminus. This was confirmed by co-immunoprecipitation of full-length endogenous proteins and by co-localisation of periplakin and plectin at cell borders of MCF-7 cells and in the cytoplasm of HaCaT keratinocytes. This co-localisation with plectin might suggest a novel mechanism of action for periplakin. Previously, it has been shown that periplakin is required for a correct targeting of

envoplakin in cultured human primary keratinocytes (DiColandrea *et al.*, 2000). Over-expression of envoplakin resulted in aggregate formation that was rescued by over-expression of periplakin (DiColandrea *et al.*, 2000). The interaction of periplakin and envoplakin is mediated by the rod domains of the proteins and the heptad repeat structure and length of the respective rod domains is compatible with heterodimerization of periplakin and envoplakin (Ruhrberg & Watt, 1997; DiColandrea *et al.*, 2000). In this study, the interaction between periplakin and plectin does not involve the periplakin rod domain and, consequently, is likely to have different functions. Studies on fully polarised MDCK cells indicated that plectin was predominantly localized underneath the lateral plasma membrane, and was barely, if at all, detectable at the basal and apical plasma membrane and throughout the cytoplasm (Eger *et al.*, 1997). These findings are identical to my results that showed periplakin and plectin co-localisation at the lateral plasma membrane of MCF-7 cells. Furthermore, anti-plectin antibodies also co-immunoprecipitated another cytolinker protein, desmoplakin (Eger *et al.*, 1997). However, the desmoplakin protein domain responsible for interaction with plectin has not been mapped in detail. It remains to be investigated whether periplakin and desmoplakin share the same plectin – binding motif. It should also be noted that it is possible that yet unidentified proteins are involved in bridging periplakin and plectin, since this option cannot be excluded by co-localisation and co-immunoprecipitation experiments.

Use of three different isoform-specific antibodies against plectin indicates that all these isoforms can co-localise with periplakin in simple epithelial cells and that the isoforms plectin-1f and plectin-1k are expressed together with periplakin in differentiated, suprabasal epidermal keratinocytes. In skin, plectin is found in hemidesmosomes that serve as anchorage sites for the intermediate filaments to mediate firm adhesion of the basal cells to the basement membrane (Borradori & Sonnenberg, 1999; Jones *et al.*, 1998). In stratified epithelia, plectin has been found in multiple locations: at the basal cell surface membranes, in peripheral areas of epithelial cells and in other layers of the skin (Wiche *et al.*, 1983). More evidence for an essential role of plectin in the integrity of muscle and skin architecture is demonstrated by plectin null mice. Plectin deficient mice exhibit severe skin blistering with a reduction of hemidesmosomes and abnormalities in skeletal heart and muscle (Andrä *et al.*, 1997). The role is further supported by human patients with plectin abnormalities, who exhibit

epidermolysis bullosa simplex (a skin blistering disease) with muscular dystrophy (EBS-MD) (Andrä *et al.*, 1997). The fact that two other plectin isoforms, plectin-1f and plectin-1k co-localise with the endogenous periplakin in suprabasal skin layers suggests an additional role for plectin, apart from being a component of hemidesmosomes. Dermal fibroblasts isolated from plectin-1 deficient mice exhibited abnormalities in their actin cytoskeleton and impaired migration potential. Similarly, plectin-1 deficient T cells isolated from lymph nodes showed diminished chemotactic migration *in vitro*. Most strikingly leukocyte infiltration during wound healing was reduced in the mutant mice (Abrahamsberg *et al.*, 2005).

A previous study has shown similar tissue-wide expression pattern of plakin genes for periplakin and plectin in the brain, liver, pancreas, placenta, skeletal muscle, colon and small intestine (Kazerounian *et al.*, 2002) which underpins our results suggesting a functional correlation between periplakin and plectin in both simple epithelia and in differentiated layers of the skin. As cytolinker proteins, both periplakin and plectin are able to directly bind keratin intermediate filaments and the fact that they co-localise in MCF-7 and HaCaT cells suggest that they might together regulate keratin intermediate filament organization.

To further investigate which domain of the periplakin amino terminus is essential for the co-localization of plectin, MCF-7 cells were transfected with different deletion constructs of the periplakin head domain labelled with an HA-tag at the C-terminal end. Immunofluorescence studies of these constructs indicated that the plectin-binding domain of periplakin is likely to reside within the first 133 amino acid residues of the N-terminus, as this fragment was required for the lateral plasma membrane localisation in MCF-7 cells. These results are in keeping with a previous study proposing that the same first 133 amino acid residues of the periplakin amino terminus is required for interaction with kazrin and membrane targeting in keratinocytes (Groot *et al.*, 2004). Though, my experiments produced similar results they also demonstrated some differences. In spite of the removal of the first 16 amino acid residues preceding the NN subdomain of the periplakin N-terminus, the construct still showed co-localization with plectin and was targeted to cell borders in contrast to data from keratinocytes. It is possible that this periplakin domain is directed to the cell borders by other proteins in simple epithelial cells while in keratinocytes, it may be that different

set of proteins are responsible for membrane targeting or that the binding sites are localised within the first 16 residues.

To conclude, in MCF-7 cells, the minimal region for periplakin to be localized at cell membrane and to be partially co-localized with endogenous plectin, is the construct PPL 16-133. Based on the plakin domain crystal structure, this region is equivalent to a spectrin repeat (SR3) (Sonnenberg et al., 2007).

3.3.5 Annexin A9 co-localise with periplakin in MCF-7 cells and in mouse skin

As a second part of this chapter, the link between periplakin and annexin A9 has been investigated. Based on the evidence above, annexin A9 was also identified as a co-immunoprecipitating partner of periplakin with a high score of mass fingerprinting. Immunoblot analysis did not shown any significant difference between the expression levels of annexin A9 in the MCF-7 ½ N-PPL cell line compared to the two control cell lines. Therefore, annexin A9 expression is unlikely to be regulated by periplakin N-terminus in MCF-7 cells.

The name “annexin” was given to these proteins in 1990 and the 12 annexins common in vertebrates were classified as Annexin A family are named ANXA1-ANXA13 leaving ANXA12 unassigned in the official nomenclature (Human genome Nomenclature Committee, www.Gene.ucl.ac.uk/nomenclature/). Annexins are found in invertebrates (family B), in fungi and unicellular eukaryotes (family C), in plants (family D) and in protists (family E). By definition, an annexin protein has to fulfill two major criteria. It has to be capable to bind negatively charged phospholipids in a Ca²⁺ dependent manner and it has to contain a conserved structure, the so-called annexin permeate (Gerke & Moss, 2002). All annexins contain two main domains, the divergent NH₂ “head” and a conserved COOH-terminus harbouring the type II and type III Ca²⁺ and membrane binding sites facing the membrane (Weng *et al.*, 1993). The C-terminus is built from four similar repeats, each with a length of 70 amino acids and forming five α -helices in all segments. Therefore, the other side of the annexin is directed away from the membrane and accessible for interactions.

Many reports have provided information about the function of the annexins, pointing out their role in membrane trafficking and organisation (Gerke & Moss, 1997),

regulation of ion-channels (Herr *et al.*, 2001) and extracellular activities such as controlling inflammatory responses (Hannon *et al.*, 2003).

Annexin A9 is a member of the annexin family (initially termed annexin 31). Its cDNA was first identified from fetal liver and spleen libraries (Morgan & Fernandez, 1998) in the data search for human expressed sequence tags (ESTs). The fact that annexin A9 cDNA was found in limited EST libraries led other scientists to imply the possibility that annexin A9 might have a specialized function which could be shared with other proteins.

Annexin A9 displays rather different properties compared to other annexins. Its type II-Ca²⁺ binding site has been altered and is most likely dysfunctional. This site, in other members of the annexin family, is normally responsible for reversible membrane binding (Goebeler *et al.*, 2003). However, data from liposome binding experiments have suggested that annexin A9 is not regulated by intracellular Ca²⁺, suggesting a novel mode of function (Goebeler *et al.*, 2003). Since the structure of the annexin A9 is closest to the annexin A2, its ability to bind actin and S100A10 protein was also studied. In neither case was annexin A9 able to bind even at high calcium concentrations, which supports a unique function for annexin A9 in the annexin family (Goebeler *et al.*, 2003). Here, it has been demonstrated an interaction between periplakin and annexin A9 in MCF-7 cells, a finding which is supported by co-localization studies. However, the functional consequence of the interaction is still unresolved. To further investigate this link, examination of protein expression level and subcellular distribution should be carried out after siRNA downregulation experiments.

Immunofluorescence studies with annexin A9 specific antibody on MCF-7 cells detected cytoplasmic and cell border staining similar to periplakin staining and revealed consistent co-localization especially at cell borders. Low level annexin A9 expression has also been detected in HepG2 cells (Goebeler *et al.*, 2003).

In this study, annexin A9 and periplakin co-localization was observed, not only in simple epithelial cells but also in newborn and adult mouse skin sections. Periplakin and annexin A9 were found to be expressed from the basal to the stratified layers of the skin. Annexin A9 has not previously been shown to localise in the stratified epithelia. Interestingly, annexin A9 is not the first annexin protein showing expression in different layers of the skin, as annexin A8 has also been reported to be found in stratified

epithelia (Runkel *et al.*, 2006). Surprisingly annexin A8, similarly to annexin A9, was also detected in the basal and suprabasal layers of the skin with an increase during postnatal days. The presence of annexin A9 and annexin A8 in the suprabasal layers may be associated with terminal differentiation of epithelial cells. A unique association of annexin A9 with skin was also published earlier. Autoantibodies isolated from patients with pemphigus vulgaris, cross-reacted with an annexin like protein named pemphaxin (Nguyen *et al.*, 2000) that is actually annexin A9. Coincidentally, periplakin with plectin (Aho *et al.*, 1999), (Mahoney *et al.*, 1998), envoplakin (Kiyakowa *et al.*, 1998) and desmoglein 3 (Ohyama *et al.*, 2001) also showed strong reactivity with paraneoplastic pemphigus (PNP) sera. It is rather intriguing that antibodies against both periplakin and the potential periplakin binding proteins, plectin and annexin A9 are found in autoimmune skin diseases.

Studying the solubility properties of annexin A9 supported the potential link between these proteins, as both periplakin and annexin A9 shared the same solubility in confluent MCF-7 cells. Therefore, an interaction between these proteins could exist in any of the three cell fractions. This is consistent with the previous proposal of annexins as cytosolic proteins with both soluble and insoluble pools which are stably or reversibly associated to components of the cytoskeleton (Moss & Morgan, 2004). Annexins are proposed to bind a wide variety of other proteins (Gerke & Moss, 2002) and many of these interactions have already been studied (**Table 3.2**).

Annexin	Interacting partners	Knock-out model	Reference
ANXA1	Epithelial growth factor receptor, formyl peptide receptor, selectin, actin, integrin A4	Changes in inflammatory response and in the effects of glucocorticoids	(Hannon <i>et al.</i> , 2003)
ANXA2	Tissue plasminogen activator, angiostatin, insulin receptors, tenascin C, caveolin I.	Defects in neurovascularization and fibrin homeostasis	(Ling <i>et al.</i> , 2004)
ANXA3	None known	Not done	
ANXA4	Lectins, glycoprotein 2	Not done	
ANXA5	Collagen type 2, vascular endothelial growth factor receptor 2, integrin B5, protein kinase C, cellular modulator of immune recognition (MIR), G-actin, helicase, DNA – methyltransferase I	Subtle phenotypes further investigation is needed	(Brachvogel <i>et al.</i> , 2003)
ANXA6	Calcium responsive heat stable protein-28, ras GTPase activating protein, chondroitin, actin		(Hawkins <i>et al.</i> , 1999)
ANXA7	Sorcin, galectin	Cause embryonic lethality in mice or changes in calcium homeostasis	(Srivastava <i>et al.</i> , 1999);(Herr <i>et al.</i> , 2001)
ANXA8	None known	Not done	
ANXA9	Periplakin	Not done	
ANXA10	None known	Not done	
ANXA11	Programmed cell death 6 (PDCD6), sorcin	Not done	
ANXA13	Neural precursor cell expressed, developmentally downregulated 4(NEDD4)	Not done	

Table 3.2: Members of the annexin family indicating interacting partners and knock-out studies. (Adapted from (Moss & Morgan, 2004)).

CHAPTER IV

KERATIN INTERMEDIATE FILAMENT ORGANIZATION IS DEPENDENT ON PERIPLAKIN AND PLECTIN IN SIMPLE EPITHELIAL CELLS

4.1 Introduction

Based on the results shown in the previous chapter, periplakin and plectin cytolinkers co-localise and co-immunoprecipitate in simple epithelia. This chapter details efforts to identify any functional relation between periplakin and plectin by using siRNA mediated downregulation in MCF-7 and HaCaT cells. In addition, the role of periplakin and plectin in keratin intermediate filament organisation during epithelial sheet migration has been investigated. Several studies have investigated the organisation of the cytoskeleton in wounded epithelia. After wounding epithelial sheets, a contractile actin purse-string cable assembles at the free wound edge (Martin & Lewis, 1992; Bement *et al.*, 1993; Danjo & Gipson, 1998) to facilitate wound closure. This cable is not exclusive to embryonic wounds, but also described in adult cells, providing a tension that contributes to wound closure. The function of the actin cable in the wound edge cells provides a dual purpose, not only to form a contractile purse-string but also to restrain front cells from forward movements (Jacinto *et al.*, 2002). Lately, a new aspect to wound healing has been found. Two hours after wounding, the keratin network is re-organised at the wound edge into a thick bundles parallel to the free edge of the epithelial sheet resembling the actin cable. (Long *et al.*, 2006) Keratin cables have been demonstrated at the edges of embryonic wounds which also show the actin purse-string (Brock *et al.*, 1996).

The carboxyl terminal domain of periplakin is considerably shorter than in the rest of the members of the plakin family, as it lacks the globular specific subdomains. However, interaction with intermediate filament proteins such as keratin 8 and vimentin gave direct evidence that periplakin can function as an IF associated protein (Kazerounian *et al.*, 2002). As opposed to the N-terminal domain of periplakin, the C-terminus has recently been shown to be involved in interaction with several other proteins. Yeast-two hybrid screening revealed that these binding partners include periphilin, a protein that can be targeted to nucleus (Kazerounian & Aho, 2003), Fc γ RI (CD64), which appears to be regulated by binding to periplakin (Beekman *et al.*, 2004) and a serine/threonine kinase, protein kinase B (PKB). Moreover, periplakin has been proposed to function as a localization signal in PKB-mediated signalling (van den Heuvel *et al.*, 2002). In addition, this technology has confirmed a specific binding of periplakin to the intracellular domain of

BPAG-2 (Aho, 2004). Furthermore, the last 208 amino acids of the C-terminal domain of periplakin has been identified as binding partner for the C-terminal region of MOP receptors (which mediate most of the actions of opiates). Periplakin is the first opioid receptor-interacting protein that disrupts agonist-mediated G-protein activation. MOP receptor signalling may be less effective in neurons that co-express the receptor and periplakin than in those that do not (Feng *et al.*, 2003). It is not yet known whether these interactions and IF binding are mutually exclusive, but it is conceivable that different periplakin pools in the cell are engaged with unique functions and interactions.

To elucidate the role of periplakin in keratin dynamics the following two stable cell lines were used: MCF-7 C-PPL clone overexpressing the C-terminal domain of periplakin and the MCF-7 ½ N-PPL cell line overexpressing the ½ N-terminus of periplakin (see **chapter 3.2.2**). To study the effect of these domains on keratin intermediate filament dynamics, scratch wound experiments (**section 2.4**) were carried out on both cell lines (MCF-7 C-PPL, MCF-7 ½ N-PPL). Subsequently, the organisation of the keratin 8 IFs was monitored at the wound margin.

4.2 Results

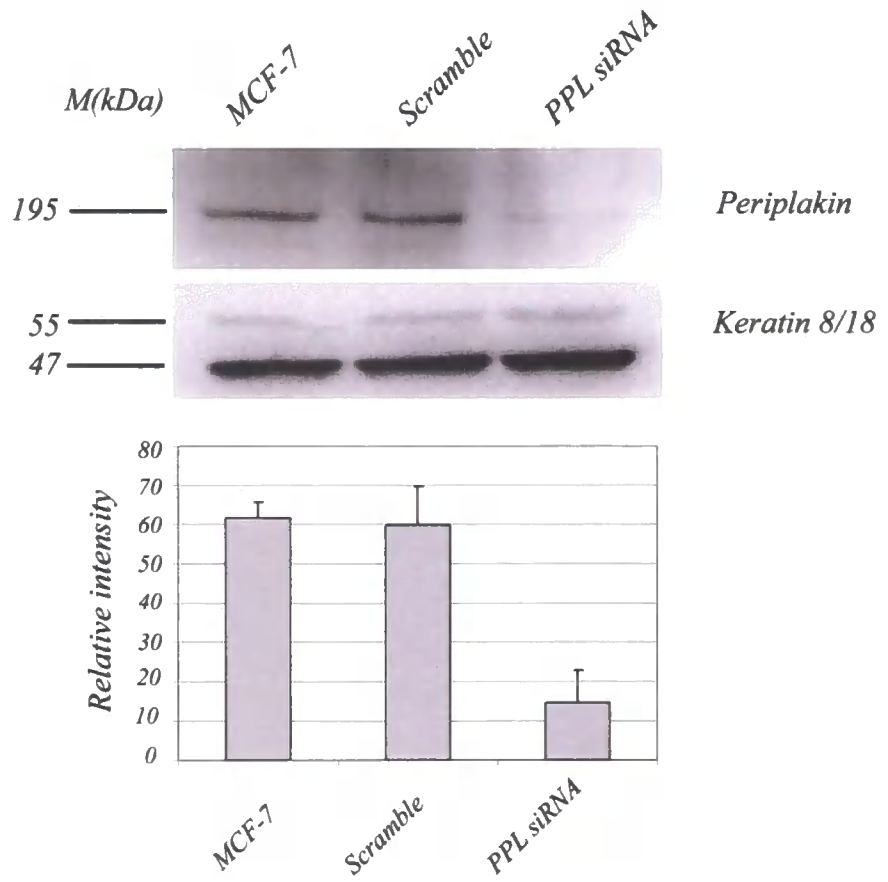
4.2.1 Transfection of short interfering RNA (siRNA) to down-regulate periplakin, plectin and keratin 8 expression

Prior to carrying out wound healing and migration assays, it was first necessary to investigate the efficiency of siRNA knock down of protein expression in MCF-7 cell lines. In this study, periplakin, plectin and keratin 8 proteins were targeted. Using the online siRNA database from Ambion, non-validated pre-designed siRNA oligonucleotides standard purity were purchased for periplakin, plectin and keratin 8. Several alternative siRNAs were tested for each protein to find the most efficient oligonucleotides. The validation of siRNAs was carried out in MCF-7 cells that were transfected with the siRNA of interest or a scrambled control siRNA. The scrambled control contains a mixed sequence of nucleotides that does not correspond to any known human mRNA sequence and therefore provides a negative control for the experiments. Furthermore, another control using water instead of any siRNA was used to demonstrate normal protein expression.

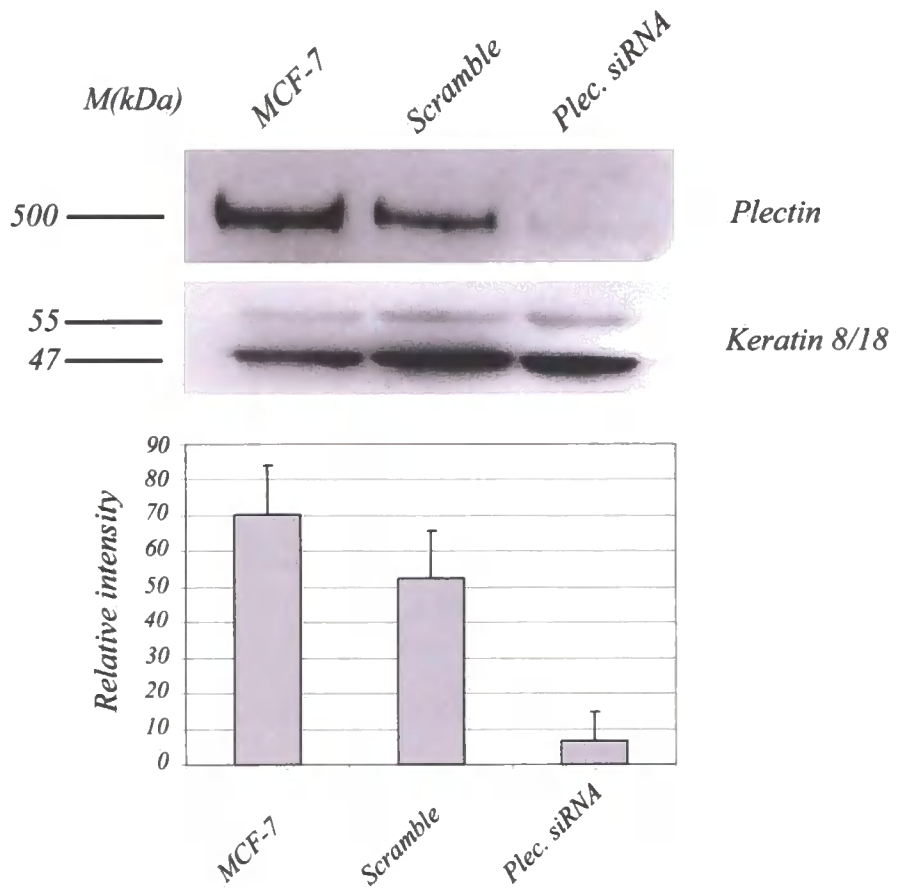
After transfection, cells were harvested at either 48 or 72 hour time points and the efficiency of protein knock-down was analysed by immunoblotting. Samples were run simultaneously on the same gel in adjacent lanes to ensure that the blotting conditions were constant. Three different target sites in the periplakin mRNA were tested. All periplakin siRNA oligonucleotides were effective and resulted in almost complete loss of periplakin protein expression. The best depletion of periplakin expression (95%) was achieved 48-72 hours after the transfection with PPL-3 siRNA. **Figure 4.1 A** shows this in comparison to transfection of the scrambled siRNA and untransfected control. Keratin 8/18 was used as a loading control showing equal loading of total proteins from each sample. This oligonucleotide was used for all siRNA transfection experiment thereafter. Plectin siRNA (Plec1) also showed prominent plectin knock-down (>95%) 72-96 hours after transfection (**Figure 4.1 B**). As before, cytokeratin bands illustrate equal loading of total proteins in each lane. This oligonucleotide was also used for all subsequent siRNA transfection experiments. To achieve keratin 8 ablation in MCF-7 cells with double-stranded siRNA oligonucleotides against keratin 8, two different siRNAs were tested. Only one of the examined keratin 8 siRNAs resulted in about 20-50% decrease of the protein expression

compared to controls (**Figure 4.1 C**). Keratin 8 siRNA transfections were carried out in HeLa and Panc-1 cells under conditions as previously described in Long *et al.*, 2006. It was observed that siRNA transfections reached the greatest efficiency when the cells were transfected 12 hours after seeding at 40% confluence. Seeding cells at over 40% confluence resulted in increasingly less efficient keratin depletion possibly due to stabilisation of the intermediate filament network.

A.



B.



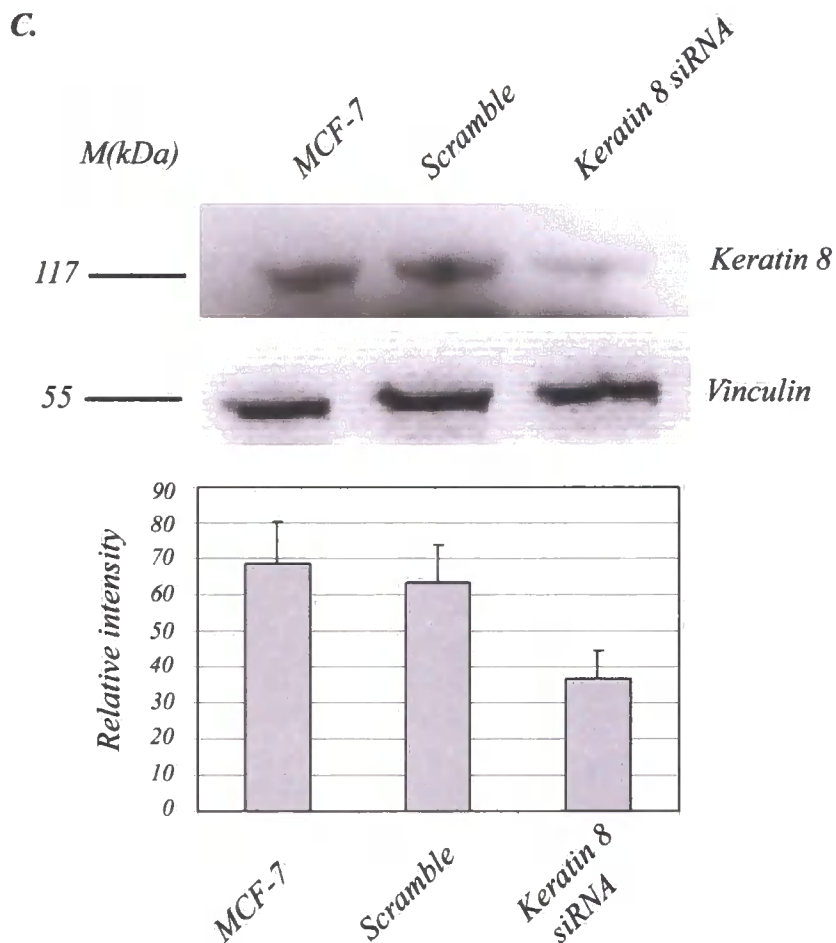


Figure 4.1: Verification of the effect of siRNA oligonucleotides using Western blot analysis in MCF-7 cells.

A. Periplakin siRNA oligonucleotide used for periplakin downregulation: PPL-3: GAGGGUAUGUAUAAAUGCtt. Target: C-terminus, exon 22. Knock-down efficiency: >95%. The above oligonucleotide was used throughout this research for periplakin ablation. As a control lane keratin 8/18 was used to demonstrate even loading of the total proteins. **B.** Immunoblot results of plectin siRNA transient transfection in MCF-7 cells. siRNA oligonucleotide: Plec-1: GGAAUGAUGACAUCGCUGAtt. Target: C-terminus, exon 5. Knock-down efficiency: >95%. Keratin bands are shown as control for loading. **C.** Immunoblot analysis of keratin 8 siRNA transfection. siRNA oligonucleotide: K8-1: AAUAUCCUCGUACUGUGCCtt. Target region: Rod, exon 6. Knock-down efficiency: 50-80%. In this case the control blot for loading was carried out with vinculin antibody (V-11-5, 1:100 dilution, Sigma).

Bar diagrams represent densitometric analysis of protein expression after periplakin, plectin and keratin 8 siRNA transfections in MCF-7 cells. Values represent means and standard deviations for three independent experiments ($n=3$). Student's T-test confirmed statistical differences ($p < 0.05$) between control and transfected cells.

4.2.2 Plectin knock-down impairs periplakin subcellular targeting in HaCaT keratinocytes

To investigate whether the link between periplakin and plectin has a functional role in epithelial cells, the periplakin or plectin expression was downregulated by siRNA transfections in MCF-7 and HaCaT cells using transfection conditions which had been established earlier (Long *et al.*, 2006).

To determine whether periplakin or plectin down-regulation changes the localization pattern of the other protein, immunofluorescence staining was performed after siRNA transfection. MCF-7 and HaCaT cells were seeded onto coverslips and left to grow for two days. After reaching 50% confluence, siRNA was applied against periplakin and plectin, respectively. Immunofluorescence microscopy using antibodies against periplakin (BOCZ-1) and plectin (c-20) was used to reveal the alterations of protein distribution and successful protein downregulation.

Both periplakin and plectin downregulation were achieved successfully in MCF-7 cells. However, in neither case were there consistent changes in the distribution of the other protein. **Figure 4.2 A** shows periplakin was mainly localised at the plasma membrane in control cells, similarly to that observed in plectin downregulated cells. Additionally, plectin distribution did not seem to be altered after periplakin ablation displaying cell border and cytoplasmic staining. Similarly, in HaCaT cells periplakin depletion did not affect plectin localisation (**Figure 4.2. B**).

In contrast, ablation of plectin in HaCaT cells caused an altered periplakin distribution (**Figure 4.2 B**). Transfection of HaCaT keratinocytes with a plectin siRNA resulted in an efficient knock-down of plectin expression (**Figure 4.3 A**) and in periplakin aggregate formation (**Figure 4.3 B**). In control transfected HaCaT keratinocytes, periplakin demonstrated mostly cytoskeletal staining where it partially co-localised with plectin (**Figure 4.2 B**). This distribution pattern is different from that seen in simple epithelial MCF-7 cells (**Figure 4.2 A**) and was confirmed by subcellular fractionation which demonstrated that in HaCaT cells the majority of both plectin and periplakin were found in the cytoskeletal, Triton insoluble P3 fraction with only a small amount of proteins present in the cytosolic S1 fraction (**Figure 4.4 A**).

Upon closer investigation of subconfluent plectin knock-down cells, it was noted that periplakin mostly aggregated in small, irregular clusters. This clustering of periplakin was accompanied by a loss of soluble periplakin and keratin 14 pools in subcellular fractionations (**Figure 4.4 A**). In addition, periplakin clusters were partially distributed along intermediate filaments or localised at tips of keratin filaments at cell periphery (**Figure 4.4 B**). Thus, plectin appears to regulate periplakin localisation in HaCaT cells.

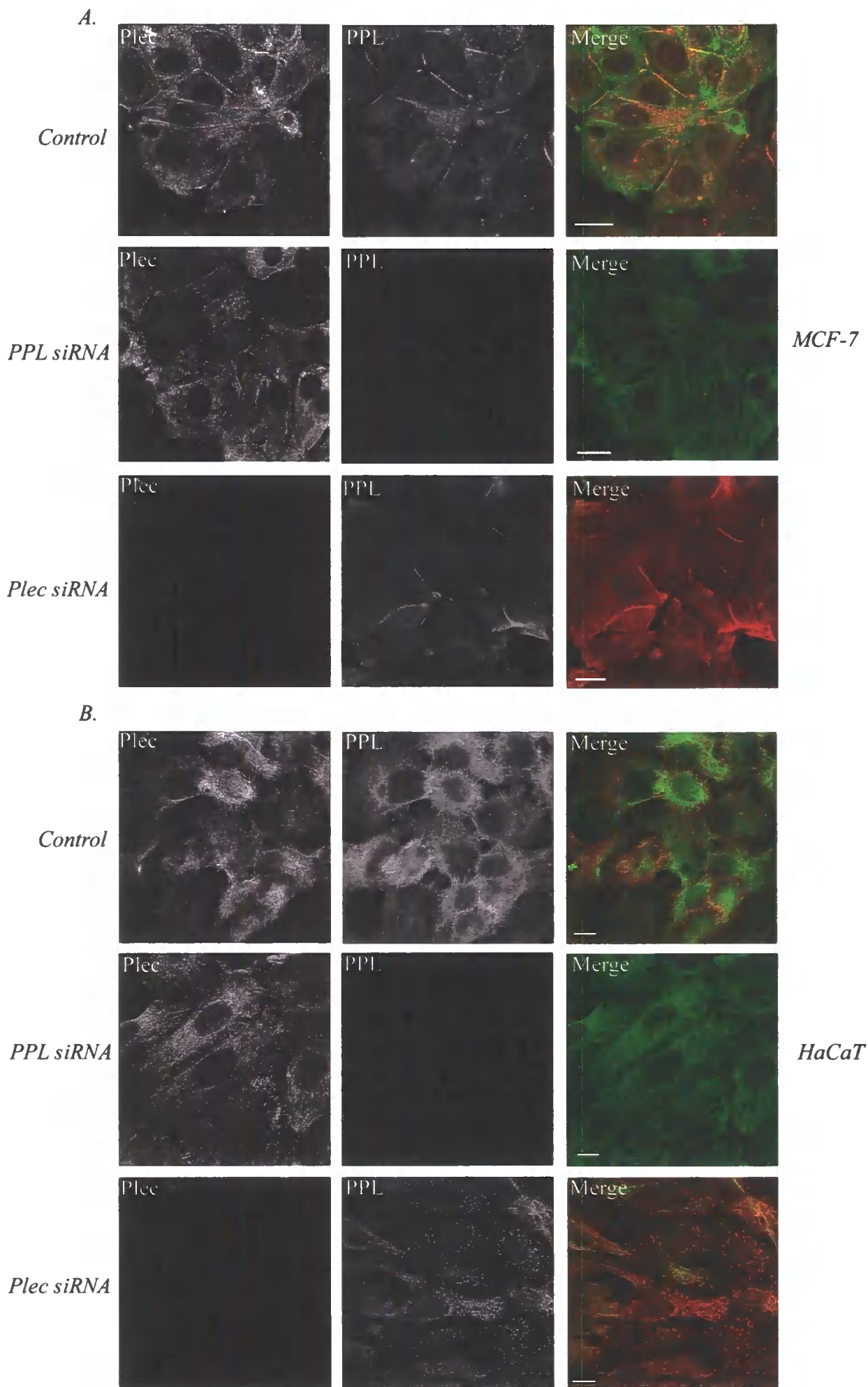
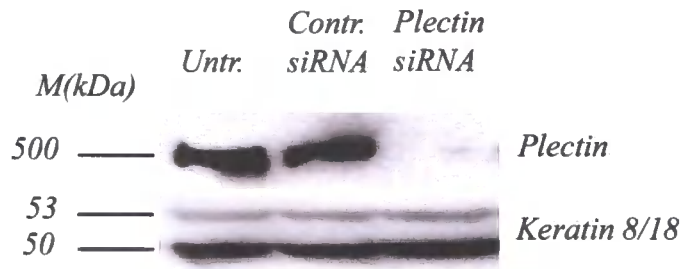


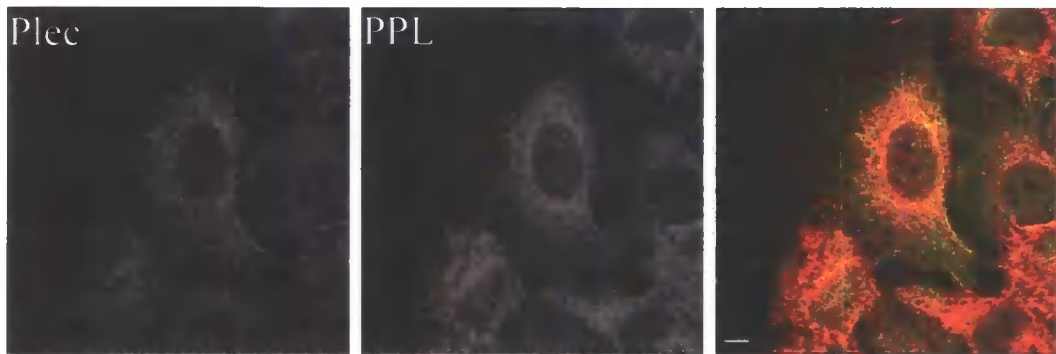
Figure 4.2: Periplakin and plectin downregulation in MCF-7 and HaCaT cells.

Control transfected MCF-7 cells (A.) and HaCaT cells (B.) (top row), periplakin siRNA transfected cells (middle row) and plectin downregulated cells (bottom row) are shown. Cells were stained with c-20 plectin antibody (green, 1:200 dilution) and periplakin BOCZ-1 antibody (red, 1:500 dilution). Scale bars equal 20 μ m.

A.



B.



C.

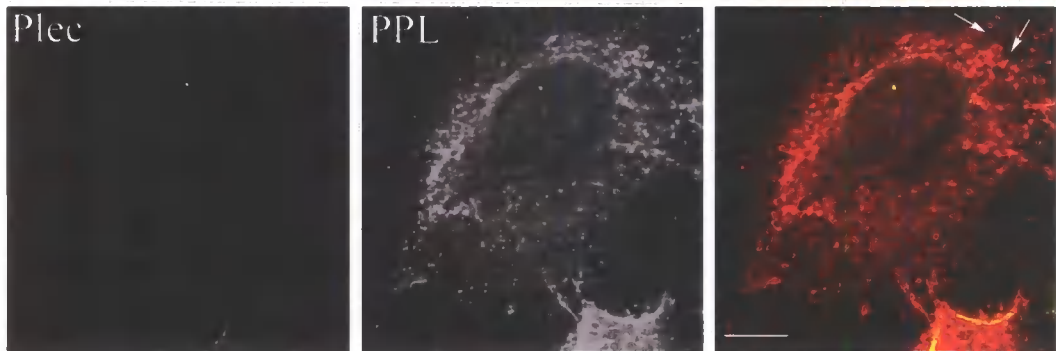
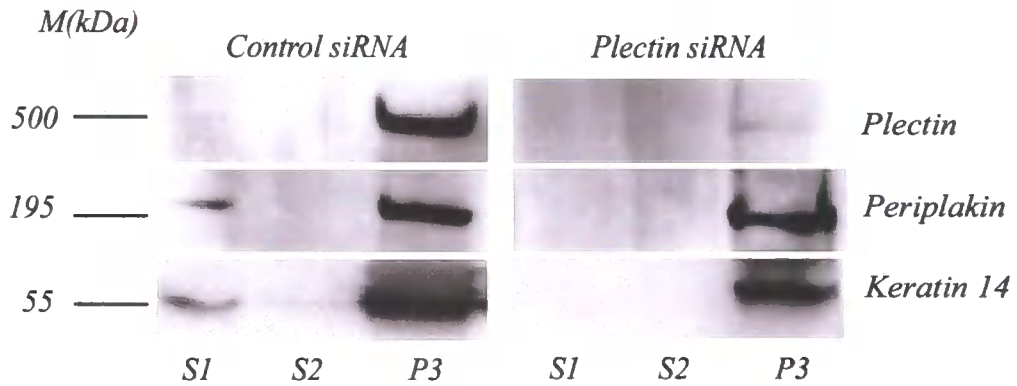


Figure 4.3: Images showing clusters of periplakin in plectin siRNA transfected HaCaT keratinocytes.

Subconfluent HaCaT keratinocytes were transfected with control siRNA or plectin siRNA oligonucleotides. **A.** Knock-down efficiency was monitored by immunoblotting of untransfected, control siRNA transfected and plectin siRNA transfected cell extracts with total plectin (c-20) antibody using keratin as loading control. **B.** Control siRNA transfected cells were stained 96 hours after transfection with plectin (green) and periplakin (red) antibodies (scale bar equals 5 μm). **C.** Plectin siRNA transfected cells stained with periplakin (red) and plectin (green) antibodies 96 hours after transfection. Arrowheads show examples of periplakin aggregates (scale bar equals 5 μm).

A.



B.



Figure 4.4: Altered periplakin distribution after plectin siRNA transfection in HaCaT keratinocytes.

A. Immunoblotting of subcellular fractions of control and plectin siRNA transfected HaCaT keratinocytes. Left and right panels indicate control and plectin downregulated samples, respectively, probed with periplakin (BOCZ-1, 1:500 dilution) and keratin 14 (1:1000 dilution) antibodies. **B.** Immunofluorescence staining of periplakin (green), and keratin 14 (red) in plectin siRNA transfected cells. Periplakin staining demonstrates aggregates distributed along the intermediate filament network (scale bar equals 20 μm).

4.2.3 Periplakin ablation inhibits intermediate filament re-organization at the wound site

To investigate the function of periplakin in simple epithelial MCF-7 cells, confluent epithelial sheets of periplakin downregulated cells were scratch wounded as shown in **Figure 2.1 A** and the organization of the keratin intermediate filaments was studied by immunofluorescence.

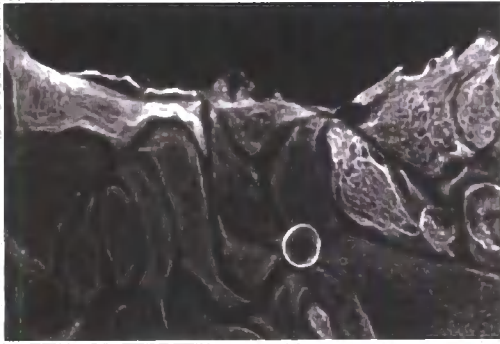
Cells were grown on glass coverslips and after reaching 50-60% confluence transient transfection with periplakin siRNA was performed. Cells were left in the transfection medium for 24 hours and after changing the medium to normal DMEM, cells were left to grow for further 3 days to reach confluence. A wound was created before staining for keratin and periplakin.

Immunolabelling revealed that even almost complete ablation of periplakin did not affect the keratin organisation of the unwounded epithelial sheets that showed normal keratin 8 intermediate filament network (Long *et al.*, 2006). In the scratch wound experiments, control siRNA transfected wound edge cells were able to re-arrange their keratin filaments into bundles parallel to the wound (**Figure 4.5 A**). In contrast, periplakin siRNA transfected cells did not re-arrange keratin filaments, showing no keratin bundling at the wound edge (**Figure 4.5 B**).

The failure of the intermediate filament cytoskeleton to reorganise was also evident by quantitative analysis. Fluorescence intensity of keratin staining in the monolayer, five rows of cells away from the wound edge was compared to the staining intensity at the area with filament bundles at the wound edge. In wounds transfected with control siRNA, keratin bundling was evident by on average 3.5 times more intense fluorescence at the wound edge. In the periplakin down-regulated cells, however, there was no difference in keratin staining intensity between the wound edge and cells away from wound site (**Figure 4.5 C**). Thus, periplakin appears to be required for the re-organisation of keratin IF network at the wound edge of simple epithelial cell monolayer.

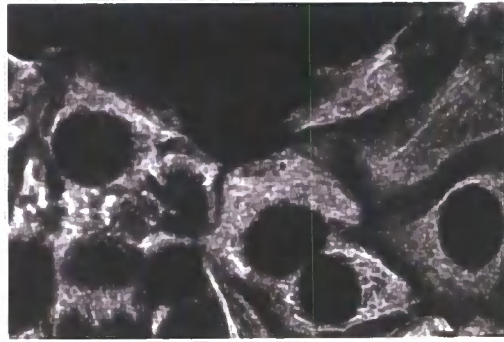
A.

Control transfected MCF-7



B.

Periplakin siRNA transfected MCF-7



C.

Fluorescence intensity

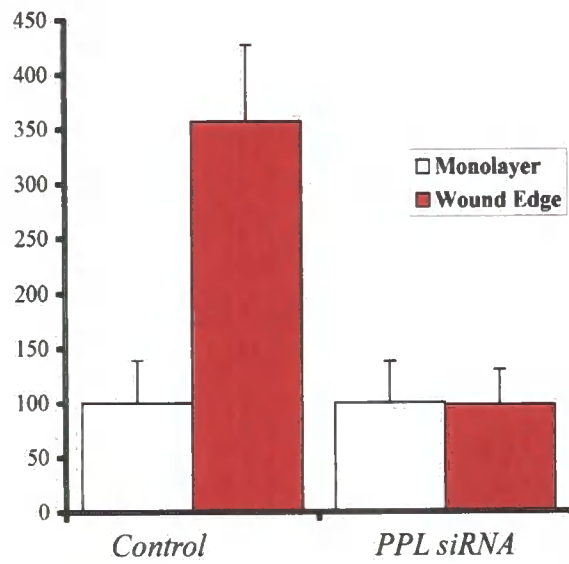


Figure 4.5: Keratin organization in periplakin downregulated wound edge cells.

Transiently transfected cells that had reached confluence were wounded 72h after transfection. A. K8 immunofluorescence in control transfected cells 2h after wounding. B. K8 immunofluorescence in periplakin siRNA transfected cells 2hours after wounding. C. Fluorescence intensity at the wound edge compared to intensity of the monolayer (set as 100 a.u.) in control and periplakin siRNA transfected cells. Fluorescence intensity was measured using raw Zeiss LSM 510 images (Merged Z-stacks) with ImageJ software from 20 cells in three independent wounds at the wound edge and in epithelial monolayer 5 to 7 cell rows away from the wound edge (Scale bar equals 20 μm).

4.2.4 Investigation of intracellular localization of periplakin C-terminus by confocal microscopy in simple epithelial cell

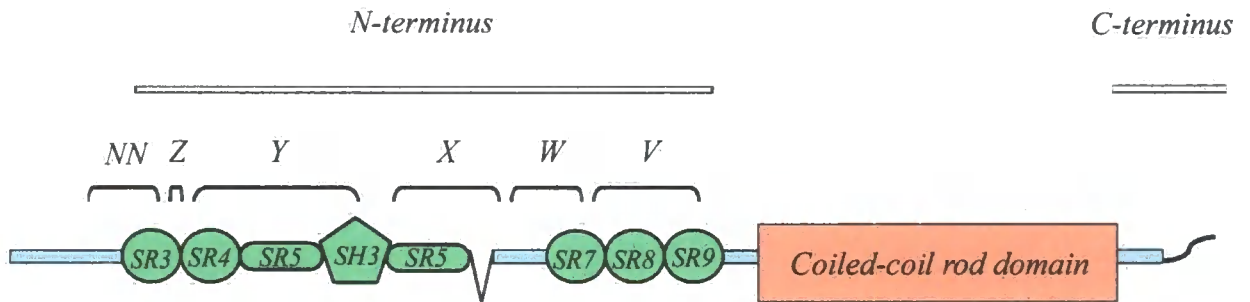
In order to investigate the association of the periplakin C-terminal linker domain and IFs, a stable cell line was created by transfection of a pCI-neo vector containing HA-tagged periplakin C-terminus. Cells were allowed to recover for 48 hours before selection with neomycin (500 µg/ml). Neomycin resistant colonies were expanded and analysed by immunoblotting and immunofluorescence. This stable cell line was named MCF-7 C-PPL. A schematic representation of the full-length periplakin and the construct used for stable transfection is shown in **figure 4.6 A., B.**

MCF-7 C-PPL cells were grown on coverslips to 50-60% confluence. Methanol/acetone (1:1) fixation was applied before staining the HA-tagged periplakin linker domain with rabbit anti-HA antibody (Y-11 Santa Cruz, in a dilution of 1:200).

This staining was different from the localization of endogenous periplakin that predominantly showed cell border staining with a weak cytoplasmic signal that did not co-localize with keratin IFs. However, the periplakin linker domain was mainly localised in the cytoplasmic region of the cell decorating the nuclear envelope and showing filamentous cytoplasmic staining resembling to the keratin intermediate filament distribution (**Figure 4.7 A**). Empty transfected MCF-7 cells (MCF-7 EV) were used as a control, where no specific staining was observed (**Figure 4.7 B**), proving the successful generation of the stable cell line.

Earlier studies demonstrated that the periplakin linker domain is a specific binding partner of the keratin 8 intermediate filaments in several cell types, such as human keratinocytes (Kazerounian *et al.*, 2002) and simple epithelial COS7 cells (Karashima & Watt, 2002). Therefore, this study has focused on the role of the linker domain in keratin reorganisation following scratch wound assays.

A.



B.



Full-length periplakin : 1-1756 aa

C-terminus of periplakin: 1639-1756 aa

Figure 4.6: Schematic diagram of the periplakin construct used for stable transfection.

A. Structure of periplakin. **B.** Structure of the periplakin construct containing HA-tagged periplakin tail domain used for the generation of MCF-7 C-PPL cell line.

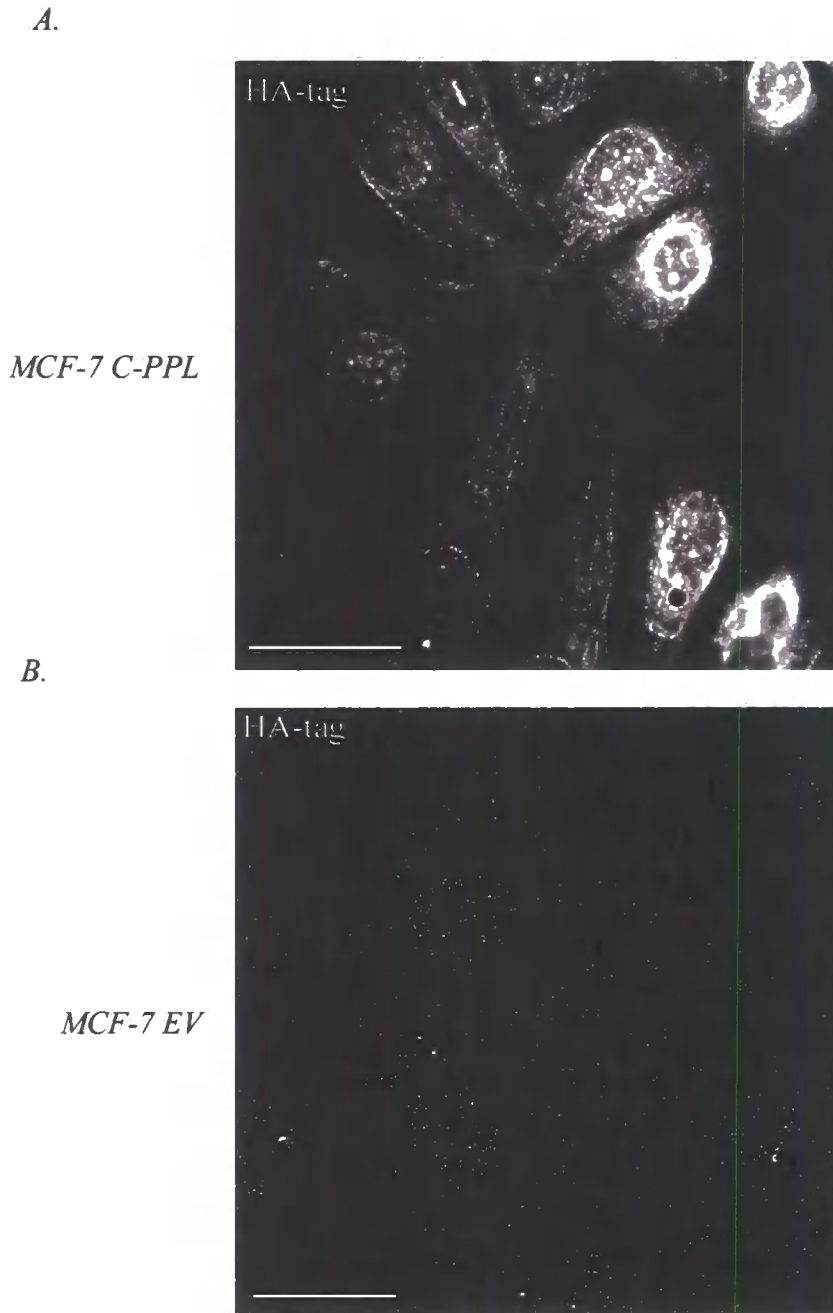


Figure 4.7: Localisation of periplakin linker domain in MCF-7 cells.

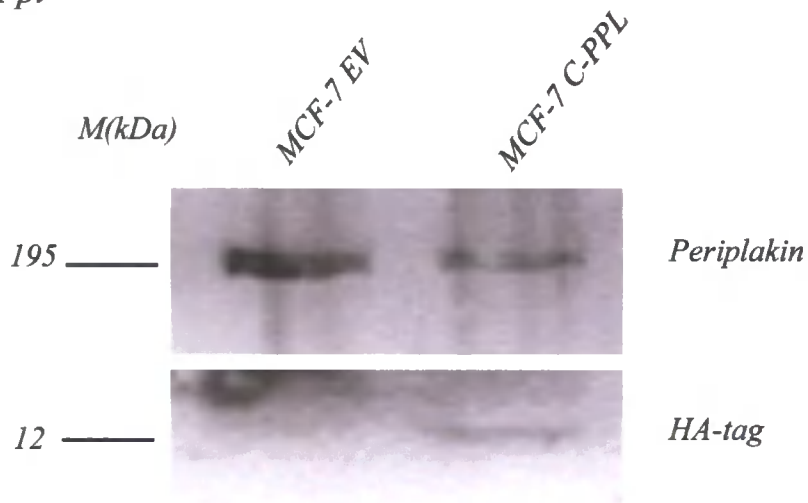
A. MCF-7 C-PPL cells expressing the HA-tagged C-terminus of periplakin showing perinuclear and cytoskeletal filamentous pattern. **B.** Control transfected MCF-7 EV cells show no specific staining with anti-HA antibody. Staining was carried out with Y-11 antibody (Santa-Cruz, 1:200 dilution, scale bars equal 20 μ m).

4.2.5 Investigation of expression levels of HA-tagged periplakin linker domain by Western blot analysis

In order to examine the expression level of HA-tagged periplakin C-terminus in stably transfected MCF-7 cells, whole cell protein extraction was carried out when cultures were at 90-100% confluence, followed by Western blot analysis. Immunoblotting of the total cell extracts showed very low amounts of tagged protein in all studied cell clones (**Figure 4.8 A**), so immunoprecipitation with anti-HA antibody was performed. Untransfected MCF-7 and a control cell line transfected with empty vector were again used as controls. The results of the immunoprecipitation and the immunoblotting thereafter confirmed the expression of the linker domain which proved the successful stable transfection (**Figure 4.8 B**). This allowed the use of this particular cell line to study the effect of periplakin linker domain on keratin organization in simple epithelial cells.

A possible explanation of the low expression level of the tagged protein is that the overexpression of periplakin C-terminus which is responsible for intermediate filament binding led to the collapse of keratin intermediate filaments in the transfected cells and therefore caused the death of these cells. In line with this, several attempts to generate stable cell lines that would constitutively express detectable level of eGFP-tagged periplakin C-terminus were unsuccessful (Long *et al.*, 2006). To overcome this limitation, MCF-7 C-PPL cells were only used at early passages.

A. WB: Ppl



B. IP: HA-tag

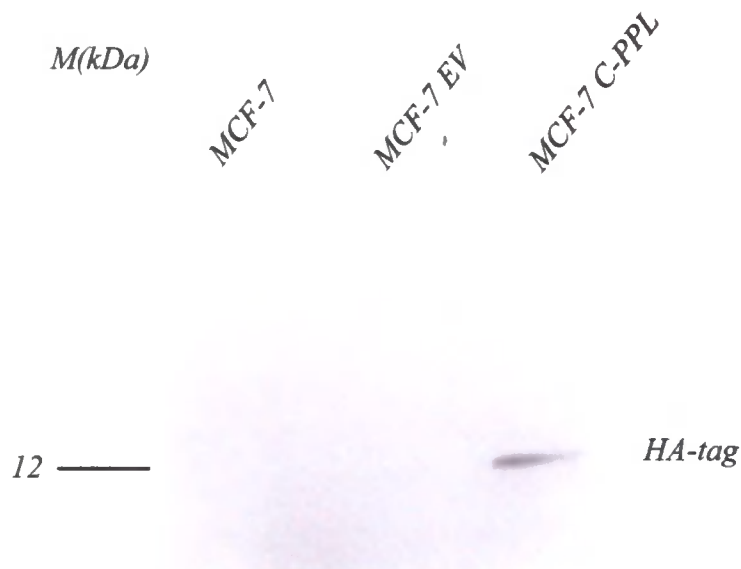


Figure 4.8: Detection of periplakin C-terminal linker domain in MCF-7 C-PPL cells by immunoprecipitation and Western blot analysis.

A. Western blot analysis of endogenous periplakin and periplakin C-terminal domain with TD-2 antibody and anti-HA antibody (both rabbit polyclonal, 1:200 dilution) in control transfected (MCF-7 EV) and stably transfected MCF-7 cells (MCF-7 C-PPL). **B.** Immunoblot analysis of HA-tag periplakin C-terminus with anti-HA rabbit antibody (1:200 dilution) after immunoprecipitation of the tagged protein. MCF-7 cells represent untransfected cells, MCF-7 EV cells refer to empty transfected control cells and MCF-7 C-PPL cells are cells expressing the periplakin tail domain.

4.2.6 Stable expression of the periplakin linker domain interferes with keratin reorganization at wound edge

This representative experiment (shown in **Figure 4.9**) demonstrates the effect of periplakin linker domain on the keratin re-organization at the wound edge in stable MCF-7 clones expressing HA-tagged periplakin C-terminus.

Cells were grown to 100% confluence and the epithelial sheet was wounded. Cells were washed with 1X PBS to clear off all the cells and cell groups that remained slightly attached to the wound edge, before normal DMED medium was applied. 30 minutes after wounding, the epithelia transfected with empty vector showed a well-organized keratin cytoskeleton and had started to re-arrange the keratin cable parallel to the wound edge (**Figure 4.9 A**). On the other hand, the wound edge cells expressing periplakin C-terminus showed a variable phenotype, containing cells with either very thick irregular keratin bundles or keratin aggregates (**Figure 4.9 B**). Many of the cells had granular staining, indicating collapsed keratin filaments in the cytoskeletal region which resembled okadaic-acid induced keratin granules (Long *et al.*, 2006).

4.2.7 Overexpression of periplakin C-terminus is associated with up-regulated Ser-431 phosphorylation in keratin 8 intermediate filament

The intracellular organization of the IF networks is under the control of protein kinases and phosphates (Inagaki *et al.*, 1987; Inagaki *et al.*, 1996; Chang & Goldman, 2004). Phosphorylation and dephosphorylation of IFs alter their biophysical and structural properties (inducing disassembly of IF and a change in solubility). Therefore, phosphorylation specific antibodies were used to recognise the phosphorylated serine/threonine residue in keratin IFs. Ser-73 and Ser-431 residues of keratin 8 IF are two of the major keratin 8 phosphorylation sites (Omary *et al.*, 1998) which are phosphorylated by the ERK 1/2 MAP kinases (Ku & Omary, 1997).

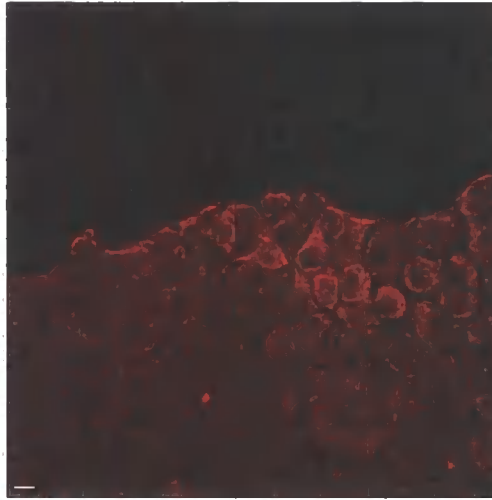
Interestingly, wound edge staining with a Ser-431-specific phosphokeratin antibody (5B3, 1:100, mouse mAB directed against keratin 8 phosphoserine residue 431, Stratech)

demonstrated that keratin bundles in control transfected MCF-7 cells contained phosphorylated keratin filaments. This phosphorylated keratin localization was evenly distributed and even far behind the wound site, the cells displayed a dense network of phosphorylated keratins (**Figure 4.10 A**). Conversely, the MCF-7 C-PPL stable cell line expressing the periplakin linker domain showed thick phosphorylated keratin bundles across the cells localised at the wound edge. Furthermore, cells behind those in the leading edge of the scratch wound displayed bundled or collapsed phosphokeratin filaments (**Figure 4.10 B**).

This increase in phosphorylated keratins at the wound site in MCF-7 C-PPL cells was also evident by Western blotting experiments. Cells were grown, transfected and wounded as described above before whole cell protein extraction. Also, whole cell proteins were extracted from monolayers without wounding as control samples. Extracted proteins were run on 12% pre-cast gel and immunoblotted with 5B3 (monoclonal, mouse anti-Ser-431 keratin 8, 1:100, Stratech) antibody. **Figure 4.10 C** confirmed that wounded MCF-7 C-PPL sheets expressed higher level of Ser-431 phosphorylated keratins than unwounded control (MCF-7 EV) cells. Cytokeratin 18 band is showed as control for even loading of the total keratins.

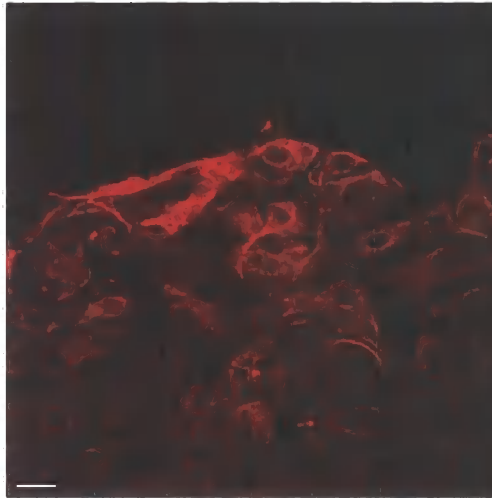
These results confirmed that increased bundling of keratin filaments close to the free wound edges was associated with a change in the distribution and amount of Ser-431 phosphorylated keratins.

A.

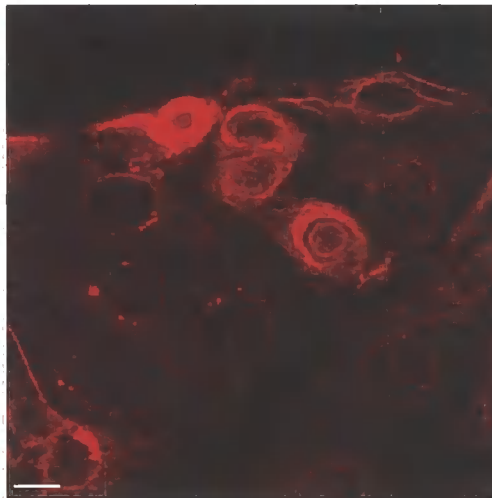


MCF-7 EV

B.



MCF-7 C-PPL



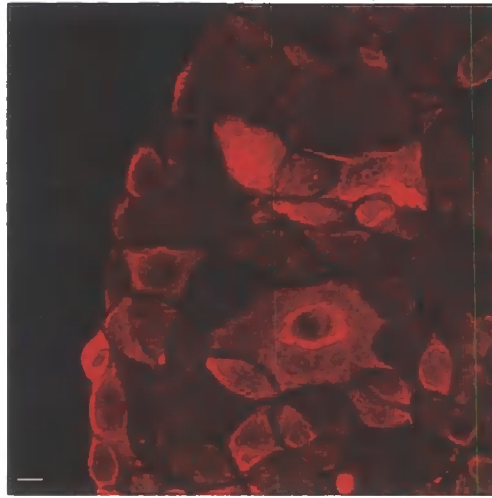
MCF-7 C-PPL

Figure 4.9: Immunofluorescence staining of keratin 8 at wound edges.

A. Empty vector transfected control cell line (MCF-7 EV) showing normal keratin 8/18 cytoskeleton (scale bar equals 100 μm). **B.** Immunofluorescence staining of keratin 8 (cytokeratin 8/18 antibody, mouse monoclonal, 1:1000 dilution) at wound edges of two independent wounds of a clone (MCF-7 C-PPL) overexpressing the HA-tagged periplakin linker domain (scale bars equals 100 (top) and 50 μm , (bottom) respectively).

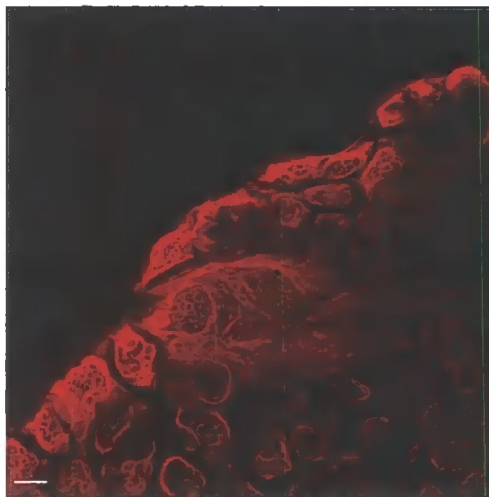
A.

MCF-7 EV



B.

MCF-7 C-PPL



C.

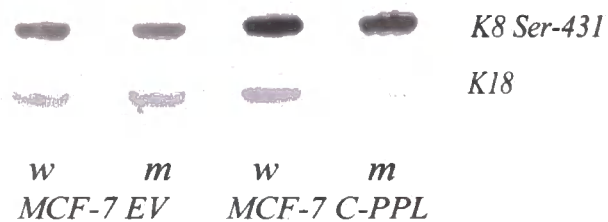


Figure 4.10: Expression of Ser-431-phosphorylated keratins at wound edges.

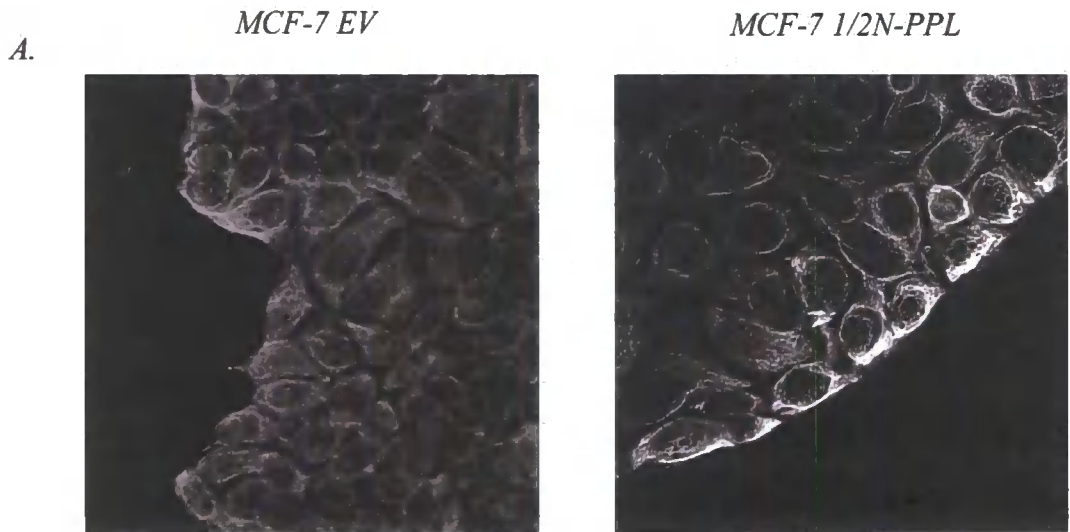
Immunofluorescence staining of control transfected MCF-7 EV cells (A.) and MCF-7 C-PPL cells (B.) expressing PPL-C-terminus 2 h after wounding. C. Western blotting of Ser431-phosphorylated keratin in monolayers (m) and wounded monolayers (w) (ten wounds per 100mm cell culture dish) in control MCF-7 EV and MCF-7 C-PPL cell clones. Keratin 18 blot of the same membrane showing no difference in the total keratin expression between the cell clones or treatments. Immunofluorescence and immunoblotting was carried out with 5B3 (monoclonal, mouse anti-Ser-431 keratin 8, 1:100 dilution, Stratech) and cytokeratin 18 (mouse, monoclonal, 1:1000 dilution) antibody (scale bars equal 100 μ m).

4.2.8 Periplakin amino-terminus accelerates keratin intermediate filament bundling at the wound edge

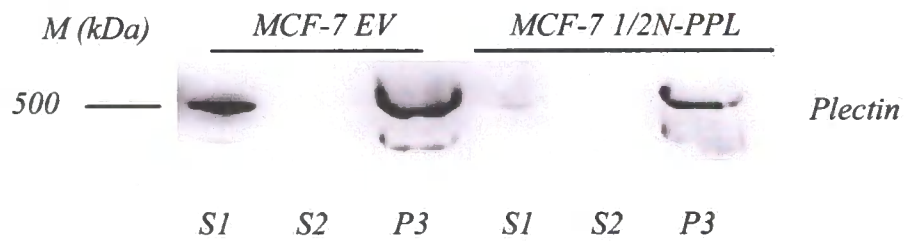
The changes in keratin organisation during migration of simple epithelial sheets of MCF-7 cells prompted the study of the ability of periplakin in cytokeratin dynamics. In addition, it was hypothesised that, if the observed co-localisation of periplakin and plectin has functional significance in these cells, over-expression of the HA-tagged periplakin N-terminus should affect the distribution or function of plectin. To investigate this, confluent MCF-7 ½ N-PPL and empty vector transfected control cell sheets were scratch wounded and the plectin subcellular distribution and keratin IF organization were followed by immunofluorescence staining.

Recent analysis of the keratin staining in MCF-7 wound edge cells revealed that 2 hours after wounding, the majority of the cells at the free edge formed a thick cable of bundled keratin filaments running parallel to the wound (Long *et al.*, 2006). For comparison, MCF-7 and MCF-7 ½ N-PPL cells were grown on glass coverslips and after forming monolayers the epithelial sheets were wounded. Immunofluorescence staining of keratin 8 demonstrated that the re-organization of keratin intermediate filaments at the scratch wound edge occurs faster in MCF-7 ½ N-PPL cells compared to control transfected cells. The MCF-7 ½ N-PPL cell line assembled a prominent keratin cable at the wound edge already 30 minutes after wounding (**Figure 4.11 A**) which was not been observed in the control cell lines.

To investigate whether this phenomenon is associated with the co-immunoprecipitation of periplakin and plectin, subcellular distribution of these proteins was examined. Biochemical fractionation of confluent monolayers of cells revealed different subcellular localization of plectin in cells overexpressing the periplakin amino-terminus (**Figure 4.11 B**). Therefore, the early keratin bundling at the wound edge seen in MCF-7 ½ N-PPL cells was correlated with a shift in subcellular distribution of plectin. Almost all plectin in MCF-7 ½ N-PPL cells was found in the Triton-insoluble cell fraction compared to empty vector transfected control cells (**Figure 4.11 B**), whereas the amount of soluble keratin subunits in the cytosolic S1 fraction and insoluble keratin in the P3 fraction was similar in both cell lines, which confirmed even loading.



B.



C.

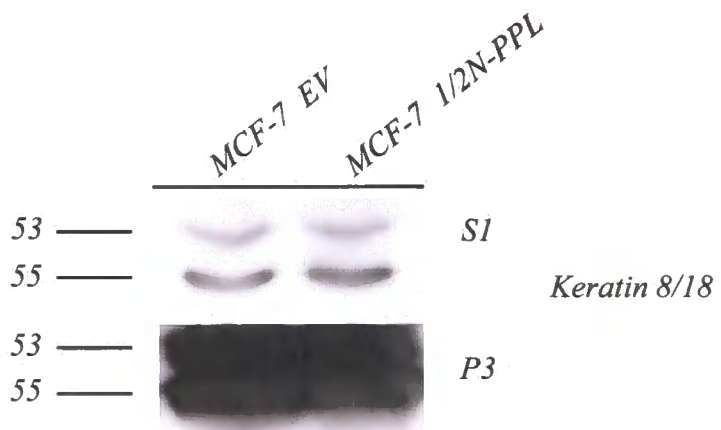


Figure 4.11: Accelerated keratin bundling in MCF-7 1/2N-PPL cells.

A. Keratin-8 immunofluorescence of scratch wounded epithelial monolayers at 30 minutes after wounding. Keratin cytoskeleton is re-arranged into a cable parallel to the wound edge in the MCF-7 1/2 N- PPL cell line (right) but not in the empty vector transfected control cell line (left). Scale bars equal 20 μm . **B.** Subcellular distribution of plectin in empty vector transfected (MCF-7 EV) cells and in cells overexpressing periplakin N-terminus (MCF-7 1/2N-PPL). S1 refers to cytosolic fraction, S2 represent Triton soluble membrane fraction and P3 indicates Triton insoluble fraction. **C.** Immunoblotting of soluble keratin 8/18 in the S1 cytosolic fractions of empty vector transfected (MCF-7 EV) and MCF-7 1/2N-PPL cells.

4.2.9 Plectin downregulation in the MCF-7 1/2N-PPL cell inhibits rapid keratin bundle formation

To confirm that plectin plays a role in the early keratin bundle formation, plectin was downregulated by transient siRNA transfection and keratin organization was followed.

Cells were grown, transfected, wounded and stained as described above. Confocal microscopy using immunofluorescence confirmed that plectin was uniformly down regulated in the scratch wound experiments in MCF-7 cells. The confocal settings for detection of fluorescent signal were unchanged for plectin-depleted cells and control cells to demonstrate the difference in fluorescent signal. Depleting MCF-7 cells of plectin resulted in decreased bundling of keratin at the free wound edge. Keratin filaments seemed to be disorganized in plectin knock-down cells and did not form a uniform cable at the wound edge (**Figure 4.12**).

Dramatic changes in keratin bundle formation at the wound edge in plectin ablated MCF-7 ½ N-PPL cells demonstrate the importance of plectin in early keratin assembly. Overall, this observation suggests that the accelerated keratin assembly into a cable at the wound edge is indeed dependent on plectin.

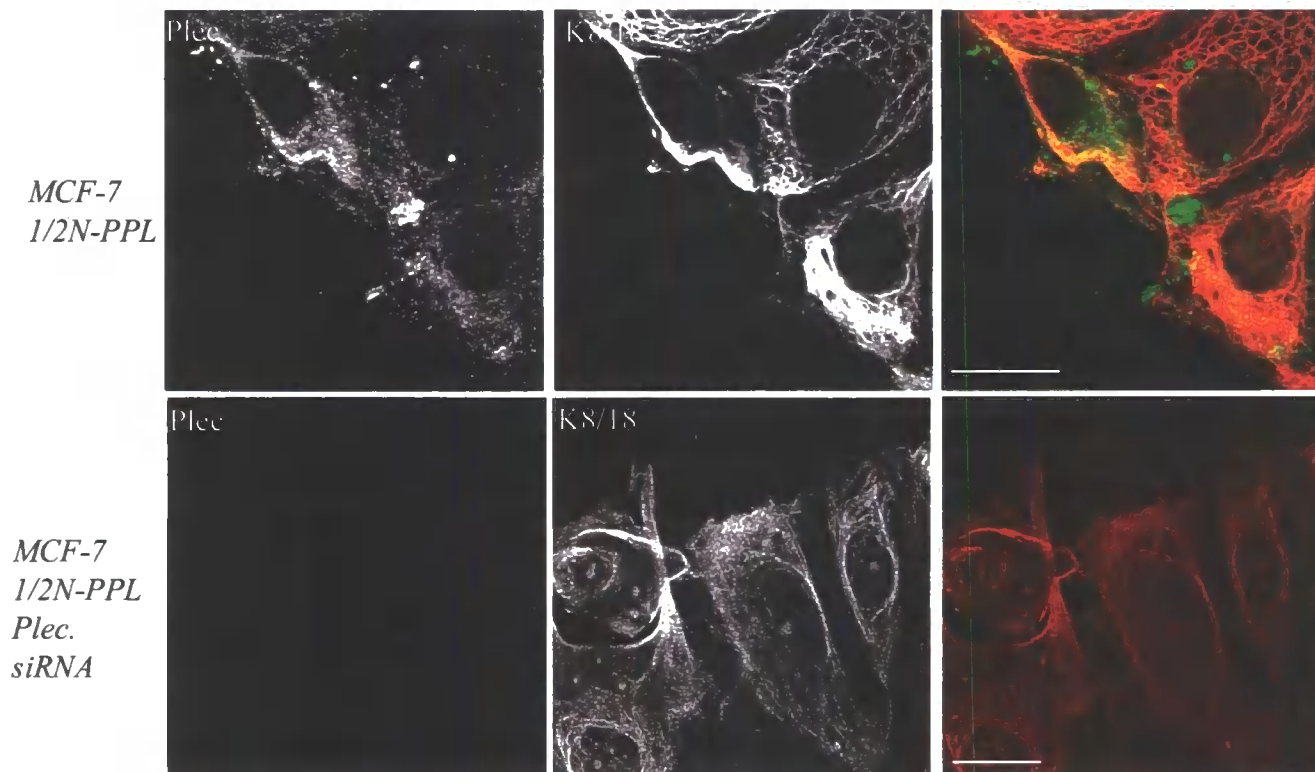


Figure 4.12: Immunofluorescence images showing that plectin is required for rapid keratin bundling at the wound edge.

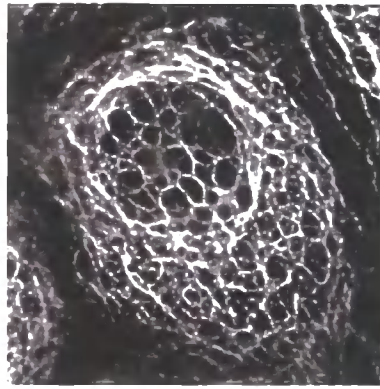
MCF-7 1/2N-PPL cell line was transfected (top) with either control or plectin (bottom) siRNA prior to scratch wounding. The cells were stained with plectin (c-20, 1:200 dilution, green) and keratin8/18 (LE-41, 1:2 dilution, red) antibodies at 30 minutes after wounding (scale bars equal 20 μm).

4.2.10 Simultaneous downregulation of periplakin and plectin results in keratin intermediate filament disorganization in MCF-7 cells

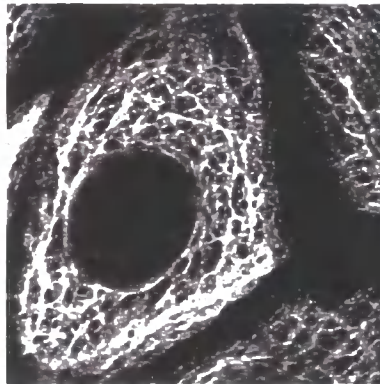
The capability of periplakin and plectin to control keratin organisation at the wound edge cells was evident in MCF-7 epithelial cells. To further examine the role of these cytolinkers, periplakin and plectin double knockdown siRNA transfected MCF-7 cells were generated. The general appearance of the keratin cytoskeleton was compared to control transfected cells using immunofluorescence microscopy.

As **figure 4.13** illustrates, the keratin filaments had a dense cytoplasmic network in control cells while those cells depleted in both periplakin and plectin displayed a strong keratin cage around the nucleus with fewer cytoplasmic keratin filaments. Interestingly, this change in the keratin network was not detected after periplakin siRNA transfection as the lack of periplakin did not result in an effect on epithelial morphology or cytokeratin organization in monolayer cells. In addition, plectin ablation on MCF-7 cells did not modify the appearance cytoskeletal network dramatically, although a small percentage of the cells demonstrated bulky keratin filaments around the nucleus. Based on this evidence, periplakin and plectin are required for normal keratin organization in simple epithelial cells and facilitate the distribution of the keratin network inside the cell.

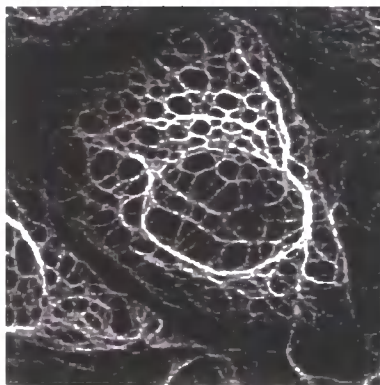
Keratin 8/18



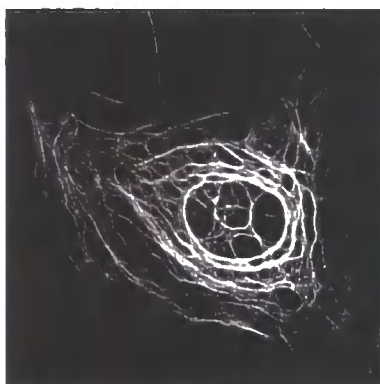
Control



PPL siRNA



Plectin siRNA



PPL and Plec siRNA

Figure 4.13: The lack of periplakin and plectin alters the appearance of keratin intermediate filament network in MCF-7 cells.

siRNA transfected MCF-7 cells were stained with keratin 8 monoclonal antibody (LE41, 1:2 dilution). Cells lacking in both periplakin and plectin show disorganised keratin network with strong bundling around the nucleus compared to single downregulated or control transfected MCF-7 cells.

4.3 Discussion

4.3.1 Effect of periplakin and plectin ablation in intact epithelial sheets

To investigate the functional significance of the interaction between periplakin and plectin, siRNA transfections were carried out in two different cell lines in order to reveal the effects of downregulation of these proteins. Immunoblotting experiments after periplakin downregulation showed unaltered plectin expression levels in both MCF-7 and HaCaT cells. Similarly, immunofluorescence studies on periplakin siRNA transfected cells did not show significant changes in the localization of the endogenous plectin. The lack of periplakin in gene targeted mice (Aho *et al.*, 2004) resulted in unaltered plectin distribution and epidermal differentiation. Taken together with our observation, it could be concluded that periplakin downregulation in either simple epithelia or in keratinocytes resulted in no obvious phenotypic differences under unwounded circumstances.

Downregulation of plectin, however, resulted in periplakin aggregation in subconfluent HaCaT keratinocytes indicating that plectin might play a role in regulating the subcellular targeting of periplakin. This periplakin aggregation appeared throughout the cytoplasm of the cells. Co-staining with periplakin and keratin 14 displayed co-localization with the tip of IFs. The changes in periplakin distribution demonstrate a functional correlation between periplakin, plectin and keratin IFs.

4.3.2 Keratin intermediate filament organization

The current work has confirmed that periplakin participates in the re-organization of keratin intermediate filaments at the wound edge. This observation suggests that periplakin is essential in normal wound healing processes in simple epithelia as its depletion leads to loss of keratin cable formation. It has been speculated that after the rapid initial wound response to assemble an actin-purse string, the actin structure is consequently used to guide the re-organization of keratins so that it reinforce the free edge of epithelia (Brock *et al.*, 1996; Long *et al.*, 2006). The formation of keratin intermediate filament cable could be mediated via periplakin that has previously been described as an actin associated protein

even though the protein lacks a classical actin-binding domain (DiColandrea *et al.*, 2000). Alternatively, plectin, which contains the ABD, could connect periplakin to the actin purse-string cable. Furthermore, it seems that the keratin filaments forming the keratin cable at the wound site are more dynamic compared to keratins in an intact monolayer. Keratin filaments at the wound edges seem to be more vulnerable to okadaic acid treatment (Long *et al.*, 2006) that causes disassembly of keratin filaments and aggregation of solubilised keratins with periplakin.

4.3.3 Influence of periplakin linker domain on keratin intermediate filaments

The N-terminus of periplakin has been shown to associate with desmosomes and interdesmosomal plasma membranes whereas the periplakin linker domain demonstrated constitutive binding to keratin intermediate filaments. To test whether the periplakin C-domain has any effect on keratin re-organization, a stable cell line was first created which expressed the linker domain of periplakin. Immunofluorescence studies revealed that periplakin COOH-domain was mainly distributed along the cytoskeleton. This stable cell line showed the same subcellular distribution of the linker domain in simple epithelia as previously seen in keratinocytes (DiColandrea *et al.*, 2000). EGFP-tagged periplakin linker domain was also associated with keratin cytoskeleton, indicating that the interaction of periplakin C-terminus and keratin filaments can take place in MCF-7 cells (Long *et al.*, 2006). Scratch wound assay on confluent monolayer revealed that wound edge cells expressing the periplakin C-terminus had collapsed keratin cytoskeleton and irregular thick keratin bundles. This phenomenon was associated with the higher phosphorylation level on keratin 8 Ser-431 residue. With regard to Ser-431 residue it is known that its phosphorylation is increased upon mitotic arrest or stimulation of cells with EGF, which suggests a role in mitogen-induced signalling (Ku & Omary, 1997). Cytoplasmic IFs are reorganized dramatically during mitosis and this reorganization is considered to be controlled by IF protein phosphorylation (Izawa & Inagaki, 2006). Furthermore, phosphorylation of these sites are correlates with disease progression in patients with chronic liver disease (Toivola *et al.*, 2004; Zatloukal *et al.*, 2004). Based on my results, it appear that periplakin linker domain expression, keratin bundling at the wound edge and

Ser-431 residue phosphorylation are connected. However, it is still not clear whether induced phosphorylation was a consequence of keratin bundling or periplakin C-terminal overexpression. It remains for future studies to map the signalling and putative phosphorylation events described above.

4.3.4 Periplakin NH₂-terminus is required in normal wound healing processes

Based on this study, wounded epithelia over-expressing periplakin N-terminus rearrange their keratin network faster than control transfected cells. The rapid bundling of keratin filaments was inhibited when the MCF-7 ½ N-PPL cells were transfected by plectin siRNA oligonucleotides indicating that the effect of the periplakin N-terminus was mediated by plectin. The role of plectin in controlling signalling pathways is beginning to be explored. Recently, plectin has been demonstrated to be a binding partner of the receptor for activated C kinase 1 (RACK1) and therefore affecting PKC signalling (Osmanagic-Myers & Wiche, 2004). Taken together with an earlier report suggesting that plectin is involved in actin filament regulation via Rho/Rac/cdc42 signalling (Andrä *et al.*, 1998), it is tempting to consider cytolinkers to be able to collaborate and provide link between cytoskeletal dynamics and signalling events. I also tested the effect of double siRNA transfection against periplakin and plectin in MCF-7 cells that, indeed, caused abnormal cytokeratin network, resulting in a perinuclear cage structure. My data support a recently investigated role of plectin as a major regulator of cytoarchitecture (Osmanagic-Myers *et al.*, 2006). The role of plectin in regulating keratin organization was studied by using plectin deficient keratinocytes where the loss of plectin resulted in larger keratin meshwork and accelerated disassembly of the keratin network in okadaic acid-treated cells (Osmanagic-Myers *et al.*, 2006). Another plakin family member, epiplakin, has also been recently implicated in organisation of intermediate filament networks. Knock-down of epiplakin in simple epithelial cells resulted in disruption of keratin and vimentin networks (Jang *et al.*, 2005). Upon cellular stress in primary keratinocytes epiplakin is translocated to the keratin intermediate filaments and protects the keratin network from rapid dissociation (Spazierer *et al.*, 2008). To summarise, siRNA experiments indicate that epiplakin is required for the maintenance of keratin network in simple epithelia and primary

keratinocytes, whereas periplakin is involved in keratin bundling at the epithelial wound edge. The respective domain organisation of periplakin and epiplakin supports this idea. Periplakin N-terminus comprises a typical 'plakin box' that can target the protein to cellular junctions and other membrane locations (Ruhrberg & Watt, 1997; DiColandrea *et al.*, 2000). Epiplakin, on the contrary, only contains a long array of IF-binding repeats (Fujiwara *et al.*, 2001). Despite this, it is notable that epiplakin null animals (Goto *et al.*, 2006; Spazierer *et al.*, 2006) as well as periplakin and envoplakin knock-out mice (Aho *et al.*, 2004; Määttä *et al.*, 2001) are viable without any major defects in epidermal differentiation, even though epiplakin deficient mice appear to have problems in keratinocyte migration and wound healing (Goto *et al.*, 2006).

It should also be noted that the keratin cytoskeleton affects subcellular localisation of plakin cytolinker proteins as demonstrated in MCF-7 cells where ablation of keratin 8 by transient siRNA transfections prevented localisation of periplakin and desmoplakin at cell borders (Long *et al.*, 2006). Likewise, plectin localisation is altered in keratin 8 null hepatocytes (Galarneau *et al.*, 2007).

Association of transiently expressed plectin domains with simple epithelial keratins in cultured cells (Wiche *et al.*, 1993; Nikolic *et al.*, 1996) indicated that plectin is involved in both the structural organisation of the peripheral cytokeratin bundles and their association with the submembrane cytoskeleton. It is also known that periplakin is localised at the desmosomal junctions and associated to intermediate filaments. Therefore it is tempting to speculate that the downregulation of plectin and periplakin weaken the intermediate filament desmosome complexes and change the shape of the cytokeratin network.

CHAPTER V

ROLE OF PLAKIN PROTEINS AND KERATIN 8 IN EPITHELIAL MIGRATION

5.1 Introduction

In the previous chapter the role of periplakin and plectin in keratin intermediate filament organisation was studied. This led to an investigation of their role in cell migration. Cell migration is important for many biological processes. It is essentially a physical process, which is regulated by a complex network of biochemical signalling and feedback pathways. In the early stages of animal embryo development, the formation of the three fundamental germ layers is achieved through the coordinated cell movements of gastrulation. In the adult, key cells in the immune response circulate in the blood until they are triggered to leave (migrate) upon detection of a pathogen.

In collective migration, cells maintain their cell-cell connections in order to move as a coherent sheet. During embryonic development, this common mechanism appears to be responsible for several processes. For example, epithelial dorsal hole closure in *Drosophila*, ventral closure of hypodermis in *C. elegans* embryos and eyelid closure of mammalian embryos (Martin & Parkhurst, 2004; Friedl *et al.*, 2004) involve collective epithelial migration. Despite the importance of this process, with many examples of multi-cell migration, the mechanisms controlling and regulating this behaviour remains poorly understood.

When a wound disrupts the continuity of an epithelial sheet, it is critical for the organism to be able to heal that breach. Two main mechanisms of epithelial wound healing have been described (Jacinto *et al.*, 2002). The first method is the so called “purse-string” mechanism. Here, closure is achieved through contraction of an actin and myosin enriched cable that runs along the leading edge of all marginal cells around the wound perimeter (Martin & Lewis, 1992). In contrast to this purse-string mechanism seen in embryonic closures, skin wounds in adults close by active migration of cells into the wounded area (Martin, 1997). This is by an acquired motility of the border cell and involves protrusions of filopodia and ruffling lamellae seen at the leading edge, while the cells crawl collectively onto the new surface. This method appears to be used in most *in vitro* investigations of wound closure. However, while there are sometimes actin cables running along the whole or a part of the adult wound edge, the cables may not be necessary for wounds to close at their normal rates. It is possible that they may contribute to the

maintenance of an even wound front (Fenteany *et al.*, 2000). It has also been shown that, at least in cultured intestinal epithelial cells, the method of closure can depend on the size of the wound (Bement *et al.*, 1993). Small wounds close by the purse-string mechanism, large wounds close by cell crawling and intermediate wounds close by the combination of the two. Despite recent advances in the understanding of how actin dynamics are regulated, there are several important unknown aspects in collective migration. For example, it is not yet fully understood how sheet migration is coordinated while the intact epithelial nature of the wound edge is maintained.

Several independent studies have indicated a role for keratin intermediate filaments in moderating cell migration. Simple epithelial, 'soft' keratins have been implicated in cell migration and invasion. For example, expression of K8 and K18 in vimentin-positive mouse L fibroblasts and in human melanoma cells has been found to increase the invasion of transfected cells through matrigel-coated filters (Chu *et al.*, 1993; Chu *et al.*, 1996). Perinuclear re-organisation of the keratin 8/18 network by sphingosylphosphorylcholine increases cellular elasticity and ability to migrate through limited-sized pores (Beil *et al.*, 2003). A study by Brock *et al.* (1996) showed no difference in embryonic wound healing between keratin 8 null and control animals. The study did, however, reveal that embryonic wounds assemble a keratin cable at wound edges in addition to the actin "purse-string" cable (Brock *et al.*, 1996). Nevertheless, the studies on simple epithelial keratins have not fully addressed the role of intermediate filament networks in the collective migration of simple epithelial sheets.

Other studies addressing the role of plakins in cell motility have shown that they mediate profound effects on cell migration. BPAG-1 knockout mice show a wound-healing defect (Guo *et al.*, 1995) due to reduced cell migration. Plectin KO fibroblasts display defects in their ability to reorganize actin microfilaments after activation of rac/rho/cdc42 signalling cascades, which results in reduced motility of plectin deficient cells (Andra *et al.*, 1998). More recently, generation of isoform-specific knock-outs for plectin have demonstrated how plectin-1 is involved in migration of fibroblasts and T-lymphocytes and is required for efficient leukocyte infiltration to wounds (Abrahamsberg *et al.*, 2005). In addition, another plakin protein, epiplakin, has also been proposed to regulate the speed of

wound healing. Epiplakin null mice had no apparent phenotypic abnormalities, but the closure of experimental wounds on their back was slightly accelerated compared to wild-type animals (Goto *et al.*, 2005). Thus, understanding the role of cytolinkers in cell migration could lead to new insights into the complex regulation of epithelial wound healing processes.

This chapter presents the results obtained when the MCF-7 C-PPL cell line was used to investigate the effect of periplakin linker domain overexpression in wound healing. During this study, a scratch wound assay was used as a tool to measure wound closure in epithelial cells. Many aspects of the migratory behaviour of cells can be conveniently studied by this classic scratch-wound assay. In this model, cells are grown on a flat surface until they form a confluent monolayer. A strip of cells is then mechanically removed using a pipette tip and the closure of this open space is observed (**Figure 2.1**). Normally, cells respond with cell spreading and migration into the denuded area until the wound is closed. The width of the wound is measured at regular timepoints, allowing comparison between different treatments. In addition, the progression of the remaining cells during healing of the wound can be easily observed by microscopy for different durations, ranging from hours to several days. In general, most cell types, for example epithelial cells, behave similarly and, characteristically, enter a lag phase (usually lasting a few hours) after wounding, followed by a steady healing process at an approximately constant rate.

In addition, the effect of downregulation of endogenous periplakin and plectin by siRNA transfection was investigated by the scratch wound assay in order to elucidate their function in cell migration. This chapter will end with data from HeLa and Panc-1 cells which extends previously published work suggesting that the keratin 8 intermediate filament network is essential for epithelial integrity in MCF-7 cells (Long *et al.*, 2006).

5.2 Results

5.2.1 Cell viability is not affected by either periplakin or keratin 8 siRNA transfections

To ensure that any effects on epithelial wound closure are not due to increased cell death survival after periplakin or keratin 8 down-regulation, cell survival was analysed 48h after transfection. In comparison to control transfected or untransfected cells, both periplakin and keratin 8 siRNA transfected cells showed similar, only slightly lower number of viable cells (**Figure 5.1**). Overall, cell viability did not change more than 5% compared to the scrambled control after periplakin or keratin 8 knock-down in these cells. Since periplakin siRNA transfection of cells had no effect on the integrity of the monolayer either, it can be concluded that the consequence of keratin 8 downregulation, described below, were not due to cell death.

5.2.2 Periplakin linker domain delays wound closure in MCF-7 cells

Wound closure of the stable cell line overexpressing the conserved linker domain of periplakin was investigated in comparison to the empty vector transfected control cell line. Compared to the control cell line, cells expressing periplakin C-terminus showed a consistent delay in wound closure. Control transfected cells migrated into the empty wound space to heal the wound in 8 hours, whereas the periplakin linker domain expressing wounds remained largely open at the same time point (**Figure 5.2 A**). Quantitative analysis of the wound closure is shown in **Figure 5.2 B**. After 8 hours, when about 40% of the control wound width remained open, the MCF-7 PPL-C wounds had only just started to close and remained still open after 24 hours (**Figure 5.2 B**). The slower migration of the epithelial sheets in the case of MCF-7 C-PPL cells corresponds to abnormal organization of keratin filaments at the wound edge which was demonstrated in chapter IV. Thus, the overexpression of the periplakin-C domain caused collapse of keratin intermediate filaments and impaired the normal rate of wound closure.

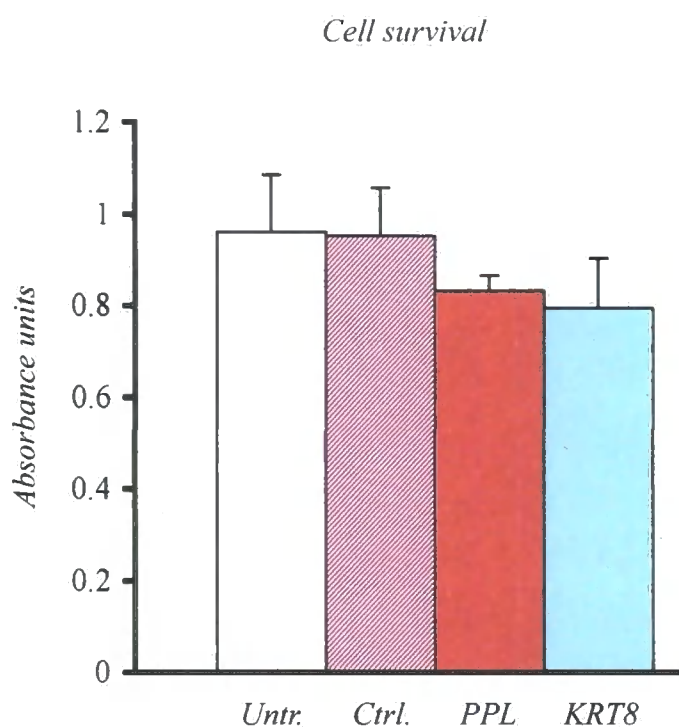
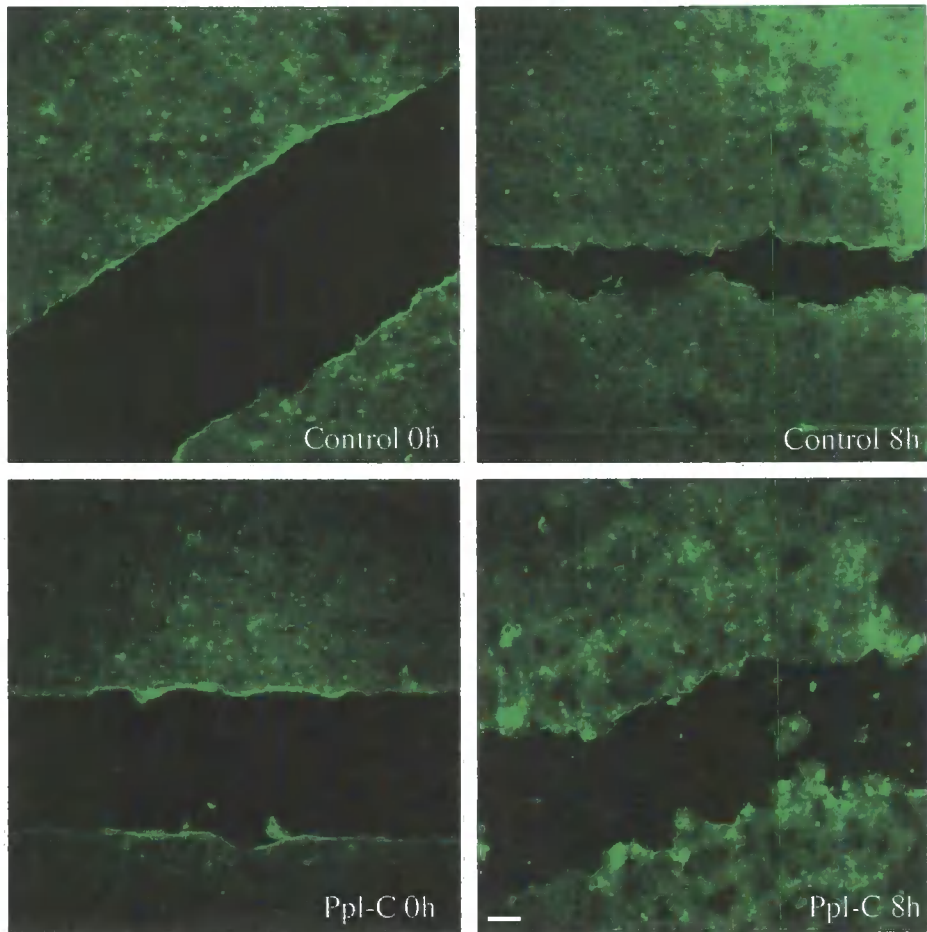


Figure 5.1: Cell survival after siRNA transfections.

The number of cells were measured using CellTiter cell proliferation kit. (Promega). Mean and standard deviation of the three measurements are shown (absorbance units at 490 nm). Cells without transfection shown in the first column under the name of Untr., control (Ctrl) transfected cells shown in the second column, whilst PPL and KRT8 refers to periplakin and keratin siRNA transfected cells, respectively.

A.



B.

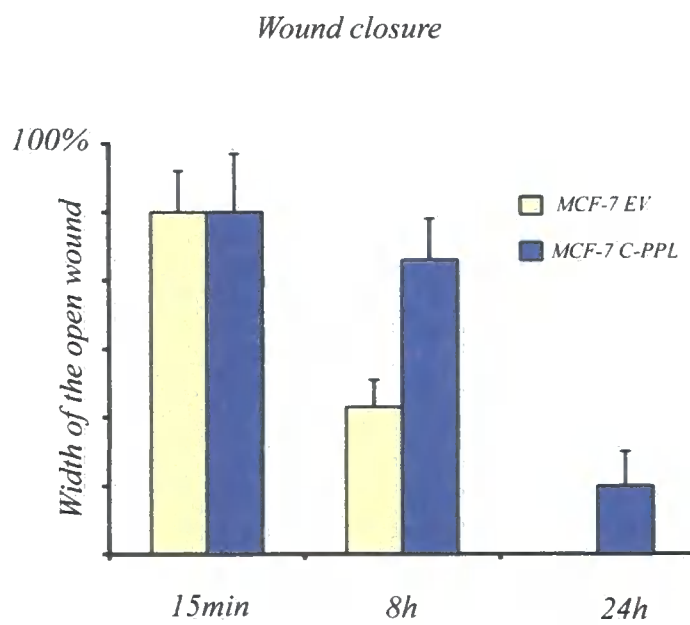


Figure 5.2: Wound closure in control and PPL-C cell lines.

A. Confluent MCF-7 C-PPL monolayers were grown in 6-well plates and wounded using 20 μl (white) pipette tips. The wound closure was monitored by phase contrast microscopy at 15 minutes, 8 hours and 24 hours time points (scale bar equals 100 μm). **B.** Quantification of the wound closure in empty vector and PPL-C terminus transfected cell clones. For each wound, the width of the 15 minute time point was designated as 100% width and subsequent time points in the graph show the mean relative width of the open wound ($n=10$). Error bars show standard deviation. As the experiment reached the 24 h time point, the control wounds were closed.

5.2.3 *In vitro* wound closure is impaired by periplakin siRNA transfection in epithelial MCF-7 and HeLa cells

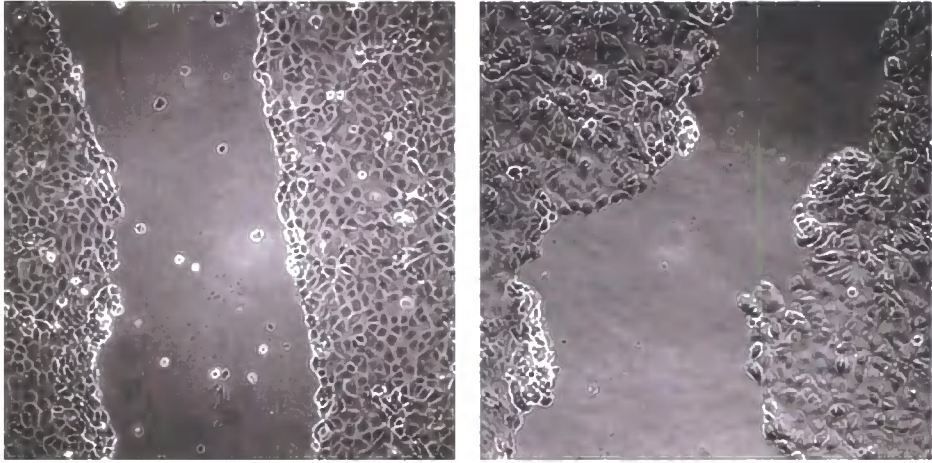
To investigate the effect of periplakin depletion on epithelial migration, epithelial sheets transfected with periplakin or control siRNA were subjected to scratch wounding. Confluent monolayers were wounded in triplicate and the wound closure was monitored using phase contrast imaging at the same area of the wound at 30 minutes, 10 hours, 20 hours and 40 hours until complete closure.

Delayed wound closure was seen in MCF-7 cells so that even 20 hours after wounding, periplakin siRNA transfected scratch wounds remained open (**Figure 5.3 A**) when compared to control transfected cells. To ensure that changes in the cell migration were not unique to the MCF-7 cell line, the same experiment was repeated using different epithelial cell lines. Similar results were found when comparing the migratory changes in periplakin ablated HeLa cells and MCF-7 cells. Both cell lines showed decreased cell migration resulting in unhealed wounds (**Figure 5.4 A**). These data indicate that regulation of wound closure is a function of periplakin regardless of the epithelial cell type. Quantification of the wound closure is displayed in **Figures 5.3 B and 5.4 B**, where bars represent mean values and standard deviation of three individual measurements.

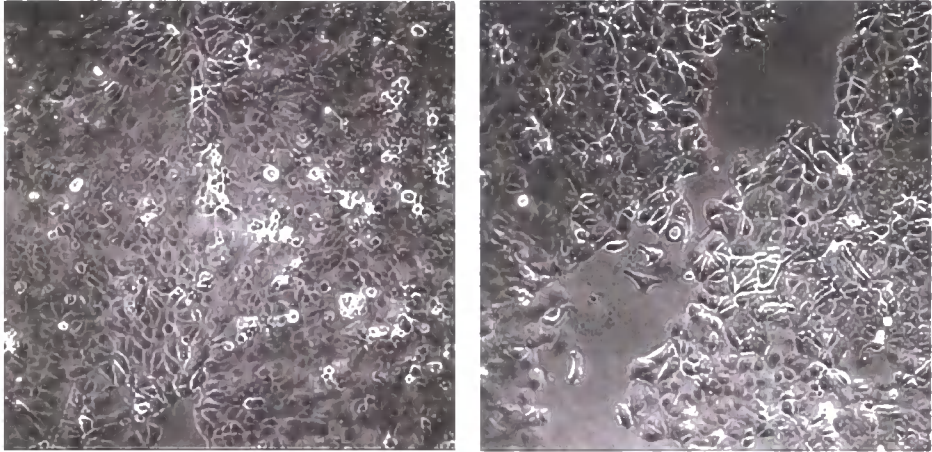
The periplakin ablated wounds displayed uneven migration characterized by irregular wound edges that nevertheless retained cell-cell contacts between the wound edge cells. Thus, it is possible that periplakin-dependent keratin bundling participates in the maintenance of co-coordinated migration of wound edge cells. The reduced cell migration in both cases demonstrates the importance of periplakin in wound healing.

A.

30 min



20 h

*Control**PPL siRNA*

B.

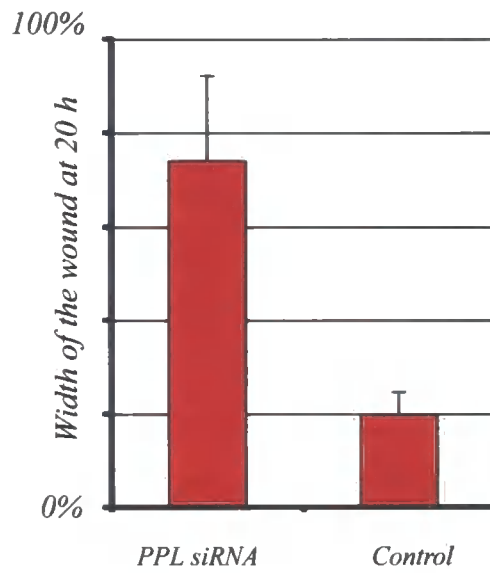
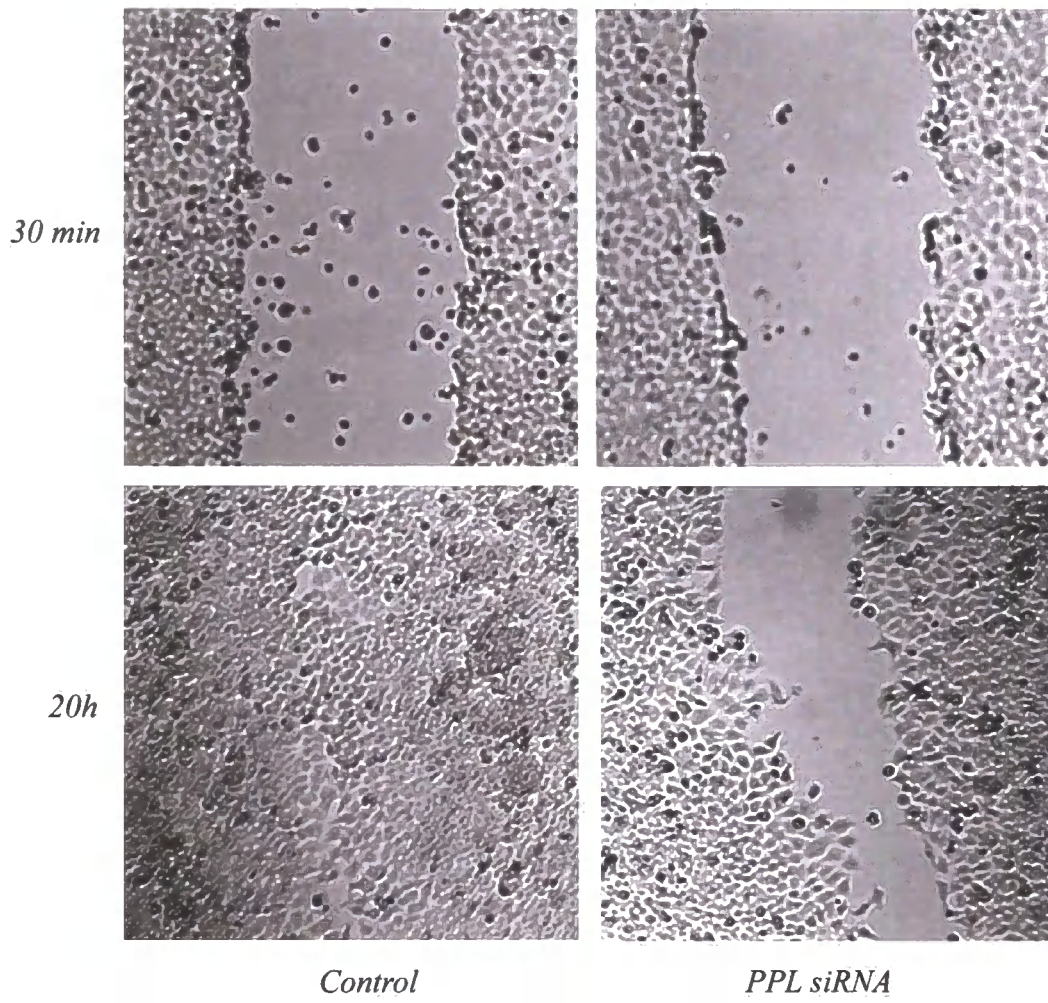


Figure 5.3: Wound migration properties of periplakin depleted MCF- 7 cells.

A. Phase contrast microscopy images of scratch wound closure of control and periplakin siRNA transfected MCF-7 monolayers (Scale bars equals 100 μ m). B. Quantification of the wound closure in MCF-7 cells. Open wound distances at the start of the experiment were designated as 100% and closure of the wounds are shown as a function of that. The width of the wounds at 20 hours time point were determined using photomicrographic images and displayed as the percentage of the remaining wound width compared to the width at 0h time point. Mean and standard deviation of the measurements from three independent transfections are shown.

A.



B.

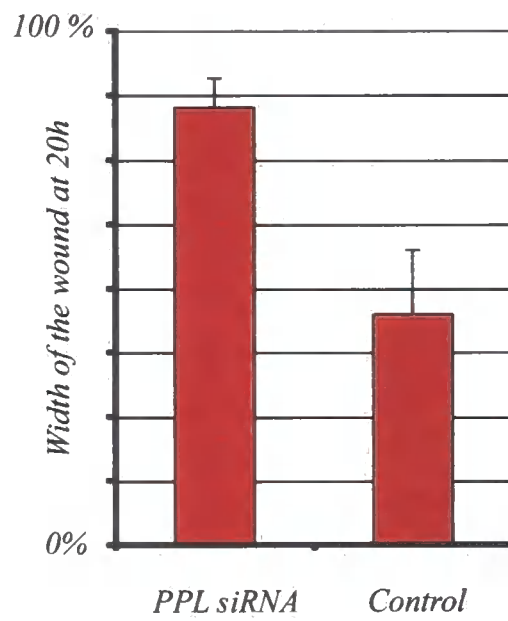


Figure 5.4: Effect of periplakin downregulation on wound healing in HeLa cells.

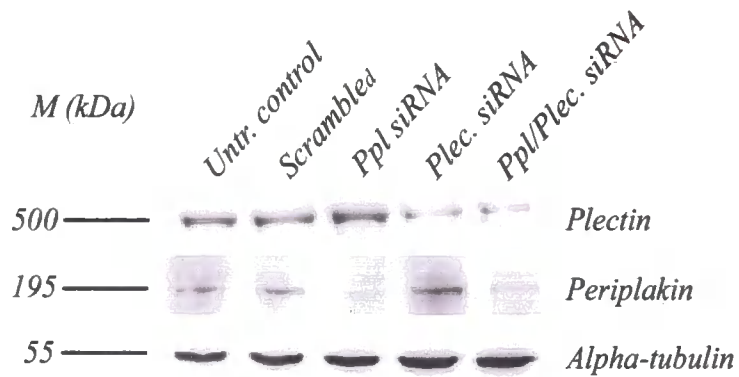
A. Phase contrast microscopy images of scratch wound closure of control transfected and periplakin siRNA transfected HeLa monolayers (Scale bars equals 100 μ m). **B.** The graphs show the mean value and standard deviation of the wound closure in HeLa cells at 20 hours time point. Quantitative analysis of three independent transfections is indicated. The widths of the open wound at the start of the experiment were designated as 100% and closure of the wounds are shown as a function of that. The width of the wounds at 20 hours time point were determined using photomicrographic images and displayed as the percentage of the remaining wound width compared to the width at 0h time point.

5.2.4 Depletion of either periplakin or plectin impairs MCF-7 wound closure in a similar manner

My earlier observations of disorganized keratin intermediate filaments at the wound edge following periplakin siRNA knockdown were associated with a reduction in the rate of normal cell migration in simple epithelia. Furthermore, since the co-immunoprecipitation experiments had revealed a link between periplakin and plectin, the effect of single and simultaneous protein downregulation was studied in MCF-7 cells. In these wound healing experiments, a higher density (50-60%) of cells is needed in order to form a monolayer at the 72 hour timepoint. As this might affect the efficiency of siRNA knock-down I first investigated the expression level of periplakin and plectin after the transfections by immunoblotting and immunocytochemistry. **Figure 5.5** shows the amount of the expressed proteins after transfections. Both single and double siRNA transfections resulted in a successful downregulation of periplakin and plectin expression (**Figure 5.5**). Triplicate samples of confluent MCF-7 epithelial sheets were thereafter subjected to scratch wounding and wound closure was monitored at 7 hours and 24 hours timepoints.

Comparing the control untransfected and control transfected epithelial wounds to periplakin and plectin siRNA transfected wounds, it is clear that the lack of plectin, just as the lack of periplakin, slows down the cell migration. Control wounds were closed 24 hours after wounding, while single transfected epithelial scratches remained invariably open (**Figure 5.6**), which was confirmed by measuring the open wounds in all three independent cases. The result shows that the closure of the cytolinker ablated wounds were delayed at 7 hours timepoint and strikingly impaired at 24 hours timepoint, when both control wounds had closed completely (**Figure 5.6**). Furthermore, epithelial wounds lacking in both periplakin and plectin cytolinker demonstrated even greater delays in cell migration, leaving a wider gap between the two epithelial faces (**Figure 5.6**).

A.



B.

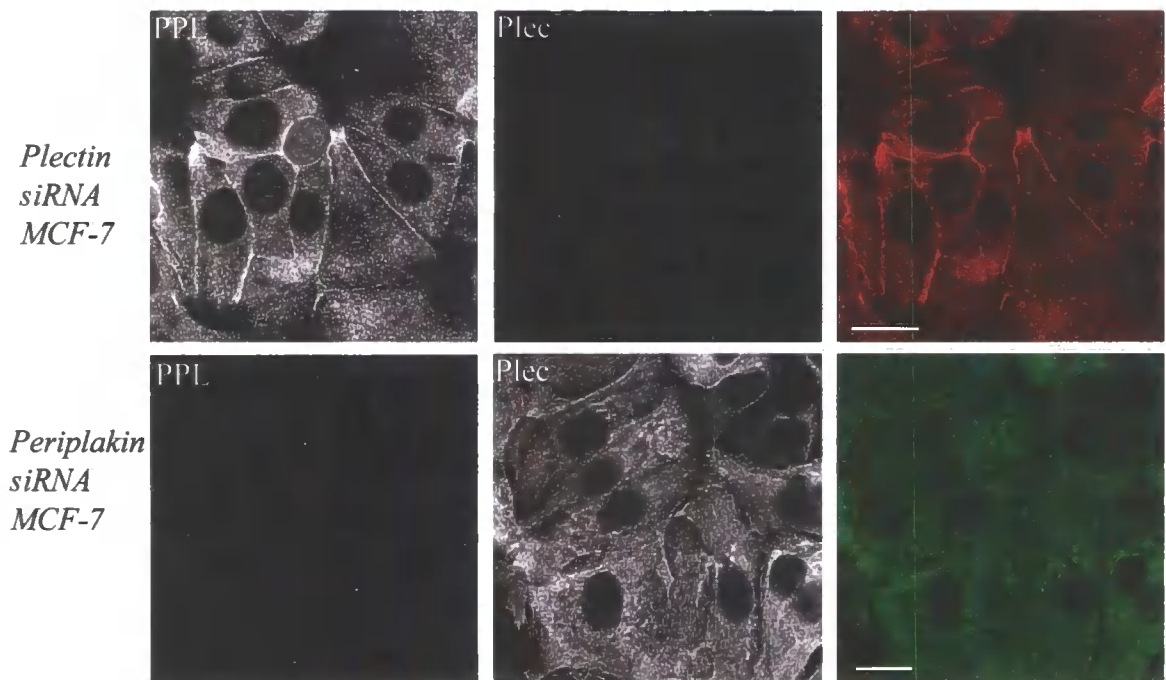


Figure 5.5: Verification of effective periplakin and plectin downregulation in wound healing experiments.

A. Western blot analysis indicating successful knock down effect in both single and double siRNA transfected cells. Actin blot shows equal loading of the total protein in each lane. **B.** Immunofluorescence staining of periplakin (red) and plectin (green) in plectin siRNA (top row) and periplakin siRNA (bottom row) transfected cell (scale bars equal 20 μm).

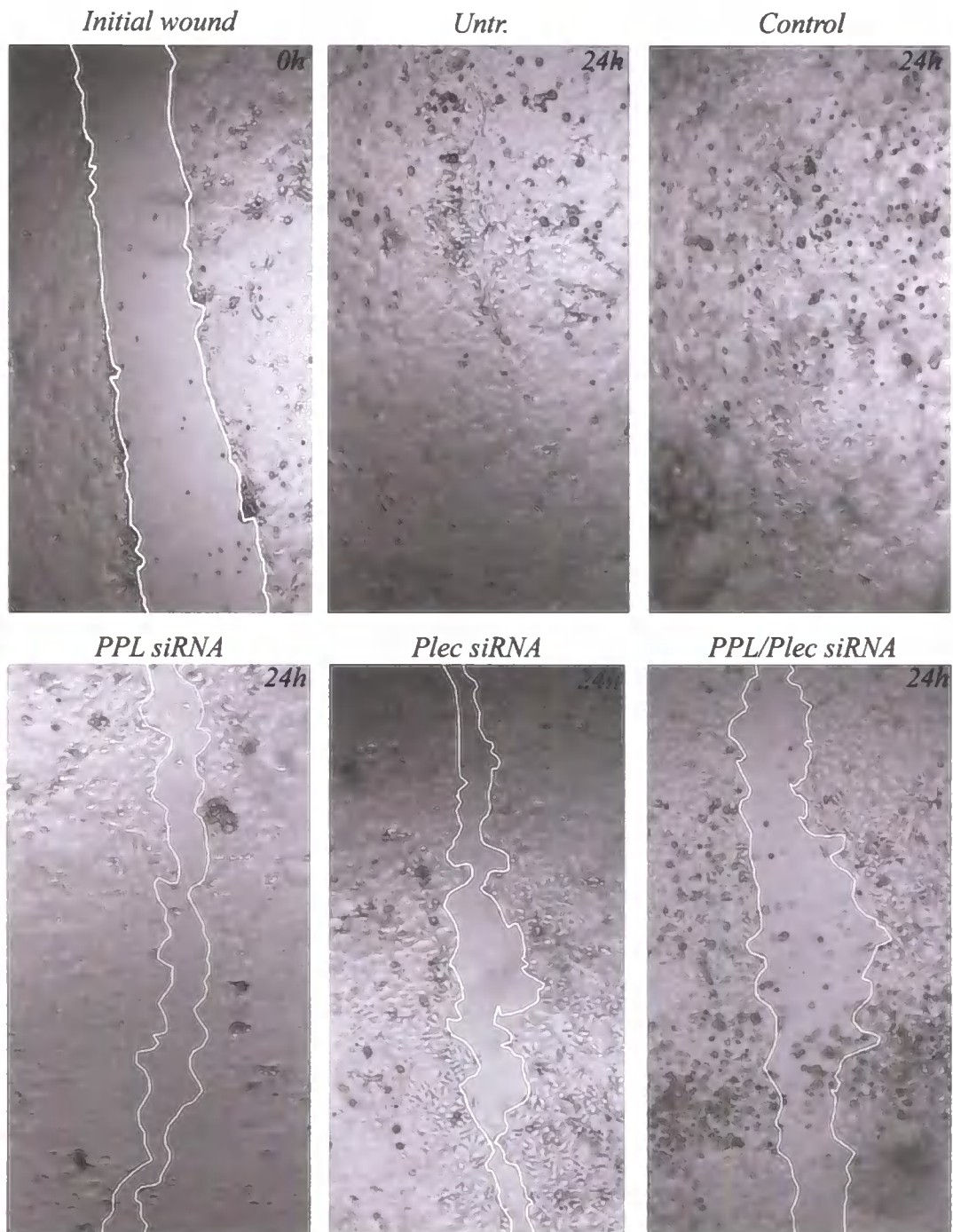


Figure 5.6: Phase contrast microscopy images showing that epithelial migration is impaired by ablation of periplakin or plectin.

Images showing representative initial wound at 0 hours time point, closed control wounds (Untr., Contr.) and open cytolinker ablated wounds (PPL siRNA, Plec siRNA, PPL/Plec siRNA) at 24 hour timepoint (wound edges are indicated by white lines). Illustrative images were taken at 10X magnification.

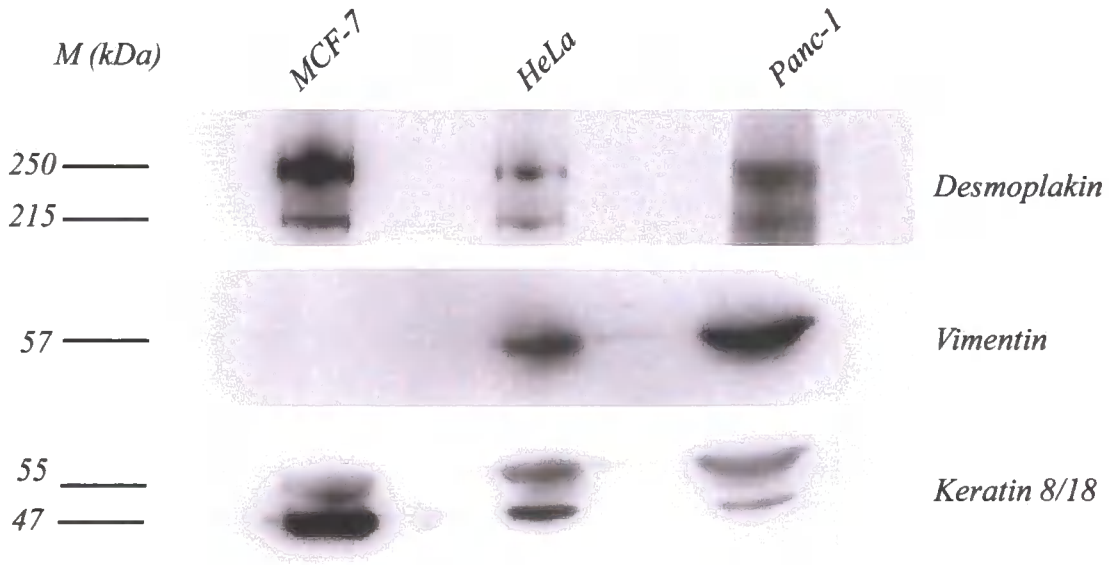
5.2.5 Ablation of keratin 8 shows disrupted desmosomes in HeLa and Panc-1 cell lines

Keratin 8 intermediate filament downregulation by siRNA transfection resulted in reduced cell-cell contacts, leading to disrupted MCF-7 epithelial sheets (Long *et al.*, 2006). It is possible that this could be due to the failure of cells to create and maintain cell-cell junctions in the absence of keratin intermediate network. Hence, this could suggest that the cohesive nature of the epithelial sheet migration of MCF-7 cells is regulated by the cytokeratin 8 network.

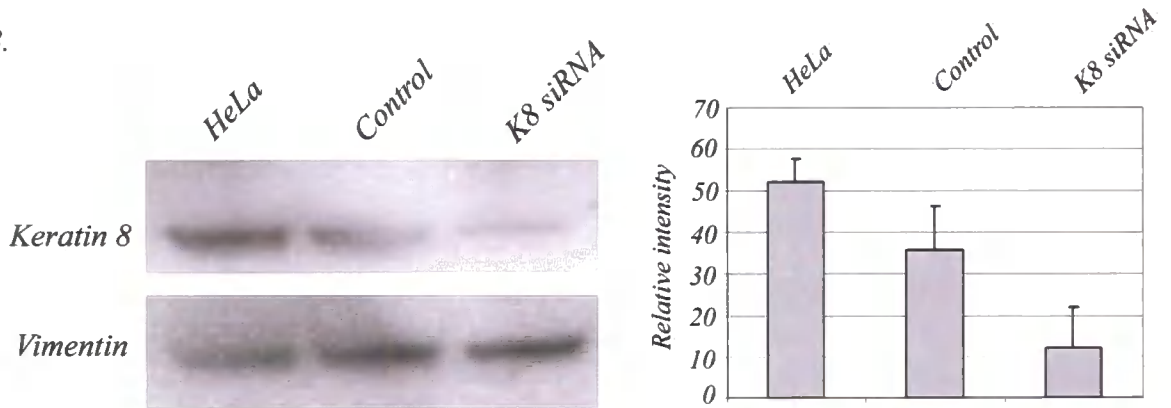
To further investigate whether keratin intermediate filaments are required for the formation and maintenance of desmosomes in other epithelial cell lines, K8 expression in HeLa and Panc-1 cells was downregulated and the expression and subcellular localisation of desmoplakin was investigated. It should be noted that both HeLa and Panc-1 cells, unlike MCF-7 cells, are vimentin positive cells (**Figure 5.7**). Immunoblotting of total cell extracts from the epithelial cell lines mentioned above allowed identification of the expressed intermediate filament proteins compared to MCF-7 cells. Keratin 8 and 18 were originally used as a loading control, but it has to be noted that the different cell lines have slight differences in keratin expression. MCF-7 cells expressed no vimentin and showed higher amount of keratin 8/18 and desmoplakin compared to Panc-1 and HeLa cells, where both vimentin and keratin intermediate filaments were expressed simultaneously.

Keratin 8 siRNA transfection was applied to both HeLa and Panc-1 cell lines. After transfection, whole cell total protein extracts were loaded on a 4-12% Nu-Page Bis-Tris pre-cast gradient gel in order to verify the knock-down efficiency. The BCA protein assay (section 2.7.2) was used to quantify protein levels prior to loading of the gel. Equal loading was further confirmed visually by staining of the filters with Ponceau S, which stains all proteins red. Immunoblotting confirmed the successful downregulation of K8 expression. The same level of keratin 8 downregulation as in MCF-7 cells was observed in both Panc-1 and HeLa cells (**Figure 5.7**).

A.



B.



C.

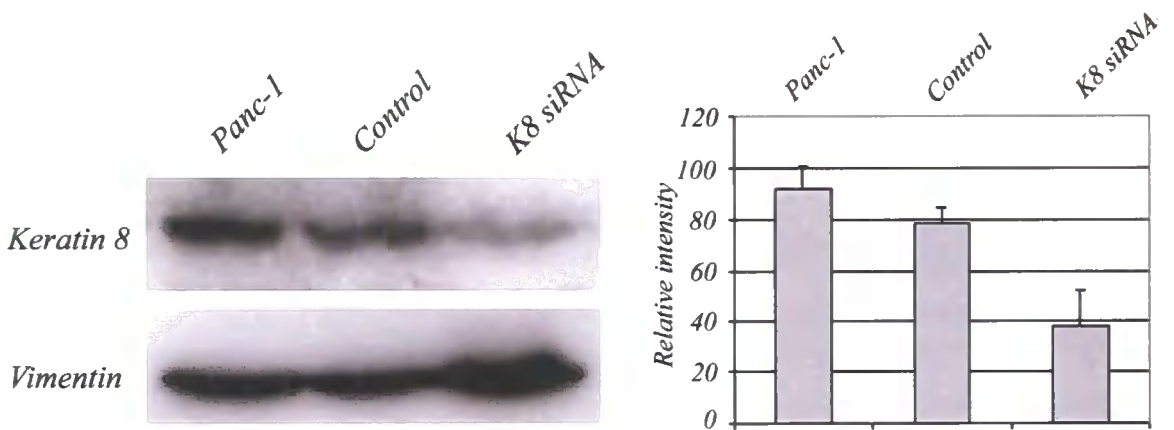


Figure 5.7: Expression of cytoskeletal proteins in MCF-7 cells in comparison to Panc-1 and HeLa cell lines.

A. Immunoblot analysis of three different epithelial cell lines. 20 µg of total cell extracts were immunoblotted with vimentin (3052, 1:2000 dilution), desmoplakin (AHP320, 1:100 dilution, Serotec) and cytokeratin 8/18 (Ab-2, 1:1000 dilution, Oncogene) antibodies. MCF-7 cells are vimentin negative cells, which is in contrast to HeLa and Panc-1 cell lines where vimentin is expressed. Cytokeratins 8 and 18 and desmoplakin are expressed in all three cell clones showing highest expression in MCF-7 cells. B. & C. Keratin 8 downregulation in HeLa and Panc-1 cell line. Vimentin immunoblot was used as a loading control. The graphs show the mean expression level and standard deviation of three independent experiments ($p > 0.05$).

Following transfection, cells were allowed to establish junctional complexes before scratch wounding of the monolayer. Indirect immunofluorescence and confocal microscopy confirmed that keratin 8 expression was uniformly downregulated in scratch-wound migration experiments of both HeLa and Panc-1 cells. Control siRNA transfected HeLa cells developed desmosome contacts with neighbouring cells, showing punctate desmoplakin staining at cell borders with keratin 8 intermediate filaments expanding from the cytoskeleton to the desmosomes (demonstrated in **Figure 5.8 A**). However, siRNA knockdown of keratin 8 intermediate filament abolished cell-border localization of desmoplakin to a large extent (**Figure 5.8 B**), the cells showing evenly distributed desmoplakin staining throughout the cytoplasm. Cells in the control transfected HeLa monolayers were immunolabelled for desmoplakin and counted 30 minutes after scratch wounding. Ninety-five percent of the control cell borders (n=73) retained desmosomal localization of desmoplakin. In contrast in keratin 8 siRNA transfected monolayers, the corresponding percentage was only 6% (n=107). Interestingly, in a transfection where a small island of HeLa cells had remained untransfected and retained prominent K8 expression, punctate desmosomal staining was established only between keratin-positive cells but not between two knock-down cells or a knock-down cell and a keratin positive cell (**Figure 5.8 C**). Higher magnification of keratin positive cells maintaining desmosomal contacts and keratin negative cells with no cell-cell contacts are displayed in **Figure 5.8 D**.

The loss of desmoplakin localization at cell borders was also observed in Panc-1 cells transfected with K8 siRNA. Punctate desmosomal staining was seen only between K8 positive cells, whereas almost no desmoplakin staining was found at cell borders of K8 knockdown cells (**Figure 5.8 D**).

HeLa

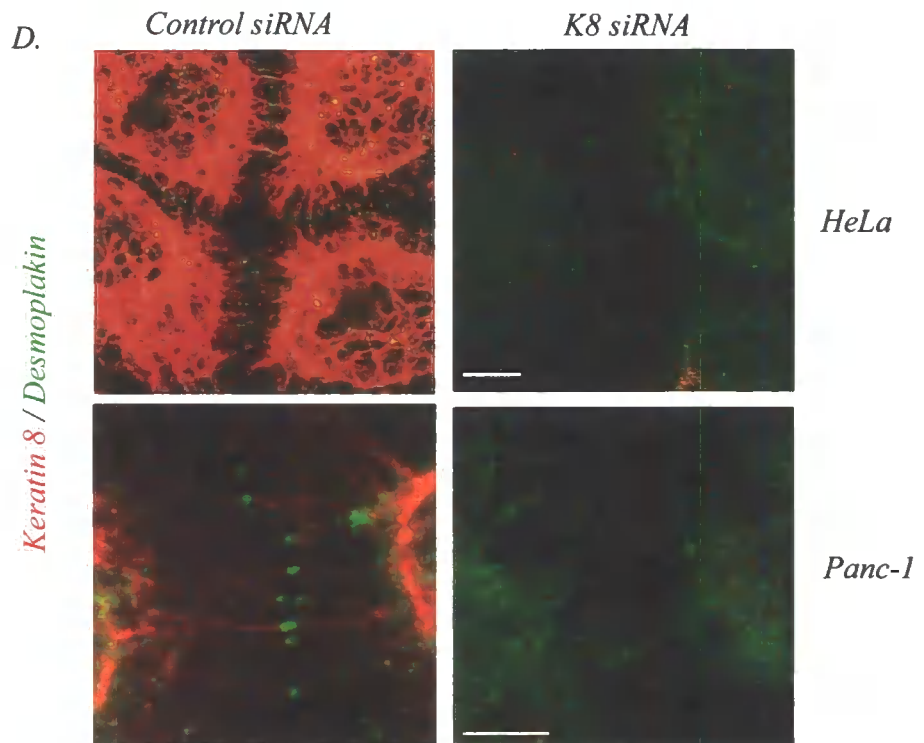
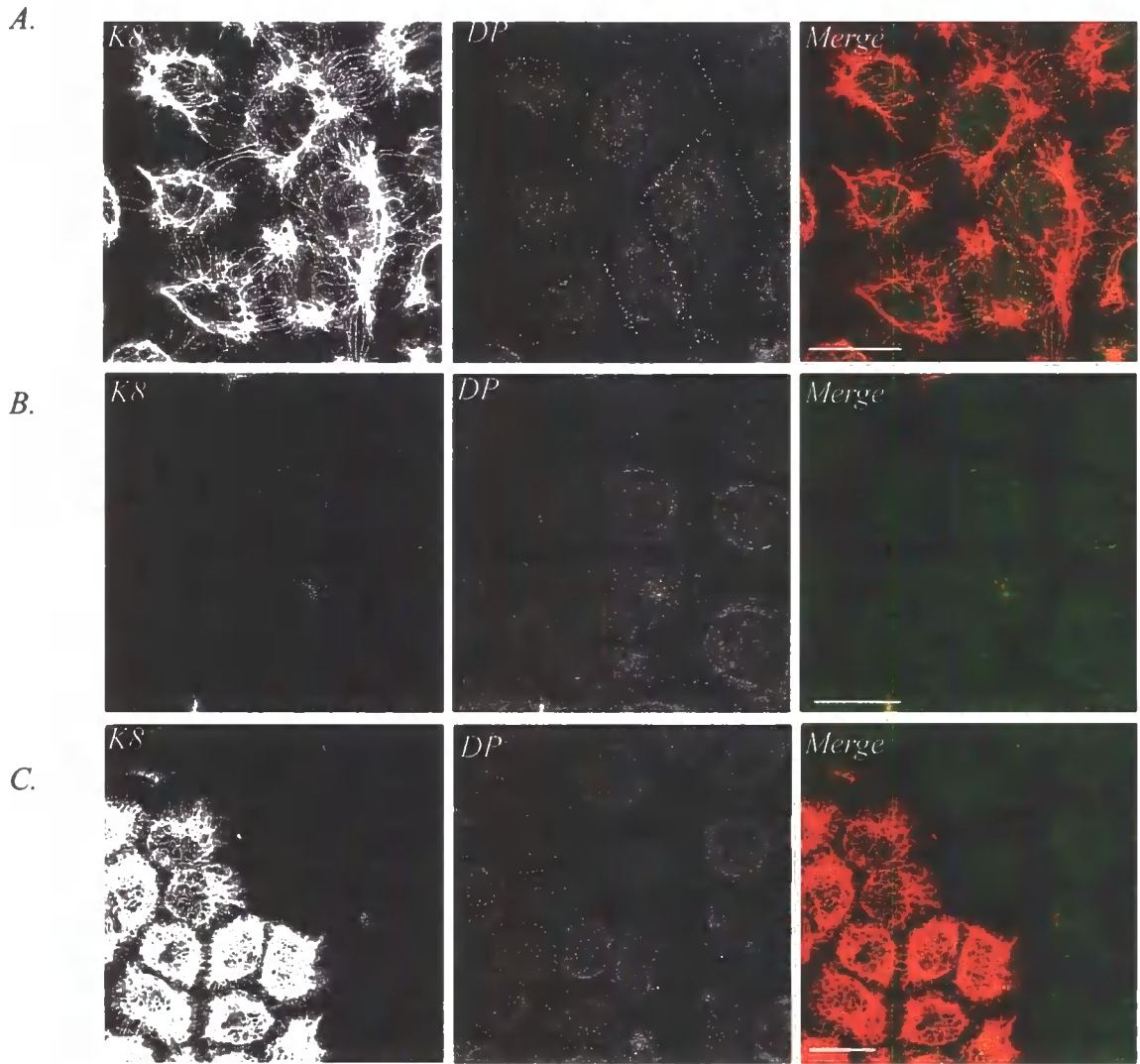


Figure 5.8: The effect of keratin 8 knock-down in HeLa and Panc-1 cells.

A. Control transfected HeLa monolayers. Red channel shows keratin 8 immunofluorescence (LE41, 1:2 dilution), green channel displays desmoplakin staining (AHP320, 1:100 dilution, Serotec). **B.** Keratin 8 and desmoplakin staining in keratin 8 siRNA transfected cells. **C.** The image displays an area of the siRNA transfected HeLa monolayer, where a small island of cells have retained their keratin 8 expression next to cells with no keratin 8 expression. Note that cells with no keratin 8 expression do not display desmoplakin staining at the cell borders. **D.** Higher magnification of desmoplakin (green) staining at HeLa cell borders shows desmosomal staining between keratin positive cells in contrast to keratin 8 negative cells (top row). Panc-1 cells (bottom row) transfected with keratin 8 siRNA were stained for keratin 8 (red) and desmoplakin (green). The desmoplakin staining at Panc-1 cells shows punctate desmosomal staining between K8-positive (red) but not between K8 knock-down cells (scale bars equals 20 μm for A, B, C and 5 μm for D).

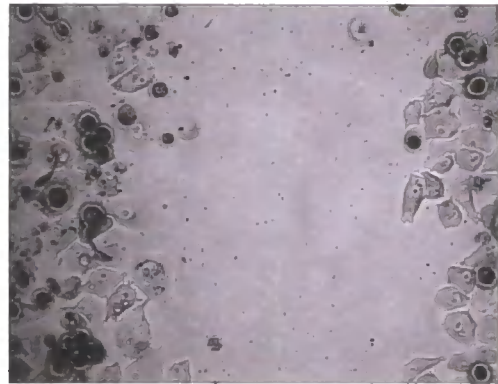
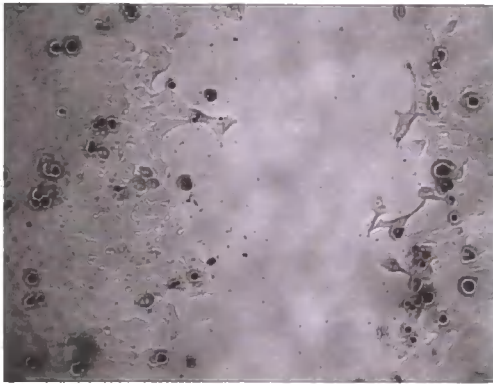
In addition, the scratch wound edges of both cell lines were irregular after K8 siRNA transfection and frequently contained cells that were attempting to migrate individually without any connection to other cells (**Figure 5.9**). Notably, K8 knockdown increased the wound closure rate due to individual cell separation in both HeLa and Panc-1 cell lines (**Figure 5.9**). Wound closure was followed at time points up to 20 hours after wounding, which confirmed this effect of keratin 8 downregulation. Both untransfected and control transfected wounds remained open, with cells in the two bordering epithelial sheets maintaining their cohesion. In contrast, epithelia lacking keratin 8 showed individual cells migrating into the denuded area without maintaining cell-cell contacts. This observation suggests that the lack of desmosomes leads to escape of individual keratin-negative cells from the wound edge.

A.

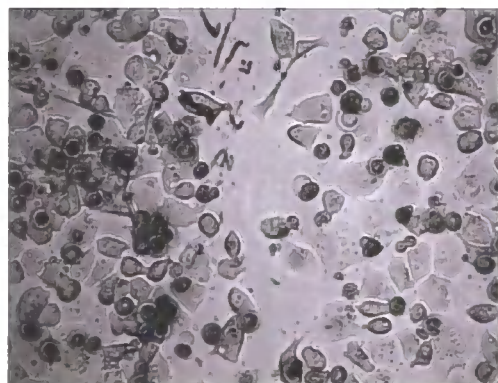
HeLa

Panc-1

Control



*Keratin 8
siRNA*



B.

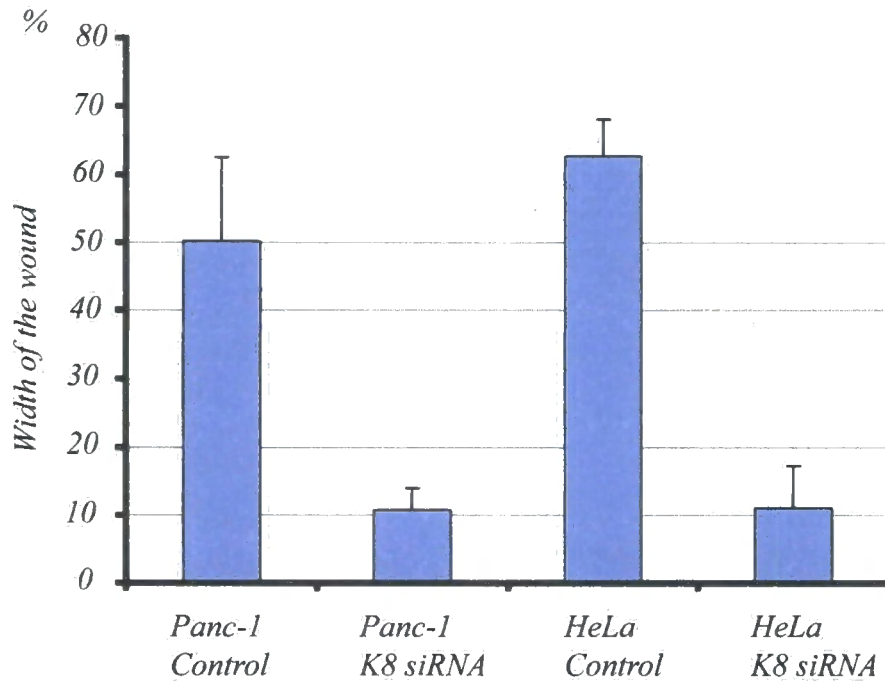


Figure 5.9: Phase contrast microscopy images of scratch wound closure in keratin 8 downregulated HeLa and Panc-1 monolayers.

A. Microphotographs showing the wounds at 20 hours time point after wounding in both HeLa and Panc-1 cell lines transfected with control or keratin 8 siRNA oligonucleotides. Note that wounds in Panc-1 and HeLa monolayers were wider than in the experiments with MCF-7 cells. **B.** Quantification of the wound closure. Open wound at 20 hours time point was measured using photomicrographs (six measurements were averaged, each from two transfection for both cell lines).

5.3 Discussion

5.3.1 Effect of ablation of periplakin and plectin on cell migration

The data presented in chapter IV demonstrated that not only plectin, but also its co-immunoprecipitating partner periplakin, is likely to be involved in the re-organization of the keratin intermediate filaments at the wound edge during the course of wound healing. In the present chapter, the ability of periplakin and plectin in the regulation of cell migration in simple epithelia was studied. Initially the effect of expression of periplakin C-terminus on wound closure was investigated. The clones expressing the periplakin C-terminus showed a consistent delay in wound healing which was associated with the abnormal organization of keratin intermediate filaments at the free wound edges. Subsequently, the effect of periplakin ablation in MCF-7 and HeLa cells was studied. Both cell lines showed identical results, which indicated that the loss of periplakin impaired wound closure. Therefore, the role of periplakin in regulating keratin re-organization and epithelial wound closure is not only evident in MCF-7 cells but likely to be seen in many epithelial cell lines.

In addition to appearing as part of the same protein complex, periplakin and plectin have been shown to regulate the architecture of the keratin filament cytoskeleton. To investigate their role in wound closure, periplakin and plectin were downregulated by siRNA transfection. Lack of periplakin and plectin in simple epithelia resulted in delayed migration compared to controls. Furthermore, epithelial sheets that had both cytolinker proteins simultaneously ablated showed even more impaired migration, suggesting a possible co-operation between these proteins in MCF-7 cells. Although periplakin knock-out mice had developed normally (Aho *et al.*, 2004), the data presented above suggest that periplakin ablation may lead to decreased cell migration in simple epithelia, although the effects within the embryo may not be evident, perhaps because of functional redundancy. The consequence of plectin ablation in cell migration has been studied more extensively in different cell types *in vitro*. In keeping with these results, cultured fibroblasts with plectin deficiency displayed prominent stress fibres and increased focal adhesion complexes, consequently demonstrating decreased cell motility (Andra *et al.*, 1998). Targeted deletion of plectin 1 isoform, which is the major plectin isoform expressed in mesenchymal tissues,

resulted in reduced recruitment of leukocytes to the location of the wound (Abrahamsberg *et al.*, 2005). However, loss of all plectin isoforms in keratinocytes resulted in larger keratin meshwork with fewer keratin filaments attached to the hemidesmosomes leading to increased vulnerability and faster collective migration (Osmanagic-Myers *et al.*, 2006). The opposite effects of plectin deficiency on cell migration in different cell lines might result from cell specific expression pattern of plectin N-terminal splice isoforms. For instance, plectin-1a is a major isoform expressed in keratinocytes, where the primary function of plectin is in the construction of hemidesmosomes. In contrast, in fibroblasts, it is likely that plectin isoforms have a much more important role in focal adhesion complexes and they may also be associated with actin stress fibres.

5.3.2 Collective migration of epithelial sheets

To investigate the role of the intermediate filament protein keratin 8 in epithelial cell migration, HeLa and Panc-1 cells were studied. My results show that knockdown of keratin 8 network in migrating epithelia results in a loss of epithelial integrity and affects wound closure similarly to that observed in keratin 8 downregulated MCF-7 cells (Long *et al.*, 2006). The role of keratin in collective epithelial migration has previously been studied, but mainly in the context of epidermal keratinocytes and skin wound healing. Studies indicate that gene targeting of both keratin 6a and keratin 6b results in impaired wound healing *in vivo* due to increased fragility of mutant keratinocytes (Wong & Coulombe, 2003). Similarly to our results in MCF-7 cells, low level of keratin 8 expression in HeLa and Panc-1 cells appeared to allow cells to escape from the migrating cell front and invade the denuded surface without any collective movement. Consequently, liberated cells migrated faster than control cells. Likewise, epidermolysis bullosa simplex cell lines carrying keratin 14 mutations display fast migration *in vivo* (Morley *et al.*, 2003). Keratin 8 ablation resulted in similar effect in vimentin negative (MCF-7) and positive (Panc-1, HeLa) cells indicating that has a role in cell migration regardless of the presence of other IF proteins.

In the light of these findings it is possible that the keratin cytoskeleton could regulate the collective motility of epidermal sheets to maintain epithelial integrity. There is an interesting difference between the results reported here and the outcome of embryonic wound healing in keratin 8 deficient mice. When embryonic wound healing was investigated in K8^{-/-} mice in FVB/N background, no difference in the wound closure was observed between gene targeted and wild type embryos, even when both mesodermal contraction and actual re-epithelialisation were taken separately into account (Brock *et al.*, 1996). In spite of this, *Xenopus* embryos depleted of maternal keratins fail to undergo normal morphogenetic tissue movements and have a defect in epithelial wound healing (Torpey *et al.*, 1992; Klymkowsky *et al.*, 1992). It is possible that there are subtle species or cell-type specific differences in the requirement for keratins in epithelial migration. It is also notable that the study by Brock *et al.* (1996) only investigated embryonic wound healing in the genetic background that supports the survival of K8^{-/-} embryos. In C57/BL6 genetic background K8 deficiency leads to embryonic lethality between 12 and 13 days of development, apparently due to structural fragility of the foetal liver (Baribault *et al.*, 1993), whereas the same mutation in FVB/N background results in viable animals that later on develop gastrointestinal hyperplasia and other related problems (Baribault *et al.*, 1994).

Adherens junctions are not the only junctions that are essential for collective cell migration, as this behaviour is also seen in fibroblasts. These cells can heal scratch wounds as a collective sheet without forming adherens junctions in culture (Bindschadler & McGrath, 2007). As the adhesiveness of desmosomes changes during wound healing from Ca²⁺ independent to dependent (Garrod *et al.*, 2005), it is likely that they play a major role in collective migration. It remains to be investigated whether the reinforcement of desmosomes to Ca²⁺-independent junctions, which is mediated by protein kinase C α (Wallis *et al.*, 2000; Garrod *et al.*, 2005), can occur without intermediate filaments. The data presented above also supports the concept that intermediate filaments are involved in correct subcellular targeting of desmosomal proteins as siRNA mediated depletion of keratin 8 resulted in apparent breakdown of cell-cell adhesions and re-distribution of desmoplakin and periplakin from cell borders to the cytosol (Long *et al.*, 2006). Specific desmoplakin mutants that either increase or abolish the association of desmoplakin with keratins have been shown to delay incorporation of desmoplakin particles into junctions

(Godsel *et al.*, 2005). Likewise, desmosomal cadherins are targeted to cell membranes in particles that are at least partially attached to keratins (Sato *et al.*, 2000). Earlier studies have shown that compromised tissue integrity can also be achieved by disturbance of either intermediate filament or desmosome anchoring counterparts (Hennies *et al.*, 1995; Fuchs & Cleveland, 1998; McMillan & Shimizu, 2001). The requirement of intermediate filaments for intercellular adhesion during epithelial migration is also supported by the work of Green and co-workers with dominant-negative desmoplakin constructs. In A431 epithelial cells, the overexpression of a desmoplakin N-terminal domain that retains plakoglobin and plakophilin binding sites, but lacks the central rod and COOH-domain results in dissociation of epithelial sheets when subjected to mechanical stress (Huen *et al.*, 2002). The role of keratins in the maintenance of desmosomes is also supported by findings of a careful histological characterisation of liver lesions in both K8 and K18 null mice (Toivola *et al.*, 2001). Livers of keratin null mice showed large areas that were devoid of both desmoplakin and filamentous actin staining (Toivola *et al.*, 2001). This is supported by the recent finding that keratin 8 is involved in the modulation of desmoplakin deposition at desmosomes through a phosphoserine dependent process (Loranger *et al.*, 2006).

Together these data suggest that maintaining epithelial integrity involves not only the presence of all desmosomal proteins building up desmosomal junctions but also it requires intact keratin cytoskeleton.

In summary, my results suggest that the cytoskeletal linker function of periplakin, allows it to act as an organiser of intermediate filament architecture and to regulate cell migration in cooperation with plectin. Furthermore, the present study supports the view that intermediate filaments can serve a structural role in epithelial cells by contributing to the maintenance of the epithelial integrity during collective migration.

CHAPTER VI

GENERAL DISCUSSION

6.1 Implications of current work

Cytolinker proteins have been extensively investigated over recent years to determine their structure, localization, regulation and function. In this thesis, I studied the function of periplakin through investigation of its binding partners in simple epithelial cells. The main findings were as follows:

A, In my first result chapter (III), I investigated the interacting partners of the periplakin head domain in the MCF-7 breast adenocarcinoma cell line. I found that periplakin is able to interact, either directly or indirectly, with another cytolinker protein, plectin. This interaction occurs not only in simple epithelia, but also in keratinocytes. Annexin A9 is another co-immunoprecipitating partner of periplakin in MCF-7 cells that colocalises with periplakin in both simple epithelial cells and in the epidermis.

B, Secondly, I describe the functional relationship between periplakin and plectin. In chapters IV and V, using siRNA techniques and scratch wound assays, I found that periplakin localisation is regulated by plectin in keratinocytes, and that periplakin and plectin together regulate keratin organization at the wound edge. Moreover, both proteins participate in the control of cell migration and wound healing processes in simple epithelia.

C, Finally, I gathered information on epithelial sheet migration. siRNA experiments revealed that keratin 8 is essential for epithelial integrity, as ablation of keratin 8 intermediate filaments leads to disrupted desmosomes and impaired epithelial sheet migration in several epithelial cell lines.

6.2 Periplakin functions

More than 20 years ago, periplakin was first identified as a constituent of the cornified envelope in terminally differentiated keratinocytes (Simon & Green, 1984; Ma & Sun, 1986). With the aim of revealing its function, periplakin knock-out mice were

generated but no apparent phenotype was found (Aho *et al.*, 2004). Recently, gene targeting of periplakin and two other CE proteins, envoplakin and involucrin, showed defects in the cornified layer including delayed barrier acquisition during embryonic development, decreased protease activity causing excessive accumulation of cornified layers during postnatal life and accumulation of CD3⁺, CD4⁺ T cells in the skin with a decrease in dendritic epidermal T cells (DETCs) (Sevilla *et al.*, 2007). The fact that these phenotypes were not observed in single knockout animals (Dijan *et al.*, 2000; Määttä *et al.*, 2001; Aho *et al.*, 2004) supports the idea of compensatory redundancy of CE scaffold proteins. Thus, no single CE protein has been found to be indispensable for barrier formation.

Periplakin expression has also been demonstrated in other tissues with a prominent epithelial component including pituitary, thyroid, salivary and mammary glands (Aho *et al.*, 1998; Kazerounian *et al.*, 2002). To date, the initial role of periplakin in these tissues remains elusive. In this study, I discovered two functions of periplakin in simple epithelial cells. The first of these is periplakin-dependent keratin IF organisation during wound healing in epithelial cells. Secondly, periplakin forms a protein complex with plectin which influences cell migration processes.

6.3 General outlook on epithelial cell migration

Injury to the surface of the epithelial monolayers in the gut could occur in many ways, including infectious colitis and inflammatory bowel disease. In order to re-establish epithelial barrier function, the epithelium must efficiently reseal the mucosal defects. A major mechanism by which wound healing is achieved involves epithelial cell migration (Nobes & Hall, 1999). Rapid resealing of the epithelial barrier following injuries is accomplished by a process termed epithelial restitution, which occurs when epithelial cells migrate and spread rapidly, prior to cell division (Fenteany *et al.*, 2000). This is followed by more delayed mechanisms of epithelial wound healing, including increased epithelial

cell proliferation and cell differentiation. The cytoskeletal networks, along with the various cytoskeletal associated proteins, are intrinsically involved in cell migration.

A central event in epithelial wound healing is the reorganization of the actin cytoskeleton, followed by the appearance of the keratin cable at the wound edge (Long *et al.*, 2006). These keratin cables have been previously reported at the free wound edge of embryonic tissues, which also showed an actin purse-string (Brock *et al.*, 1996). The results presented in this thesis demonstrate that two cytolinker proteins, namely periplakin and plectin, form a protein complex that affects the organization of the keratin cytoskeleton and regulates cell migration in simple epithelial cells. The lack of each plakin in isolation resulted in decreased cell migration, while simultaneous ablation slowed down the wound healing even more. Emerging data suggest that plakin proteins play roles in signal transduction, being large modular proteins, they can interact with a variety of signalling molecules and have an impact on various signalling processes (Sonnenberg & Liem, 2007). It has to be noted that this involvement in signalling processes could be achieved indirectly, via their effect on stabilizing the cytoskeleton (Sonnenberg & Liem, 2007). I demonstrated that simultaneous periplakin and plectin downregulation in MCF-7 cells resulted in alterations in the keratin cytoskeleton, which might lead to downstream modifications in the signalling pathways involved in epithelial cell migration. Interestingly, in keratinocytes, plectin deficiency results in an altered keratin network, which affects ERK 1/2 MAP kinases leading to faster *in vitro* migration (Osmanagic-Myers *et al.*, 2006). Not only plectin and periplakin, but also other cytolinker proteins, such as BPAG-1 and epiplakin, have been associated with epithelial migration. Loss of BPAG-1 in mice disrupted the connection of keratin IFs to hemidesmosomes and led to reduced cell migration (Guo *et al.*, 1995). Epiplakin has also been shown to regulate the intermediate filament network, as epiplakin depletion in HeLa cells resulted in a disorganized keratin and vimentin network (Jang *et al.*, 2005). Surprisingly, epiplakin knock-out mice have a similar phenotype to that observed in plectin downregulation, with accelerated keratinocyte migration (Goto *et al.*, 2006). Thus, cytolinkers may have an impact on signalling processes that regulate cell migration.

In recent years, the term “collective migration” has gained use to describe the type of migration in which cells maintain intercellular junctions (Friedl *et al.*, 2004). Several groups have shown previously that the modification of intermediate filaments or intracellular junctions can alter the cohesiveness of cell sheets using dissociation assay (Huen *et al.*, 2002; Setzer *et al.*, 2004; Yin *et al.*, 2005). In this study, I confirmed that the loss of keratin 8 caused desmosome disruption and led to a disturbance in cohesive epithelial sheet migration in breast carcinoma cells. Understanding collective cell migration is important in cancer cell research, as some metastatic cells migrate as a group (Hegerfeldt *et al.*, 2002) and are able to invade surrounding tissues as multicellular aggregates (Friedl & Wolf, 2003). This type of migration has also been observed among colorectal and breast tumour cells, which can migrate as protruding sheets and tubules connected to the primary tumour (Nabeshima *et al.*, 2000). 90% of cancers originate from epithelial tissues and show characteristics of epithelial to mesenchymal transition (Christofori, 2006), although recent studies suggest that loss of epithelial morphology is not required for invasion and metastasis of the carcinoma cells (Christiansen & Rajasekaran, 2006). Primary metastatic tissue samples taken from patients suffering from mammary ductal carcinoma, contained tight junctions, adherens junctions, and desmosomes, that were abundantly evident by electron microscopy (Ng, 2002). More recently, alterations in cell-cell adhesion have been shown to have a central role in facilitating tumour cell migration (Kartenbeck *et al.*, 2005; Lyons & Jones, 2007).

In conclusion, understanding the role of cytolinkers in the regulation of the keratin intermediate filament network, and their influence on collective cell migration, is important. Together, these findings might lead to a better understanding of diseases involving simple epithelial injury and carcinoma cell migration.

6.4 Possible future directions

There are several aspects of this study which merit future investigation.

- To continue the co-immunoprecipitation experiments that revealed periplakin and plectin protein complexes, it would be of great interest to investigate the molecular interactions of periplakin with each alternative N-terminal plectin isoform, study the effect of these interactions, and map the exact binding sites.
- siRNA mediated ablation of either periplakin or plectin caused disorganization of the cytoskeleton and impairment of simple epithelial cell migration *in vitro*. With the emerging data implicating periplakin and plectin in various signal transduction pathways, it would be interesting to study whether there is any co-operation between these proteins in the previously identified signalling functions.
- Isoform specific antibodies against plectin isoforms demonstrated that plectin is not only localized in the basal layer of the skin, but at least two isoforms (plectin-1f and plectin-1k) were present and co-localised with periplakin in the spinous and granular layers as well. Studying their specific roles in the assembly of the epidermal barrier would provide a better understanding of barrier formation.
- An in-depth study of the function of keratin 8 intermediate filaments in desmosome formation and maintenance could be carried out by investigating other protein members of the desmosome complex following keratin 8 depletion. This could be complemented by phosphorylation studies, as desmoplakin deposition in hepatocytes is dependent on the phosphorylation of keratin 8 at the Ser24 residue (Loranger *et al.*, 2006).
- With regard to my results showing annexin A9 and periplakin co-immunoprecipitation, it would be interesting to show whether this is a direct or indirect interaction by yeast-two-hybrid analyses and/or by carrying out functional

studies including siRNA transfections in simple epithelial cells and keratinocytes. Simultaneous periplakin – annexin A9 depletion could further reveal a functional role for these proteins.

- Studies should be continued to investigate whether periplakin, plectin and annexin A9 are part of the same protein complex, as all three proteins are found to be localized in the suprabasal layer of the skin and located at the plasma membrane in MCF-7 cells.

REFERENCES

- Abrahamsberg, C., Fuchs, P., Osmanagic-Myers, S., Fischer, I., Propst, F., Elbe-Bürger, A. & Wiche, G.** (2005) Targeted ablation of plectin isoform 1 uncovers role of cytolinker proteins in leukocyte recruitment. *Proc. Natl. Acad. Sci. U S A.* **102**, 18449-18454.
- Aebersold, R. & Mann, M.** (2003) Mass spectrometry-based proteomics. *Nature* **422**, 198-207.
- Aho, S.** (2004) Many faces of periplakin: domain-specific antibodies detect the protein throughout the epidermis, explaining the multiple protein-protein interactions. *Cell Tissue Res.* **316**, 87-97.
- Aho, S., Li, K., Ryoo, Y., McGee, C., Ishida-Yamamoto, A., Uitto, J. & Klement, J.F.** (2004) Periplakin gene targeting reveals a constituent of the cornified cell envelope dispensable for normal mouse development. *Mol Cell Biol* **24**(14), 6410-6418.
- Aho, S., Mahoney, M.G. & Uitto, J.** (1999) Plectin serves as an autoantigen in paraneoplastic pemphigus. *J. Invest. Dermatol.* **113**, 422-423.
- Aho, S., Mclean, W.H.I., Li, K. & Uitto, J.** (1998) cDNA cloning, mRNA expression, and chromosomal mapping of human and mouse periplakin gene. *Genomics* **48**, 242-247.
- Alberts, B.e.a.** (2002) *Molecular Biology of the Cell*. New York: Garland Science.
- Alexander, D., B. & Goldberg, G., S.** (2003) Transfer of biologically important molecules between cells through gap junction channels. *Curr. Med. Chemistry and Function* **10**, 2045-2058.
- Allen, P.G. & Shah, J.V.** (1999) Brains and brawn: plectin as regulator and reinforcer of the cytoskeleton. *Bioessays* **21**(6), 451-454.
- Amagai, M.** (2003) Desmoglein as a target in autoimmunity and infection. *J. Am. Acad. Dermatol.* **48**, 244-252.
- Amagai, M., Nishikawa, T., Nousari, H., C., Anhalt, G., J. & Hashimoto, T.** (1998) Antibodies against desmoglein 3 (pemphigus vulgaris antigen) are present in sera from patients with paraneoplastic pemphigus and cause acantholysis in vivo in neonatal mice. *J. Clin. Invest.* **102**(4), 775-782.
- Amagai, M., Tsunoda, K., Zillikens, D., Nagai, T. & Nishikawa, T.** (1999) The clinical phenotype of pemphigus is defined by the anti-desmoglein autoantibody profile. *J. Am. Acad. Dermatol.* **40**, 167-170.
- Anderson, J., M., Van Itallie, C., M. & Fanning, A., S.** (2004) Setting up a selective barrier at the apical junction complex. *Curr. Opin. Cell Biol.* **16**, 140-145.
- Andrä, K., Lassmann, H., Bittner, R., Shorny, S., Fässler, R., Propst, F. & Wiche, G.** (1997) Targeted inactivation of plectin reveals essential function in maintaining the integrity of skin, muscle, and heart cytoarchitecture. *Genes Dev.* **11**(23), 3143-3156.
- Andrä, K., Nikolic, B., Stöcher, M., Drenckhahn, D. & Wiche, G.** (1998) Not just scaffolding: plectin regulates actin dynamics in cultured cells. *Genes Dev.* **12**(21):. **12**, 3442-3451.

- Anhalt, G., J.** (1999) Making sense of antigens and antibodies in pemphigus. *J. Am. Acad. Dermatol.* **40**, 763-766.
- Anhalt, G., J., Kim, S., C., Stanley, J., R., Korman, N., J., Jabs, D., A., Kory, M., Izumi, H., Ratrie, H.r., Mutasim, D. & Ariss-Abdo, L.** (1990) Paraneoplastic pemphigus. An autoimmune mucocutaneous disease associated with neoplasia. *N. Engl. J. Med.* **323**(25), 1729-1735.
- Aoyama, Y., Owada, M.K. & Kitajima, Y.** (1999) A pathogenic autoantibody, pemphigus vulgaris-IgG, induces phosphorylation of desmoglein 3, and its dissociation from plakoglobin in cultured keratinocytes. *Eur. J. Immunol.* **29**, 2233-2240.
- Armstrong, D., K., McKenna, K., E., Purkis, P., E., Green, K., J., Eady, R., A., Leigh, I., M. & Hughes, A., E.** (1999) Haploinsufficiency of desmoplakin causes a striate subtype of palmoplantar keratoderma. *Hum. Mol. Genet.* **8**, 143-148.
- Backendorf, C. & Hohl, D.** (1992) A common origin for cornified envelope proteins? *Nat. Genetics* **2**, 91.
- Bader, J., S., Chaudhuri, A., Rothberg, J., M. & Chant, J.** (2004) Gaining confidence in high-throughput protein interaction networks. *Nat. Biotechnol.* **22**(1), 78-85.
- Balda, M., S. & Matter, K.** (1998) Tight junctions. *J. Cell. Sci.* **111**(5), 541-547.
- Bañuelos, S., Saraste, M. & Djinović Carugo, K.** (1998) Structural comparisons of calponin homology domains: implications for actin binding. *Structure* **15**, 1419-1431.
- Baribault, H., Penner, J., Iozzo, R., V. & Wilson-Heiner, M.** (1994) Colorectal hyperplasia and inflammation in keratin 8-deficient FVB/N mice. *Genes. Dev.* **8**(24), 2964-2973.
- Baribault, H., Price, J., Miyai, K. & Oshima, R.G.** (1993) Mid-gestational lethality in mice lacking keratin 8. *Genes Dev.* **7**, 1191-1202.
- Bass, B., L.** (2001) RNA interference, the short answer. *Nature* **411**, 428-429.
- Batta, K., Rugg, E., L., Wilson, N., J., West, N., Goodyear, H., Lane, E., B., Gratian, M., Dopping-Hepenstal, P., Moss, C. & Eady, R., A.** (2000) A keratin 14 'knockout' mutation in recessive epidermolysis bullosa simplex resulting in less severe disease. *Br. J. Dermatol.* **143**, 621-627.
- Beekman, J.M., Bakema, J.E., van der Linden, J., Tops, B., Hinten, M., van Vugt, M., van de Winkel, J.G. & Leusen, J.H.** (2004) Modulation of FcγRI (CD64) ligand binding by blocking peptides of periplakin. *J. Biol. Chem.* **279**, 33875-33881.
- Begg, D., A., Rodewald, R. & Rebhun, L., I.** (1978) The visualization of actin filament polarity in thin sections. Evidence for the uniform polarity of membrane-associated filaments. *J. Cell Biol.* **79**, 846-852.
- Beil, M., Micoulet, A., von Wichert, G., Paschke, S., Walther, P., Omary, M.B., Van Veldhoven, P.P., Gern, U., Wolff-Hieber, E., Eggermann, J., Waltenberger, J., Adler, G., Spatz, J. & Seufferlein, T.** (2003) Sphingosylphosphorylcholine regulates keratin network architecture and visco-elastic properties of human cancer cells. *Nat. Cell Biol.* **5**, 803-811.
- Bement, W.M., Forscher, P. & Mooseker, M.** (1993) A novel cytoskeletal structure involved in purse string wound closure and cell polarity maintenance. *J. Cell Biol.* **121**, 565-578.

- Berkowitz, P., Hu, P., Liu, Z., Diaz, L., A., Enghild, J., J., Chua, M., P. & Rubenstein, D., S.** (2005) Desmosome signaling. Inhibition of p38MAPK prevents pemphigus vulgaris IgG-induced cytoskeleton reorganization. *J. Biol. Chem.* **280**, 23778-23784.
- Bernier, G., Brown, A., Dalpé, G., De Repentigny, Y., Mathieu, M. & Kothary, R.** (1995) Dystonin expression in the developing nervous system predominates in the neurons that degenerate in dystonia musculorum mutant mice. *Mol. Cell Neurosci.* **6**, 509-520.
- Betz, R., C., Planko, L., Eigelshoven, S., Hanneken, S., Pasternack, S., M., Bussow, H., Van Den Bogaert, K., Wenzel, J., Braun-Falco, M., Rutten, A., Rogers, M., A., Ruzicka, T., Nöthen, M., M., Magin, T., M., & Kruse, R.** (2006) Loss-of-function mutations in the keratin 5 gene lead to Dowling-Degos disease. *Am. J. Hum. Genet.* **78**, 510-519.
- Beutner, E., H. & Jordon, R., E.** (1964) Demonstration of skin antibodies in sera of pemphigus vulgaris patients by indirect immunofluorescent staining. *Proc. Soc. Exp. Biol. Med.* **117**, 505-510.
- Bierkamp, C., McLaughlin, K., J., Schwarz, H., Huber, O. & Kemler, R.** (1996) Embryonic heart and skin defects in mice lacking plakoglobin. *Dev. Biol.* **180**, 780-785.
- Bindschadler, M. & McGrath, J.L.** (2007) Sheet migration by wounded monolayers as an emergent property of single-cell dynamics. *J. Cell Sci.* **120**, 876-884.
- Birchmeier, W. & Behrens, J.** (1994) Cadherin expression in carcinomas: role in the formation of cell junctions and the prevention of invasiveness. *Biochim. Biophys. Acta.* **1198**(1), 11-26.
- Bonder, E., M. & Mooseker, M., S.** (1983) Direct electron microscopic visualization of barbed end capping and filament cutting by intestinal microvillar 95-kdalton protein (villin): a new actin assembly assay using the limulus acrosomal process. *J. Cell Biol.* **96**, 1097-1107.
- Bonder, E., M., Fishkind, D., J. & Mooseker, M., S.** (1983) Direct measurement of critical concentrations and assembly rate constants at the two ends of an actin filament. *Cell* **34**, 491-501.
- Bornslaeger, E., A., Godsel, L., M., Corcoran, C., M., Park, J., K., Hatzfeld, M., Kowalczyk, A., P., & Green, K., J.** (2001) Plakophilin 1 interferes with plakoglobin binding to desmoplakin, yet together with plakoglobin promotes clustering of desmosomal plaque complexes at cell-cell borders. *J. Cell Sci.* **114**, 727-738.
- Bornslaeger, E.A., Corcoran, C.M., Stappenbeck, T.S. & Green, K.J.** (1996) Breaking the connection: Displacement of the desmosomal plaque protein desmoplakin from cell-cell interfaces disrupts intermediate filament bundles and alters intercellular junction assembly. *J. Cell Biol.* **134**, 985-1001.
- Borradori, L. & Sonnenberg, A.** (1996) Hemidesmosomes: roles in adhesion, signaling and human diseases. *Curr. Opin. Cell Biol.* **8**(5), 647-656.
- Borradori, L. & Sonnenberg, A.** (1999) Structure and function of hemidesmosomes: more than simple adhesion complexes. *J. Invest. Dermatol.* **112**(4), 411-418.
- Borradori, L., Koch, P., J., Niessen, C., M., Erkeland, S., van Leusden, M., R. & Sonnenberg, A.** (1997) The localization of bullous pemphigoid antigen 180 (BP180) in

hemidesmosomes is mediated by its cytoplasmic domain and seems to be regulated by the beta4 integrin subunit. *J. Cell Biol.* **136**, 1333-1347.

- Borrmann, C., M., Grund, C., Kuhn, C., Hofmann, I., Pieperhoff, S. & Franke, W., W.** (2006) The area composita of adhering junctions connecting heart muscle cells of vertebrates. II. Colocalizations of desmosomal and fascia adhaerens molecules in the intercalated disk. *Eur. J. Cell Biol.* **85**, 469-85.
- Bosher, J., M., Hahn, B., S., Legouis, R., Sookhareea, S., Weimer, R., M., Gansmuller, A., Chisholm, A., D., Rose, A., M., Bessereau, J., L. & Labouesse, M.** (2003) The *Caenorhabditis elegans* vab-10 spectraplaklin isoforms protect the epidermis against internal and external forces. *J. Cell Biol.* **161**, 757-768.
- Brachvogel, B., Dikschas, J., Moch, H., Welzel, H., von der Mark, K., Hofmann, C. & Poschl, E.** (2003) Annexin A5 is not essential for skeletal development. *Mol. Cell Biol.* **23**, 2907-2913.
- Braga, V., M.** (2002) Cell-cell adhesion and signalling. *Curr. Opin. Cell Biol.* **14**(5), 546-556.
- Bray, D.** (1992) *Cell movements*. New York: Garland Publishing.
- Brock, J., McCluskey, J., Baribault, H. & Martin, P.** (1996) Perfect wound healing in the keratin 8 deficient mouse embryo. *Cell Motil. Cytoskeleton.* **35**, 358-366.
- Brown, A., Bernier, G., Mathieu, M., Rossant, J. & Kothary, R.** (1995) The mouse dystonia musculorum gene is a neural isoform of bullous pemphigoid antigen 1. *Nat. Genet.* **10**, 301-306.
- Brown, M., C. & Turner, C., E.** (2004) Paxillin: adapting to change. *Physiol. Rev.* **84**, 1315-1339.
- Buckley, I., K. & Porter, K., R.** (1975) Electron microscopy of critical point dried whole cultured cells. *J. Microsc.* **104**, 107-120.
- Budunova, I., V., Carbajal, S. & Slaga, T., J.** (1995) The expression of gap junctional proteins during different stages of mouse skin carcinogenesis. *Carcinogenesis* **16**, 2717-2724.
- Burgeson, R., E. & Christiano, A., M.** (1997) The dermal-epidermal junction. *Curr. Opin. Cell Biol.* **9**(5), 651-658.
- Burridge, K., Fath, K., Kelly, T., Nuckolls, G. & Turner, C.** (1988) Focal adhesions: transmembrane junctions between the extracellular matrix and the cytoskeleton. *Annu. Rev. Cell Biol.* **4**, 487-525.
- Byers, H., R., Maheshwary, S., Amodeo, D., M. & Dykstra, S., G.** (2003) Role of cytoplasmic dynein in perinuclear aggregation of phagocytosed melanosomes and supranuclear melanin cap formation in human keratinocytes. *J. Invest. Dermatol.* (121), 813-820.
- Calkins, C., C., Setzer, S., V., Jennings, J., M., Summers, S., Tsunoda, K., Amagai, M. & Kowalczyk, A., P.** (2006) Desmoglein endocytosis and desmosome disassembly are coordinated responses to pemphigus autoantibodies. *J. Biol. Chem.* **281**, 7623-7634.

- Camargo L, M., Collura, V., Rain, J., C., Mizuguchi, K., Hermjakob, H., Kerrien, S., Bonnert, T., P., Whiting, P., J. & Brandon, N., J.** (2007) Disrupted in Schizophrenia 1 Interactome: evidence for the close connectivity of risk genes and a potential synaptic basis for schizophrenia. *Mol. Psychiatry*. **12**, 74-86.
- Candi E, Schmidt R, Melino G.** (2005) The cornified envelope: a model of cell death in the skin. *Nat Rev Mol Cell Biol*. **4**, 328-40.
- Carlier, M., F.** (1991a) Actin: protein structure and filament dynamics. *J. Biol. Chem.* **266**, 1-4.
- Carlier, M., F.** (1991b) Nucleotide hydrolysis in cytoskeletal assembly. *Curr. Opin. Cell Biol.* **3**, 12-17.
- Chan, Y., Anton-Lamprecht, I., Yu, Q., C., Jäckel, A., Zabel, B., Ernst, J., P. & Fuchs, E.** (1994) A human keratin 14 "knockout": the absence of K14 leads to severe epidermolysis bullosa simplex and a function for an intermediate filament protein. *Genes Dev.* **8**, 2574-2587.
- Chang, L. & Goldman, R.D.** (2004) Intermediate filaments mediate cytoskeletal crosstalk. *Nat. Rev. Mol. Cell Biol.* **5**, 601-613.
- Charlesworth, A., Gagnoux-Palacios, L., Bonduelle, M., Ortonne, J., P., De Raeve, L. & Meneguzzi, G.** (2003) Identification of a lethal form of epidermolysis bullosa simplex associated with a homozygous genetic mutation in plectin. *J. Invest. Dermatol.* **121**, 1344-1348.
- Chen, H., J., Lin, C., M., Lin, C., S., Perez-Olle, R., Leung, C., L. & Liem, R., K.** (2006) The role of microtubule actin cross-linking factor 1 (MACF1) in the Wnt signaling pathway. *Genes. Dev.* **20**, 1933-1945.
- Choi, H., J., Park-Snyder, S., Pascoe, L., T., Green, K., J. & Weis, W., I.** (2002) Structures of two intermediate filament-binding fragments of desmoplakin reveal a unique repeat motif structure. *Nat. Struct. Biol.* **9**, 612-620.
- Choquet, D., Felsenfeld, D., P. & Sheetz, M., P.** (1997) Extracellular matrix rigidity causes strengthening of integrin-cytoskeleton linkages. *Cell* **88**, 39-48.
- Christiansen, J., J. & Rajasekaran, A., K.** (2006) Reassessing epithelial to mesenchymal transition as a prerequisite for carcinoma invasion and metastasis. *Cancer Research* **66**, 8319-8326.
- Christofori, G.** (2006) New signals from the invasive front. *Nature* **441**, 444-450.
- Chu, Y.W., Runyan, R.B., Oshima, R.G. & Hendrix, M.J.** (1993) Expression of complete keratin filaments in mouse L cells augments cell migration and invasion. *Proc. Natl. Acad. Sci.* **90**, 4261-4265.
- Chu, Y.W., Seftor, E.A., Romer, L.H. & Hendrix, M.J.** (1996) Experimental coexpression of vimentin and keratin intermediate filaments in human melanoma cells augments motility. *Am. J. Pathol.* **148**(1), 63-69.
- Cooper, G.** (2000) *The cell-A molecular approach*. Sunderland: Sinauer Associates Inc.
- Coulombe, P., A. & Wong, P.** (2004) Cytoplasmic intermediate filaments revealed as dynamic and multipurpose scaffolds. *Nat. Cell Biol.* **6**(8), 699-706.

- Coulombe, P., A., Ma, L., Yamada, S. & Wawersik, M.** (2001) Intermediate filaments at a glance. *J. Cell Sci.* **114**, 4345-4347.
- Cowin, A., J.** (2006) Wound healing is defective in mice lacking tetraspanin CD151. *J. Invest. Dermatol.* **126**, 680-689.
- Coy, D., L., Hancock, W., O., Wagenbach, M. & Howard, J.** (1999) Kinesin's tail domain is an inhibitory regulator of the motor domain. *Nat. Cell Biol.* **1**, 288-292.
- Cozzani, E., Christana, K., Mastrogiacomo, A., Rampini, P., Drosera, M., Casu, M., Murialdo, G. & Parodi, A.** (2007) Pemphigus vegetans Neumann type with anti-desmoglein and anti-periplakin autoantibodies. *Eur. J. Dermatol.* **17**, 530-533.
- Critchley, D., R.** (2005) Genetic, biochemical and structural approaches to talin function. *Biochem. Soc. Trans.* **33**, 1308-1312.
- Dalpé, G., Leclerc, N., Vallée, A., Messer, A., Mathieu, M., De Repentigny, Y. & Kothary, R.** (1998) Dystonin Is Essential for Maintaining Neuronal Cytoskeleton Organization. *Mol. Cell Neurosci.* **10**, 243-257.
- Dalpé, G., Mathieu, M., Comtois, A., Zhu, E., Wasiak, S., De Repentigny, Y., Leclerc, N. & Kothary, R.** (1999) Dystonin-deficient mice exhibit an intrinsic muscle weakness and an instability of skeletal muscle cytoarchitecture. *Dev. Biol.* **210**, 367-380.
- Danjo, Y. & Gipson, I.K.** (1998) Actin 'purse string' filaments are anchored by E-cadherin-mediated adherens junctions at the leading edge of the epithelial wound, providing coordinated cell movement. *J. Cell Sci.* **111**, 3323-3332
- Davies, E., L., Gee, J., M., Cochrane, R., A., Jiang, W., G., Sharma, A., K., Nicholson, R., I., Mansel, R., E. & 1999** (1999) The immunohistochemical expression of desmoplakin and its role in vivo in the progression and metastasis of breast cancer. *Eur. J. Cancer.* **35**, 902-907.
- Den, Z., Cheng, X., Merched-Sauvage, M. & Koch, P., J.** (2006) Desmocollin 3 is required for pre-implantation development of the mouse embryo. *J. Cell Sci.* **119**, 482-489.
- Denli, A.M., Hannon, G.J. &** (2003) RNAi: an ever-growing puzzle. *Trends Biochem. Sci.* **28**(4), 196-201.
- Desai, A. & Mitchison, T., J.** (1997) Microtubule polymerization dynamics. *Annu. Rev. Cell Dev. Biol.* **13**, 83-117.
- DiColandrea, T., Karashima, T., A., M. & F.M., W.** (2000) Subcellular distribution of envoplakin and periplakin: insights into their role as precursors of the epidermal cornified envelope. *J. Cell Biol.* **151**, 573-586.
- Dijan, P., Easley, K. & Green, H.** (2000) Targetted ablation of the murine involucrin gene. *J. Cell Biol.* **151**, 381-388.
- Ding, X., Diaz, L., A., Fairley, J., A., Giudice, G., J. & Liu, Z.** (1999) The anti-desmoglein 1 autoantibodies in pemphigus vulgaris sera are pathogenic. *J. Invest. Dermatol.* **112**(5), 739-743.
- Duchen, L., W., Strich, S., J. & Falconer, D., S.** (1964) Clinical and pathological studies of an hereditary neuropathy in mice (dystonia musculorum). *Brain* **87**, 367-378.

- Eckert, R., L., Crish, J., F. & Robinson, N., A.** (1997) The epidermal keratinocyte as a model for the study of gene regulation and cell differentiation. *Physiol. Rev.* **77**(2), 397-424.
- Eger, A., Stockinger, A., Wiche, G. & Foisner, R.** (1997) Polarisation-dependent association of plectin with desmoplakin and the lateral submembrane skeleton in MDCK cells. *J. Cell Sci.* **110**, 1307-1316.
- Elbashir, S., Harborth, J., Lendeckel, W., Yalcin, A., Weber, K. & Tuschl, T.** (2001) Duplexes of 21-nucleotide RNAs mediate RNA interference in cultured mammalian cells. *Nature* **411**(6836), 494-498.
- Elias, P., M. & Feingold, K., R.** (2001) Coordinate regulation of epidermal differentiation and barrier homeostasis. *Skin Pharmacol. Appl. Skin Physiol.* **14**, 28-34.
- Elliott, C., E., Becker, B., Oehler, S., Castañón, M., J., Hauptmann, R. & Wiche, G.** (1997) Plectin transcript diversity: identification and tissue distribution of variants with distinct first coding exons and rodless isoforms. *Genomics* **42**, 115-125.
- Engelkamp, D., Schafer, B., W., Mattei, M., G., Erne, P. & Heizmann, C., W.** (1993) Six S100 genes are clustered on human chromosome 1q21: Identification of two genes coding for the two previously unreported calcium-binding proteins S100D and S100E. *Proc. Natl. Acad. Sci. USA* **90**, 6547-6551.
- Erber, A., Riemer, D., Bovenschulte, M. & Weber, K.** (1998a) Molecular phylogeny of metazoan intermediate filament proteins. *J. Mol. Evol.* **47**, 751-762.
- Erber, A., Riemer, D., Bovenschulte, M. & Weber, K.** (1998b) Molecular phylogeny of metazoan intermediate filament proteins. *J. Mol. Evol.* **47**, 751-762.
- Eriksson, J., E., He, T., Trejo-Skalli, A., V., Härmälä-Braskén, A., S., Hellman, J., Chou, Y., H. & Goldman, R., D.** (2004) Specific in vivo phosphorylation sites determine the assembly dynamics of vimentin intermediate filaments. *J. Cell Sci.* **117**, 919-932.
- Eshkind, L., Tian, Q., Schmidt, A., Franke, W., W., Windoffer, R. & Leube, R., E.** (2002) Loss of desmoglein 2 suggests essential functions for early embryonic development and proliferation of embryonal stem cells. *Eur. J. Cell Biol.* **81**, 592-598.
- Eckes, B., Colucci-Guyon, E., Smola, H., Nodder, S., Babinet, C., Krieg, T. & Martin, P.** (2000) Impaired wound healing in embryonic and adult mice lacking vimentin. *J. Cell Sci.* **113**, 2455-2462.
- Evans, R., M. & Fink, L., M.** (1982) An alteration in the phosphorylation of vimentin-type intermediate filaments is associated with mitosis in cultured mammalian cells. *Cell* **29**, 43-52.
- Favre, B., Fontao, L., Koster, J., Shafaatian, R., Jaunin, F., Saurat, J., H., Sonnenberg, A. & Borradori, L.** (2001) The hemidesmosomal protein bullous pemphigoid antigen 1 and the integrin beta 4 subunit bind to ERBIN. Molecular cloning of multiple alternative splice variants of ERBIN and analysis of their tissue expression. *J. Biol. Chem.* **276**, 32427-32436.
- Feng, G.J., Kellett, E., Scorer, C.A., Wilde, J., White, J.H. & Milligan, G.** (2003) Selective interactions between helix VIII of the human mu-opioid receptors and the C terminus of periplakin disrupt G protein activation. *J. Biol. Chem.* , 33400-33407.

- Fenteany, G., Janmey, P.A. & Stossel, T.P.** (2000) Signaling pathways and cell mechanics involved in wound closure by epithelial cell sheets. *Curr. Biol.* **10**, 831-838.
- Fey, S.J. & Larsen, P.M.** (2001) 2D or not 2D? *Curr. Opin. Chem. Biol.* **5**, 26-33.
- Fire, A., Xu, S., Montgomery, M., Kostas, S., Driver, S. & Mello, C.** (1998) Potent and specific genetic interference by double-stranded RNA in *Caenorhabditis elegans*. *Nature* **391**, 806-811.
- Fontao, L., Dirrig, S., Owaribe, K., Kedinger, M. & Launay, J., F.** (1997) Polarized expression of HD1: relationship with the cytoskeleton in cultured human colonic carcinoma cells. *Exp. Cell Res.* **231**(2), 319-327.
- Fontao, L., Favre, B., Riou, S., Geerts, D., Jaunin, F., Saurat, J., H., Green, K., J., Sonnenberg, A. & Borradori, L.** (2003) Interaction of the bullous pemphigoid antigen 1 (BP230) and desmoplakin with intermediate filaments is mediated by distinct sequences within their COOH terminus. *Mol. Biol. Cell.* **14**, 1978-1992.
- Fontao, L., Geerts, D., Kuikman, I., Koster, J., Kramer, D. & Sonnenberg, A.** (2001) The interaction of plectin with actin: evidence for cross-linking of actin filaments by dimerization of the actin-binding domain of plectin. *J. Cell Sci.* **114**, 2065-2076.
- Fontao, L., Stutzmann, J., Gendry, P. & Launay, J., F.** (1999) Regulation of the type II hemidesmosomal plaque assembly in intestinal epithelial cells. *Exp. Cell Res.* **250**(2), 298-312.
- Friedl, P. & Wolf, K.** (2003) Tumour-cell invasion and migration: diversity and escape mechanisms. *Nat. Rev. Cancer* **3**, 362-374.
- Friedl, P., Hegerfeldt, Y. & Tusch, M.** (2004) Collective cell migration in morphogenesis and cancer. *Int. J. Dev. Biol.* **48**, 441-449.
- Fuchs, E. & Cleveland, D.W.** (1998) A structural scaffolding of intermediate filaments in health and disease. *Science* **279**, 514-519.
- Fuchs, E. & Karakesisoglou, I.** (2001) Bridging cytoskeletal intersections. *Genes. Dev.* **15**, 1-14.
- Fuchs, E. & Weber, K.** (1994) Intermediate filaments: Structure, dynamics, function, and disease. *Annu. Rev. Biochem.* **63**, 345-382.
- Fuchs, P., Zörer, M., Reznicek, G., A., Spazierer, D., Oehler, S., Castañón, M., J., Hauptmann, R. & Wiche, G.** (1999) Unusual 5' transcript complexity of plectin isoforms: novel tissue-specific exons modulate actin binding activity. *Hum. Mol. Genet.* **8**, 2461-2472.
- Fudge, D., S., Gardner, K., H., Forsyth, V., T., Riekkel, C. & Gosline, J., M.** (2003) The mechanical properties of hydrated intermediate filaments: insights from hagfish slime threads. *Biophys. J.* **85**, 2015-2027.
- Fujita, T., Maturana A, D., Ikuta, J., Hamada, J., Walchli, S., Suzuki, T., Sawa, H., Wooten, M., W., Okajima, T., Tatematsu, K., Tanizawa, K. & Kuroda, S.** (2007) Axonal guidance protein FEZ1 associates with tubulin and kinesin motor protein to transport mitochondria in neurites of NGF-stimulated PC12 cells. *Biochem Biophys Res Commun.* **361**(3), 605-10.

- Fujiwara, S., Takeo, N., Otani, Y., Parry, D., A., Kunimatsu, M., Lu, R., Sasaki, M., Matsuo, N., Khaleduzzaman, M. & Yoshioka, H.** (2001) Epiplakin, a novel member of the Plakin family originally identified as a 450-kDa human epidermal autoantigen. Structure and tissue localization. *J. Biol Chem.* **276**, 13340-13347.
- Furuse, M. & Tsukita, S.** (2006) Claudins in occluding junctions of humans and flies. *Trends Cell Biol.* **16**, 181-188.
- Furuse, M., Hata, M. & Furuse, K.** (2002) Claudin-based tight junctions are crucial for the mammalian epidermal barrier: a lesson from claudin-1-deficient mice. *J. Cell Biol.* **156**, 1099-1111.
- Fusenig, N., E., Breitkreutz, D., Dzarlieva, R., T., Boukamp, P., Herzmann, E., Bohnert, A., Pöhlmann, J., Rausch, C., Schiitz, S. & J., H.** (1982) Epidermal cell differentiation and malignant transformation in culture. *Cancer Forum* **6**, 209-240.
- Gache, Y., Chavanas, S., Lacour, J., P., Wiche, G., Owaribe, K., Meneguzzi, G. & Ortonne, J., P.** (1996) Defective expression of plectin/HD1 in epidermolysis bullosa simplex with muscular dystrophy. *J. Clin. Invest.* **97**(10), 2289-2298.
- Galarneau, L., Loranger, A., Gilbert, S. & Marceau, N.** (2007) Keratins modulate hepatic cell adhesion, size and G1/S transition. *Exp. Cell Res.* **313**, 179-194.
- Gallicano, G., I., Bauer, C. & Fuchs, E.** (2001) Rescuing desmoplakin function in extra-embryonic ectoderm reveals the importance of this protein in embryonic heart, neuroepithelium, skin and vasculature. *Development* **128**(6), 929-941.
- Gallicano, G., I., Kouklis, P., Bauer, C., Yin, M., Vasioukhin, V., Degenstein, L. & Fuchs, E.** (1998) Desmoplakin is required early in development for assembly of desmosomes and cytoskeletal linkage. *J. Cell Biol.* **143**, 2009-2022.
- Garcia-Gras, E., Lombardi, R., Giocondo, M., J., Willerson, J., T., Schneider, M., D., Khoury, D., S. & Marian, A., J.** (2006) Suppression of canonical Wnt/beta-catenin signaling by nuclear plakoglobin recapitulates phenotype of arrhythmogenic right ventricular cardiomyopathy. *J. Clin. Invest.* **116**, 2012-2021.
- Garrod, D., Chidgey, M. & North, A.** (1996) Desmosomes: differentiation, development, dynamics and disease. *Curr. Opin. Cell Biol.* **8**, 670-678.
- Garrod, D., R.** (1993) Desmosomes and hemidesmosomes. *Curr. Opin. Cell Biol.* **5**(1), 30-40.
- Garrod, D., R.** (1996) Epithelial development and differentiation: the role of desmosomes. *J. R. Coll. Physicians Lond.* **30**, 366-373.
- Garrod, D., R., Berika, M., Y., Bardsley, W., F., Holmes, D. & Taberner, L.** (2005) Hyper-adhesion in desmosomes: its regulation in wound healing and possible relationship to cadherin crystal structure. *J. Cell Sci.* **118**, 5743-5754.
- Garrod, D., R., Merritt, A., J. & Nie, Z.** (2002) Desmosomal adhesion: structural basis, molecular mechanism and regulation. *Mol. Membr. Biol.* **19**(2), 81-94.
- Geerts, D., Fontao, L., Nievers, M., G., Schaapveld, R., Q., Purkis, P., E., Wheeler, G., N., Lane, E., B., Leigh, I., M. & Sonnenberg, A.** (1999) Binding of integrin alpha6beta4 to plectin prevents plectin association with F-actin but does not interfere with intermediate filament binding. *J. Cell Biol.* **147**, 417-434.

- Geiger, B. & Ginsberg, D.** (1991) The cytoplasmic domain of adherens-type junctions. *Cell Motil. Cytoskeleton* **20**(1), 1-6.
- Gerke, V. & Moss, S., E.** (1997) Annexins and membrane dynamics. *Biochim. Biophys. Acta.* **1357**, 129-154.
- Gerke, V. & Moss, S.E.** (2002) Annexins: From structure to function. *Physiol. Rev.* **82**, 331-371.
- Getsios, S., Huen, A., C. & Green, K., J.** (2004) Working out the strength and flexibility of desmosomes. *Nat. Rev. Mol. Cell Biol.* **5**, 271-281.
- Geuijen, C., A. & Sonnenberg, A.** (2002) Dynamics of the alpha6beta4 integrin in keratinocytes. *Mol. Biol. Cell.* **13**, 3845-3858.
- Giancotti, F., G.** (1996) Signal transduction by the alpha 6 beta 4 integrin: charting the path between laminin binding and nuclear events. *J. Cell Sci.* **109**(6), 1165-1172.
- Gillard, B., Clement, R., Colucci-Guyon, E., Babinet, C., Schwarzmann, G., Taki, T., Kasama, T. & Marcus, D.M.** (1998) Decreased synthesis of glycosphingolipids in cells lacking vimentin intermediate filaments. *Exp. Cell Res.* **242** 561-572.
- Gimona, M., Djinic-Carugo, K., Kranewitter, W., J. & Winder, S., J.** (2002) Functional plasticity of CH domains. *FEBS Lett.* **513**, 98-106.
- Giorda, R., Cerritello, A., Bonaglia, M., C., Bova, S., Lanzi, G., Repetti, E., Giglio, S., Baschiroto, C., Pramparo, T., Avolio, L., Bragheri, R., Maraschio, P. & Zuffardi, O.** (2004) Selective disruption of muscle and brain-specific BPAG1 isoforms in a girl with a 6;15 translocation, cognitive and motor delay, and tracheo-oesophageal atresia. *J. Med. Genet.* **41**, e71.
- Godsel, L., M., , Hobbs, R., P. & Green, K., J.** (2008) Intermediate filament assembly: dynamics to disease. *Trends Cell Biol.* **18**, 28-37.
- Godsel, L., M., , Getsios, S., Huen, A., C. & Green, K., J.** (2004) *The Molecular Composition and Function of Desmosomes.* SPRINGER VERLAG KG.
- Godsel, L., M., Hsieh, S., N., Amargo, E., V., Bass, A., E., Pascoe-McGillicuddy, L., T., Huen, A., C., Thorne, M., E., Gaudry, C., A., Park, J., K., Myung, K., Goldman, R., D., Chew, T., L. & Green, K., J.** (2005) Desmoplakin assembly dynamics in four dimensions: multiple phases differentially regulated by intermediate filaments and actin. *J. Cell Biol.* **171**(6), 1045-1059.
- Goebeler, V., Ruhe, D., Gerke, V. & Rescher, U.** (2003) Atypical properties displayed by annexin A9, a novel member of the annexin family of Ca²⁺ and lipid binding proteins. *FEBS letters* **546**, 359-364.
- Gong, X., Q., Shao, Q., Lounsbury, C., S., Bai, D. & Laird, D., W.** (2006) Functional characterization of a GJA1 frame-shift mutation causing oculodentodigital dysplasia and palmoplantar keratoderma. *J. Biol. Chem.* **281**, 31801-31811.
- Gonzales, M., Weksler, B., Tsuruta, D., Goldman, R., D., Yoon, K., J., Hopkinson, S., B., Flitney, F., W. & Jones, J., C.** (2001) Structure and function of a vimentin-associated matrix adhesion in endothelial cells. *Mol. Biol. Cell.* **12**, 85-100.

- Goto, M., Sumiyoshi, H., Sakai, T., Fässler, R., Ohashi, S., Adachi, E., Yoshioka, H. & Fujiwara, S.** (2006) Elimination of epiplakin by gene targeting results in acceleration of keratinocyte migration in mice. *Mol. Cell Biol.* **26**, 548-558.
- Green, K., J., Parry, D., A., Steinert, P., M., Virata, M., L., Wagner, R., M., Angst, B., D. & Nilles, L., A.** (1990) Structure of the human desmoplakins. Implications for function in the desmosomal plaque. *J. Biol Chem.* **265**(5), 2603-2612.
- Green, K.J., Bohringer, M., Gocken, T. & Jones, J.C.** (2005) Intermediate filament associated proteins. *Adv. Protein Chem.* **70** 143-202.
- Green, K.J., Virata, M.L.A., Elgart, G.W., Stanley, J. & Parry, D.A.D.** (1992) Comparative structural analysis of desmoplakin, bullous pemphigoid antigen and plectin: Members of a new gene family involved in organization of intermediate filaments. *Int. J. Biol. Macromol.* **14**, 145-153.
- Gregory, S., L. & Brown, N., H.** (1998) kakapo, a gene required for adhesion between and within cell layers in Drosophila, encodes a large cytoskeletal linker protein related to plectin and dystrophin. *J. Cell Biol.* **143**, 1271-1282.
- Groot, K.R., Sevilla, L.M., Nishi, K., DiColandrea, T. & Watt, F.M.** (2004) Kazrin, a novel periplakin-interacting protein associated with desmosomes and the keratinocyte plasma membrane. *J. Cell Biol.* **166**, . 653-659.
- Gross, S., P., Vershinin, M. & Shubeita, G., T.** (2007) Cargo transport: two motors are sometimes better than one. *Curr. Biol.* **17**, 478-486.
- Grossmann, K., S, Grund, C., Huelsken, J., Behrend, M., Erdmann, B., Franke, W., W. & Birchmeier, W.** (2004) Requirement of plakophilin 2 for heart morphogenesis and cardiac junction formation. *J. Cell Biol.* **167**, 149-160.
- Gumbiner, B.** (1988) Cadherins: a family of Ca²⁺-dependent adhesion molecules. *Trends. Biochem. Sci.* **13**(3), 75-76.
- Guo, L., Degenstein, L., Dowling, J., Yu, Q., C., Wollmann, R., Perman, B. & Fuchs, E.** (1995) Gene targeting of BPAG1: abnormalities in mechanical strength and cell migration in stratified epithelia and neurologic degeneration. *Cell* **81**, 233-243.
- Hämmerling, B., Grund, C., Boda-Heggemann, J., Moll, R. & Franke, W., W.** (2006) The complexus adhaerens of mammalian lymphatic endothelia revisited: a junction even more complex than hitherto thought. *Cell Tissue Res.* **324**, 55-67.
- Hannon, R., Croxtall, J., D., Getting, S., J., Roviezzo, F., Yona, S., Paul-Clark, M., J. , Gavins, F., N., Perretti, M., Morris, J., F. , Buckingham, J., C. & Flower, R., J.** (2003) Aberrant inflammation and resistance to glucocorticoids in annexin 1^{-/-} mouse. *FASEB J.* **17**, 253-255.
- Harborth, J., Elbashir, S., M. , Bechert, K., Tuschl, T. & Weber, K.** (2001) Identification of essential genes in cultured mammalian cells using small interfering RNAs. *J. Cell Sci.* **114**, 4557-4565.
- Harel, A., Bergman, R., Indelman, M. & Sprecher, E.** (2006) Epidermolysis bullosa simplex with mottled pigmentation resulting from a recurrent mutation in KRT14. *J. Invest. Dermatol.* **126**, 1654-1657.

- Hashimoto, T., Komai, A., Futei, Y., Nishikawa, T. & Amagai, M.** (2001) Detection of IgA autoantibodies to desmogleins by an enzyme-linked immunosorbent assay: the presence of new minor subtypes of IgA pemphigus. *Arch. Dermatol.* **137**(6), 735-738.
- Hatzfeld, M.** (1999) The armadillo family of structural proteins. *Int. Rev. Cytol.* **186**, 179-224.
- Hawkins, T.E., Roes, J., Rees, D., Monkhouse, J. & Moss, S.E.** (1999) Immunological development and cardiovascular function are normal in annexin VI null mutant mice. *Mol. Cell Biol.* **19**, 8028-8032.
- Hegerfeldt, Y., Tusch, M., Bröcker, E., B. & Friedl, P.** (2002) Collective cell movement in primary melanoma explants: plasticity of cell-cell interaction, beta1-integrin function, and migration strategies. *Cancer Res.* **62**, 2125-2130.
- Helfand, B., T., Loomis, P., Yoon, M. & Goldman, R., D.** (2003) Rapid transport of neural intermediate filament protein. *J. Cell Sci.* **116**, 2345-2359.
- Hendrychová, J., Vítová, M., Bisová, K., Wiche, G. & Zachleder, V.** (2002) Plectin-like proteins are present in cells of *Chlamydomonas eugametos* (Volvocales). *Folia Microbiol (Praha)*. **47**, 535-539.
- Hennies, H., C., Küster, W., Mischke, D. & Reis, A.** (1995) Localization of a locus for the striated form of palmoplantar keratoderma to chromosome 18q near the desmosomal cadherin gene cluster. *Hum. Mol. Genet.* **4**(6), 1015-1020.
- Herr, C., Smyth, N., Ullrich, S., Yun, F., Sasse, P., Hescheler, J., Fleischmann, B., Lasek, K., Brixius, K., Schwinger, R., H., Fässler, R., Schröder, R. & Noegel, A., A.** (2001) Loss of annexin A7 leads to alterations in frequency-induced shortening of isolated murine cardiomyocytes. *Mol. Cell Biol.* **21**, 4119-4128.
- Herrmann, H. & Aebi, U.** (2004) Intermediate filaments: Molecular structure, assembly mechanism, and integration into functionally distinct intracellular scaffolds. *Annu. Rev. Biochem.* **73**, 749-789.
- Hesse, M., Magin, T., M. & Weber, K.** (2001) Genes for intermediate filament proteins and the draft sequence of the human genome: novel keratin genes and a surprisingly high number of pseudogenes related to keratin genes 8 and 18. *J. Cell Sci.* **114**, 2569-2575.
- Hesse, M., Zimek, A., Weber, K. & Magin, T., M.** (2004) Comprehensive analysis of keratin gene clusters in humans and rodents. *Eur. J. Cell Biol.* **83**, 19-26.
- Hieda, Y., Nishizawa, Y., Uematsu, J. & Owaribe, K.** (1992) Identification of a new hemidesmosomal protein, HD1: a major, high molecular mass component of isolated hemidesmosomes. *J. Cell Biol.* **116**, 1497-1506.
- Hirokawa, N.** (1998) Kinesin and dynein superfamily proteins and the mechanism of organelle transport. *Science* **279**, 519-526.
- Hoffman, P., N. & Lasek, R., J.** (1975) The slow component of axonal transport. Identification of major structural polypeptides of the axon and their generality among mammalian neurons. *J. Cell Biol.* **66**, 351-366.
- Hofmann, I., Casella, M., Schnölzer, M., Schlechter, T., Spring, H. & Franke, W., W.** (2006) Identification of the junctional plaque protein plakophilin 3 in cytoplasmic particles containing RNA-binding proteins and the recruitment of plakophilins 1 and 3 to stress granules. *Mol. Biol. Cell* **17**, 1388-1398.

- Hohl, D.** (1990) Cornified cell envelope. *Dermatologica* **180**(4), 201-211.
- Hollenbeck, P., J. & Swanson, J., A.** (1990) Radial extension of macrophage tubular lysosomes supported by kinesin. *Nature* **346**, 864-866.
- Hopkinson, S., B. & Jones, J., C.** (2000) The N terminus of the transmembrane protein BP180 interacts with the N-terminal domain of BP230, thereby mediating keratin cytoskeleton anchorage to the cell surface at the site of the hemidesmosome. *Mol. Biol. Cell.* **11**(1), 277-286.
- Huen, A., C., Park, J., K., Godsel, L., M., Chen, X., Bannon, L., J., Amargo, E., V., Hudson, T., Y., Mongiu, A., K., Leigh, I., M., Kelsell, D., P., Gumbiner, B., M. & Green, K., J.** (2002) Intermediate filament-membrane attachments function synergistically with actin-dependent contacts to regulate intercellular adhesive strength. *J. Cell Biol.* **159**, 1005-1017.
- Hunt, D., M., Rickman, L., Whittock, N., V. , Eady, R., A. , Simrak, D., Dopping-Hepenstal, P., J. , Stevens, H., P., Armstrong, D., K. , Hennies, H., C. , Küster, W., Hughes, A., E. , Arnemann, J., Leigh, I., M., McGrath, J., A. , Kelsell, D., P. & Buxton, R., S.** (2001) Spectrum of dominant mutations in the desmosomal cadherin desmoglein 1, causing the skin disease striate palmoplantar keratoderma. *Eur. J. Hum. Genet.* **9**, 197-203.
- Hutvagner, G. & Zamore, P.D.** (2002) RNAi: nature abhors a double-strand. *Curr. Opin. Genet. Dev.* **12**(2), 225-232.
- Inagaki, M., Matsuoka, Y. & Tsujimura, K.** (1996) Dynamic property of intermediate filaments: Regulation by phosphorylation. *Bioessays* **18**, 481-487.
- Inagaki, M., Nishi, Y., Nishizawa, K., Matsuyama, M. & Sato, C.** (1987) Site-specific phosphorylation induces disassembly of vimentin filaments in vivo. *Nature* **328**, 649-652.
- Ishii, K. & Green, K., J.** (2001) Cadherin function: breaking the barrier. *Curr. Biol.* **11**, 569-572.
- Ishikawa, H., Bischoff, R. & Holtzer, H.** (1968) Mitosis and intermediate-sized filaments in developing skeletal muscle. *J. Cell Biol.* **38**, 538-555
- Izawa, I. & Inagaki, M.** (2006) Regulatory mechanisms and functions of intermediate filaments: a study using site- and phosphorylation state-specific antibodies. *Cancer Sci.* **97**(3), 167-174.
- Jacinto, A., Wood, W., Woolner, S., Hiley, C., Turner, L., Wilson, C., Martinez-Arias, A. & Martin, P.** (2002) Dynamic Analysis of Actin Cable Function during Drosophila Dorsal Closure. *Current Biology* **12**, 1245-1250.
- Jackson, B., Claudia, M., L. , Tilli, J., Hardman, M., J., Avilion A, A., MacLeod M, C., Ashcroft, G., S. & Byrne, C.** (2005) Late Cornified Envelope Family in Differentiating Epithelia—Response to Calcium and Ultraviolet Irradiation. *J. Invest. Dermatol.* **124**, 1062-1070.
- Jang, S.-I., Kalinin, A., Takahashi, K., Marekov, L.N. & M., S.P.** (2005) Characterization of human epiplakin: RNAi-mediated epiplakin depletion leads to the disruption of keratin and vimentin IF networks. *J. Cell Sci.* **118**, 781-793.

- Jarnik, M., de Viragh, P., A., Schärer, E., Bundman, D., Simon, M., N., Roop, D., R. & Steven, A., C.** (2002) Quasi-normal cornified cell envelopes in loricrin knockout mice imply the existence of a loricrin backup system. *J. Invest. Dermatol.* **118**, 102-109.
- Jarnik, M., Simon, M., N. & Steven, A., C.** (1998) Cornified cell envelope assembly: a model based on electron microscopic determinations of thickness and projected density. *J. Cell. Sci.* **1051-1060**.
- Jefferson, J.J., Leung, C.L. & Liem, R.K.** (2004) Plakins: Goliaths that link cell junctions and the cytoskeleton. *Nat. Rev. Mol. Cell Biol.* **5**, 542-553.
- Joly, P., Richard, C., Gilbert, D., Courville, P., Chosidow, O., Roujeau, J., C., Beylot-Barry, M., D'incan, M., Martel, P., Lauret, P. & Tron, F.** (2000) Sensitivity and specificity of clinical, histologic, and immunologic features in the diagnosis of paraneoplastic pemphigus. *J. Am. Acad. Dermatol.* **43(4)**, 619-626.
- Jonca, N., Guerrin, M., Hadjiolova, K., Caubet, C., Gallinaro, H., Simon, M. & Serre, G.** (2002) Corneodesmosin, a component of epidermal corneocyte desmosomes, displays homophilic adhesive properties. *J. Biol. Chem.* **277**, 5024-5029.
- Jones, J.C., Hopkinson, S.B. & Goldfinger, L.E.** (1998) Structure and assembly of hemidesmosomes. *Bioessays* **20(6)**, 488-494.
- Jonkman, M., F., Pasmooij, A., M., Pasmans, S., G., van den Berg, M., P., Ter Horst, H., J., Timmer, A. & Pas, H., H.** (2005) Loss of desmoplakin tail causes lethal acantholytic epidermolysis bullosa. *Am. J. Hum. Genet.* **77**, 653-660.
- Kalinin, A.E., Kalinin, A.E., Aho, M., Uitto, J. & Aho, S.** (2005) Breaking the connection: caspase 6 disconnects intermediate filament-binding domain of periplakin from its actin-binding N-terminal region. *J. Invest. Dermatol.* **124**, 46-55.
- Karamatic, C.V., Burton, N., Kagan, A., Green, C., A., Levene, C., Flintner, F., Brady, R., L., Daniels, G. & Anstee, D., J.** (2004) CD151, the first member of the tetraspanin (TM4) superfamily detected on erythrocytes, is essential for the correct assembly of human basement membranes in kidney and skin. *Blood* **104**, 2217-2223.
- Karashima, T. & Watt, F.M.** (2002) Interaction of periplakin and envoplakin with intermediate filaments. *J. Cell Sci.* **115**, 5027-5037.
- Kartenbeck, J., Haselmann, U. & Gassler, N.** (2005) Synthesis of junctional proteins in metastasizing colon cancer cells. *Eur. J Cell Biol.* **84**, 417-430.
- Karty, J.A., Ireland, M.M.E., Brun, Y.V. & Reilly, J.P.** (2002) Artifacts and unassigned masses encountered in peptide mass mapping. *J. Chromatogr.* **782**, 363-383.
- Kazerounian, S. & Aho, S.** (2003) Characterization of periphilin, a widespread, highly insoluble nuclear protein and potential constituent of the keratinocyte cornified envelope. *J. Biol. Chem.* **278**, 36707-36717.
- Kazerounian, S., Mahoney, M., G., Uitto, J. & Aho, S.** (2000) Envoplakin and periplakin, the paraneoplastic pemphigus antigens, are also recognized by pemphigus foliaceus autoantibodies. *J. Invest. Dermatol.* **115(3)**, 505-507.
- Kazerounian, S., Uitto, J. & Aho, S.** (2002) Unique role for the periplakin tail in intermediate filament association: specific binding to keratin 8 and vimentin. *Exp. Dermatol.* **11**, 428-438.

- Kee, S., H. & Steinert, P., M.** (2001) Microtubule disruption in keratinocytes induces cell-cell adhesion through activation of endogenous E-cadherin. *Mol. Biol. Cell* **12**(7), 1983-1993.
- Kelsell, D., P., Wilgoss, A., L., Richard, G., Stevens, H., P., Munro, C., S. & Leigh, I., M.** (2000) Connexin mutations associated with palmoplantar keratoderma and profound deafness in a single family. *Eur. J. Hum. Genet.* **8**, 469-472.
- Kim, S. & Coulombe, P.A.** (2007) Intermediate filament scaffolds fulfill mechanical, organizational, and signalling functions in the cytoplasm. *Genes and Development* **21**, 1581-1597.
- Kimura, T., E., Merritt, A., J. & Garrod, D., R.** (2007) Calcium-independent desmosomes of keratinocytes are hyper-adhesive. *J. Invest. Dermatol.* **127**, 775-781.
- Kirchhoff, S., Nelles, E. & Hagendorff, A.** (1998) Reduced cardiac conduction velocity and predisposition to arrhythmias in connexin40- deficient mice. *Curr. Biol.* **8**, 299-302.
- Kirmse, R., Portet, S., Mücke, N., Aebi, U., Herrmann, H. & Langowski, J.** (2007) A quantitative kinetic model for the in vitro assembly of intermediate filaments from tetrameric vimentin. *J. Biol. Chem.* **282**, 18563-18572.
- Kitajima, Y., Aoyama, Y. & Seishima, M.** (1999) Transmembrane signaling for adhesive regulation of desmosomes and hemidesmosomes, and for cell-cell attachment induced by pemphigus IgG in cultured keratinocytes: involvement of protein kinase. *C. J. Investig. Dermatol. Symp. Proc.* **4**, 137-144.
- Kiyokawa, C., Ruhrberg, C., Nie, Z., Karashima, T., Mori, O., Nishikawa, T., Green, K., J., Anhalt, G., J., DiColandrea, T., Watt, F., M. & Hashimoto, T.** (1998) Envoplakin and periplakin are components of the paraneoplastic pemphigus antigen complex. *J. Invest. Dermatol.* **111**(6), 1236-1238.
- Kljuic, A., Bazzi, H., Sundberg, J., P., Martinez-Mir, A., O'Shaughnessy, R., Mahoney, M., G., Levy, M., Montagutelli, X., Ahmad, W., Aita, V., M., Gordon, D., Uitto, J., D., W., Ott, J., Fischer, S., Gilliam, T., C., Jahoda, C., A., Morris, R., J., Panteleyev, A., A., Nguyen, V., T. & Christiano, A., M.** (2003) Desmoglein 4 in hair follicle differentiation and epidermal adhesion: evidence from inherited hypotrichosis and acquired pemphigus vulgaris. *Cell* **113**, 249-260.
- Klymkowsky, M.W., Shook, D.R. & Maynell, L.A.** (1992) Evidence that the deep keratin filament systems of the *Xenopus* embryo act to ensure normal gastrulation. *Proc. Natl. Acad. Sci.* **89**, 8736-8740.
- Knudsen, K., A., Frankowski, C., Johnson, K., R. & Wheelock, M., J.** (1998) A role for cadherins in cellular signaling and differentiation. *J. Cell Biochem. Suppl.* **30-31**, 168-176.
- Kosako, H., Amano, M., Yanagida, M., Tanabe, K., Nishi, Y., Kaibuchi, K. & Inagaki, M.** (1997) Phosphorylation of glial fibrillary acidic protein at the same sites by cleavage furrow kinase and Rho-associated kinase. *J. Biol. Chem.* **272**, 10333-10336.
- Koss-Harnes, D., Høyheim, B., Anton-Lamprecht, I., Gjesti, A., Jørgensen, R., S., Jahnsen, F., L., Olaisen, B., Wiche, G. & Gedde-Dahl, T.J.** (2002) A site-specific

- plectin mutation causes dominant epidermolysis bullosa simplex Ogna: two identical de novo mutations. *J. Invest Dermatol.* **118**, 87-93.
- Koster, J., Geerts, D., Favre, B., Borradori, L. & Sonnenberg, A.** (2003) Analysis of the interactions between BP180, BP230, plectin and the integrin alpha6beta4 important for hemidesmosome assembly. *J. Cell Sci.* **116**, 387-399.
- Koster, J., van Wilpe, S., Kuikman, I., Litjens, S., H. & Sonnenberg, A.** (2004) Role of binding of plectin to the integrin beta4 subunit in the assembly of hemidesmosomes. *Mol. Biol Cell.* **15**, 1211-1223.
- Kowalczyk, A.P., Bornslaeger, E.A., Norvell, S.M., Palka, H.L. & Green, K.J.** (1999) Desmosomes: intercellular adhesive junctions specialized for attachment of intermediate filaments. *Int. Rev. Cytol.* **185**, 237-302.
- Kreplak, L., Ba" r, H., Leterrier, J., F. & Herrmann, H.** (2005) Exploring the mechanical behavior of single intermediate filaments. *J. Mol. Biol.* **354**, 569-577.
- Kretz, M., Euwens, C., Hombach, S., Eckardt, D., Teubner, B. & Traub, O.** (2003) Altered connexin expression and wound healing in the epidermis of connexin-deficient mice. *J. Cell Sci.* **116**, 3443-3452.
- Ku, N., O., Michie, S., A., Soetikno, R., M., Resurreccion, E., Z., Broome, R., L. & Omary, M., B.** (1998a) Mutation of a major keratin phosphorylation site predisposes to hepatotoxic injury in transgenic mice. *J. Cell Biol.* **143**, 2023-2032.
- Ku, N.O. & Omary, M.B.** (1997) Phosphorylation of human keratin 8 in vivo at conserved head domain serie 23 and at epidermal growth factor-stimulated tail domain serine 431. *The Journal Of Biological Chemistry* **272**, 7556-7564.
- Lampugnani, M., G.** (1999) Cell migration into a wounded area in vitro. *Methods Mol. Biol.* **96**, 177-182.
- Lauffenburger, D., A. & Horwitz, A., F.** (1996) Cell migration: a physically integrated molecular process. *Cell* **84**, 359-369.
- Lechler, T. & Fuchs, E.** (2007) Desmoplakin: an unexpected regulator of microtubule organization in the epidermis. *J. Cell Biol.* **176**, 147-154.
- Lee, M.K. & Cleveland, D.W.** (1996) Neuronal intermediate filaments. **19** 187-217
- Leung, C., L., Sun, D., Zheng, M., Knowles, D., R. & Liem, R., K.** (1999) Microtubule actin cross-linking factor (MACF): a hybrid of dystonin and dystrophin that can interact with the actin and microtubule cytoskeletons. *J. Cell Biol.* **147**, 1275-1286.
- Leung, C., L., Zheng, M., Prater, S., M. & Liem, R., K.** (2001) The BPAG1 locus: Alternative splicing produces multiple isoforms with distinct cytoskeletal linker domains, including predominant isoforms in neurons and muscles. *J. Cell Biol.* **154**(4), 691-697.
- Leung, C.L., Green, K.J. & Liem, R.K.** (2002) Plakins: a family of versatile cytolinker proteins. *Trends. Cell Biol.* **12**, 37-45.
- Liao, H., Zhao, Y., Baty, D., U., McGrath, J., A., Mellerio, J., E. & McLean, W., H.** (2007) A heterozygous frameshift mutation in the V1 domain of keratin 5 in a family with Dowling-Degos disease. *J. Invest. Dermatol.* **127**, 298-300.

- Liao, J. & Omary, M., B.** (1996) 14-3-3 proteins associate with phosphorylated simple epithelial keratins during cell cycle progression and act as a solubility cofactor. *J. Cell Biol.* **133**, 345-357.
- Lieber, M., Mazzetta, J., Nelson-Rees, W., Kaplan, M. & Todaro, G.** (1975) Establishment of a continuous tumor-cell line (panc-1) from a human carcinoma of the exocrine pancreas. *Int. J. Cancer.* **15**, 741-747.
- Ling, Q., Jacovina, A.T., Deora, A., Febbraio, M., Simantov, R., Silverstein, R.L., Hempstead, B., Mark, W.H. & Hajjar, K.A.** (2004) Annexin II regulates fibrin homeostasis and neoangiogenesis in vivo. *J. Clin. Invest.* **113**, 38-48.
- Liovic, M., Mogensen, M., M., Prescott, A., R. & Lane, E., B.** (2003) Observation of keratin particles showing fast bidirectional movement colocalized with microtubules. *J. Cell Sci.* **116**, 1417-1427.
- Lippincott-Schwartz, J., Cole, N., B., Marotta, A., Conrad, P., A. & Bloom, G., S.** (1995) Kinesin is the motor for microtubule-mediated Golgi-to-ER membrane traffic. *J. Cell Biol.* **128**, 293-306.
- Litjens, S.H., de Pereda, J.M. & Sonnenberg, A.** (2006) Current insights into the formation and breakdown of hemidesmosomes. *Trends Cell Biol.* **16**, 376-383.
- Liu, J., J., Ding, J., Wu, C., Bhagavatula, P., Cui, B., Chu, S., Mobley, W., C. & Yang, Y.** (2007) Retrolinkin, a membrane protein, plays an important role in retrograde axonal transport. *Proc. Natl. Acad. Sci. U S A.* **104**, 2223-2228.
- Liu, J., J., Ding, J., Kowal, A., S., Nardine, T., Allen, E., Delcroix, J., D., Wu, C., Mobley, W., Fuchs, E. & Yang, Y.** (2003) BPAG1n4 is essential for retrograde axonal transport in sensory neurons. *J. Cell Biol.* **163**, 223-229.
- Lloyd, C., Yu, Q., C., Cheng, J., Turksen, K., Degenstein, L., Hutton, E. & Fuchs, E.** (1995) The basal keratin network of stratified squamous epithelia: defining K15 function in the absence of K14. *J. Cell Biol.* **129**, 1329-1344.
- Long, H.A., Boczonadi, V., McInroy, L., Goldberg, M. & Maatta, A.** (2006) Periplakin-dependent re-organization of keratin cytoskeleton and loss of collective migration in keratin-8-downregulated epithelial sheets. *J. Cell Sci.* **119**, 5147-5159.
- Loranger, A., Gilbert, S., Brouard, J., S., Magin, T., M. & Marceau, N.** (2006) Keratin 8 modulation of desmoplakin deposition at desmosomes in hepatocytes. *Exp. Cell Res.* **312**(20), 4108-4119.
- Lugassy, J., Itin, P., Ishida-Yamamoto, A., Holland, K., Huson, S., Geiger, D., Hennies, H., C., Indelman, M., Bercovich, D., Uitto, J., Bergman, R., McGrath, J., A., Richard, G. & Sprecher, E.** (2006) Naegeli-Franceschetti-Jadassohn syndrome and dermatopathia pigmentosa reticularis: two allelic ectodermal dysplasias caused by dominant mutations in KRT14. *Am. J. Hum. Genet.* **79**, 724-730.
- Lunter, P., C. & Wiche, G.** (2002) Direct binding of plectin to Fer kinase and negative regulation of its catalytic activity. *Biochem. Biophys. Res. Commun.* **296**, 904-910.
- Luo, B., H. & Springer, T., A.** (2006) Integrin structures and conformational signaling. *Curr. Opin. Cell Biol.* **18**, 579-586.
- Lyons, A., J. & Jones, J.** (2007) Cell adhesion molecules, the extracellular matrix and oral squamous carcinoma. *Int. J. Oral Maxillofac. Surg.* (36), 671-679.

- Ma, A.S.-P. & Sun, T.-T.** (1986) Differentiation-dependent changes in the solubility of a 195-kD protein in human epidermal keratinocytes. *J. Cell Biol.* **103**, 41-48.
- Määttä, A., DiColandrea, T., Groot, K. & Watt, F.M.** (2001) Gene targeting of envoplakin, a cytoskeletal linker protein and precursor of the epidermal cornified envelope. *Mol. Cell Biol.* **21**, 7047-7053.
- Määttä, A., Hutchison, C., J. & Watson, M., D.** (2004) Spectraplakins and nesprins, giant spectrin repeat proteins participating in the organization of the cytoskeleton and the nuclear envelope. *Symp. Soc. Exp. Biol.* **56**, 265-277.
- Macari, F., Landau, M., Cousin, P., Mevorah, B., Brenner, S. & Panizzon, R.** (2000) Mutation in the gene for connexin 30.3 in a family with erythrokeratoderma variabilis. *Am. J. Hum. Genet.* **67**, 1296-1301.
- Maciver, S.** (1996) Myosin II function in non-muscle cells. *Bioessays* **18**, 179-182.
- Maeda, O., Usami, N., Kondo, M., Takahashi, M., Goto, H., Shimokata, K., Kusugami, K. & Sekido, Y.** (2004) Plakoglobin (gamma-catenin) has TCF/LEF family-dependent transcriptional activity in beta-catenin-deficient cell line. *Oncogene* **23**, 964-972.
- Magin, T., M., Vijayaraj, P. & Leube, R., E.** (2007) Structural and regulatory functions of keratins. *Exp. Cell Res.* **313**, 2021-2032.
- Mahoney, M.G., Aho, S., Uitto, J. & Stanley, J.R.** (1998) The members of the plakin family of proteins recognized by paraneoplastic pemphigus antibodies include periplakin. *J. Invest. Dermatol.* **111**, 308-313.
- Manser, E., Huang, H., Y., Loo, T., H., Chen, X., Q., Dong, J., M., Leung, T. & L., L.** (1997) Expression of constitutively active alpha-PAK reveals effects of the kinase on actin and focal complexes. *Mol. Cell Biol.* **17**, 1129-1143.
- Margolis, S., S., Perry, J., A., Forester, C., M., Nutt, L., K., Guo, Y., Jardim, M., J., Thomenius, M., J., Freel, C., D., Darbandi, R., Ahn, J., H., Arroyo, J., D., Wang, X., F., Shenolikar, S., Nairn, A., C., Dunphy, W., G., Hahn, W., C., Virshup, D., M. & Kornbluth, S.** (2006) Role for the PP2A/B56delta phosphatase in regulating 14-3-3 release from Cdc25 to control mitosis. *Cell* **127**, 759-773.
- Marshall, D., Hardman, M., J., Nield, K., M. & Byrne, C.** (2001) Differentially expressed late constituents of the epidermal cornified envelope. *Proc. Natl. Acad. Sci. USA* **98**, 13031-13036.
- Martin, P. & Lewis, J.** (1992) Actin cables and epidermal movement in embryonic wound healing. *Nature* **360**, 179-183
- Martin, P. & Parkhurst, S.M.** (2004) Parallels between tissue repair and embryo morphogenesis. *Development* **131**, 3021-3034.
- Martin, P.** (1997) Wound healing--aiming for perfect skin regeneration. *Science* **276**, 75-81.
- Matsuki, M., Yamashita, F., Ishida-Yamamoto, A., Yamada, K., Kinoshita, C., Fushik, i.S., Ueda, E., Morishima, Y., Tabata, K., Yasuno, H., Hashida, M., Iizuka, H., Ikawa, M., Okabe, M., Kondoh, G., Kinoshita, T., Takeda, J. & Yamanishi, K.** (1998) Defective stratum corneum and early neonatal death in mice lacking the gene for

- transglutaminase 1 (keratinocyte transglutaminase). *Proc. Natl. Acad. Sci. U S A.* **95**(3), 1044-1049.
- Matsuzawa, K., Kosako, H., Azuma, I., Inagaki, N. & Inagaki, M.** (1998) Possible regulation of intermediate filament proteins by Rho-binding kinases. *Subcell. Biochem.* **31**, 423-435.
- Mattey, D., L. & Garrod, D., R.** (1986) Splitting and internalization of the desmosomes of cultured kidney epithelial cells by reduction in calcium concentration. *J. Cell Sci.* **85**, 113-124.
- McGrath, J., A.** (2005) Inherited disorders of desmosomes. *Australas J. Dermatol.* **46**, 221-229.
- McInroy, L. & Maatta, A.** (2007) Down-regulation of vimentin expression inhibits carcinoma cell migration and adhesion. *Biochemical and Biophysical Research Communications* **360**, 109-114.
- McKoy, G., Protonotarios, N., Crosby, A., Tsatsopoulou, A., Anastasakis, A., Coonar, A., Norman, M., Baboonian, C., Jeffery, S. & McKenna, W., J.** (2000) Identification of a deletion in plakoglobin in arrhythmic right ventricular cardiomyopathy with palmoplantar keratoderma and woolly hair (Naxos disease). *Lancet.* **355**, 2119-2124.
- McLean, W., H., Pulkkinen, L., Smith, F., J., Rugg, E., L., Lane, E., B., Bullrich, F., Burgeson, R., E., Amano, S., Hudson, D., L., Owaribe, K., McGrath, J., A., McMillan, J., R., Eady, R., A., Leigh, I., M., Christiano, A., M. & Uitto, J.** (1996) Loss of plectin causes epidermolysis bullosa with muscular dystrophy: cDNA cloning and genomic organization. *Genes. Dev.* **10**, 1724-1735.
- McMillan, J.R. & Shimizu, H.** (2001) Desmosomes: structure and function in normal and diseased epidermis. *J. Dermatol.* **28**, 291-298.
- Mejillano, M., R., Kojima, S., Applewhite, D., A., Gertler, F., B., Svitkina, T., M. & Borisy, G., G.** (2004) Lamellipodial versus filopodial mode of the actin nanomachinery: pivotal role of the filament barbed end. *Cell* **118**, 363-373.
- Meng, J.J., Bornslaeger, E.A., Green, K.J., Steinert, P.M. & Ip, W.** (1997) Two-hybrid analysis reveals fundamental differences in direct interactions between desmoplakin and cell type-specific intermediate filaments. *J. Biol. Chem.* **272**, 21495-21503.
- Mertens, C., Hofmann, I., Wang, Z., Teichmann, M., Sepehri Chong, S., Schnölzer, M. & Franke, W., W.** (2001) Nuclear particles containing RNA polymerase III complexes associated with the junctional plaque protein plakophilin 2. *Proc. Natl. Acad. Sci. U S A.* **98**, 7795-7800.
- Michel, S., Schmidt, R., Shroot, B. & Reichert, U.** (1988) Morphological and biochemical characterization of the cornified envelopes from human epidermal keratinocytes of different origin. *J. Invest. Dermatol.* **91**(1), 11-5.
- Miravet, S., Piedra, J., Castaño, J., Raurell, I., Francí, C., Duñach, M. & García de Herreros, A.** (2003) Tyrosine phosphorylation of plakoglobin causes contrary effects on its association with desmosomes and adherens junction components and modulates beta-catenin-mediated transcription. *Mol. Cell Biol.* **23**, 7391-402.

- Mischke, D., Korge, B., P., Marenholz, I., Volz, A. & Ziegler, A.** (1996) Genes encoding structural proteins of epidermal cornification and S100 calcium-binding proteins form a gene complex ("epidermal differentiation complex") on human chromosome 1q21. . *J. Invest. Dermatol.* **106**, 989–992.
- Mitchison, T. & Kirschner, M.** (1984) Dynamic instability of microtubule growth. . *Nature* **312**, 237–242.
- Mitchison, T., J. & Cramer, L., P.** (1996) Actin-based cell motility and cell locomotion. *Cell* **84**, 371–379.
- Moore, B., W. & Perez, V., J.** (1967) *Specific acidic proteins of the nervous system*. NJ.: Prentice-Hall, Englewood Cliffs.
- Morgan, R., O. & Fernandez, M., P.** (1998) Expression profile and structural divergence of novel human annexin 31. *FEBS Lett.* **434**, 300–304.
- Morley, S.M., D'Alessandro, M., Sexton, C., Rugg, E.L., Navsaria, H., Shemanko, C.S., Huber, M., Hohl, D., Heagerty, A.I., Leigh, I.M. & Lane, E.B.** (2003) Generation and characterization of epidermolysis bullosa simplex cell lines: scratch assays show faster migration with disruptive keratin mutations. *Br. J. Dermatol.* **149**, 46–58.
- Moss, S.E. & Morgan, R.O.** (2004) The annexins. *Genome Biology* **5**(4), 219.
- Motil, J., Chan, W., K., Dubey, M., Chaudhury, P., Pimenta, A., Chylinski, T., M., Ortiz, D., T. & Shea, T., B.** (2006) Dynein mediates retrograde neurofilament transport within axons and anterograde delivery of NFs from perikarya into axons: regulation by multiple phosphorylation events. *Cell Motil. Cytoskeleton.* **63**, 266–286.
- Musil, L., S., Le, A., C., VanSlyke, J., K. & Roberts, L., M.** (2000) Regulation of connexin degradation as a mechanism to increase gap junction assembly and function. . *J. Biol. Chem.* **275**, 25207–25215.
- Nabeshima, K., Inoue, T. & Shima, Y.** (2000) Front-cell-specific expression of membrane-type 1 matrix metalloproteinase and gelatinase A during cohort migration of colon carcinoma cells induced by hepatocyte growth factor/scatter factor. . *Cancer Res.* **60**, 3364–3369.
- Nagafuchi, A.** (2001) Molecular architecture of adherens junctions. . *Curr. Opin. Cell Biol.* **13**, 600–603.
- Nagata, Y., Karashima, T., Watt, F., M., Salmhofer, W., Kanzaki, T. & Hashimoto, T.** (2001) Paraneoplastic pemphigus sera react strongly with multiple epitopes on the various regions of envoplakin and periplakin, except for the c-terminal homologous domain of periplakin. *J. Invest. Dermatol.* **116**(4), 556–563.
- Nayal, A., Webb, D., J., Brown, C., M., Schaefer, E., M., Vicente-Manzanares, M. & Horwitz, A., R.** (2006) Paxillin phosphorylation at Ser273 localizes a GIT1-PIX-PAK complex and regulates adhesion and protrusion dynamics. *J. Cell Biol.* **173**, 587–589.
- Nemes, Z. & Steinert, P., M.** (1999) Bricks and mortar of the epidermal barrier. *Exp. Mol. Med.* **31**(1), 5–19.
- Ng, W., K.** (2002) Fine-needle aspiration cytology findings of an uncommon micropapillary variant of pure mucinous carcinoma of the breast: review of patients over an 8-year period. *Cancer Res.* **96**, 280–288.

- Nguyen, V., T., Ndoye, A., Bassler, K., D., Shultz, L., D., Shields, M., C., Ruben, B., S., Webber, R., J., Pittelkow, M., R., Lynch, P., J. & Grando, S., A.** (2001) Classification, clinical manifestations, and immunopathological mechanisms of the epithelial variant of paraneoplastic autoimmune multiorgan syndrome: a reappraisal of paraneoplastic pemphigus. *Arch. Dermatol.* **137**(2), 193-206.
- Nguyen, V.T., Ndoye, A. & Grando, S.A.** (2000) A novel keratinocyte annexin -like molecule binding acetylcholine. *J. Biol.Chem.* **275**, 29466-29476.
- Niessen, C., M., Hulsman, E., H., Oomen, L., C., Kuikman, I. & Sonnenberg, A.** (1997) A minimal region on the integrin beta4 subunit that is critical to its localization in hemidesmosomes regulates the distribution of HD1/plectin in COS-7 cells. *J. Cell Sci.* **110**, 1705-1716.
- Niessen, C., M., Hogervorst, F., Jaspars, L., H., de Melker, A., A., Delwel, G., O., Hulsman, E., H., Kuikman, I. & Sonnenberg, A.** (1994) The alpha 6 beta 4 integrin is a receptor for both laminin and kalinin. *Exp. Cell Res.* **211**(2), 360-367.
- Nikolic, B., Mac Nulty, E., Mir, B. & Wiche, G.** (1996) Basic amino acid residue cluster within nuclear targeting sequence motif is essential for cytoplasmic plectin-vimentin network junctions. *J. Cell Biol.* **134**, 1455-1467.
- Nishimori, T., Tomonaga, T., Matsushita, K., Oh-Ishi, M., Kodera, Y., Maeda, T., Nomura, F., Matsubara, H., Shimada, H. & Ochiai, T.** (2006) Proteomic analysis of primary esophageal squamous cell carcinoma reveals downregulation of a cell adhesion protein, periplakin. *Proteomics* **6**, 1011-1018.
- Nobes, C., D. & Hall, A.** (1999) Rho GTPases control polarity, protrusion, and adhesion during cell movement. *J. Cell Biol.* **144**, 1235-1244.
- Norgett, E., E., Hatsell, S., J., Carvajal-Huerta, L., Cabezas, J., C., Common, J., Purkis, P., E., Whittock, N., Leigh, I., M., Stevens, H., P. & Kelsell, D., P.** (2000) Recessive mutation in desmoplakin disrupts desmoplakin-intermediate filament interactions and causes dilated cardiomyopathy, woolly hair and keratoderma. *Hum. Mol. Genet.* **9**, 2761-2766.
- North, A., J., Chidgey, M., A., Clarke, J., P., Bardsley, W., G. & Garrod, D., R.** (1996) Distinct desmocollin isoforms occur in the same desmosomes and show reciprocally graded distributions in bovine nasal epidermis. *Proc. Natl. Acad. Sci. U. S. A.*, 7701-7705.
- Nuber, U., A., Schafer, S., Stehr, S., Rackwitz, H., R. & Franke, W., W.** (1996) Patterns of desmocollin synthesis in human epithelia: immunolocalization of desmocollins 1 and 3 in special epithelia and in cultured cells. *Eur. J. Cell Biol.* **71**, 1-13.
- Ohyama, M., Amagai, M. & Hashimoto, T.** (2001) Clinical phenotype and anti-desmoglein autoantibody profile in paraneoplastic pemphigus. *J. Invest. Dermatol.* **44**, 593-593.
- O'Keefe, E., J., Erickson, H., P. & Bennett, V.** (1989) Desmoplakin I and desmoplakin II. Purification and characterization. *J. Biol. Chem.* **264**, 8310-8318.
- Okuda, T., Matsuda, S., Nakatsugawa, S., Ichigotani, Y., Iwahashi, N., Takahashi, M., Ishigaki, T. & Hamaguchi, M.** (1999) Molecular cloning of macrophin, a human homologue of *Drosophila* kakapo with a close structural similarity to plectin and dystrophin. *Biochem. Biophys. Res. Commun.* **264**, 568-574.

- Omary, M., B., Coulombe, P., A. & McLean, W., H.** (2004) Intermediate filament proteins and their associated diseases. *N. Engl. J. Med.* **351**, 2087-2100.
- Omary, M.B., Ku, N.O., Liao, J. & Price, D.** (1998) Keratin modifications and solubility properties in epithelial cells and in vitro. *Subcell. Biochem.* **31**, 105-140.
- Omary, M.B., Ku, N.O., Tao, G.Z., Toivola, D.M. & Liao, J.** (2006) 'Heads and tails' of intermediate filament phosphorylation: Multiple sites and functional insights. *Trends Biochem. Sci.* **31**, 383-394.
- Orian-Rousseau, V., D., A., Fontao, L., Chevalier, L., Meneguzz, i.G., Kedinger, M. & Simon-Assmann, P.** (1996) Developmental expression of laminin-5 and HD1 in the intestine: epithelial to mesenchymal shift for the laminin gamma-2 chain subunit deposition. *Dev. Dyn.* **206**(1), 12-23.
- Oriolo, A., S., Wald, F., A., Ramsauer, V., P. & Salas, P., J.** (2007) Intermediate filaments: a role in epithelial polarity. *Exp. Cell Res.* **313**(10), 2255-2264.
- Osmanagic-Myers, S. & Wiche, G.** (2004) Plectin-RACK1 (receptor for activated C kinase 1) scaffolding: a novel mechanism to regulate protein kinase C activity. *J. Biol. Chem.* **279**, 18701-18710.
- Osmanagic-Myers, S., Gregor, M., Walko, G., Burgstaller, G., Reipert, S. & Wiche, G.** (2006) Plectin-controlled keratin cytoarchitecture affects MAP kinases involved in cellular stress response and migration. *J. Cell Biol.* **174**, 557-568.
- Owaribe, K., Nishizawa, Y. & Franke, W., W.** (1991) Isolation and characterization of hemidesmosomes from bovine corneal epithelial cells. *Exp. Cell Res.* **192**, 622-630.
- Pachter, J., S. & Liem, R., K.** (1985) alpha-Interneixin, a 66-kD intermediate filament-binding protein from mammalian central nervous tissues. *J. Cell Biol.* **101**, 1316-1322.
- Paddison, P., J. & Hannon, G., J.** (2002) RNA interference: the new somatic cell genetics? *Cancer Cell* **2**(1), 17-23.
- Palka, H., L. & Green, K., J.** (1997) Roles of plakoglobin end domains in desmosome assembly. *J. Cell Sci.* **110**, 2359-2371.
- Pallari, H., M. & Eriksson, J., E.** (2006) Intermediate filaments as signaling platforms. *Sci. STKE.* **366**, pe53.
- Pappin, D., J. , Hojrup, P. & Bleasby, A., J.** (1993) Rapid identification of proteins by peptide-mass fingerprinting. *Curr. Biol.* **3**(6), 327-332.
- Park, G., T. , Quan, G. & Lee, J., B.** (2006) Sera from patients with toxic epidermal necrolysis contain autoantibodies to periplakin. *Br. J. Dermatol.* **155**(2), 337-343.
- Parry, D., A. , Strelkov, S., V., Burkhard, P., Aebi, U. & Herrmann, H.** (2007) Towards a molecular description of intermediate filament structure and assembly. *Exp. Cell Res.* **313**, 2204-2216.
- Paznekas, W., A., Boyadjiev, S., A., Shapiro, R., E. , Daniels, O., Wollnik, B. & Keegan, C., E.** (2003) Connexin 43 (GJA1) mutations cause the pleiotropic phenotype of oculodentodigital dysplasia. *Am. J. Hum. Genet.* **72**, 408-418.
- Perez-Moreno, M., Jamora, C. & Fuchs, E.** (2003) Sticky business: orchestrating cellular signals at adherens junctions. *Cell* **112**(4), 535-548.

- Peters, B., Kirfel, J., Büssow, H., Vidal, M. & Magin, T., M.** (2001) Complete cytolysis and neonatal lethality in keratin 5 knockout mice reveal its fundamental role in skin integrity and in epidermolysis bullosa simplex. *Mol. Biol. Cell.* **12**, 1775-1789.
- Pfendner, E. & Uitto, J.** (2005) Plectin gene mutations can cause epidermolysis bullosa with pyloric atresia. *J. Invest. Dermatol.* **124**, 111-115.
- Polakowska, R., Herting, E. & Goldsmith, L., A.** (1991) Isolation of cDNA for human epidermal type I transglutaminase. *J. Invest. Dermatol.* **96**(2), 285-288.
- Porter, R., M.** (2006) The new keratin nomenclature. *J. Invest. Dermatol.* **126**, 2366-2368.
- Prahlad, V., Yoon, M., Moir, R., D., Vale, R., D. & Goldman, R., D.** (1998) Rapid movements of vimentin on microtubule tracks: kinesin-dependent assembly of intermediate filament networks. *J. Cell Biol.* **143**, 159-170.
- Prout, M., Damania, Z., Soong, J., Fristrom, D. & Fristrom, J., W.** (1997) Autosomal mutations affecting adhesion between wing surfaces in *Drosophila melanogaster*. *Genetics* **146**, 275-285.
- Puck, T., T., Marcus, P., I. & Cieciura, S., J.** (1956) Clonal growth of mammalian cells in vitro; growth characteristics of colonies from single HeLa cells with and without a feeder layer. *J. Exp Med.* **103**, 273-283.
- Pulkkinen, L. & Uitto, J.** (1999) Mutation analysis and molecular genetics of epidermolysis bullosa. *Matrix Biol.* **18**, 29-42.
- Puviani, M., Marconi, A., Cozzani, E. & Pincelli, C.** (2003) Fas ligand in pemphigus sera induces keratinocyte apoptosis through the activation of caspase-8. *J. Invest. Dermatol.* **120**, 164-167.
- Pytela, R. & Wiche, G.** (1980) High molecular weight polypeptides (270,000-340,000) from cultured cells are related to hog brain microtubule-associated proteins but copurify with intermediate filaments. *Proc. Natl. Acad. Sci. U S A.* **77**, 4808-4812.
- Rampazzo, A., Nava, A., Malacrida, S., Beffagna, G., Bauce, B., Rossi, V., Zimbello, R., Simionati, B., Basso, C., Thiene, G., Towbin, J., A. & Danieli, G., A.** (2002) Mutation in human desmoplakin domain binding to plakoglobin causes a dominant form of arrhythmogenic right ventricular cardiomyopathy. *Am. J. Hum. Genet.* **71**, 1200-1206.
- Rash, J., E., Shay, J., W. & Biesele, J., J.** (1970) Preliminary biochemical investigations of the intermediate filaments. *J. Ultrastruct. Res.* **33**, 399-407.
- Regnier, M., Caron, D., Reichert, U. & Schaefer, H.** (1993) Barrier function of human skin and human reconstructed epidermis. *J. Pharm. Sci.* **82**, 404-407.
- Ren, X., Kiosses, W., Sieg, D., Otey, C., Schlaepfer, D. & M., S.** (2000) Focal adhesion kinase suppresses Rho activity to promote focal adhesion turnover. *J. Cell Sci.* **113**, 3673-3678.
- Revel, J., P. & Karnovsky, M., J.** (1967) Hexagonal array of subunits in intercellular junctions of the mouse heart and liver. *J. Cell Biol.* **33**(3), C7-C12.

- Reynolds, A., B., Daniel, J., McCrea, P., D., Wheelock, M., J., Wu, J. & Zhang, Z.** (1994) Identification of a new catenin: the tyrosine kinase substrate p120cas associates with E-cadherin complexes. *Mol. Cell Biol.* **14**(12), 8333-8342.
- Reynolds, A., B., Herbert, L., Cleveland, J., L., Berg, S., T. & Gaut, J., R.** (1992) p120, a novel substrate of protein tyrosine kinase receptors and of p60v-src, is related to cadherin-binding factors beta-catenin, plakoglobin and armadillo. *Oncogene* **7**(12), 2439-2445.
- Rezniczek, G., A., Abrahamsberg, C., Fuchs, P., Spazierer, D. & Wiche, G.** (2003) Plectin 5'-transcript diversity: short alternative sequences determine stability of gene products, initiation of translation and subcellular localization of isoforms. *Hum. Mol. Genet.* **12**, 3181-3194.
- Rezniczek, G., A., Janda, L. & Wiche, G.** (2004) Plectin. *Methods. Cell Biol.* **78**, 721-755.
- Rezniczek, G., A., Konieczny, P., Nikolic, B., Reipert, S., Schneller, D., Abrahamsberg, C., Davies, K., E., Winder, S., J. & Wiche, G.** (2007) Plectin 1f scaffolding at the sarcolemma of dystrophic (mdx) muscle fibers through multiple interactions with beta-dystroglycan. *J. Cell Biol.* (176), 965-977.
- Rezniczek, G.A., Abrahamsberg, C., Fuchs, P., Spazierer, D. & Wiche, G.** (2003) Plectin 5'-transcript diversity: short alternative sequences determine stability of gene products, initiation of translation and subcellular localization of isoforms. *Hum. Mol. Genet.* **12**, 3181-3194.
- Richard, G., Smith, L., E., Bailey, R., A., Itin, P., Hohl, D. & Epstein, E., H. Jr.** (1988) Mutations in the human connexin gene GJB3 cause erythrokeratoderma variabilis. *Nat. Genet.* **20**, 366-369.
- Richard, G., Smith, L., E., Bailey, R., A., Itin, P., Hohl, D. & Epstein, E., H. Jr.** (1998a) Mutations in the human connexin gene GJB3 cause erythrokeratoderma variabilis. *Nat. Genet.* **20**, 366-369.
- Richard, G., White, T., W., Smith, L., E., Bailey, R., A., Compton, J., G. & Paul, D., L.** (1998b) Functional defects of Cx26 resulting from a heterozygous missense mutation in a family with dominant deaf-mutism and palmoplantar keratoderma. *Hum. Genet.* **103**, 393-399.
- Rimm, D., L., Koslov, E., R., Kebriaci, P., Cianci, C., D. & Morrow, J., S.** (1995) Alpha 1(E)-catenin is an actin-binding and -bundling protein mediating the attachment of F-actin to the membrane adhesion complex. *Proc. Natl. Acad. Sci. U S A.* **92**(19), 8813-8817.
- Robertson, J., D.** (1963) The occurrence of a subunit pattern in the unit membranes of club endings in mauthner cell synapses in goldfish brains. *TJ. Cell Biol.* **19**, 201-221.
- Rogalski, A., A. & Singer, S., J.** (1984) Associations of elements of the Golgi apparatus with microtubules. *J. Cell Biol.* **99**, 1092-1100.
- Rogers, M., A., Edler, L., Winter, H., Langbein, L., Beckmann, I. & Schweizer, J.** (2005) Characterization of new members of the human type II keratin gene family and a general evaluation of the keratin gene domain on chromosome 12q13.13. *J. Invest. Dermatol.* **124**, 536-544.

- Rogers, M., A., Winter, H., Langbein, L., Bleiler, R. & Schweizer, J.** (2004) The human type I keratin gene family: characterization of new hair follicle specific members and evaluation of the chromosome 17q21.2 gene domain. *Differentiation* **72**, 527-540.
- Röper, K. & Brown, N., H.** (2003) Maintaining epithelial integrity: a function for gigantic spectraplaklin isoforms in adherens junctions. *J. Cell Biol.* **162**, 1305-1315.
- Röper, K., Gregory, S., L. & Brown, N., H.** (2002) The 'spectraplaklins': cytoskeletal giants with characteristics of both spectrin and plaklin families. *J. Cell Sci.* **115**, 4215-4225.
- Rugg, E., L. , McLean, W., H., Lane, E., B., Pitera, R., McMillan, J., R., Dopping-Hepenstal, P., J., Navsaria, H., A., Leigh, I., M. & Eady, R., A.** (1994) A functional "knockout" of human keratin 14. *Genes Dev.* **8**, 2563-2573.
- Ruhrberg, C. & Watt, F.M.** (1997) The plaklin family: versatile organizers of cytoskeletal architecture. *Curr. Opin. Genet. Dev* **7**, 392 -397.
- Ruhrberg, C., Hajibagheri, M., A., Parry, D., A. & Watt, F., M.** (1997) Periplakin, a novel component of cornified envelopes and desmosomes that belongs to the plaklin family and forms complexes with envoplakin. *J. Cell Biol.* **139**(7), 1835-1849.
- Ruhrberg, C., Hajibagheri, M., A., Simon, M., Dooley, T., P. & Watt, F., M.** (1996) Envoplakin, a novel precursor of the cornified envelope that has homology to desmoplakin. *J. Cell Biol.* **134**(3), 715-729.
- Ruiz, P., Brinkmann, V., Ledermann, B., Behrend, M., Grund, C., Thalhammer, C., Vogel, F., Birchmeier, C., Günthert, U., Franke, W., W. & Birchmeier, W.** (1996) Targeted mutation of plakoglobin in mice reveals essential functions of desmosomes in the embryonic heart. *J. Cell Biol.* **135**, 215-225.
- Runkel, F., Michels, M., Franken, S. & Franz, F.** (2006) Specific expression of annexin A8 in adult murine stratified epithelia. *Journal of Molecular Histology* **37**, 353-359.
- Saez, J., C. , Connor, J., A. , Spray, D., C. & Bennett, M., V.** (1989) Hepatocyte gap junctions are permeable to the second messenger, inositol 1,4,5-trisphosphate, and to calcium ions. . *Proc. Natl. Acad. Sci. U S A* **86**, 2708– 2712.
- Sánchez-Aparicio, P., Martínez de Velasco, A., M., Niessen, C., M., Borradori, L., Kuikman, I., Hulsman, E., H., Fässler, R., Owaribe, K. & Sonnenberg, A.** (1997) The subcellular distribution of the high molecular mass protein, HD1, is determined by the cytoplasmic domain of the integrin beta 4 subunit. *J. Cell Sci.* **110**, 169-178.
- Sato, M., Aoyama, Y. & Kitajima, Y.** (2000) Assembly pathway of desmoglein 3 to desmosomes and its perturbation by pemphigus vulgaris-IgG in cultured keratinocytes, as revealed by time-lapsed labeling immunoelectron microscopy. *Lab Invest.* **80**, 1583-1592.
- Schmidt, A. & Hall, M., N.** (1998) Signaling to the actin cytoskeleton. *Annu. Rev. Cell Dev. Biol.* **14**, 305-338.
- Schmidt, A. & Jäger, S.** (2005) Plakophilins--hard work in the desmosome, recreation in the nucleus? *Eur. J. Cell Biol.* **84**(2-3), 189-204.
- Schweizer, J., Bowden, P., E., Coulombe, P., A., Langbein, L., Lane, E., B., Magin, T., M. , Maltais, L., Omary, M., B. , Parry, D., A., Rogers, M., A. & Wright, M., W.**

- (2006) New consensus nomenclature for mammalian keratins. *J. Cell Biol.* **174**, 169-174.
- Seifert, G., J., Lawson, D. & Wiche, G.** (1992) Immunolocalization of the intermediate filament-associated protein plectin at focal contacts and actin stress fibers. *Eur. J. Cell Biol.* **59**, 138-147.
- Serre, G., Mils, V., Haftek, M., Vincent, C., Croute, F., Réano, A., Ouhayoun, J., P., Bettinger, S., Soleilhavoup, J., P. & Iizuka, H.** (1991) Identification of late differentiation antigens of human cornified epithelia, expressed in re-organized desmosomes and bound to cross-linked envelope. *J. Invest. Dermatol.* **97**(6), 1061-1072.
- Setzer, S., V., Calkins, C., C., Garner, J., Summers, S., Green, K., J. & Kowalczyk, A., P.** (2004) Comparative analysis of armadillo family proteins in the regulation of a431 epithelial cell junction assembly, adhesion and migration. *J. Invest. Dermatol.* **123**, 426-433.
- Sevcík, J., Urbániková, L., Kost'an, J., Janda, L. & Wiche, G.** (2004) Actin-binding domain of mouse plectin. Crystal structure and binding to vimentin. *Eur. J. Biochem.* **271**, 1873-1884.
- Sevilla, L.M., Nachat, R., Groot, K.R., Klement, J.F., Uitto, J., Djian, P., Maatta, A. & Watt, F.M.** (2007) Mice deficient in involucrin, envoplakin and periplakin have a defective epidermal barrier. *J. Cell Biol.* **179**(7), 1599--1612.
- Shimizu, H., Masunaga, T., Ishiko, A., Kikuchi, A., Hashimoto, T. & Nishikawa, T.** (1995) Pemphigus vulgaris and pemphigus foliaceus sera show an inversely graded binding pattern to extracellular regions of desmosomes in different layers of human epidermis. *J. Invest. Dermatol.* **105**, 153-159.
- Simon, A., M., Goodenough, D., A. & Paul, D., L.** (1998) Mice lacking connexin40 have cardiac conduction abnormalities characteristic of atrioventricular block and bundle branch block. *Curr. Biol.* **8**, 295 - 298.
- Simon, M. & Green, H.** (1984) Participation of membrane-associated proteins in the formation of the cross-linked envelope of the keratinocyte. *Cell* **36**, 827-834.
- Sjöblom, T., Jones, S., Wood, L., D., Parsons, D., W., Lin, J., Barber, T., D., Mandelker, D., Leary, R., J., Ptak, J., Silliman, N., Szabo, S., Buckhaults, P., Farrell, C., Meeh, P., Markowitz, S., D., Willis, J., Dawson, D., Willson, J., K., Gazdar, A., F., Hartigan, J., Wu, L., Liu, C., Parmigiani, G., Park, B., H., Bachman, K., E., Papadopoulos, N., Vogelstein, B., Kinzler, K., W. & Velculescu, V., E.** (2006) The consensus coding sequences of human breast and colorectal cancers. *Science* **314**, 268-274.
- Skerrow, C., J. & Matoltsy, A., G.** (1974) Isolation of epidermal desmosomes. *J. Cell Biol.* **63**, 515-523.
- Small, J., V.** (1995) Getting the actin filaments straight: nucleation-release or treadmilling? *Trends. Cell Biol.* **5**, 52-55.
- Smith, E., A. & Fuchs, E.** (1998) Defining the interactions between intermediate filaments and desmosomes. *J. Cell Biol.* **141**, 1229-1241.

- Sokolova, A., V., Kreplak, L., Wedig, T., Mücke, N., Svergun, D., I., Herrmann, H., Aebi, U. & Strelkov, S., V.** (2006) Monitoring intermediate filament assembly by small-angle x-ray scattering reveals the molecular architecture of assembly intermediates. *Proc. Natl. Acad. Sci. USA* **103**, 16206-16211.
- Sonnenberg, A. & Liem, R.K.H.** (2007) Plakins in development and disease. *Experimental Cell Research* **313**, 2189-2203.
- Soule, H., D., Vazquez, J., Long, A., Albert, S. & Brennan, M.** (1973) A human cell line from a pleural effusion derived from a breast carcinoma. *J. Natl. Cancer Inst.* **51**, 1409-1416.
- Spazierer, D., Fuchs, P., Pröll, V., Janda, L., Oehler, S., Fischer, I., Hauptmann, R. & Wiche, G.** (2003) Epiplakin gene analysis in mouse reveals a single exon encoding a 725-kDa protein with expression restricted to epithelial tissues. *J. Biol Chem.* **278**, 31657-31666.
- Spazierer, D., Fuchs, P., Reipert, S., Fischer, I., Schmuth, M., Lassmann, H. & Wiche, G.** (2006) Epiplakin is dispensable for skin barrier function and for integrity of keratin network cytoarchitecture in simple and stratified epithelia. *Mol. Cell Biol.* **26**, 559-568.
- Spazierer, D., Raberger, J., Groß, K., Fuchs, P. & Wiche, G.** (2008) Stress-induced recruitment of epiplakin to keratin networks increases their resistance to hyperphosphorylation-induced disruption. *J. Cell Sci.* **121**, 825-833.
- Spiegelman, B., M., Penningroth, S., M. & Kirschner, M., W.** (1977) Turnover of tubulin and the N site GTP in Chinese hamster ovary cells. *Cell* **12**, 587-600.
- Spinardi, L., Ren, Y., L., Sanders, R. & Giancotti, F., G.** (1993) The beta 4 subunit cytoplasmic domain mediates the interaction of alpha 6 beta 4 integrin with the cytoskeleton of hemidesmosomes. *Mol. Biol. Cell.* **4**, 871-884.
- Srivastava, M., Atwater, I., Glasman, M., Leighton, X., Goping, G., Caohuy, H., Miller, G., Pichel, J., Westphal, H. & Mears, D.** (1999) Defects in inositol 1,4,5-trisphosphate receptor expression, Ca²⁺ signaling, and insulin secretion in the *anx7(+/-)* knock-out mouse. *Proc. Natl. Acad. Sci. USA* **96**, 13783-13788.
- Stanley, J., R.** (1993) Cell adhesion molecules as targets of autoantibodies in pemphigus and pemphigoid, bullous diseases due to defective epidermal cell adhesion. *Adv. Immunol.* **53**, 291-325.
- Stanley, J., R., Alvarez, O., M., Bere, E., W. Jr., Eaglstein, W., H. & Katz, S., I.** (1981) Detection of basement membrane zone antigens during epidermal wound healing in pigs. *J. Invest. Dermatol.* **77**(2), 240-243.
- Stanley, J., R., Yaar, M., Hawley-Nelson, P. & Katz, S., I.** (1982) Pemphigus antibodies identify a cell surface glycoprotein synthesized by human and mouse keratinocytes. *J. Clin. Invest.* **70**(2), 281-288.
- Stanley, J., R., Tanaka, T., Mueller, S., Klaus-Kovtun, V. & Roop, D.** (1988) Isolation of complementary DNA for bullous pemphigoid antigen by use of patients' autoantibodies. *J. Clin. Invest.* **82**, 1864-1870.
- Stauffer, K., A. & Unwin, N.** (1992) Structure of gap junctions channels. *Semin. Cell Biol.* **3**, 17-20.

- Stegh, A., H., Herrmann, H., Lampel, S., Weisenberger, D., Andrä, K., Seper, M., Wiche, G., Krammer, P., H. & Peter, M., E.** (2000) Identification of the cytolinker plectin as a major early in vivo substrate for caspase 8 during CD95- and tumor necrosis factor receptor-mediated apoptosis. *Mol. Cell Biol.* **20**, 5665-5679.
- Steinert, P., M. & Marekov, L., N.** (1995) The proteins elafin, filaggrin, keratin intermediate filaments, loricrin, and small proline-rich proteins 1 and 2 are isodipeptide cross-linked components of the human epidermal cornified cell envelope. *J. Biol. Chem.* **270**(30), 17702-17711.
- Sterk, L., M., Geuijen, C., A., Oomen, L., C., Calafat, J., Janssen, H. & Sonnenberg, A.** (2000) The tetraspan molecule CD151, a novel constituent of hemidesmosomes, associates with the integrin alpha6beta4 and may regulate the spatial organization of hemidesmosomes. *J. Cell Biol.* **149**(4), 969-982.
- Steven, A.C., Hainfeld, J.F., Trus, B.L., Wall, J.S. & P.M., S.** (1983) Epidermal Keratin Filaments Assembled in vitro Have Masses-per-Unit-Length That Scale According to Average Subunit Mass: Structural Basis for Homologous Packing of Subunits in Intermediate Filaments. *The Journal of Cell Biology* **97**, 1939-1944.
- Stradal, T., Kranewitter, W., Winder, S., J. & Gimona, M.** (1998) CH domains revisited. *FEBS Lett.* **431**, 134-137.
- Straub, B.K., Boda, J., Kuhn, C., Schnoelzer, M., Korf, U., Kempf, T., Spring, H., Hatzfeld, M. & Franke, W.W.** (2003) A novel cell-cell junction system: the cortex adhaerens mosaic of lens fiber cells *Journal of Cell Science* **116**, 4985-4995
- Strelkov, S., V., Herrmann, H. & Aebi, U.** (2003) Molecular architecture of intermediate filaments. *Bioessays* **25**(3), 243-251.
- Sun, D., Leung, C., L. & Liem, R., K.** (2001) Characterization of the microtubule binding domain of microtubule actin crosslinking factor (MACF): identification of a novel group of microtubule associated proteins. *J. Cell Sci.* **114**, 161-172.
- Sun, Y., Zhang, J., Kraeft, S., K., Auclair, D., Chang, M., S., Liu, Y., Sutherland, R., Salgia, R., Griffin, J., D., Ferland, L., H. & Chen, L., B.** (1999) Molecular cloning and characterization of human trabeculin-alpha, a giant protein defining a new family of actin-binding proteins. *J. Biol Chem.* **274**, 33522-33530.
- Svitkina, T.M., Verkhovskiy, A.B. & Borisy, G.G.** (1996) Plectin sidearms mediate interaction of intermediate filaments with microtubules and other components of the cytoskeleton. *J. Cell Biol.* **135**, 991-1007.
- Szent-Györgyi, A.** (1949) Attacks on Muscle. *Science* **110**, 411-413.
- Szent-Györgyi, A., G.** (1951) A new method for the preparation of actin. *J. Biol Chem.* **192**(1), 361-369.
- Tadokoro, S., Shattil, S., J., Eto, K., Tai, V., Liddington, R., C., de Pereda, J., M., Ginsberg, M., H. & Calderwood, D., A.** (2003) Talin binding to integrin beta tails: a final common step in integrin activation. *Science* **302**, 103-106.
- Takai, Y. & Nakanishi, H.** (2003) Nectin and afadin: novel organizers of intercellular junctions. *J. Cell Sci.* **116**, 17-27.

- Takeichi, M.** (1995) Morphogenetic roles of classic cadherins. *Curr. Opin. Cell Biol.* **7**(5), 619-627.
- Teulière, J., Faraldo, M., M., Shtutman, M., Birchmeier, W., Huelsken, J., Thiery, J., P. & Glukhova, M., A.** (2004) beta-catenin-dependent and -independent effects of DeltaN-plakoglobin on epidermal growth and differentiation. *Mol. Cell Biol.* **24**, 8649-8661.
- Thoreson, M., A., Anastasiadis, P., Daniel, J., M., Ireton, R., C., Wheelock, M., J., Johnson, K., R., Hummingbird, D., K. & Reynolds, A., B.** (2000) Selective uncoupling of p120(ctn) from E-cadherin disrupts strong adhesion. *J. Cell Biol.* **148**(1), 189-202.
- Toivola, D., M., Nieminen, M., I., Hesse, M., He, T., Baribault, H., Magin, T., M., Omary, M., B. & Eriksson, J., E.** (2001) Disturbances in hepatic cell-cycle regulation in mice with assembly-deficient keratins 8/18. *Hepatology* **34**, 1174-1183.
- Toivola, D.M., Ku, N.O., Resurreccion, E.Z., Nelson, D.R., Wright, T.L. & Omary, M.B.** (2004) Keratin 8 and 18 hyperphosphorylation is a marker of progression of human liver disease. *Hepatology* **40**, 459-466.
- Torpey, N., Wylie, C.C. & Heasman, J.** (1992) Function of maternal cytokeratin in *Xenopus* development. *Nature* **357**, 413-415.
- Tsukita, S., Furuse, M. & Itoh, M.** (1999) Structural and signalling molecules come together at tight junctions. *Curr. Opin. Cell Biol.* **11**(5), 628-633.
- Tsukita, S., Furuse, M. & Itoh, M.** (2001) Multifunctional strands in tight junctions. *Nat. Rev. Mol. Cell Biol.* **2**(4), 285-293.
- Tucker, J.** (1992) The microtubule-organizing center. *Bioessays* **14**, 861-867.
- Uematsu, J., Nishizawa, Y., Sonnenberg, A. & Owaribe, K.** (1994) Demonstration of type II hemidesmosomes in a mammary gland epithelial cell line, BMGE-H. *J. Biochem.* **115**(3), 469-476.
- Uitto, J., Pulkkinen, L., Smith, F., J. & McLean, W., H.** (1996) Plectin and human genetic disorders of the skin and muscle. The paradigm of epidermolysis bullosa with muscular dystrophy. *Exp. Dermatol.* **5**, 237-246.
- Uitto, J., Richard, G. & McGrath, J., A.** (2007) Diseases of epidermal keratins and their linker proteins. *Exp. Cell Res.* **313**, 1995-2009.
- Ulmer, T., S., Calderwood, D., A., Ginsberg, M., H. & Campbell, I., D.** (2003) Domain-specific interactions of talin with the membrane-proximal region of the integrin beta3 subunit. *Biochemistry* **42**, 8307-8312.
- Ursitti, J., A., Petrich, B., G., Lee, P., C., Resneck, W., G., Ye, X., Yang, J., Randall, W., R., Bloch, R., J. & Wang, Y.** (2007) Role of an alternatively spliced form of alpha1-spectrin in localization of connexin 43 in cardiomyocytes and regulation by stress-activated protein kinase. *J. Mol. Cell Cardiol.* **42**, 572-581.
- Vactor, D., V., Sink, H., Fambrough, D., Tsoo, R. & Goodman, C., S.** (1993) Genes that control neuromuscular specificity in *Drosophila*. *Cell* **73**, 1137-1153.

- Valiunas, V., Polosina, Y., Y., Miller, H., Potapova, I., A., Valiuniene, L. & Doronin, S.** (2005) Connexin-specific cell-to-cell transfer of short interfering RNA by gap junctions. *J. Physiol.* **568**, 459–468.
- van den Heuvel, A., de Vries-Smits, A., M., van Weeren, P., C., Dijkers, P., F., de Bruyn, K., M., Riedl, J., A. & Burgering, B., M.** (2002) Binding of protein kinase B to the plakin family member periplakin. *J. Cell Sci.* **115**, 3957–3966.
- Vasioukhin, V., Bowers, E., Bauer, C., Degenstein, L. & Fuchs, E.** (2001) Desmoplakin is essential in epidermal sheet formation. *Nat. Cell Biol.* **3**, 1076–1085.
- Venetianer, A., Schiller, D.L., Magin, T. & Franke, W.W.** (1983) Cessation of cytokeratin expression in a rat hepatome cell line lacking differentiated functions. *Nature* **305**, 730–733.
- Vikstrom, K., L., Lim, S., S., Goldman, R., D. & Borisy, G., G.** (1992) Steady state dynamics of intermediate filament networks. *J. Cell Biol.* **118**, 121–129.
- Vinken, M., Vanhaecke, T., Papcleu, P., Snykers, S., Henkens, T. & Rogiers, V.** (2006) Connexins and their channels in cell growth and cell death. *Cell Signal* **18**, 592–600.
- Vybiral, T., Winkelmann, J., C., Roberts, R., Joc, E., Casey, D., L., Williams, J., K. & Epstein, H., F.** (2001) Human cardiac and skeletal muscle spectrins: differential expression and localization. *Cell. Motil. Cytoskel.* **21**, 293–304.
- Wallis, S., Lloyd, S., Wise, I., Ireland, G., Fleming, T., P. & Garrod, D.** (2000) The alpha isoform of protein kinase C is involved in signaling the response of desmosomes to wounding in cultured epithelial cells. *Mol. Biol. Cell.* **11**, 1077–1092.
- Wang, A., Johnson, D., G. & MacLeod, M., C.** (2001) Molecular cloning and characterization of a novel mouse epidermal differentiation gene and its promoter. *Genomics* **73**, 284–290.
- Wang, L., Ho, C., L., Sun, D., Liem, R., K. & Brown, A.** (2000) Rapid movement of axonal neurofilaments interrupted by prolonged pauses. *Nat. Cell Biol.* **2**, 137–141.
- Waschke, J., Bruggeman, P., Baumgartner, W., Zillikens, D. & Drenckhahn, D.** (2005) Pemphigus foliaceus IgG causes dissociation of desmoglein 1-containing junctions without blocking desmoglein 1 transinteraction. *J Clin Invest.* **115**, 3157–3165.
- Waterman-Storer, C., M. & Salmon, E., D.** (1998) How microtubules get fluorescent speckles. *Biophys. J.* **75**(4), 2059–2069.
- Watt, F., M., Matthey, D., L. & Garrod, D., R.** (1984) Calcium-induced reorganization of desmosomal components in cultured human keratinocytes. *J. Cell Biol.* **99**, 2211–2215.
- Webb, D.J., Donais, K., Whitmore, L., A., Thomas, S., M., Turner, C., E., Parsons, J., T. & Horwitz, A., F.** (2004) FAK-Src signalling through paxillin, ERK and MLCK regulates adhesion disassembly. *Nat. Cell Biol.* **6**, 154–161.
- Weng, X., Luecke, H., Song, I.S., Kang, D.S., Kim, S.H. & Huber, R.** (1993) Crystal structure of human annexin I at 2.5 Å resolution. *Protein sci.* **2**, 448–458.
- Werner, N.S., Windoffer, R., Strnad, P., Grund, C., Leube, R.E. & Magin, T.M.** (2004) Epidermolysis bullosa simplex-type mutations alter the dynamics of the keratin cytoskeleton and reveal a contribution of actin to the transport of keratin subunits. *Mol. Biol. Cell.* **15**, 990–1002.

- Wertz, P., W. & Downing, D., T.** (1990) Metabolism of linoleic acid in porcine epidermis. *J. Lipid. Res.* **31**(10), 1839-1844.
- Wheelock, M., J. & Jensen, P., J.** (1992) Regulation of keratinocyte intercellular junction organization and epidermal morphogenesis by E-cadherin. *J. Cell Biol.* **117**(2), 415-425.
- Whitlock, N., V., Ashton, G., H., Dopping-Hepenstal, P., J., Gratian, M., J., Keane, F., M., Eady, R., A. & McGrath, J., A.** (1999) Striate palmoplantar keratoderma resulting from desmoplakin haploinsufficiency. *J. Invest. Dermatol.* **113**, 940-946.
- Whitlock, N., V., Wan, H., Morley, S., M., Garzon, M., C., Kristal, L., Hyde, P., McLean, W., H., Pulkkinen, L., Uitto, J., Christiano, A., M., Eady, R., A. & McGrath, J., A.** (2002) Compound heterozygosity for non-sense and mis-sense mutations in desmoplakin underlies skin fragility/woolly hair syndrome. *J. Invest. Dermatol.* **118**, 232-238.
- Wiche, G., Becker, B., Lubert, K., Weitzer, G., Castañón, M.J., Hauptmann, R., Stratowa, C. & Stewart, M.** (1991) Cloning and sequencing of rat plectin indicates a 466-kD polypeptide chain with a three-domain structure based on a central alpha-helical coiled coil. *J. Cell Biol.* **114**, 83-99.
- Wiche, G., Gromov, D., Donovan, A., Castanon, M., J. & Fuchs, E.** (1993) Expression of plectin mutant cDNA in cultured cells indicates a role of COOH-terminal domain in intermediate filament association. *J. Cell Biol.* **121**, 607-619.
- Wiche, G., Krepler, R., Artlieb, U., Pytela, R. & Denk, H.** (1983) Occurrence and immunolocalization of plectin in tissues. *J. Cell Biol.* **97**, 887-901.
- Wilhelmsen, K., Litjens, S., Kuikman, I., Tshimbalanga, N., Janssen, H., van den Bout, I., Raymond, K. & Sonnenberg, A.** (2005) Nesprin-3, a novel outer nuclear membrane protein, associates with the cytoskeletal linker protein plectin. *J. Cell Biol.* **171** (5), 799-810.
- Winder, S., J., Hemmings, L., Maciver, S., K., Bolton, S., J., Tinsley, J., M., Davies, K., E., Critchley, D., R. & Kendrick-Jones, J.** (1995) Utrophin actin binding domain: analysis of actin binding and cellular targeting. *J. Cell Sci.* **108**, 63-71.
- Windoffer, R., Borchert-Stuhlträger, M. & Leube, R., E.** (2002) Desmosomes: interconnected calcium-dependent structures of remarkable stability with significant integral membrane protein turnover. *J. Cell Sci.* **115**, 1717-1732.
- Windoffer, R., Kölsch, A., Wöll, S. & Leube, R., E.** (2006) Focal adhesions are hotspots for keratin filament precursor formation. *J. Cell Biol.* **173**, 341-348.
- Windoffer, R., Wöll, S., Strnad, P. & Leube, R., E.** (2004) Identification of novel principles of keratin filament network turnover in living cells. *Mol. Biol. Cell.* **15**(5), 2436-2448.
- Winsor, B. & Schiebe, I.E.** (1997) Review: an overview of the *Saccharomyces cerevisiae* microtubule and microfilament cytoskeleton. *Yeast* **13**(5), 399-434.
- Wiszniewski, L., Limat, A., Saurat, J., H., Meda, P. & Salomon, D.** (2000) Differential expression of connexins during stratification of human keratinocytes. *J. Invest. Dermatol.* **115**, 278-285.

- Wolkenstein, P., C., Adle, H., Wechsler, J., Garchon, H., J., Revuz, J. & Roujeau, J., C.** (1996) Apoptosis as a mechanism of keratinocyte death in toxic epidermal necrolysis. *Br. J. Dermatol.* **134**, 710-714.
- Wöll, S., Windoffer, R. & Leube, R., E.** (2005) Dissection of keratin dynamics: different contributions of the actin and microtubule systems. *Eur. J. Cell Biol.* **84**, 311-328.
- Wong, P. & Coulombe, P.A.** (2003) Loss of keratin 6 (K6) proteins reveals a function for intermediate filaments during wound repair. *J. Cell Biol.* **163**, 327-337.
- Yang, Y., Bauer, C., Strasser, G., Wollman, R., Julien, J., P. & Fuchs, E.** (1999) Integrators of the cytoskeleton that stabilize microtubules. *Cell* **98**, 229-238.
- Yap, A., S., Niessen, C., M. & Gumbiner, B., M.** (1998) The juxtamembrane region of the cadherin cytoplasmic tail supports lateral clustering, adhesive strengthening, and interaction with p120ctn. *J. Cell Biol.* **141**(3), 779-789.
- Yin, T. & Green, K., J.** (2004) Regulation of desmosome assembly and adhesion. *Semin. Cell Dev. Biol.* **15**, 665-677.
- Yin, T., Getsios, S., Caldelari, R., Godsel, L., M., Kowalczyk, A., P., Müller, E., J. & Green, K., J.** (2005) Mechanisms of plakoglobin-dependent adhesion: desmosome-specific functions in assembly and regulation by epidermal growth factor receptor. *J. Biol Chem.* **280**, 40355-40363.
- Yoon, K., H., Yoon, M., Moir, R., D., Khuon, S., Flitney, F., W. & Goldman, R., D.** (2001) Insights into the dynamic properties of keratin intermediate filaments in living epithelial cells. *J. Cell Biol.* **153**, 503-516.
- Yoon, M., Moir, R., D., Prahlad, V. & Goldman, R., D.** (1998) Motile properties of vimentin intermediate filament networks in living cells. *J. Cell Biol.* **143**, 147-157.
- Young, K., G., Pool, M. & Kothary, R.** (2003) Bpag1 localization to actin filaments and to the nucleus is regulated by its N-terminus. *J. Cell Sci.* **116**, 4543-4555.
- Younus, J. & Ahmed, A., R.** (1990) The relationship of pemphigus to neoplasia. *J. Am. Acad. Dermatol.* **23**, 498-502.
- Zamir, E. & Geiger, B.** (2001) Molecular complexity and dynamics of cell-matrix adhesions. *J. Cell Sci.* **114**, 3583-3590.
- Zamore, P.D., Tuschl, T., Sharp, P.A. & Bartel, D.P.** (2000) RNAi: double-stranded RNA directs the ATP-dependent cleavage of mRNA at 21 to 23 nucleotide intervals. *Cell* **101**(1), 25-33.
- Zatloukal, K., Stumtner, C., Fuchsbichler, A., Fickert, P., Lackner, C., Trauner, M. & Denk, H.** (2004) The keratin cytoskeleton in liver diseases. *J. Pathol.* **204**, 367-376.
- Zernig, G. & Wiche, G.** (1985) Morphological integrity of single adult cardiac myocytes isolated by collagenase treatment: immunolocalization of tubulin, microtubule-associated proteins 1 and 2, plectin, vimentin, and vinculin. *Eur. J. Cell Biol.* **38**, 113-122.
- Zhang, T., Haws, P. & Wu, Q.** (2004) Multiple variable first exons: a mechanism for cell- and tissue-specific gene regulation. *Genome Res.* **14**, 79-89.

- Zhao, X., P. & Elder, J., T.** (1997) Positional cloning of novel skin-specific genes from the human epidermal differentiation complex. *Genomics* **42**, 250–258.
- Zhao, Z., S., Manser, E., Loo, T., H. & L., L.** (2000) Coupling of PAK- interacting exchange factor PIX to GIT1 promotes focal complex disassembly. *Mol. Cell. Biol.* **20**, 6354–6363.
- Zhou, X., Stuart, A., Dettin, L., E., Rodriguez, G., Hoel, B. & Gallicano, G., I.** (2004) Desmoplakin is required for microvascular tube formation in culture. *J. Cell Sci.* **117**, 3129-3140.
- Zhu, H., Bilgin, M. & Snyder, M.** (2003) Proteomics. *Annu. Rev. Biochem.* **72**, 783-812.
- Zhurinsky, J., Shtutman, M. & Ben-Ze'ev, A.** (2000) Plakoglobin and beta-catenin: protein interactions, regulation and biological roles. *J. Cell Sci.* **113**, 3127-3139.

